doi : 10.17596/0003796

JAMSTEC *Chikyu* SCORE Expedition 910

"The west off Cape Erimo Drilling"

September 19 (Hachinohe) to September 23 (Hakodate), 2017

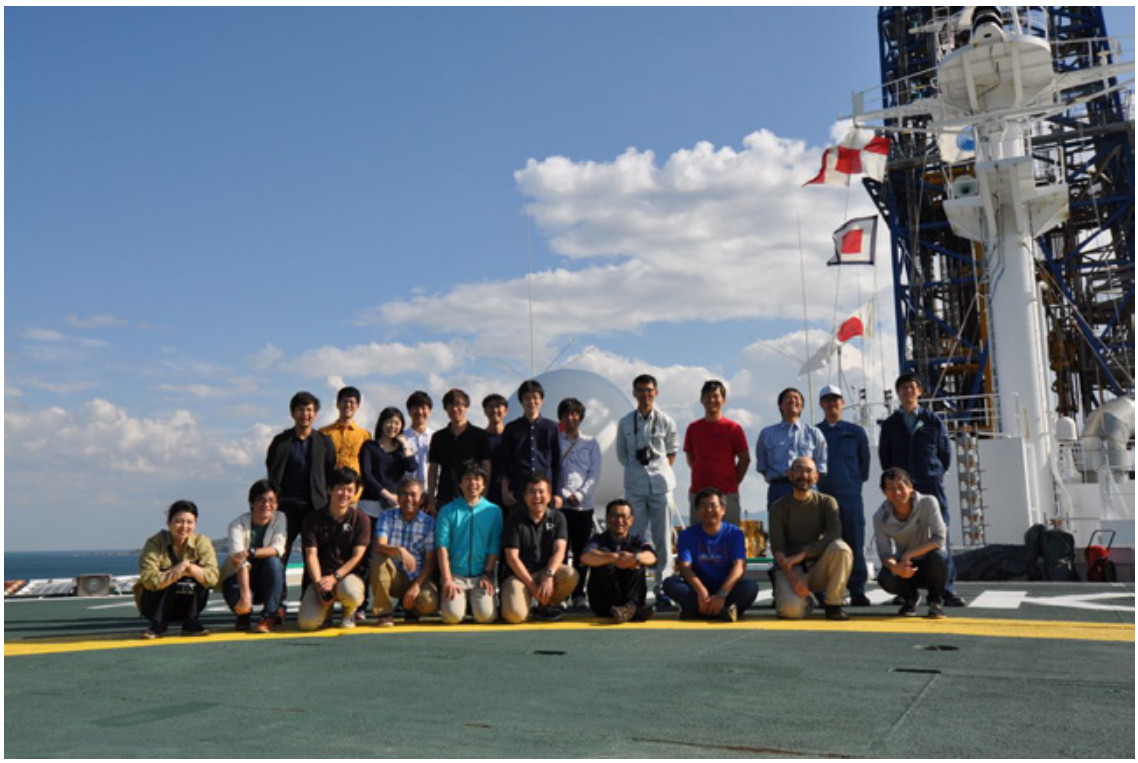

Preliminary Cruise Report

Yusuke Kubo, Fumio Inagaki and the Expedition 910 Shipboard Scientists

Acknowledgements

Expedition 910 shipboard scientists thank all MQJ drilling staff and MWJ laboratory technical staff of the D/V *Chikyu* for the wonderful cruise and taking high-quality core samples. Special thanks T. Ikawa, the CDEX Operation Superintendent of the expedition, for successful sampling. This cruise was implemented as the first of the SCORE program of J-DESC. The proponents would like to thank J-DESC and CDEX for providing the opportunity of this short expedition.

Expedition 910 Shipboard Scientists

Yusuke Kubo (Expedition Project Manager, Chief Scientist)
Center for Deep Earth Exploration (CDEX)
Japan Agency for Marine-Earth Science and Technology (JAMSTEC)
Showa-machi 3173-25, Kanazawa-ku, Yokohama 236-0001, Japan.
E-mail: kuboy@jamstec.go.jp

Fumio Inagaki (Lead Proponent)
Research and Development Center for Ocean Drilling Science
Japan Agency for Marine-Earth Science and Technology (JAMSTEC)
Showa-machi 3173-25, Kanazawa-ku, Yokohama 236-0001, Japan.
E-mail: inagaki@jamstec.go.jp

Tatsuhiko Hoshino (Microbiologist)
Kochi Institute for Core Sample Research
Japan Agency for Marine-Earth Science and Technology (JAMSTEC)
Monobe B200, Nankoku, Kochi 783-8502, Japan
E-mail: hoshinot@jamstec.go.jp

Hiroaki Kurano (Sedimentologist)
Graduate school of frontier science, The University of Tokyo
5-1-5 kashiwanoha, kashawa, Chiba 277-8564, Japan
E-mail: hkurano@aori.u-tokyo.ac.jp

Akira Ijiri (Organic Geochemist)
Kochi Institute for Core Sample Research
Japan Agency for Marine-Earth Science and Technology (JAMSTEC)
Monobe B200, Nankoku, Kochi 783-8502, Japan
E-mail: iijiri@jamstec.go.jp

Yuki Morono (Microbiologist)
Kochi Institute for Core Sample Research

Japan Agency for Marine-Earth Science and Technology (JAMSTEC)
Monobe B200, Nankoku, Kochi 783-8502, Japan
E-mail: morono@jamstec.go.jp

Yuichi Okuma (Sedimentologist)
Faculty of Science, Kochi University
Akebono-cho 2-5-1, Kochi, 780-8072, Japan
Email: single.pe.8746112345p02b.6530@gmail.com

Fumiaki Okumura (Organic Geochemist)
Japan Petroleum Exploration Co., Ltd (JAPEX)
1-2-1 Hamada, Mihama-ku, Chiba 261-0025, Japan
E-mail: fumiaki.okumura@japex.co.jp

Satoko Owari (Inorganic Geochemist)
Graduate school of science, Chiba University
1-33 Yayoi-cho, Inage-ku, Chiba 263-8522, Japan
E-mail: owari.stk@chiba-u.jp

Donald Pan (Microbiologist)
Japan Agency for Marine-Earth Science and Technology (JAMSTEC)
2-15 Natsushima-cho, Yokosuka, Kanagawa 237-0061, Japan
E-mail: donald.pan@jamstec.go.jp

Wataru Tanikawa (Physical Property Specialist)
Kochi Institute for Core Sample Research
Japan Agency for Marine-Earth Science and Technology (JMSTEC),
Monobe B200, Nankoku, Kochi 783-8502, Japan
E-mail: tanikawa@jamstec.go.jp

Takeshi Terada (Microbiologist)
Marine Works Japan, Ltd.,
Oppamahigashi 3-54-1, Yokosuka, 237-0063, Japan

E-mail: teradat@mwj.co.jp

Hitoshi Tomaru (Inorganic Geochemist)
Chiba University
1-33 Yayoi-cho, Inage-ku, Chiba 263-8522 Japan
E-mail: tomaru@chiba-u.jp

Goichiro Uramoto (Physical Properties Specialist)
Center for Advanced Marine Core Research, Kochi University
Monobe B200, Nankoku, Kochi 782-8502, Japan
Email: uramoto.go@kochi-u.ac.jp

Expedition 910 Shore-based contributors

Satoshi Tonai (Core descriptions)
Faculty of Science and Technology, Kochi University
2-5-1 Akebono-cho, Kochi 780-8520, Japan
Email: s-tonai@kochi-u.ac.jp

1 General Background

Scientific ocean drilling has demonstrated that Earth's biosphere extends far below our planet surface, at least down to ~2.5 km beneath the ocean floor on the continental margin (e.g., Inagaki et al., 2015). A recent numerical model study estimated that a total of ~1030 microbial cells are present in the global subseafloor biosphere, accounting for 4 Pg of biomass carbon on Earth (Kallmeyer et al., 2012). In addition, these communities in subseafloor sedimentary habitats consist mainly of phylogenetically distinct species from known microbes on Earth's surface biosphere (e.g., Inagaki et al., 2003, 2006), and therefore the physiology and metabolic functions are still largely unpredictable based on the currently existing metagenomic information (Biddle et al., 2006).

Despite the recent progress of our understanding on the deep subseafloor biosphere, little is known about whether several important elements (e.g., carbon) are sequestered for millions of years or returned to the ocean as active agents with an impact on life and climate (Hinrichs and Inagaki, 2012). It remains unsolved how geological and geochemical instability associated with active tectonic processes do influence the functionality of subseafloor microbial communities.

To address this important scientific question, we drilled and cut core down to ~100 meters below the ocean floor west off Cape Erimo, Hokkaido Island, Japan, where Pliocene-Pleistocene sedimentary sequence is intercalated with multiple mass-transport deposits (MTDs). Here we report the shipboard scientific activity during the expedition and the preliminary dataset from the core samples.

2 Scientific Objectives

The non-riser drilling and coring operations at the proposed site using the *Chikyu*'s Hydraulic Piston Coring System (HPCS) technology will provide a unique opportunity to address two overarching scientific questions as outlined below.

Q1. How does the subseafloor sedimentary biosphere sensitively respond to environmental changes? What are the recovery processes of the subseafloor sedimentary biosphere after the occurrence of submarine landslide? More generally, do adaptive evolution occur in the deep subseafloor biosphere?

A recent study of near-surface sedimentary habitats in Aarhus Bay, Denmark

showed that relative abundances of bacteria in bioturbation layers are up to 60-fold higher than that of archaea, suggesting that seawater-migration by macrofauna activity is one of the key factors controlling bacterial and archaeal abundances and overall community structure during the initial depositional stage (Chen et al., 2017). Similarly, but on larger scale, we hypothesize that submarine landslides introduce fresh organic matter and high-energy electron acceptors (e.g., sulfate) from the overlying seawater into the deep subseafloor biosphere, subsequently stimulate biomass, activity and diversification of organic-fueled microbial communities in the newly constituted sedimentary habitat.

Q2. What are the impact of submarine landslides and subsequent biospheres' roles on global biogeochemical carbon cycles and climate?

It has been hypothesized that earthquake-triggered submarine landslides affect gas hydrate-instability and subsequently impact on paleoceanographic conditions and climates. Carbon isotopic and biomarker analyses of methanotrophic microbial communities also supported that aerobic methanotrophic microbial communities play significant roles in preventing methane release from the hydrosphere to the atmosphere (Hinrichs et al., 2003; Uchida et al., 2004). Despite the past fossil records of the water column ecosystem in response to submarine landslide-associated methane emission have been documented through scientific ocean drilling, it remains largely unknown how the deep subseafloor biosphere responded to submarine landslides and played roles in biogeochemical carbon cycles, as a mediator of the climate change. Since submarine landslides episodically supplied water and electron acceptors (i.e., oxygen, nitrate, sulfate) from the overlying seawater during the mass movement and its depositional phases, it is conceivable that subseafloor sedimentary microbial communities also sensitively respond to those changes in environmental factors and therefore mediate carbon cycling in marine sediments: for example, it might occur that submarine landslides accelerate biomass production and activity of sedimentary microbial communities in MTDs, such as anaerobic oxidation of methane (AOM) coupled with sulfate reduction (Hinrichs et al., 1999; Boetius et al., 2000; Orphan et al., 2001).

There are some additional scientific questions that could be addressed by scientific ocean drilling at the proposed site):

・ What are the origins and generation processes of MTDs-hosted methane and other hydrocarbons?

・ What are the modes and scales of sediment remobilization? When and how did they occur?

・ What are the depositional processes of individual mass-movements in the sedimentary sequence at the proposed site? Can slump facies on seismic images be categorized with lithological characteristics and physical properties of the sediment cores?

Our scientific objectives aforementioned are congruent not only with Challenge 7 "How sensitive are ecosystem and biodiversity to environmental change?" and Challenge 5 "What are the origin, composition, and global significance of subseafloor communities?" in the Chapter 3 "Biosphere Frontiers" of IODP Science Plan 2013-2023, but also significantly relevant to Challenge 12 "What mechanisms control the occurrence of destructive earthquakes, landslides, and tsunami?", Challenge 13 "What properties and processes govern the flow and storage of carbon in the subseafloor?", and Challenge 14 "How do fluids link subseafloor tectonic, thermal, and biogeochemical processes?" in Chapter 5 "Earth in Motion: Processes and hazards on human time scales".

3 Geological background

The Hidaka Trough is located in an arc-arc junction between the northeastern Japan arc and Kuril arc in the southern part of Hokkaido, and extends southward to offshore the Shimokita Peninsula (Fig. 3.1). The Hidaka Trough originated from a forearc basin developed along the Pacific Plate subduction zone (~8 cm/y, west-northwest plate motion vector; Seno et al., 1996), and later converted to a foreland basin adjacent to the Hidaka Block collision zone due to the westward migration of the Kuril forearc sliver (Kimura and Kusunoki, 1997; Takano et al., 2017). A large-scale fore-deep subsidence and a tremendous amount of clastic inflow derived from the uplifted Hidaka Mountains resulted in the thick sedimentary piles of the Neogene foreland basin succession in the Hidaka Trough (Itoh and Tsuru, 2005). The 5,000 m-thick fore-land basin-filling succession comprises submarine-fan

turbidites, MTDs, siliceous shale and hemipelagic mudstones, depending on the background tectonic conditions at the depositional time and the inside-basin locations (JOGMEC, 2005).

Multiple two dimensional (2D)/three dimensional (3D) seismic surveys have been conducted in the Hidaka Trough, including the Ministry of Economy, Trade, and Industry of Japan (MITI) geophysical surveys "Hidaka Shujo Kaibon 3D (JOGMEC, 2005)" and "Hidaka Shujo Kaibon West 3D (JOGMEC, 2006)", providing seismic stratigraphic and structural information on the both deeper and shallower parts of the basin-filling succession. Some seismic sections of the 3D seismic survey cubes indicate that the shallower part below the seafloor is dominated by interbedded MTDs and hemipelagic shales. The 3D-topographic maps of the seafloor clearly indicate that a large-scale slump scar structure (escarpment) developed along the shelf break westward offshore Cape Erimo. Depth contour map and dip magnitude display of the seafloor surface also depict that debris flow lobes and fragmented slump blocks widely distributed in the downstream part of the shelf break slump scar, indicating that the slump scar provided wider-scale MTDs in the central part of the Hidaka Trough. We propose the drilling site in this MTD development area. The shallowest sedimentary sequence (~100 m below seafloor [mbsf]) in the proposed drilling area off Cape Erimo primary consists of Quaternary sedimentary sequence overlying Pliocene units. The 3D-seismic profiles represent the Quaternary sedimentary sequence intercalates at least 3 thinner MTDs, underlying a thicker MTD (Fig. 3.2). As suggested by the prominent collapse of landward escarpment described above, the past gigantic earthquakes have repeatedly triggered massive submarine landslides (and tsunamis) around this area and subsequently formed MTDs with rapid sedimentation in the semicircular basin.

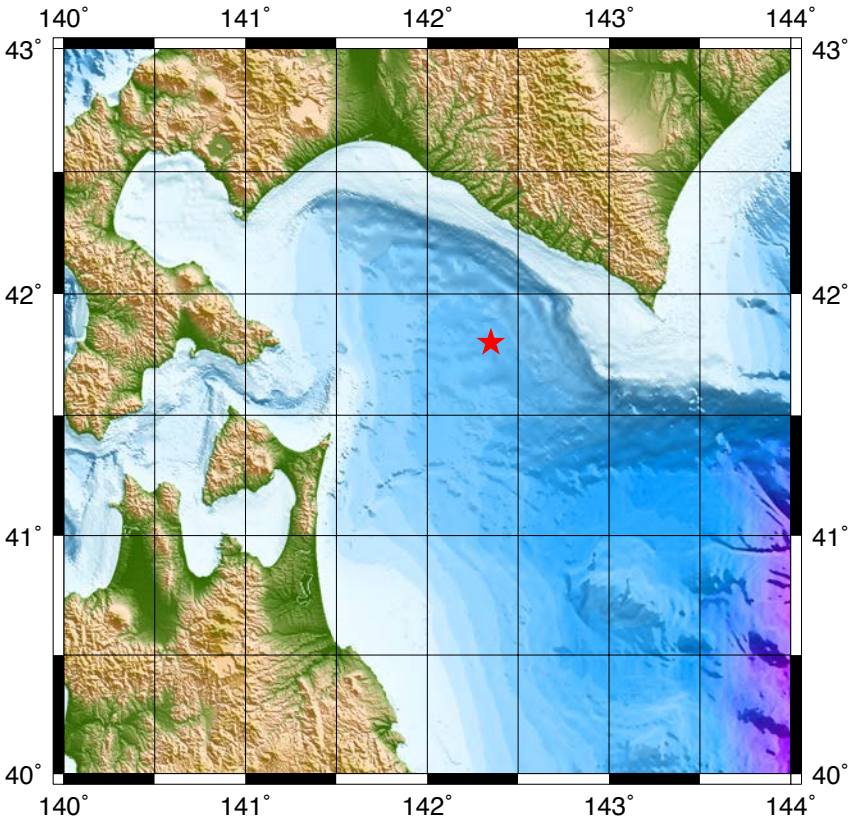

Fig. 3.1. 3D seafloor topographic map around the Hidaka Trough off Cape Erimo and Shimokita Peninsula, northeast Japan. The star shows the proposed drilling site.

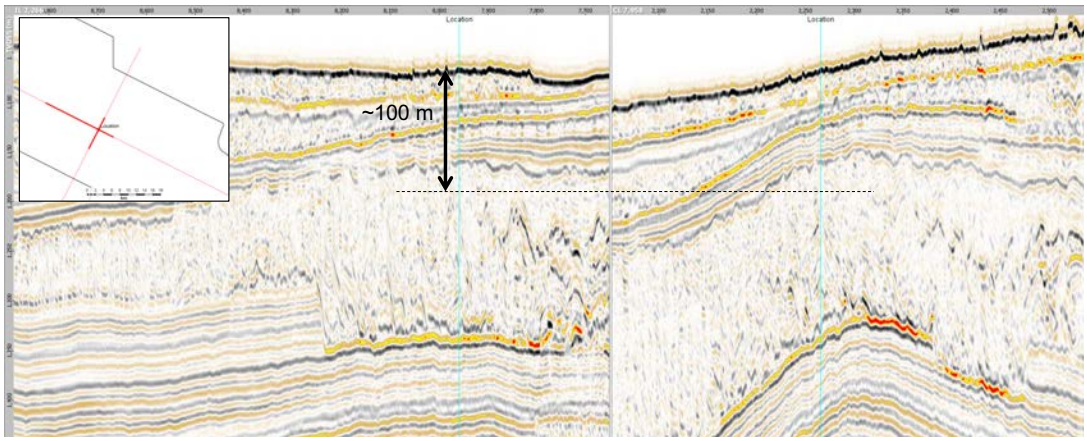

Fig. 3.2. Seismic sections around the proposed drilling site, showing interbedded MTDs and hemipelagic mudstones in the shallowest interval of the foreland basin-filling succession (JOGMEC, 2005, 2006).

4 Shipboard core analysis flow

Three holes were drilled for coring at Site C9033 (Table 4.1). All core sample was taken by using hydraulic piston coring system (HPCS) of *Chikyu*. A short stroke HPCS was used for the last core of Hole C. Formation temperature measurements with APCT-3 tool were conducted at five intervals in Hole A.

Core samples from Hole A were used for shipboard sampling and analysis. Once the core was delivered to the Core Cutting Area, a 10-m long core was cut into sections of 1.4 m long after quick view with an infrared camera for a search of indications of hydrate bearing interval. Small holes were made on core liner to release gases from the sediments. Gas samples were collected at two void intervals before releasing the trapped gas. Plug samples were collected from section ends for headspace gas analysis and microbial cell enumeration. Short whole round core (WRC) samples were also taken at the core cutting area. A few sections were selected for fast-track handling to minimize the time from core recovery to whole round sampling.

All the sections, except for core catcher samples and short WRs, were examined with X-ray Computed Tomography (X-CT). Based on the X-CT images, WRC sampling plan was quickly determined. WRCs were cut out from sections and stored either in refrigerated or frozen condition. Cell Alive System (CAS) was used for freezing the samples.

Two to three WRCs per core were squeezed to obtain interstitial water (IW) sample. IW samples were also distributed to shipboard analyses and post-cruise studies.

Physical properties measurements were carried out after the sections reached equilibrium with room temperature. Thermal conductivity was measured with a needle-type probe. Penetration strength measurement, and sampling for moisture and density were conducted at the same surface, whenever possible, with thermal conductivity measurements.

General core analysis flow is shown in Fig 4.1, and detailed protocol is described in *6. Method and Results* chapter.

Core sample from Hole B was used only for interstitial water extraction after X-CT observation. The sections were packed in an aerobic condition for the use of post

cruise study. All sections from Hole C was examined only with X-CT. No shipboard sample was taken during the expedition.

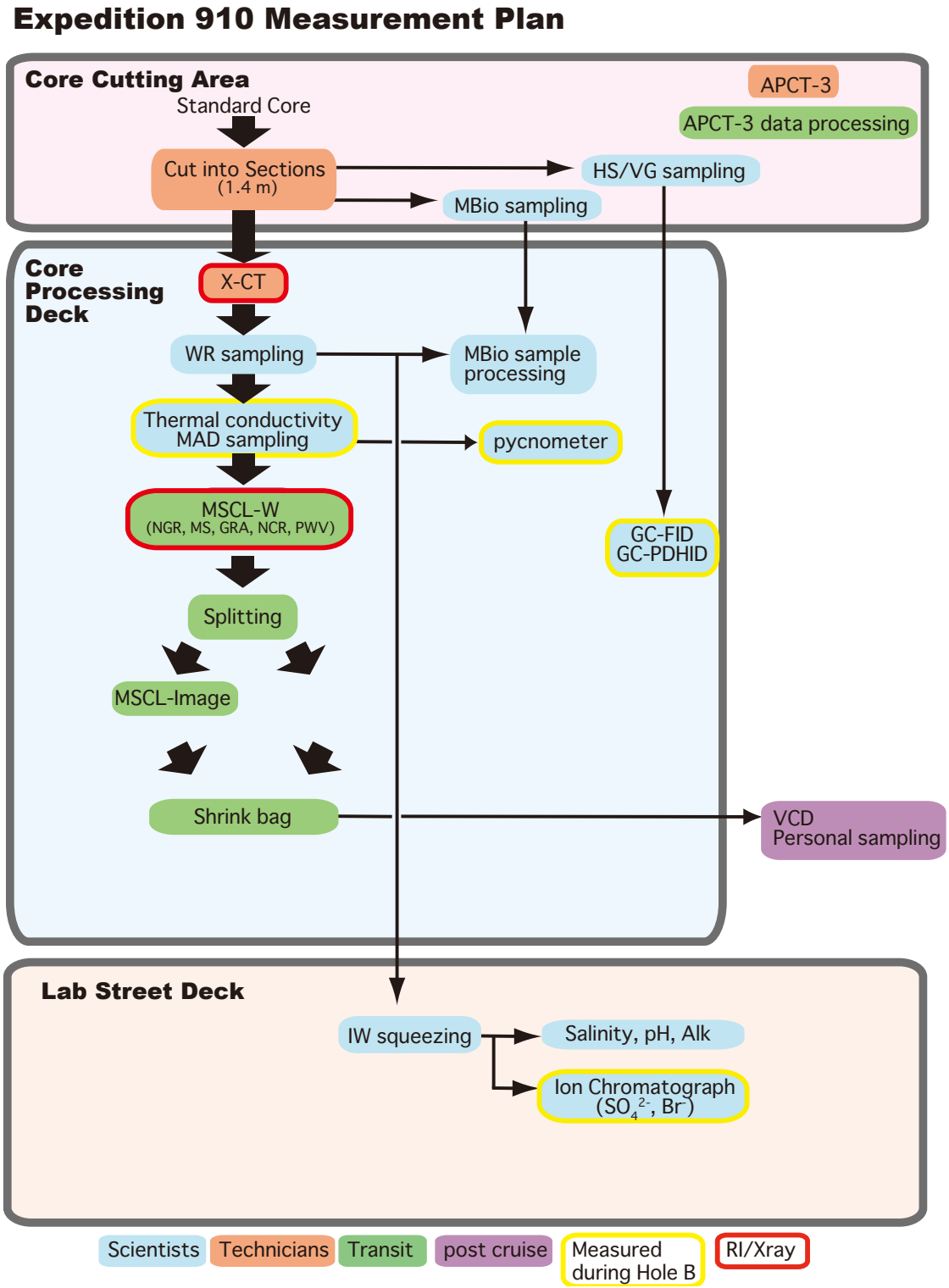

Fig. 4.1. Schematic illustration of shipboard core analysis flow.

Hole	Location	Water depth (mbsl)	Cores (N)	Cored (m)	Recovered (m)	Recovery (%)
A	41°48'08.33" N 142°21'27.88" E	1068.5	12	100.0	109.64	109.8
B	41°48'08.56" N 142°21'28.19" E	1069.0	1	7.0	7.25	103.8
C	41°48'08.56" N 142°21'28.19" E	1069.0	11	99.5	107.47	108.0

Table 4.1. Hole summary of Site C9033.

4.1 Extended work during the transit

After the science party disembarked, cores were logged and split by shipboard technicians during the transit period from September 23 to September 30. All whole round sections after WRC sampling were examined with multi-sensor core logger for whole round cores (MSCL-W). After MSCL-W, sections were split into working and archive halves. The split surface of archive halves was scanned for image archive. All sections were packed and stored at +4ºC until shipping to Kochi Core Center.

5 Operation

Chikyu departed Hachinohe port at 1400 h on September 19 after boarding of the science party. The ship arrived at the proposed site on 0030 h on September 20, and started running HPCS assembly at 0230 after confirmation of low current. Shooting of HPCS was started a few tens of meter above the expected sea floor due to lack of visual observation of the seafloor. The first core was recovered in the 7th shooting, which was registered as C9033A-1H. The water depth turned out to be 1097 mBRT. Continuous HPCS coring continued to C9033A-5H by the end of the day. Formation temperature survey with APCT-3 was conducted in coring of 3H and 5H.

On September 21, HPCS coring at C9033A continued to 100 mbsf. The last core C9033A-12H was recovered on deck at 1430 h. Another three surveys with APCT-

3 were conducted at 7H, 10H and 12H. After pulling out of the hole, a new hole C9033B was started at 10 m NE of Hole A. The mudline core of 7.25 m long was successfully recovered at 1600 h, and continuous coring was resumed at a new hole C9033C. Six HPCS cores were recovered at C9033C by the end of the day.
On September 22, coring at C9033C was completed when C9033C-11F reached 99.5 mbsf. The last core 11F using a short stroke HPCS with 4.5 m advance was recovered on deck at 0830 h. After spotting 1.30 sg Kill mud, we completed pulling out of the hole to surface at 1400 h. The ship started sailing, and arrived at the crew change point 4 miles south of Hakodate Port at 0230 h on September 23.

6 Method and results

In this chapter the methods and preliminary results of shipboard sampling, sample processing and analysis are described. The depth scale, mbsf, represents the core depth below seafloor after compressing the excess (>100%) recovery to fit into the coring advance length, unless otherwise noted.

6.1 X-ray Computed Tomography

The preliminary assessment of core quality was performed using X-ray CT images. Scanning for preliminary assessment was done immediately after dividing the core into sections. All sections were screened to avoid destruction of key geological features and drilling disturbance for WRCs. Our methods followed those used during previous expeditions (e.g., Integrated Ocean Drilling Program Expeditions 337 and 348). The X-ray CT instrument on the *Chikyu* is a Discovery CT 750HD (GE Medical Systems) capable of generating thirty-two 0.625 mm thick slice images every 1.0 second, the time for one revolution of the X-ray source around the sample. Data generated for each core consist of core-axis-normal planes of X-ray attenuation values with dimensions of 512 × 512 pixels. Data were stored on the server as Digital Imaging and Communication in Medicine (DICOM) formatted files. The DICOM files were restructured to create 3-D images for further investigation.

6.2 WRC sampling

In total, 260 WRCs were taken from Holes A and B cores during the expedition (Table 6.1, Appendix Table 2). This includes the entire sections of C9033A-6H-10, which showed features of typical mass transport deposits, and all of 7 sections from C9033B-1H after taking IW samples with Rhizon sampler. These sections were packed in an anaerobic condition and kept aside for post cruise study.

For cutting of WRCs for microbiology purpose (sample codes 910DNA, 910VIR, 910IPL, 910CULT, 910ACT1, and ACT2), pre-sterilized (by autoclaving) scrapers were used to avoid cross-contamination between samples.

The storage procedures for each type of WRC are summarized in Table 6.1. Samples for 910DNA, 910VIR, and 910IPL were frozen in CAS freezer. The parameters for CAS freezer were set as follows; CAS energy: 50%, freezing temperature -45ºC, freezing wind volume: 100%. The WRCs were placed in CAS freezer for at least 3 hours to reach terminal temperature throughout the WRC (Morono et al. 2015) and transferred to -80ºC freezer for storage.

Code	Number	Length	Treatment	Temperature
910ACT1	23	15 cm	Vacuum seal with N2 flushing	4ºC
910ACT2	24	15 cm	Vacuum seal with N2 flushing	4ºC
910BIO	8	Entire section	Vacuum seal with N2 flushing	4ºC
910CULT	21	15 cm	Vacuum seal with N2 flushing	4ºC
910DNA	38	15 cm	Freezing with CAS freezer	-80ºC
910GAS	33	6 cm	Used for shipboard analysis	N/A
910GEO	11	40 cm	Vacuum seal with N2 flushing	4ºC
910IPL	32	10 cm	Freezing with CAS freezer	-80ºC
910PP	24	20 cm	Vacuum seal with N2 flushing	4ºC
910VIR	14	10 cm	Freezing with CAS freezer	-80ºC
IW	32	15 cm	Used for shipboard analysis	N/A
Total	260			

Table 6.1. Number, standard length, packing and storage temperature of whole round samples.

6.3 Microbiology

Plug samples were collected in the Core Cutting Area immediately upon core arrival. By inserting a pre-sterilized, cut-off syringe, ~5 cc samples were taken from the bottom of each section. Full list of discrete samples is available in Appendix Table 3. The sample processing and storage conditions were as follows;

910CELL: From 5 cc syringe, 2 cc of the sediment was ejected into 8 ml of 4% PFA in 15 ml round bottom tubes. In the microbiology lab, the samples were mixed until the sediment was completely suspended. The suspension was stored at 4˚C at least 6 hours for fixation. After the fixation, the sediment was centrifuged at 5,000 x g for 10 min and the supernatant was removed. The fixed sediment was washed with 3 x PBS twice, re-suspended with 8 ml of 50% ethanol/ 3 x PBS, and stored at -20˚C.

910VIRC: 1 cc of the sediment remaining in the syringe after 910CELL was ejected into 3 ml of 10% formalin in 15 ml conical tubes. The sediment samples were rapidly frozen by immersing tubes in liquid nitrogen for approximately 5 min and stored at -80˚C.

6.4 Organic Geochemistry

6.4.1 Sampling

Short whole round samples (6 cm length) were taken at about 3 m intervals from each core at the Core Cutting Area. Three plug samples were immediately collected with a cut-off syringe from the freshly exposed end of the whole round sample. Two plug-samples were used for the shipboard gas analyses (see "Shipboard gas analyses").

The remaining one plug sample was kept for the shore-based gas analyses of carbon and hydrogen isotopic compositions of light hydrocarbon (910AIHS). Approximately 5 cm^3 sediment was extruded into a 24 mL glass vial with milli-Q water. About 0.5 mL of 10% benzalkonium chloride solution was

added into the vial to suppressing microbial activity, and sealed with an air headspace.

After the plug sampling, the residual whole round sample was collected for the shore-based analysis of clumped isotopologue of methane ($^{13}CH_3D$) (910GAS). For the sampling of 910GAS, Iso-Jar™ (Isotech Laboratories, USA) or 500 mL Duran bottle were used. About 400 cm^3 of sediment was put into an Iso-Jar™ or Duran bottle with milli-Q water. About 15 mL of 10% benzalkonium chloride solution was added into the bottle to suppress microbial activity, and sealed with an air headspace.

When a void space was observed in a core liner, a void gas sample was collected for clumped isotopologue measurement of methane (VAC) and ship-board analysis of C_1–C_4 hydrocarbon gas from the void space by sticking a needle of a gas-tight syringe into the core liner. The sample was transferred to a pre-vacuumed 24 ml glass vial.

6.4.2 Shipboard hydrocarbon gas analysis

A 5 cm^3 sediment was extruded into a 24 mL glass vial and immediately sealed with a Teflon septum and metal crimp cap. For C_1–C_4 hydrocarbon gas analysis, the vial was placed in a headspace sampler (Agilent Technologies 7697A network headspace sampler), where it was heated at 70°C for 30 min before an aliquot of the headspace gas was automatically injected into an Agilent 7890B GC equipped with a capillary column (HP-PLOT Q) and FID. Chromatographic response on the GC was calibrated against five different authentic standards with variable quantities of low molecular weight hydrocarbons.

Downhole profile of the methane (C_1) concentration in the headspace gas is shown in Fig. 6.1 (left). The C_1 concentration at 1.715 m below seafloor (mbsf) was 10,000 ppmv, and increased with depth to 30,000 ppm at 9.3 mbsf. Between 9.3 mbsf and 32 mbsf, the C_1 concentration showed high value ranging from 18,000 ppm to 35,000 ppm. Below 37 mbsf, the C_1 concentrations were relatively lower than those shallower than 37 mbsf (3,000–10,000 ppm), except for the sample at 52 mbsf (23,000 ppm).

Ethane (C_2) and propane (C_3) were detected in all samples at Hole C9033A. $C_1/(C_2+C_3)$ concentration ratio increased from 21,000 at 1.7 mbsf to 35,000 at 9.3 mbsf, and then decreased with depth to 9,000 ppm at 37 mbsf. Below 37 mbsf, the ratio was constant at 3,000–8,000 ppm except for the sample at 52 mbsf (20,000) (Fig. 6.1, right).

The void spaces were observed only below 20 mbsf. The $C_1/(C_2+C_3)$ ratios of the void gas were one order of magnitude higher than those of headspace gas (Fig. 6.1, right). The downhole trend of $C_1/(C_2+C_3)$ ratio of void gas was similar to that of headspace gas sample below 20 mbsf. The ratio was consistently high in 20 - 33 mbsf (ca. 110,000), decreasing to 57,000 at 60 mbsf and the ratio gradually decreased to 50,000 at the bottom of the hole.

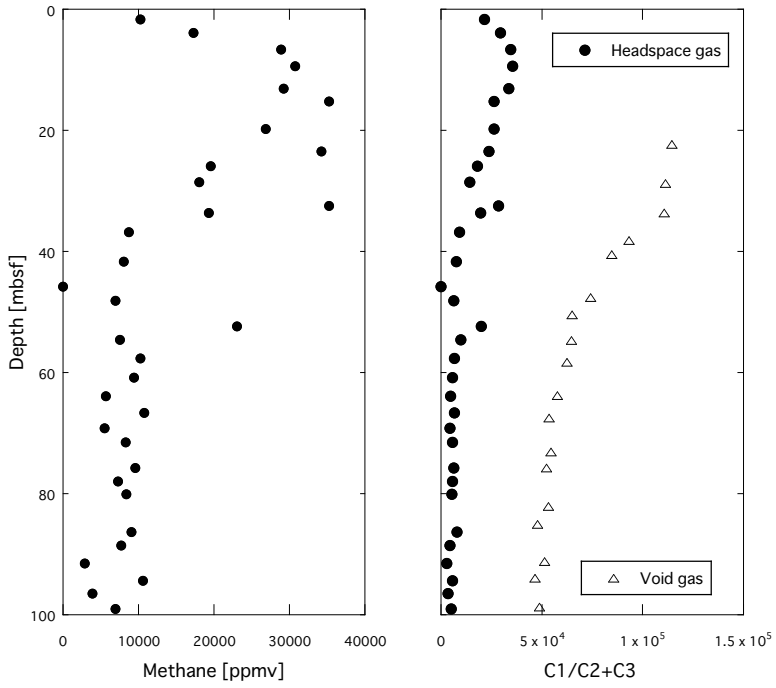

Fig. 6.1. Downhole profiles of the methane concentration (left) and ratio of $C_1/(C_2+C_3)$ (right).

6.4.3 Shipboard hydrogen gas analysis

A 5 cm^3 sediment was collected with a cut-off plastic syringe, and was extruded into a 24 mL glass vial and immediately sealed with a butyl-rubber septum and metal crimp cap. For H_2 analysis, the vial was placed in a headspace sampler (Agilent Technologies 7697A network headspace

sampler), where it was heated at 70°C for 30 min before an aliquot of the headspace gas was automatically injected into an Agilent 7890B GC equipped with a HP PLOT-Q and HP PLOT-Q capillary columns and a pulsed discharge helium ionization detector (PDHID) to determine the H_2 concentration.

Hydrogen gas was detected throughout Hole C9033A (Fig. 6.2). The concentration near the sediment surface (1.7 mbsf) was 1.4 ppm, which was close to the blank value (1.2 ppm) analyzed without sediment sample in the vial. Between 3.9 mbsf and 37 mbsf, the concentrations scattered in the range of 2.4 - 12.4 ppm. The highest concentration (12.4 ppm) was observed at 29 mbsf. Below 37 mbsf, the H_2 concentrations were constant at 1.6–3.2 ppm.

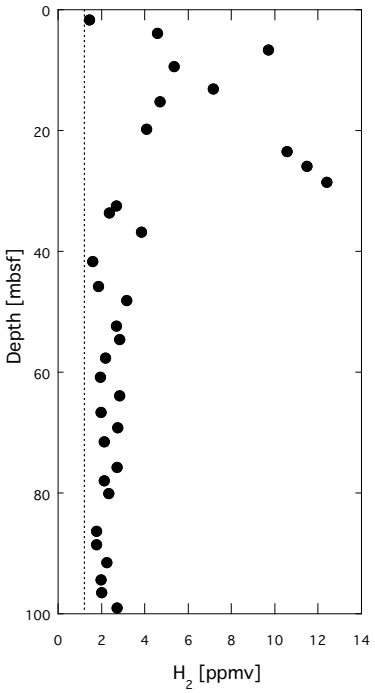

Fig. 6.2. Downhole profile of the hydrogen concentration. Dashed line shows the blank value.

6.5 Inorganic Geochemistry

6.5.1 Method

A 15 to 20 cm-long WRC sample was used for interstitial water extraction soon after X-ray CT observation. Three WRC samples were

provided per core, except for 9033A-1H and -12H. The collected WRCs were transferred into a N_2-filled glove bag and pushed out from the plastic core liner. The surface of the sediments was carefully removed to avoid any contamination and/or disturbance with core liner. The interstitial water was extracted from the trimmed sediment core using hydraulic squeezing system onboard (90 mm ø) with a pressure up to 17.5 MPa into the pre-washed plastic syringe following the standard IODP/*Chikyu* protocol. If the squeezing was not carried out immediately, the sample was preserved in a N_2-filled plastic bag in the refrigerator at ~4 °C up to 3hrs. The interstitial water was sub-sampled through the 0.2 μm disposable disk filter for onboard analyses (IWIC; salinity, pH-alkalinity) and onshore analyses of dissolved organic matter (910VFA, 910OM, 910FTMS), DIC (910DIC), δ^{18}O-D/H (910H2O), and major/minor elementals using IC, ICP-MS, and ICP-AES (910HTIW). In addition, the interstitial water was collected more frequently from Hole C9033B Core 1 using Rhizon fluid sampler of 10 mL, three samples from Section 1 and two samples from Sections 2 to 6, in the cold room at ~4 °C for 10 hours. These samples were sub-sampled through the 0.2 μm disposable disk filter for the onboard (IWIC) and onshore (910VFA, 910DIC, 910H2O, 910HTIW) analyses.

The refractive index of interstitial water, corresponding to the salinity, was measured using a digital refractometer (RX-5000α, ATAGO) with the experimental error better than 0.002% RSD. The standard seawater provided by the International Association for the Physical Sciences of the Oceans (IAPSO) and RO-EDI purified water was used for the calibration of the refractometer. The pmH and total alkalinity were determined by acid (0.1 mol/L HCl) titration using an automatic titrator (794 Basic Titrino, Metrohm) with the precision better than 3%.

6.5.2 Sub-sampling

Table 1 shows the list of requested sub-samples of interstitial water. Detailed sample distribution (volume) is included in Appendix Table 4.

Sample ID	Analysis
IWIC	pH and alkalinity (onboard analyses)
910VFA	Volatile fatty acid
910DIC	Dissolved inorganic carbon ($\delta^{13}C$)
910H2O	^{16}O, ^{17}O, ^{18}O, D/H
910OM	Dissolved organic matter
910FTMS	Dissolved organic matter using FTICR
910HTIW	SO_4, Cl, ICP-MS, ICP-AES, Iodine

Table 6.2. List of interstitial water sub-samples.

6.5.3 Results

Analytical results are shown in Fig. 6.3. Although the salinity of the shallowest sample at Hole C9033A (0.6 mbsf) is anomalously high compared with other samples, it decreases to the lowest value of 34.12 at 3.7 mbsf at Hole C0033B. The salinity then gradually increases with depth, reaching 37.8 at 98.1 m CSF. The pmH value contrary increases from 7.77 in the first ~3.3 m and decreases rapidly to 7.73 at 14.9 mbsf, and gently decrease to 7.63 at 89.0 mbsf. Relatively higher values are observed at >91.8 mbsf. The alkalinity of interstitial water rapidly increases with depth from near-seawater level to >10 times higher at 4.2 mbsf. The gradient of alkalinity then decreases and the alkalinity values gradually increase with depth below 4.2 mbsf.

The shallow interstitial waters at <4 mbsf may reflect strong influence of seawater and rapid changes of geochemical environments. Linear downhole trends in the deeper parts indicate mixing with fluid derived from deep sediments probably characterized by high salinity and alkalinity. These overall trends show kinky/discontinuous points at ~12, ~28, ~50, ~85 mbsf. More dataset, such as changes in lithology, physical property, etc. is required for further discussion.

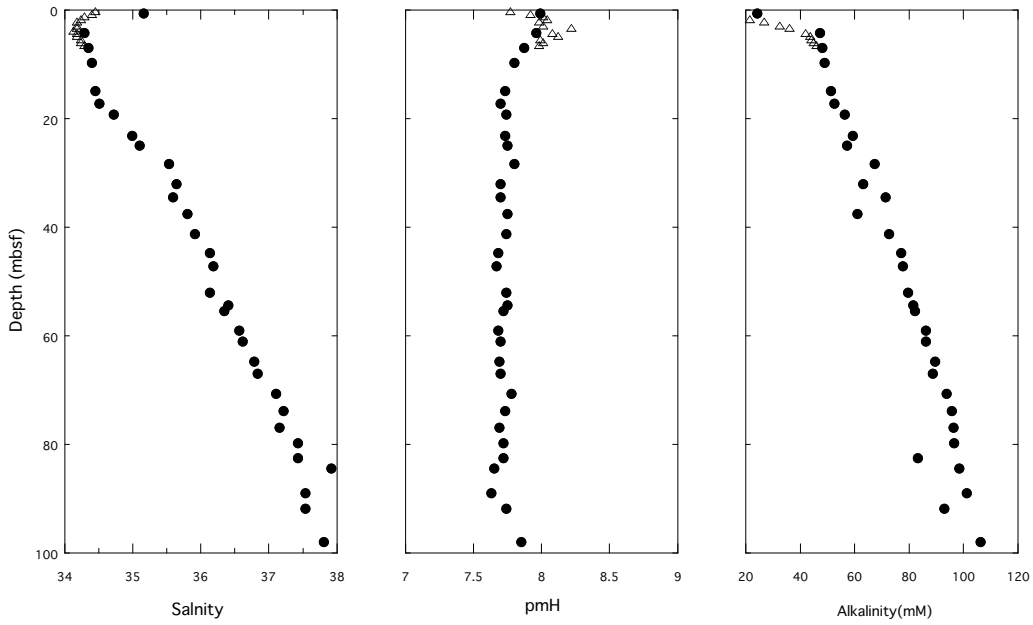

Fig. 6.3. Analytical results of interstitial waters; salinity, pmH and alkalinity from left. Circles are samples from squeezing of whole round samples in Hole A, and triangles are samples from Rhizon sampling in Hole B.

6.6 Physical property measurement

6.6.1 Method

Thermal conductivity, penetration strength, and moisture and density (MAD) measurements were conducted for two to three intervals per cores at the same core depths in Hole C9033A. Thermal conductivity measurements were carried out for whole-round core sample. Penetration strength test and MAD discrete sampling were routinely carried out at the same depth intervals where thermal conductivity was measured. Several personal discrete samples (Sample code: 910WTW and 910WTX) were taken from the same depths after physical property measurements. In-situ temperature measurement was performed at the same hole using APCT-3 system to estimate the in-situ temperature, geothermal gradient, and heat flow.

6.6.2 Thermal conductivity

Thermal conductivity measurements were conducted using two TeKa TK04 units (Blum, 1997) on whole-round core samples (Von Herzen and Maxwell, 1959; Vacquier, 1985). The measurement frequency was two per core for full length cores. A needle probe of 2 mm in diameter was inserted to the bottom of whole-round section in the vertical direction to the depth. A small hole was drilled in the center of the end cap of the core liner in order to insert the needle probe.

All thermal conductivity measurements were made after the cores had equilibrated to room temperature (> three hours of waiting time at the core processing deck). A section was placed in a thermal insulation box to stabilize air temperature during the measurement. At the beginning of each measurement, temperature in the sediment was monitored to ensure that thermal drift becomes small enough (typically within a couple of minutes). After it was established that the temperature was near equilibrium, a calibrated linear heat (1.5~2.0 W/m) was applied, and the rise in temperature was recorded for 80 seconds. Values of thermal conductivity were calculated based on the observed rise in temperature for a given quantity of heat. Each thermal conductivity measurement was performed repeatedly three times, and the arithmetic mean was calculated as a representative value.

Empirical tests to check system condition or performances were conducted with a certified MACOR ceramic standard sample (k = 1.623 W/[m·K] ± 2%). 3.5 W/m of heat power was applied for the standard sample measurement. The empirical tests were performed at least once a day.

6.6.3 Penetrometer strength

The penetrometer provides a measure of unconfined compressive strength (UCS) of sediment samples. The UCS is calculated by dividing the penetration resistance generated by pushing a cylindrical probe into the core surface to a 5 mm penetration depth by the area of the penetration probe (Blum, 1997). All measurements in this expedition were conducted using a probe with a nominal diameter of 6.35 mm (0.25 inches). The UCS values were calculated from the average of three

penetration trials conducted at adjacent points on the core. The unit was converted from kg/cm^2 to kPa by the following equation as,

UCS (kPa) = UCS (kg/cm^2) * 9.81 * 10.

In this report, UCS in kPa is used, but the value of UCS (kPa) divided by two were uploaded to the J-CORES database as penetration strength (kPa).

Typical spatial separation between trials was on the order of 1 cm. As the center of a section after thermal conductivity measurement was mechanically disturbed, the strength was measured a few cm away from the center.

6.6.4 Moisture and density measurements

Index properties (bulk density, grain density, water content, porosity, and void ratio) of core samples were calculated from measurements of wet masses, dry masses, and dry volumes on discrete samples. Basically, ~10 cm^3 of sediment was sampled by a plastic syringe (20 mm in diameter) from one to two intervals of each core. Each discrete sample for MAD were collected from the surface of the section end by avoiding the core disturbance caused by the thermal conductivity measurement and the strength tests.

6.6.5 Weight and volume measurements

Wet and dry masses were measured using a paired electronic balance system designed to compensate for the ship's heave. The sample mass was counterbalanced with a precisely known mass (40 g) that was suitable for 30–50 g sample mass measurements. The sample mass was determined to a precision of ±0.01 g. The balance system was calibrated every day. Immediately after the samples were collected, wet sediment mass was measured. Dry sediment mass and volume were measured after drying the samples in a convection oven for 24 h at 105° ± 5°C. Dried samples were then cooled in a dry desiccator for 1 h before the measurement of dry mass. Dry volume was measured by using a helium-displacement five-cell pycnometer with a nominal precision of ±0.04 cm3. Cell volumes were calibrated every day. A reference volume (calibrated sphere) was run with each set of four samples, and the sphere

was rotated in the cells in order to check any systematic error. For calculation of bulk wet and dry density, grain density, porosity, and void ratio, the traditional ODP method is used (Method C in Blum, 1997). Water content, porosity, and void ratio are defined by the mass or volume of extracted water before and after removal of interstitial water through the drying process. Standard seawater density (1.024 g/cm^3) was assumed for the density of interstitial water calculation.

6.6.6 *In situ* temperature and heat flow

In situ temperature measurement was carried out using the APCT-3 (Heesemann et al., 2006), which was installed on the cutting shoe of HPCS. The APCT-3 consists of three components: electronics, coring hardware, and software. During this expedition, *in situ* temperature measurement was taken at five depths of Hole A. To equilibrate with surrounding temperature, the cutting shoe was held at the mudline for 10 min before shooting, and within the formation for another 10 min after shooting. Shooting the barrel into the formation normally causes a rapid increase in temperature by frictional heating. After that, temperature decreases with time along a decay curve. Temperature was measured as a time series with a sampling rate of 1 second. Temperature data were logged onto a microprocessor within the downhole tool. When the tool was retrieved, data were downloaded into a computer.

In situ temperatures are extrapolated from the APCT-3 measurements for 10 min, using the *tpfit3.exe* program developed by Heesemann et al. (2006), which includes the 3-D geometry effect and the dependence of the thermal diffusion process on thermal properties (e.g., thermal conductivity).

6.6.7 Result

The downhole profiles of physical properties are shown in Fig. 6.4. Thermal conductivity of sediment near the seafloor was approximately 0.8 W/[m*K] at 1.4 mbsf and slightly increases with depth. Most thermal conductivity of mud ranged from 0.8 to 1.0 W/[m*K], and the minimum and the maximum values showed 0.738 W/[m*K] (80 mbsf) and 1.023 W/[m*K] (65 mbsf), respectively.

Unconfined compressive strength of sediment near the seafloor (1.4 mbsf) was approximately 33 kPa, and gradually increased with depth to ~193 kPa at 64 mbsf. Below 64 mbsf, the strength was nearly constant ranging from 150 to 180 kPa. Anomalously high strength (~300 kPa) were observed at ~50 mbsf and 90 mbsf.

Grain density gradually decreased from 2.7 to 2.6 g/cm3 at depth from 10 to 40 mbsf. Below 40 to 90 mbsf, grain density was nearly constant, ranging from 2.55 to 2.6 g/cm^3. Relatively high grain density (~2.7 g/cm^3) was observed at ~50 mbsf and 100 mbsf. Bulk density ranges from 1.5 g/cm^3 to 1.8 g/cm^3, except the shallowest sample showing 1.4 g/cm^3 at 1.4 mbsf. Porosity of sediment near sea surface (1.4 mbsf) was approximately 0.75, and gradually decreased with depth to 0.64. Relatively low porosity (0.53 ~ 0.55) were observed at ~50 mbsf where strength anomaly was detected. Grain density of sediment near sea surface (1.4 mbsf) was approximately 0.263.

APCT-3 measurements at four depths downhole to 100 mbsf provided a linear geothermal gradient of 28.9 mK/m at depth from 0 to 100 mbsf (Fig. 6.5). The quality of APCT-3 data at 56.5 mbsf was not good, therefore we disregarded this data to evaluate the geotherm. Heat flow value is estimated as 26 mW/m^2 by using the average thermal conductivity at this hole (0.895 W/[m*K])

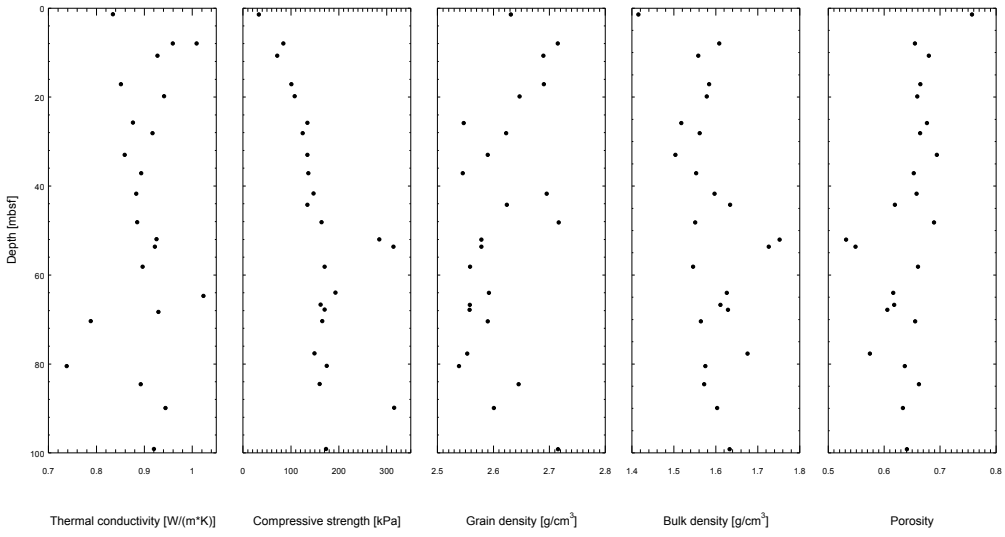

Fig. 6.4. Downhole plofiles of thermal conductivity, penetration strength, and MAD data (grain density, bulk density and porosity) at Hole C9033A.

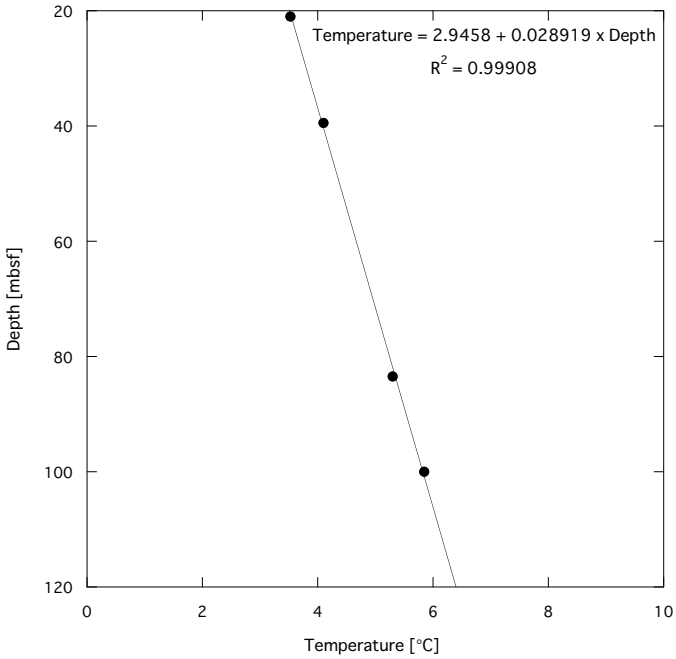

Fig. 6.5. *In situ* formation temperature at Hole C9033A estimated from APCT-3 operations.

7 Extended analysis during the transit

All sections were examined with MSCL-W. P-wave velocity, magnetic susceptibility, no-contact resistivity, and gamma-ray attenuation were measured at 4 cm interval, and natural gamma radiation was measured at 16 cm interval. The results from Hole C9033A and C9033C are shown in Figs. 7.1 and 7.2, respectively.

Following MSCL-W measurements, the sections were split and the image of split surface of archive half sections was scanned with MSCL-I. Digital images of archive-half cores were acquired by a line-scan camera equipped with three charge-coupled devices. A calibration is conducted before scanning each core to compensate for pixel-to-pixel response variation, uneven lighting, and lens effects. Resolution of the images obtained on the *Chikyu* is 100 pixels per cm.

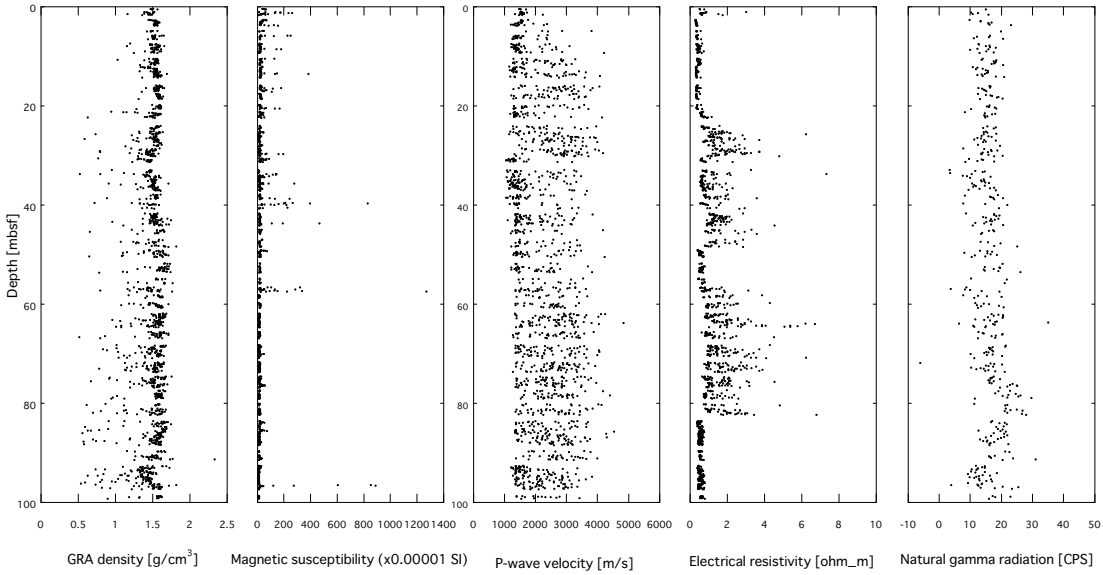

Fig. 7.1. Downhole profiles gamma ray attenuation density, magnetic susceptibility, P-wave velocity, electric resistivity, and natural gamma ray radiation of whole round cores from Hole C9033A.

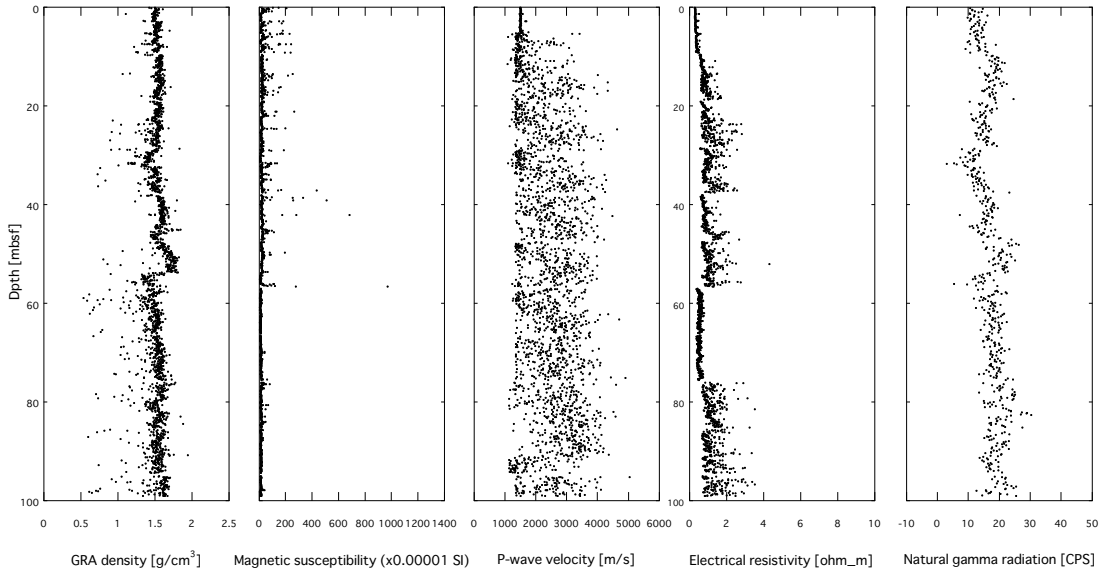

Fig. 7.2. Downhole profiles gamma ray attenuation density, magnetic susceptibility, P-wave velocity, electric resistivity, and natural gamma ray radiation of whole round cores from Hole C9033C.

8 Post-cruise core description

All core sections were transferred to the core repository of Kochi Core Center, after *Chikyu* arrived at Sasebo. Core description using the split sections were conducted in October 25-27, and sampling from working halves was carried out in November 14-17, 2017.

8.1 Visual core description

The thickness of cored sediments was 100.0 m at Hole C9033A and 99.5 m at Hole C9033C, respectively (Table 4.1, Fig. 8.1). Main lithology of the cores was dark olive to olive gray silty clay. Silty clay consisted of clay minerals with quartz, feldspar, volcanic glass, and microfossils of calcareous nannofossils, diatoms, and sponge spicules. These sediments were generally unconsolidated. Bioturbation was commonly observed.

The uppermost part of core sediments mainly consisted of silty clay, which alternated with medium thick volcaniclastic sediments. Volcaniclastic sediments mainly consisted of pumice, scoria, and volcanic glass. The thickness of the volcaniclastic sediment layers was up to 18 cm, showing light to dark gray color. Inverse grading or symmetric grading reverse to normal were common in volcaniclastic sediment. In X-ray CT image, a massive volcaniclastic sediment cutting laminae of silty clay was observed at C9033A-1H-2, 9 cm.

The underlying sediments were characterized by alternations of silty clay and very fine to coarse sand. Pyrite grains were present, with a few aggregates up to 2 mm in diameter. Several echinoid-concentrated layers were observed. Sand beds were 1–14 cm thick, and commonly show sharp base and normal grading. Pumice, scoria, and volcanic glass were rich in some sand beds. According to the visual core description and X-ray CT images, four layers of chaotic deposits including mud clasts of irregular shapes were identified and correlated between Holes C9033A and C9033C (orange color in Fig. 8.1). An interval from 90.3 mbsf to 95.0 mbsf in C9033C was heavily disturbed by flow-in.

Deformed intervals

Four intervals containing deformed features such as chaotic deposits and/or inclined bedding were recognized and correlated between Holes C9033A and C9033C (Fig. 8.1). A folded mud clast (C9033A-8H-10, 63 cm) was observed in a

chaotic deposit. An overturned sand bed (C9033A-9H-4, 19cm), which apparently showed sharp top and inversed grading, was observed.

Deformed interval 1 occurred at the top of this site and was more than 20 m-thick. This interval mainly consisted of silty clay with inclined bedding and several volcaniclastic sediments. Volcaniclastic sediments in this interval showed inclined base and horizontal top. The lower boundary was transitional at 22.3 mbsf in C9033A and 20.7 mbsf in C9033C. Deformed interval 2 was about 10 m-thick and consisted of two chaotic deposits and silty clay with inclined bedding. The upper boundary was well defined by the top of a chaotic deposit at 46.0 mbsf in C9033A and 45.0 mbsf in C9033C. The lower boundary was transitional at 55.0–56.5 mbsf in C9033A and 54.5–56.1 mbsf in C9033C. Deformed interval 3 was about 9 m-thick in C9033A and 7 m-thick in C9033C respectively, and consisted of a chaotic deposit and silty clay with inclined bedding. The upper boundary was defined by the top of the chaotic deposit at 60.3 mbsf in C9033A and 59.5 mbsf in C9033C. The lower boundary was transitional at 68.0–69.0 mbsf in C9033A and 66.0–69.0 mbsf in C9033C. Deformed interval 4 occurred at the bottom of this site and was more than 8 m-thick. This interval mainly consisted of chaotic deposits and silty clay with inclined bedding. The upper boundary was defined by the top of a chaotic deposit at 91.0 mbsf in C9033A and by the top of an inclined silty clay interval at 95.0 mbsf in Hole 9033C. The lower boundary was not identified and probably deeper than 100 mbsf.

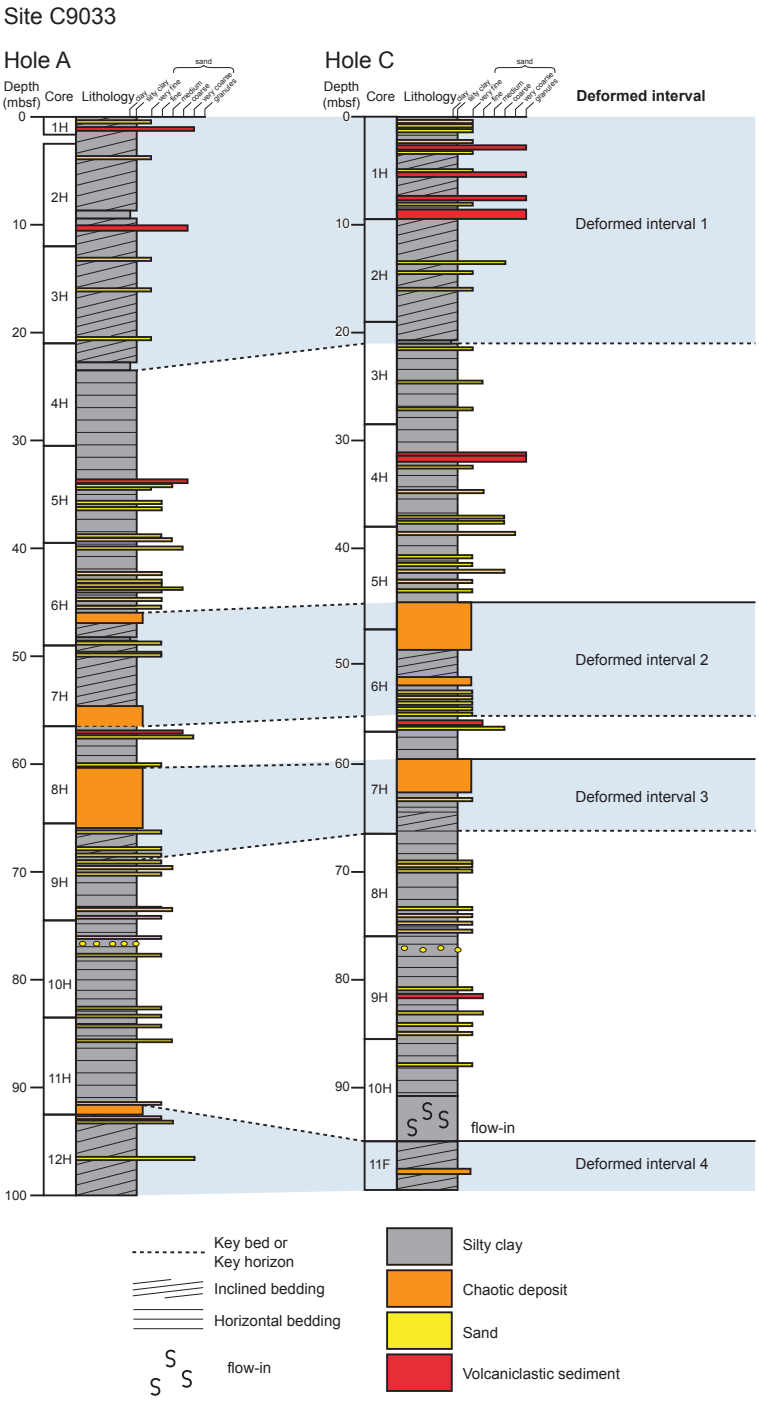

Fig. 8.1 Lithostratigraphy sketch of Holes C9033A and C9033C. Four intervals of deformed sediments were correlated between the holes.

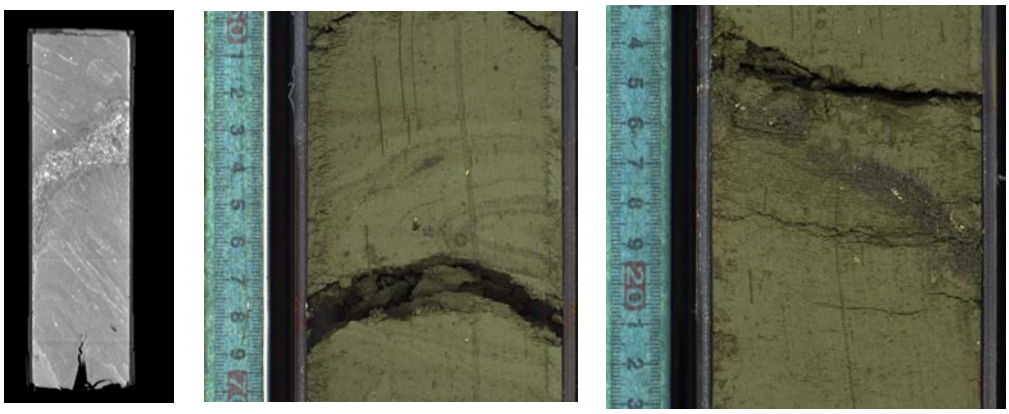

Fig. 8.2 Examples of core samples. Left: X-ray CT image of volcanic sediments (C9033A-1H-2, 0-25 cm), middle: folded mud clast (C9033A-8H-10, 60-70 cm), and right: overturned sand bed (C9033A-9H-4, 13-23 cm).

8.2 Personal sampling

Personal samples based on sample requests were collected, and will be used for each post-cruise research program, such as nannofossil age and organic matter analysis. Data from post-cruise research will be published when the moratorium period ends in two years.

9 Reference

Biddle, J. F., Lipp, J. S., Lever, M. A., Lloyd, K. G., Sørensen, K. B., Anderson, R., Fredricks, H. F., Elvert, M., Kelly, T. J., Schrag, D. P., Sogin, M. L., Brenchley, J. E., Teske, A., House, C. H., and Hinrichs, K.-U., 2006. Heterotrophic Archaea dominate sedimentary subsurface ecosystems off Peru. *Proc. Natl. Acad. Sci. U.S.A.,* **103**, 3846–3851.

Blum, P., 1997. Physical properties handbook: a guide to the shipboard measurement of physical properties of deep-sea cores. *Ocean Drilling Program Technical Note,* **26**. doi: 10.2973/odp.tn.26.1997

Boetisu, A., Ravenschlag, K., Schubert, C., Rickert, D., Widdel, F., Gieseke, A., Aman, R., Jørgensen, B. B., Witte, U., and Pfannkuche, O., 2000. A marine microbial consortium apparently mediating anaerobic oxidation of methane. *Nature*, **407**, 623-626.

Heesemann, M., Villinger, H., Fisher, A.T., Tréhu, A.M., and White, S., 2006. Data report: testing and deployment of the new APCT-3 tool to determine in situ temperatures while piston coring. *In* Riedel, M., Collett, T.S., Malone, M.J., and the Expedition 311 Scientists. *Proceedings of the Integrated Ocean Drilling Program,* 311: Washington, DC (Integrated Ocean Drilling Program Management International, Inc.). doi:10.2204/iodp.proc.311.108.2006

Hinrichs, K.-U., and Inagaki, F., 2012. Downsizing the deep biosphere. *Science*, **338**, 204-205.

Hinrichs, K.-U., Hayes, J. M., Sylva, S. P., Brewer, P. G., and DeLong, E. F., 1999. Methane-consuming archaeabacteria in marine sediments. *Nature*, **398**, 802-805.

Hinrichs, K.-U., Hmelo, L R., and Sylva, S. P., 2003. Molecular fossil record of elevated methane levels in late Pleistocene coastal waters. *Science*, **299**, 1214-1217.Inagaki, F., Suzuki, M., Takai, K., Oida, H., Sakamoto, T., Aoki, K., Nealson, K. H. and Horikoshi, K., 2003. Microbial communities associated with geological horizons in coastal subseafloor sediments from the Sea of Okhotsk. *Appl. Environ. Microbiol.,* **69,** 7224-7235.

Inagaki, F., Nunoura, T., Nakagawa, S., Teske, A., Lever, M., Lauer, A., Suzuki, M., Takai, K., Delwiche, M., Colwell, F. S., Nealson, K. H., Horikoshi, K., D'Hondt, S., and Jørgensen, B. B., 2006. Biogeographical distribution and diversity of microbes in methane hydrate-bearing deep marine sediments on the Pacific Ocean Margin. *Proc. Natl. Acad. Sci. U.S.A.*, **103,** 2815-2820.

Inagaki, F., Hinrichs, K.-U., Kubo, Y., Bowles, M. W., Heuer, V. B., Hong, W.-L., Hoshino, T., Ijiri, A., Imachi, H., Ito, M., Kaneko, M., Lever, M. A., Lin, Y.-S., Methé, B. A., Morita, S., Morono, Y., Tanikawa, W., Bihan, M., Bowden, S. A., Elvert, M., Glombitza, C., Gross, D., Harrington, G. J., Hori, T., Li, K., Limmer, D., Liu, C.-H., Murayama, M., Ohkouchi, N., Ono, S., Park, Y.-S., Phillips, S. C., Prieto-Mollar, X., Purkey, M., Riedinger, N., Sanada, Y., Sauvage, J., Snyder, G., Susilawati, R., Takano, Y., Tasumi, E., Terada, T., Tomaru, H., Trembath-Reichert, E., Wang, D. T., and Yamada, Y., 2015. Exploring deep microbial life down to ~2.5 km below the ocean floor. *Science*, **349**, 420-424.

Itoh, Y. and Tsuru, T., 2005. Evolution history of the Hidaka-oki (offshore Hidaka) basin in the southern central Hokkaido, as revealed by seismic interpretation, and

related tectonic events in an adjacent collision zone. *Phys. Earth Planet. Int.*, **153**, 220-226.

Japan Oil, Gas and Metals National Corporation (JOGMEC), 2005. *Data interpretation report of the geophysical survey "Hidaka Shujo Kaibon 3D"*. Japan Oil, Gas and Metals National Corporation, Tokyo.

Japan Oil, Gas and Metals National Corporation (JOGMEC), 2006. *Data interpretation report of the geophysical survey "Hidaka Shujo Kaibon West 3D"*. Japan Oil, Gas and Metals National Corporation, Tokyo.

Kallmeyer, J., Pockalny, R., Adhikari, R. R., Smith, D., and D'Hondt, S., 2012. Global distribution of microbial abundance and biomass in subseafloor sediment. *Proc. Natl. Acad. Sci. U.S.A.*, **109**, 16213-16216.

Kimura, G. and Kusunoki, K., 1997. The Hidaka orogeny and tectonics of arc-arc junction. *Mem. Geol. Soc. Japan,* **47**, 295-305.

Morono, Y., Terada, T. Yamamoto, Y., Xiao, N., Hirose, T., Sugeno, M., Ohwada, N. and Inagaki, F., 2015. Intact preservation of environmental samples by freezing under an alternating magnetic field. *Environmental microbiology reports* **7**(2): 243-251.

Orphan, V. J., House, C. H., Hinrichs, K.-U., McKeegan, K. D., and DeLong, E. F., 2001. Methane-consuming archaea revealed by directly coupled isotopic and phylogenetic analysis. *Science*, **293**, 484-487.

Seno, T., Sakurai, T., and Stein, S., 1996. Can the Okhotsk plate be discriminated from the North American plate? *J. Geophys. Res., [Solid Earth],* **101**(B5):11305–11315. doi:10.1029/ 96JB00532

Takano, O., 2017. Intermittent formation, sedimentation and deformation history of Cenozoic forearc basins along the northwestern Pacific margins as an indicator of tectonic scenarios. *In*: Itoh, Y., Takano, O. and Takashima, R. (eds.), Dynamics of Arc Migration and Amalgamation – Architectural Examples from the NW Pacific Margin*, InTech*, pp. 1-24. doi:10.5772/intechopen.68290

Uchida, M., Ohkushi, K., Kimoto, K., Inagaki, F., Ishimura, T., Tsunogai, U., TuZino, T., and Shibata, Y., 2008. Radiocarbon-based carbon source quantification of anomalous isotopic foraminifera in last glacial sediments in the western North Pacific. *Geochem. Geophys. Geosyst.*, **9,** Q04N14, doi:10.1029/2006GC001558.

Vacquier, V., 1985. The measurement of thermal conductivity of solids with a transient linear heat source on the plane surface of a poorly conducting body. *Earth and Planetary Science Letters,* **74**(2–3):275–279. doi:10.1016/0012-821X(85)90027-5

Von Herzen, R., and Maxwell, A.E., 1959. The measurement of thermal conductivity of deep-sea sediments by a needle-probe method. *Journal of Geophysical Research,* **64**(10):1557–1563. doi:10.1029/JZ064i010p01557

Appendix Table 1. Coring record

Appendix Table 2. List of whole round samples

Appendix Table 3. Discrete sample list

Appendix Table 4: List of interstitial water sub-samples**.**

Appendix Figure: Visual core description sheets of core sections.

Core	Type	Core on Deck Time (JST)	Depth Below Rotary Table (mBRT)		Depth Below Seafloor (mbsf)		Advance (m)	Initial Core Length (m)	Initial Recovery (%)	Curated Liner Length (m)
			Top	Bottom	Top	Bottom				
Hole C9033A										
1	H	2017/09/20 15:33	1097.00	1099.50	0.00	2.50	2.50	1.92	76.8	1.95
2	H	2017/09/20 16:27	1099.50	1109.00	2.50	12.00	9.50	9.92	104.4	9.99
3	H	2017/09/20 20:38	1109.00	1118.00	12.00	21.00	9.00	9.84	109.3	9.89
4	H	2017/09/20 21:34	1118.00	1127.50	21.00	30.50	9.50	10.21	107.5	10.44
5	H	2017/09/20 23:26	1127.50	1136.50	30.50	39.50	9.00	10.10	112.2	10.45
6	H	2017/09/21 02:40	1136.50	1146.00	39.50	49.00	9.50	10.18	107.2	10.36
7	H	2017/09/21 04:50	1146.00	1153.50	49.00	56.50	7.50	7.74	103.2	7.96
8	H	2017/09/21 06:41	1153.50	1162.50	56.50	65.50	9.00	9.88	109.8	10.50
9	H	2017/09/21 08:12	1162.50	1171.50	65.50	74.50	9.00	10.28	114.2	10.49
10	H	2017/09/21 10:32	1171.50	1180.50	74.50	83.50	9.00	10.57	117.4	10.68
11	H	2017/09/21 12:08	1180.50	1189.50	83.50	92.50	9.00	9.77	108.6	10.13
12	H	2017/09/21 13:45	1189.50	1197.00	92.50	100.00	7.50	9.23	123.1	9.75
Hole C9033B										
1	H	2017/09/21 15:35	1097.50	1104.50	0.0	7.00	7.00	7.25	103.6	7.25
Hole C9033C										
1	H	2017/09/21 16:17	1097.50	1107.00	0.0	9.50	9.50	9.93	104.5	9.91
2	H	2017/09/21 17:12	1107.00	1116.50	9.50	19.00	9.50	10.04	105.7	10.04
3	H	2017/09/21 19:31	1116.50	1126.00	19.00	28.50	9.50	10.03	105.6	10.06
4	H	2017/09/21 20:38	1126.00	1135.50	28.50	38.00	9.50	10.75	113.2	10.74
5	H	2017/09/21 21:56	1135.50	1145.00	38.00	47.50	9.50	10.07	106.0	10.07
6	H	2017/09/21 23:09	1145.00	1154.50	47.50	57.00	9.50	10.17	107.1	10.25
7	H	2017/09/22 01:32	1154.50	1164.00	57.00	66.50	9.50	10.68	112.4	11.15
8	H	2017/09/22 03:10	1164.00	1173.50	66.50	76.00	9.50	10.37	109.2	10.70
9	H	2017/09/22 04:23	1173.50	1183.00	76.00	85.50	9.50	10.20	107.4	10.72
10	H	2017/09/22 06:43	1183.00	1192.50	85.50	95.00	9.50	10.13	106.6	10.17
11	F	2017/09/22 08:23	1192.50	1197.00	95.00	99.50	4.50	5.10	113.3	5.32

Sample source	Top Core depth (below sea floor) [m CSF-A]	Top Core depth (below sea floor) [m CSF-B]	Bottom Core depth (below sea floor) [m CSF-A]	Bottom Core depth (below sea floor) [m CSF-B]	Sample code
C9033A-1H-1 WR, 70.0--85.0 cm	0.7	0.7	0.85	0.85	910ACT1
C9033A-2H-3 WR, 40.0--55.0 cm	4.37	4.268	4.52	4.41	910ACT1
C9033A-2H-6 WR, 40.0--55.0 cm	7.245	6.985	7.395	7.127	910ACT1
C9033A-2H-9 WR, 40.0--55.0 cm	10.15	9.731	10.3	9.873	910ACT1
C9033A-3H-4 WR, 40.0--55.0 cm	14.89	14.646	15.04	14.783	910ACT1
C9033A-3H-9 WR, 50.0--65.0 cm	19.71	19.059	19.86	19.196	910ACT1
C9033A-4H-2 WR, 75.0--90.0 cm	23.15	22.92	23.3	23.054	910ACT1
C9033A-4H-9 WR, 40.0--55.0 cm	28.485	27.683	28.635	27.817	910ACT1
C9033A-5H-2 WR, 60.0--75.0 cm	32.075	31.84	32.225	31.967	910ACT1
C9033A-5H-10 WR, 60.0--75.0 cm	38.575	37.369	38.725	37.497	910ACT1
C9033A-6H-3 WR, 65.0--80.0 cm	41.25	41.096	41.4	41.233	910ACT1
C9033A-6H-7 WR, 65.0--80.0 cm	44.925	44.448	45.075	44.585	910ACT1
C9033A-7H-4 WR, 23.0--38.0 cm	51.52	51.367	51.67	51.508	910ACT1
C9033A-7H-7 WR, 60.0--75.0 cm	54.32	53.997	54.47	54.138	910ACT1
C9033A-8H-5 WR, 50.0--65.0 cm	59.555	59.111	59.705	59.239	910ACT1
C9033A-8H-8 WR, 52.0--67.0 cm	62.055	61.248	62.205	61.376	910ACT1
C9033A-9H-4 WR, 57.0--70.0 cm	67.41	67.133	67.54	67.244	910ACT1
C9033A-9H-9 WR, 85.0--100.0 cm	72.015	71.071	72.165	71.199	910ACT1
C9033A-10H-5 WR, 20.0--35.0 cm	77.465	76.993	77.615	77.119	910ACT1
C9033A-10H-8 WR, 60.0--75.0 cm	80.54	79.578	80.69	79.704	910ACT1
C9033A-11H-9 WR, 80.0--95.0 cm	89.97	89.231	90.12	89.364	910ACT1
C9033A-11H-13 WR, 45.0--60.0 cm	93.015	91.929	93.165	92.062	910ACT1
C9033A-12H-8 WR, 65.0--80.0 cm	99.505	97.864	99.655	97.979	910ACT1
C9033A-1H-1 WR, 85.0--100.0 cm	0.85	0.85	1	1	910ACT2
C9033A-2H-3 WR, 55.0--70.0 cm	4.52	4.41	4.67	4.551	910ACT2
C9033A-2H-6 WR, 55.0--70.0 cm	7.395	7.127	7.545	7.269	910ACT2
C9033A-2H-9 WR, 55.0--70.0 cm	10.3	9.873	10.45	10.015	910ACT2
C9033A-3H-4 WR, 25.0--40.0 cm	14.74	14.509	14.89	14.646	910ACT2
C9033A-3H-9 WR, 35.0--50.0 cm	19.56	18.922	19.71	19.059	910ACT2
C9033A-4H-2 WR, 60.0--75.0 cm	23	22.786	23.15	22.92	910ACT2
C9033A-4H-9 WR, 25.0--40.0 cm	28.335	27.549	28.485	27.683	910ACT2
C9033A-5H-2 WR, 45.0--60.0 cm	31.925	31.712	32.075	31.84	910ACT2
C9033A-5H-10 WR, 45.0--60.0 cm	38.425	37.242	38.575	37.369	910ACT2
C9033A-6H-3 WR, 50.0--65.0 cm	41.1	40.959	41.25	41.096	910ACT2
C9033A-6H-7 WR, 50.0--65.0 cm	44.775	44.312	44.925	44.448	910ACT2
C9033A-7H-4 WR, 38.0--53.0 cm	51.67	51.508	51.82	51.649	910ACT2
C9033A-7H-7 WR, 45.0--60.0 cm	54.17	53.856	54.32	53.997	910ACT2
C9033A-8H-5 WR, 65.0--80.0 cm	59.705	59.239	59.855	59.368	910ACT2
C9033A-8H-8 WR, 67.0--82.0 cm	62.205	61.376	62.355	61.504	910ACT2
C9033A-9H-4 WR, 70.0--84.0 cm	67.54	67.244	67.68	67.364	910ACT2
C9033A-9H-4 WR, 84.0--95.0 cm	67.68	67.364	67.79	67.458	910ACT2
C9033A-9H-9 WR, 100.0--115.0 cm	72.165	71.199	72.315	71.328	910ACT2
C9033A-10H-5 WR, 35.0--50.0 cm	77.615	77.119	77.765	77.245	910ACT2
C9033A-10H-8 WR, 30.0--45.0 cm	80.24	79.326	80.39	79.452	910ACT2
C9033A-11H-9 WR, 65.0--80.0 cm	89.82	89.098	89.97	89.231	910ACT2

C9033A-11H-13 WR, 10.0--25.0 cm	92.665	91.619	92.815	91.752	910ACT2
C9033A-12H-8 WR, 50.0--65.0 cm	99.355	97.749	99.505	97.864	910ACT2
C9033B-1H-1 WR, 0.0--140.5 cm	0	0	1.405	1.351	910BIO
C9033B-1H-2 WR, 0.0--100.5 cm	1.405	1.351	2.41	2.317	910BIO
C9033B-1H-3 WR, 0.0--141.5 cm	2.41	2.317	3.825	3.678	910BIO
C9033B-1H-4 WR, 0.0--99.5 cm	3.825	3.678	4.82	4.635	910BIO
C9033B-1H-5 WR, 0.0--100.5 cm	4.82	4.635	5.825	5.601	910BIO
C9033B-1H-6 WR, 0.0--110.0 cm	5.825	5.601	6.925	6.659	910BIO
C9033B-1H-CC WR, 0.0--35.5 cm	6.925	6.659	7.28	7	910BIO
C9033A-6H-10 WR, 0.0--120.0 cm	46.45	45.839	47.65	46.934	910BIO
C9033A-2H-3 WR, 70.0--85.0 cm	4.67	4.551	4.82	4.693	910CULT
C9033A-2H-6 WR, 70.0--85.0 cm	7.545	7.269	7.695	7.411	910CULT
C9033A-2H-9 WR, 95.0--110.0 cm	10.7	10.251	10.85	10.393	910CULT
C9033A-3H-4 WR, 10.0--25.0 cm	14.59	14.371	14.74	14.509	910CULT
C9033A-3H-9 WR, 20.0--35.0 cm	19.41	18.784	19.56	18.922	910CULT
C9033A-4H-2 WR, 45.0--60.0 cm	22.85	22.652	23	22.786	910CULT
C9033A-4H-9 WR, 0.0--15.0 cm	28.085	27.326	28.235	27.46	910CULT
C9033A-5H-2 WR, 30.0--45.0 cm	31.775	31.585	31.925	31.712	910CULT
C9033A-5H-10 WR, 30.0--45.0 cm	38.275	37.114	38.425	37.242	910CULT
C9033A-6H-3 WR, 35.0--50.0 cm	40.95	40.823	41.1	40.959	910CULT
C9033A-6H-7 WR, 35.0--50.0 cm	44.625	44.175	44.775	44.312	910CULT
C9033A-7H-4 WR, 9.0--23.0 cm	51.38	51.235	51.52	51.367	910CULT
C9033A-7H-7 WR, 30.0--45.0 cm	54.02	53.715	54.17	53.856	910CULT
C9033A-8H-5 WR, 80.0--95.0 cm	59.855	59.368	60.005	59.496	910CULT
C9033A-8H-8 WR, 82.0--99.0 cm	62.355	61.504	62.525	61.65	910CULT
C9033A-9H-4 WR, 105.0--120.0 cm	67.89	67.544	68.04	67.672	910CULT
C9033A-9H-9 WR, 60.0--75.0 cm	71.765	70.857	71.915	70.986	910CULT
C9033A-10H-5 WR, 50.0--65.0 cm	77.765	77.245	77.915	77.371	910CULT
C9033A-10H-8 WR, 45.0--60.0 cm	80.39	79.452	80.54	79.578	910CULT
C9033A-11H-9 WR, 30.0--45.0 cm	89.47	88.788	89.62	88.921	910CULT
C9033A-12H-8 WR, 35.0--50.0 cm	99.205	97.634	99.355	97.749	910CULT
C9033A-1H-1 WR, 0.0--15.0 cm	0	0	0.15	0.15	910DNA
C9033A-2H-3 WR, 0.0--15.0 cm	3.97	3.89	4.12	4.031	910DNA
C9033A-2H-6 WR, 0.0--15.0 cm	6.845	6.607	6.995	6.749	910DNA
C9033A-2H-9 WR, 0.0--15.0 cm	9.75	9.353	9.9	9.495	910DNA
C9033A-2H-9 WR, 80.0--95.0 cm	10.55	10.11	10.7	10.251	910DNA
C9033A-3H-4 WR, 85.0--100.5 cm	15.34	15.058	15.495	15.2	910DNA
C9033A-3H-7 WR, 105.0--123.0 cm	17.83	17.338	18.01	17.503	910DNA
C9033A-3H-9 WR, 90.0--105.0 cm	20.11	19.425	20.26	19.563	910DNA
C9033A-3H-9 WR, 105.0--120.5 cm	20.26	19.563	20.415	19.705	910DNA
C9033A-4H-2 WR, 115.0--131.0 cm	23.55	23.277	23.71	23.42	910DNA
C9033A-4H-5 WR, 0.0--15.0 cm	25.15	24.705	25.3	24.839	910DNA
C9033A-4H-5 WR, 118.0--133.0 cm	26.33	25.759	26.48	25.893	910DNA
C9033A-4H-9 WR, 115.0--131.0 cm	29.235	28.353	29.395	28.496	910DNA
C9033A-5H-2 WR, 108.0--123.0 cm	32.555	32.248	32.705	32.376	910DNA
C9033A-5H-6 WR, 20.0--35.0 cm	34.445	33.856	34.595	33.984	910DNA
C9033A-5H-6 WR, 104.0--121.0 cm	35.285	34.57	35.455	34.715	910DNA

C9033A-5H-10 WR, 101.0--116.0 cm	38.985	37.718	39.135	37.846	910DNA
C9033A-6H-3 WR, 105.0--120.5 cm	41.65	41.461	41.805	41.603	910DNA
C9033A-6H-7 WR, 105.0--120.5 cm	45.325	44.813	45.48	44.955	910DNA
C9033A-6H-11 WR, 106.0--121.0 cm	48.71	47.901	48.86	48.038	910DNA
C9033A-6H-13 WR, 37.5--52.5 cm	49.295	48.435	49.445	48.571	910DNA
C9033A-7H-4 WR, 105.0--121.0 cm	52.34	52.137	52.5	52.287	910DNA
C9033A-7H-7 WR, 106.0--121.0 cm	54.78	54.429	54.93	54.57	910DNA
C9033A-7H-9 WR, 50.0--65.0 cm	55.49	55.096	55.64	55.237	910DNA
C9033A-8H-5 WR, 105.0--120.5 cm	60.105	59.581	60.26	59.714	910DNA
C9033A-8H-8 WR, 106.0--121.5 cm	62.595	61.709	62.75	61.842	910DNA
C9033A-8H-12 WR, 115.0--131.5 cm	66.355	64.923	66.52	65.064	910DNA
C9033A-9H-4 WR, 120.0--130.5 cm	68.04	67.672	68.145	67.762	910DNA
C9033A-9H-9 WR, 115.0--130.0 cm	72.315	71.328	72.465	71.456	910DNA
C9033A-9H-13 WR, 65.0--80.5 cm	75.465	74.021	75.62	74.154	910DNA
C9033A-10H-5 WR, 115.0--130.0 cm	78.415	77.792	78.565	77.918	910DNA
C9033A-10H-8 WR, 105.0--120.0 cm	80.99	79.956	81.14	80.082	910DNA
C9033A-10H-12 WR, 123.0--138.0 cm	84.2	82.655	84.35	82.781	910DNA
C9033A-11H-3 WR, 72.0--87.0 cm	85.11	84.926	85.26	85.059	910DNA
C9033A-11H-9 WR, 105.0--120.0 cm	90.22	89.453	90.37	89.586	910DNA
C9033A-11H-13 WR, 60.0--69.5 cm	93.165	92.062	93.26	92.146	910DNA
C9033A-12H-8 WR, 115.0--130.5 cm	100.005	98.247	100.16	98.365	910DNA
C9033A-12H-11 WR, 29.5--44.5 cm	101.39	99.307	101.54	99.422	910DNA
C9033A-1H-3 WR, 0.0--7.0 cm	1.645	1.645	1.715	1.715	910GAS
C9033A-2H-2 WR, 0.0--7.0 cm	3.9	3.823	3.97	3.89	910GAS
C9033A-2H-5 WR, 0.0--6.0 cm	6.785	6.551	6.845	6.607	910GAS
C9033A-2H-8 WR, 0.0--6.0 cm	9.69	9.297	9.75	9.353	910GAS
C9033A-3H-2 WR, 0.0--6.0 cm	13.105	13.012	13.165	13.067	910GAS
C9033A-3H-5 WR, 0.0--6.0 cm	15.495	15.2	15.555	15.255	910GAS
C9033A-3H-10 WR, 0.0--6.0 cm	20.415	19.705	20.475	19.759	910GAS
C9033A-4H-3 WR, 0.0--6.0 cm	23.71	23.42	23.77	23.473	910GAS
C9033A-4H-6 WR, 0.0--6.0 cm	26.48	25.893	26.54	25.946	910GAS
C9033A-4H-10 WR, 0.0--6.0 cm	29.395	28.496	29.455	28.549	910GAS
C9033A-5H-3 WR, 0.0--6.0 cm	32.705	32.376	32.765	32.427	910GAS
C9033A-5H-5 WR, 0.0--22.0 cm	34.025	33.499	34.245	33.686	910GAS
C9033A-5H-9 WR, 0.0--6.0 cm	37.915	36.808	37.975	36.859	910GAS
C9033A-6H-4 WR, 0.0--6.0 cm	41.805	41.603	41.865	41.657	910GAS
C9033A-6H-9 WR, 0.0--6.0 cm	46.39	45.785	46.45	45.839	910GAS
C9033A-6H-12 WR, 0.0--6.0 cm	48.86	48.038	48.92	48.092	910GAS
C9033A-7H-5 WR, 0.0--6.0 cm	52.5	52.287	52.56	52.344	910GAS
C9033A-7H-8 WR, 0.0--6.0 cm	54.93	54.57	54.99	54.626	910GAS
C9033A-8H-3 WR, 0.0--8.0 cm	57.71	57.534	57.79	57.603	910GAS
C9033A-8H-7 WR, 0.0--7.0 cm	61.465	60.744	61.535	60.803	910GAS
C9033A-8H-11 WR, 0.0--7.0 cm	65.135	63.88	65.205	63.94	910GAS
C9033A-9H-3 WR, 0.0--10.0 cm	66.74	66.56	66.84	66.646	910GAS
C9033A-9H-7 WR, 0.0--10.0 cm	69.76	69.143	69.86	69.228	910GAS
C9033A-9H-10 WR, 0.0--7.0 cm	72.47	71.46	72.54	71.52	910GAS
C9033A-10H-3 WR, 0.0--7.0 cm	75.895	75.673	75.965	75.732	910GAS

C9033A-10H-6 WR, 0.0--7.0 cm	78.565	77.918	78.635	77.976	910GAS
C9033A-10H-9 WR, 0.0--7.0 cm	81.14	80.082	81.21	80.141	910GAS
C9033A-11H-5 WR, 0.0--7.0 cm	86.675	86.313	86.745	86.375	910GAS
C9033A-11H-8 WR, 0.0--7.0 cm	89.1	88.461	89.17	88.523	910GAS
C9033A-11H-12 WR, 0.0--7.0 cm	92.495	91.468	92.565	91.53	910GAS
C9033A-12H-3 WR, 0.0--7.0 cm	94.93	94.361	95	94.414	910GAS
C9033A-12H-6 WR, 0.0--7.0 cm	97.65	96.443	97.72	96.497	910GAS
C9033A-12H-10 WR, 0.0--7.0 cm	101.025	99.028	101.095	99.081	910GAS
C9033A-2H-4 WR, 1.0--50.0 cm	5.39	5.232	5.88	5.695	910GEO
C9033A-3H-6 WR, 0.0--40.0 cm	15.555	15.255	15.955	15.621	910GEO
C9033A-4H-4 WR, 20.0--60.0 cm	23.97	23.652	24.37	24.009	910GEO
C9033A-5H-11 WR, 0.0--40.0 cm	39.135	37.846	39.535	38.186	910GEO
C9033A-6H-2 WR, 45.0--85.0 cm	40.075	40.025	40.475	40.389	910GEO
C9033A-7H-3 WR, 33.0--73.0 cm	50.62	50.522	51.02	50.897	910GEO
C9033A-8H-4 WR, 0.0--45.0 cm	57.79	57.603	58.24	57.987	910GEO
C9033A-9H-5 WR, 20.0--60.0 cm	68.345	67.933	68.745	68.275	910GEO
C9033A-10H-10 WR, 40.0--80.0 cm	81.61	80.478	82.01	80.814	910GEO
C9033A-11H-10 WR, 35.0--75.0 cm	90.72	89.896	91.12	90.25	910GEO
C9033A-12H-9 WR, 0.0--40.0 cm	100.16	98.365	100.56	98.672	910GEO
C9033A-1H-1 WR, 15.0--25.0 cm	0.15	0.15	0.25	0.25	910IPL
C9033A-2H-3 WR, 15.0--25.0 cm	4.12	4.031	4.22	4.126	910IPL
C9033A-2H-6 WR, 15.0--25.0 cm	6.995	6.749	7.095	6.844	910IPL
C9033A-2H-9 WR, 15.0--25.0 cm	9.9	9.495	10	9.59	910IPL
C9033A-2H-9 WR, 70.0--80.0 cm	10.45	10.015	10.55	10.11	910IPL
C9033A-3H-4 WR, 75.0--85.0 cm	15.24	14.966	15.34	15.058	910IPL
C9033A-3H-7 WR, 80.0--90.0 cm	17.58	17.109	17.68	17.2	910IPL
C9033A-3H-9 WR, 80.0--90.0 cm	20.01	19.334	20.11	19.425	910IPL
C9033A-4H-2 WR, 105.0--115.0 cm	23.45	23.188	23.55	23.277	910IPL
C9033A-4H-5 WR, 30.0--40.0 cm	25.45	24.973	25.55	25.063	910IPL
C9033A-4H-9 WR, 90.0--100.0 cm	28.985	28.13	29.085	28.219	910IPL
C9033A-5H-2 WR, 95.0--108.0 cm	32.425	32.138	32.555	32.248	910IPL
C9033A-5H-10 WR, 90.0--101.0 cm	38.875	37.624	38.985	37.718	910IPL
C9033A-6H-3 WR, 95.0--105.0 cm	41.55	41.37	41.65	41.461	910IPL
C9033A-6H-7 WR, 80.0--90.0 cm	45.075	44.585	45.175	44.676	910IPL
C9033A-6H-11 WR, 96.0--106.0 cm	48.61	47.81	48.71	47.901	910IPL
C9033A-7H-4 WR, 53.0--63.0 cm	51.82	51.649	51.92	51.743	910IPL
C9033A-7H-7 WR, 75.0--85.0 cm	54.47	54.138	54.57	54.232	910IPL
C9033A-7H-9 WR, 65.0--75.0 cm	55.64	55.237	55.74	55.331	910IPL
C9033A-8H-5 WR, 20.0--30.0 cm	59.255	58.855	59.355	58.94	910IPL
C9033A-8H-8 WR, 40.0--52.0 cm	61.935	61.145	62.055	61.248	910IPL
C9033A-8H-12 WR, 105.0--115.0 cm	66.255	64.838	66.355	64.923	910IPL
C9033A-9H-4 WR, 46.0--57.0 cm	67.3	67.039	67.41	67.133	910IPL
C9033A-9H-9 WR, 75.0--85.0 cm	71.915	70.986	72.015	71.071	910IPL
C9033A-9H-13 WR, 55.0--65.0 cm	75.365	73.936	75.465	74.021	910IPL
C9033A-10H-5 WR, 105.0--115.0 cm	78.315	77.707	78.415	77.792	910IPL
C9033A-10H-8 WR, 95.0--105.0 cm	80.89	79.872	80.99	79.956	910IPL
C9033A-10H-12 WR, 90.0--103.0 cm	83.87	82.378	84	82.487	910IPL

C9033A-11H-3 WR, 60.0--72.0 cm	84.99	84.82	85.11	84.926	910IPL
C9033A-11H-9 WR, 95.0--105.0 cm	90.12	89.364	90.22	89.453	910IPL
C9033A-11H-13 WR, 0.0--10.0 cm	92.565	91.53	92.665	91.619	910IPL
C9033A-12H-8 WR, 100.0--115.0 cm	99.855	98.132	100.005	98.247	910IPL
C9033A-2H-3 WR, 120.0--141.0 cm	5.17	5.024	5.38	5.222	910PP
C9033A-2H-4 WR, 0.0--10.0 cm	5.38	5.222	5.48	5.317	910PP
C9033A-2H-7 WR, 83.0--103.0 cm	9.08	8.72	9.28	8.909	910PP
C9033A-3H-6 WR, 40.0--50.0 cm	15.955	15.621	16.055	15.713	910PP
C9033A-3H-9 WR, 0.0--20.0 cm	19.21	18.601	19.41	18.784	910PP
C9033A-4H-2 WR, 15.0--35.0 cm	22.55	22.384	22.75	22.563	910PP
C9033A-4H-4 WR, 0.0--20.0 cm	23.77	23.473	23.97	23.652	910PP
C9033A-5H-2 WR, 0.0--20.0 cm	31.475	31.329	31.675	31.5	910PP
C9033A-5H-11 WR, 40.0--60.0 cm	39.535	38.186	39.735	38.356	910PP
C9033A-6H-2 WR, 85.0--97.5 cm	40.475	40.389	40.6	40.503	910PP
C9033A-6H-8 WR, 49.0--69.0 cm	45.97	45.402	46.17	45.584	910PP
C9033A-7H-3 WR, 73.0--100.0 cm	51.02	50.897	51.29	51.151	910PP
C9033A-7H-9 WR, 0.0--20.0 cm	54.99	54.626	55.19	54.814	910PP
C9033A-8H-4 WR, 45.0--60.0 cm	58.24	57.987	58.39	58.115	910PP
C9033A-8H-5 WR, 0.0--20.0 cm	59.055	58.684	59.255	58.855	910PP
C9033A-8H-8 WR, 0.0--20.0 cm	61.535	60.803	61.735	60.974	910PP
C9033A-8H-10 WR, 0.0--20.0 cm	63.935	62.855	64.135	63.026	910PP
C9033A-9H-5 WR, 0.0--20.0 cm	68.145	67.762	68.345	67.933	910PP
C9033A-9H-11 WR, 0.0--20.0 cm	72.54	71.52	72.74	71.691	910PP
C9033A-10H-8 WR, 0.0--30.0 cm	79.94	79.074	80.24	79.326	910PP
C9033A-10H-10 WR, 80.0--100.0 cm	82.01	80.814	82.21	80.982	910PP
C9033A-11H-9 WR, 10.0--30.0 cm	89.27	88.611	89.47	88.788	910PP
C9033A-11H-10 WR, 75.0--95.0 cm	91.12	90.25	91.32	90.427	910PP
C9033A-12H-8 WR, 0.0--25.0 cm	98.855	97.366	99.105	97.557	910PP
C9033A-1H-1 WR, 25.0--35.0 cm	0.25	0.25	0.35	0.35	910VIR
C9033A-2H-3 WR, 85.0--95.0 cm	4.82	4.693	4.92	4.788	910VIR
C9033A-3H-4 WR, 0.0--10.0 cm	14.49	14.28	14.59	14.371	910VIR
C9033A-4H-2 WR, 35.0--45.0 cm	22.75	22.563	22.85	22.652	910VIR
C9033A-5H-2 WR, 20.0--30.0 cm	31.675	31.5	31.775	31.585	910VIR
C9033A-6H-3 WR, 25.0--35.0 cm	40.85	40.731	40.95	40.823	910VIR
C9033A-7H-4 WR, 0.0--9.0 cm	51.29	51.151	51.38	51.235	910VIR
C9033A-7H-7 WR, 20.0--30.0 cm	53.92	53.621	54.02	53.715	910VIR
C9033A-8H-5 WR, 95.0--105.0 cm	60.005	59.496	60.105	59.581	910VIR
C9033A-8H-8 WR, 99.0--106.0 cm	62.525	61.65	62.595	61.709	910VIR
C9033A-9H-4 WR, 95.0--105.0 cm	67.79	67.458	67.89	67.544	910VIR
C9033A-10H-5 WR, 95.0--105.0 cm	78.215	77.623	78.315	77.707	910VIR
C9033A-11H-9 WR, 0.0--10.0 cm	89.17	88.523	89.27	88.611	910VIR
C9033A-12H-8 WR, 25.0--35.0 cm	99.105	97.557	99.205	97.634	910VIR
C9033A-1H-1 WR, 55.0--70.0 cm	0.55	0.55	0.7	0.7	IW
C9033A-2H-3 WR, 25.0--40.0 cm	4.22	4.126	4.37	4.268	IW
C9033A-2H-6 WR, 25.0--40.0 cm	7.095	6.844	7.245	6.985	IW
C9033A-2H-9 WR, 25.0--40.0 cm	10	9.59	10.15	9.731	IW
C9033A-3H-4 WR, 55.0--75.0 cm	15.04	14.783	15.24	14.966	IW

C9033A-3H-7 WR, 90.0--105.0 cm	17.68	17.2	17.83	17.338	IW
C9033A-3H-9 WR, 65.0--80.0 cm	19.86	19.196	20.01	19.334	IW
C9033A-4H-2 WR, 90.0--105.0 cm	23.3	23.054	23.45	23.188	IW
C9033A-4H-5 WR, 15.0--30.0 cm	25.3	24.839	25.45	24.973	IW
C9033A-4H-9 WR, 100.0--115.0 cm	29.085	28.219	29.235	28.353	IW
C9033A-5H-2 WR, 75.0--95.0 cm	32.225	31.967	32.425	32.138	IW
C9033A-5H-6 WR, 90.0--104.0 cm	35.145	34.451	35.285	34.57	IW
C9033A-5H-10 WR, 75.0--90.0 cm	38.725	37.497	38.875	37.624	IW
C9033A-6H-3 WR, 80.0--95.0 cm	41.4	41.233	41.55	41.37	IW
C9033A-6H-7 WR, 90.0--105.0 cm	45.175	44.676	45.325	44.813	IW
C9033A-6H-11 WR, 15.0--35.0 cm	47.8	47.071	48	47.253	IW
C9033A-7H-4 WR, 85.0--105.0 cm	52.14	51.949	52.34	52.137	IW
C9033A-7H-7 WR, 85.0--106.0 cm	54.57	54.232	54.78	54.429	IW
C9033A-7H-9 WR, 75.0--95.0 cm	55.74	55.331	55.94	55.519	IW
C9033A-8H-5 WR, 30.0--50.0 cm	59.355	58.94	59.555	59.111	IW
C9033A-8H-8 WR, 20.0--40.0 cm	61.735	60.974	61.935	61.145	IW
C9033A-8H-12 WR, 90.0--105.0 cm	66.105	64.709	66.255	64.838	IW
C9033A-9H-4 WR, 31.0--46.0 cm	67.15	66.911	67.3	67.039	IW
C9033A-9H-9 WR, 24.0--44.0 cm	71.405	70.549	71.605	70.72	IW
C9033A-9H-13 WR, 35.0--55.0 cm	75.165	73.765	75.365	73.936	IW
C9033A-10H-5 WR, 0.0--20.0 cm	77.265	76.825	77.465	76.993	IW
C9033A-10H-8 WR, 75.0--95.0 cm	80.69	79.704	80.89	79.872	IW
C9033A-10H-12 WR, 103.0--123.0 cm	84	82.487	84.2	82.655	IW
C9033A-11H-3 WR, 0.0--25.0 cm	84.39	84.288	84.64	84.51	IW
C9033A-11H-9 WR, 45.0--65.0 cm	89.62	88.921	89.82	89.098	IW
C9033A-11H-13 WR, 25.0--45.0 cm	92.815	91.752	93.015	91.929	IW
C9033A-12H-8 WR, 80.0--100.0 cm	99.655	97.979	99.855	98.132	IW

Appendix Table 3. List of discrete samples.						
Sample source	Top Core depth (below sea floor) [m CSF-A]	Top Core depth (below sea floor) [m CSF-B]	Bottom Core depth (below sea floor) [m CSF-A]	Bottom Core depth (below sea floor) [m CSF-B]	Sample code	Sample volume (cm3)
C9033A-1H-3 WR, 0.0--7.0 cm	1.645	1.645	1.715	1.715	910AIHS	5
C9033A-2H-2 WR, 0.0--7.0 cm	3.9	3.823	3.97	3.89	910AIHS	5
C9033A-2H-5 WR, 0.0--6.0 cm	6.785	6.551	6.845	6.607	910AIHS	5
C9033A-2H-8 WR, 0.0--6.0 cm	9.69	9.297	9.75	9.353	910AIHS	5
C9033A-3H-2 WR, 0.0--6.0 cm	13.105	13.012	13.165	13.067	910AIHS	5
C9033A-3H-5 WR, 0.0--6.0 cm	15.495	15.2	15.555	15.255	910AIHS	5
C9033A-3H-10 WR, 0.0--6.0 cm	20.415	19.705	20.475	19.759	910AIHS	5
C9033A-4H-3 WR, 0.0--6.0 cm	23.71	23.42	23.77	23.473	910AIHS	5
C9033A-4H-6 WR, 0.0--6.0 cm	26.48	25.893	26.54	25.946	910AIHS	5
C9033A-4H-10 WR, 0.0--6.0 cm	29.395	28.496	29.455	28.549	910AIHS	5
C9033A-5H-3 WR, 0.0--6.0 cm	32.705	32.376	32.765	32.427	910AIHS	5
C9033A-5H-5 WR, 0.0--22.0 cm	34.025	33.499	34.245	33.686	910AIHS	5
C9033A-5H-9 WR, 0.0--6.0 cm	37.915	36.808	37.975	36.859	910AIHS	5
C9033A-6H-4 WR, 0.0--6.0 cm	41.805	41.603	41.865	41.657	910AIHS	5
C9033A-6H-9 WR, 0.0--6.0 cm	46.39	45.785	46.45	45.839	910AIHS	5
C9033A-6H-12 WR, 0.0--6.0 cm	48.86	48.038	48.92	48.092	910AIHS	5
C9033A-7H-5 WR, 0.0--6.0 cm	52.5	52.287	52.56	52.344	910AIHS	5
C9033A-7H-8 WR, 0.0--6.0 cm	54.93	54.57	54.99	54.626	910AIHS	5
C9033A-8H-3 WR, 0.0--8.0 cm	57.71	57.534	57.79	57.603	910AIHS	5
C9033A-8H-7 WR, 0.0--7.0 cm	61.465	60.744	61.535	60.803	910AIHS	5
C9033A-8H-11 WR, 0.0--7.0 cm	65.135	63.88	65.205	63.94	910AIHS	5
C9033A-9H-3 WR, 0.0--10.0 cm	66.74	66.56	66.84	66.646	910AIHS	5
C9033A-9H-7 WR, 0.0--10.0 cm	69.76	69.143	69.86	69.228	910AIHS	5
C9033A-9H-10 WR, 0.0--7.0 cm	72.47	71.46	72.54	71.52	910AIHS	5
C9033A-10H-3 WR, 0.0--7.0 cm	75.895	75.673	75.965	75.732	910AIHS	5
C9033A-10H-6 WR, 0.0--7.0 cm	78.565	77.918	78.635	77.976	910AIHS	5
C9033A-10H-9 WR, 0.0--7.0 cm	81.14	80.082	81.21	80.141	910AIHS	5
C9033A-11H-5 WR, 0.0--7.0 cm	86.675	86.313	86.745	86.375	910AIHS	5
C9033A-11H-8 WR, 0.0--7.0 cm	89.1	88.461	89.17	88.523	910AIHS	5
C9033A-11H-12 WR, 0.0--7.0 cm	92.495	91.468	92.565	91.53	910AIHS	5
C9033A-12H-3 WR, 0.0--7.0 cm	94.93	94.361	95	94.414	910AIHS	5
C9033A-12H-6 WR, 0.0--7.0 cm	97.65	96.443	97.72	96.497	910AIHS	5
C9033A-12H-10 WR, 0.0--7.0 cm	101.025	99.028	101.095	99.081	910AIHS	5
C9033A-1H-1 WR, 0.0--4.0 cm	0	0	0.04	0.04	910CELL	2
C9033B-1H-1 WR, 0.0--4.0 cm	0	0	0.04	0.039	910CELL	2
C9033B-1H-1 WR, 136.5--140.5 cm	1.365	1.313	1.405	1.351	910CELL	2
C9033A-1H-2 WR, 21.0--25.0 cm	1.605	1.605	1.645	1.645	910CELL	2
C9033B-1H-2 WR, 96.5--100.5 cm	2.37	2.279	2.41	2.317	910CELL	2
C9033B-1H-3 WR, 137.5--141.5 cm	3.785	3.639	3.825	3.678	910CELL	2
C9033A-2H-2 WR, 0.0--4.0 cm	3.9	3.823	3.94	3.861	910CELL	2
C9033B-1H-4 WR, 95.5--99.5 cm	4.78	4.596	4.82	4.635	910CELL	2
C9033A-2H-4 WR, 0.0--4.0 cm	5.38	5.222	5.42	5.26	910CELL	2
C9033B-1H-5 WR, 96.5--100.5 cm	5.785	5.563	5.825	5.601	910CELL	2
C9033A-2H-6 WR, 0.0--4.0 cm	6.845	6.607	6.885	6.645	910CELL	2
C9033B-1H-6 WR, 106.0--110.0 cm	6.885	6.62	6.925	6.659	910CELL	2
C9033A-2H-7 WR, 0.0--4.0 cm	8.25	7.935	8.29	7.973	910CELL	2
C9033A-2H-9 WR, 0.0--4.0 cm	9.75	9.353	9.79	9.391	910CELL	2
C9033A-2H-9 WR, 95.0--110.0 cm	10.7	10.251	10.85	10.393	910CELL	2
C9033A-2H-10 WR, 0.0--4.0 cm	11.165	10.691	11.205	10.729	910CELL	2
C9033A-2H-10 WR, 111.0--115.0 cm	12.275	11.74	12.315	11.778	910CELL	2
C9033A-3H-1 WR, 106.5--110.5 cm	13.065	12.975	13.105	13.012	910CELL	2
C9033A-3H-3 WR, 128.5--132.5 cm	14.45	14.243	14.49	14.28	910CELL	2
C9033A-3H-4 WR, 96.5--100.5 cm	15.455	15.163	15.495	15.2	910CELL	2
C9033A-3H-6 WR, 118.5--122.5 cm	16.74	16.34	16.78	16.376	910CELL	2
C9033A-3H-7 WR, 119.0--123.0 cm	17.97	17.466	18.01	17.503	910CELL	2
C9033A-3H-8 WR, 116.0--120.0 cm	19.17	18.565	19.21	18.601	910CELL	2
C9033A-3H-9 WR, 116.5--120.5 cm	20.375	19.668	20.415	19.705	910CELL	2
C9033A-3H-11 WR, 91.5--95.5 cm	21.39	20.597	21.43	20.634	910CELL	2
C9033A-4H-2 WR, 127.0--131.0 cm	23.67	23.384	23.71	23.42	910CELL	2
C9033A-4H-4 WR, 134.0--138.0 cm	25.11	24.67	25.15	24.705	910CELL	2
C9033A-4H-5 WR, 129.0--133.0 cm	26.44	25.857	26.48	25.893	910CELL	2
C9033A-4H-7 WR, 128.0--132.0 cm	27.82	27.089	27.86	27.125	910CELL	2
C9033A-4H-9 WR, 127.0--131.0 cm	29.355	28.46	29.395	28.496	910CELL	2
C9033A-4H-11 WR, 127.0--131.0 cm	30.725	29.683	30.765	29.719	910CELL	2

C9033A-4H-12 WR, 48.0--52.0 cm	31.245	30.147	31.285	30.183	910CELL	2
C9033A-5H-1 WR, 93.5--97.5 cm	31.435	31.295	31.475	31.329	910CELL	2
C9033A-5H-2 WR, 119.0--123.0 cm	32.665	32.342	32.705	32.376	910CELL	2
C9033A-5H-4 WR, 122.0--126.0 cm	33.985	33.465	34.025	33.499	910CELL	2
C9033A-5H-6 WR, 117.0--121.0 cm	35.415	34.681	35.455	34.715	910CELL	2
C9033A-5H-7 WR, 122.0--126.0 cm	36.675	35.753	36.715	35.787	910CELL	2
C9033A-5H-8 WR, 116.0--120.0 cm	37.875	36.774	37.915	36.808	910CELL	2
C9033A-5H-10 WR, 112.0--116.0 cm	39.095	37.811	39.135	37.846	910CELL	2
C9033A-5H-11 WR, 110.0--114.0 cm	40.235	38.781	40.275	38.815	910CELL	2
C9033A-6H-3 WR, 116.5--120.5 cm	41.765	41.566	41.805	41.603	910CELL	2
C9033A-6H-5 WR, 117.0--121.0 cm	43.035	42.724	43.075	42.761	910CELL	2
C9033A-6H-6 WR, 116.0--120.0 cm	44.235	43.819	44.275	43.856	910CELL	2
C9033A-6H-7 WR, 116.5--120.5 cm	45.44	44.918	45.48	44.955	910CELL	2
C9033A-6H-8 WR, 87.0--91.0 cm	46.35	45.748	46.39	45.785	910CELL	2
C9033A-6H-10 WR, 116.0--120.0 cm	47.61	46.898	47.65	46.934	910CELL	2
C9033A-6H-11 WR, 117.0--121.0 cm	48.82	48.001	48.86	48.038	910CELL	2
C9033A-6H-13 WR, 48.5--52.5 cm	49.405	48.535	49.445	48.571	910CELL	2
C9033A-7H-2 WR, 90.0--94.0 cm	50.25	50.174	50.29	50.212	910CELL	2
C9033A-7H-3 WR, 96.0--100.0 cm	51.25	51.113	51.29	51.151	910CELL	2
C9033A-7H-4 WR, 117.0--121.0 cm	52.46	52.25	52.5	52.287	910CELL	2
C9033A-7H-6 WR, 112.0--116.0 cm	53.68	53.396	53.72	53.433	910CELL	2
C9033A-7H-7 WR, 117.0--121.0 cm	54.89	54.532	54.93	54.57	910CELL	2
C9033A-8H-2 WR, 66.0--70.0 cm	57.67	57.5	57.71	57.534	910CELL	2
C9033A-8H-4 WR, 122.5--126.5 cm	59.015	58.65	59.055	58.684	910CELL	2
C9033A-8H-5 WR, 116.5--120.5 cm	60.22	59.68	60.26	59.714	910CELL	2
C9033A-8H-6 WR, 116.5--120.5 cm	61.425	60.709	61.465	60.744	910CELL	2
C9033A-8H-8 WR, 117.0--121.0 cm	62.705	61.803	62.745	61.838	910CELL	2
C9033A-8H-9 WR, 114.0--118.0 cm	63.89	62.816	63.93	62.85	910CELL	2
C9033A-8H-10 WR, 116.0--120.0 cm	65.095	63.846	65.135	63.88	910CELL	2
C9033A-8H-12 WR, 127.0--131.0 cm	66.475	65.026	66.515	65.06	910CELL	2
C9033A-9H-2 WR, 69.0--73.0 cm	66.7	66.526	66.74	66.56	910CELL	2
C9033A-9H-4 WR, 126.0--130.0 cm	68.1	67.723	68.14	67.758	910CELL	2
C9033A-9H-5 WR, 126.0--130.0 cm	69.405	68.839	69.445	68.873	910CELL	2
C9033A-9H-6 WR, 27.0--31.0 cm	69.715	69.104	69.755	69.139	910CELL	2
C9033A-9H-8 WR, 126.0--130.0 cm	71.12	70.306	71.16	70.34	910CELL	2
C9033A-9H-9 WR, 126.0--130.0 cm	72.425	71.422	72.465	71.456	910CELL	2
C9033A-9H-11 WR, 126.0--130.0 cm	73.8	72.597	73.84	72.632	910CELL	2
C9033A-9H-12 WR, 93.0--97.0 cm	74.775	73.431	74.815	73.465	910CELL	2
C9033A-9H-13 WR, 76.0--80.0 cm	75.575	74.115	75.615	74.149	910CELL	2
C9033A-10H-2 WR, 103.0--107.0 cm	75.855	75.639	75.895	75.673	910CELL	2
C9033A-10H-4 WR, 126.0--130.0 cm	77.225	76.791	77.265	76.825	910CELL	2
C9033A-10H-5 WR, 126.0--130.0 cm	78.525	77.884	78.565	77.918	910CELL	2
C9033A-10H-7 WR, 126.5--130.5 cm	79.9	79.04	79.94	79.074	910CELL	2
C9033A-10H-8 WR, 116.0--120.0 cm	81.1	80.049	81.14	80.082	910CELL	2
C9033A-10H-10 WR, 126.5--130.5 cm	82.475	81.205	82.515	81.238	910CELL	2
C9033A-10H-11 WR, 41.5--45.5 cm	82.93	81.587	82.97	81.621	910CELL	2
C9033A-10H-12 WR, 134.0--138.0 cm	84.31	82.748	84.35	82.781	910CELL	2
C9033A-11H-3 WR, 0.0--4.0 cm	84.39	84.288	84.43	84.324	910CELL	2
C9033A-11H-3 WR, 83.0--87.0 cm	85.22	85.024	85.26	85.059	910CELL	2
C9033A-11H-4 WR, 137.5--141.5 cm	86.635	86.277	86.675	86.313	910CELL	2
C9033A-11H-6 WR, 101.0--104.0 cm	87.755	87.269	87.785	87.296	910CELL	2
C9033A-11H-7 WR, 126.5--130.5 cm	89.06	88.425	89.1	88.461	910CELL	2
C9033A-11H-9 WR, 116.0--120.0 cm	90.33	89.55	90.37	89.586	910CELL	2
C9033A-11H-10 WR, 116.0--120.0 cm	91.53	90.613	91.57	90.649	910CELL	2
C9033A-11H-11 WR, 88.5--92.5 cm	92.455	91.433	92.495	91.468	910CELL	2
C9033A-11H-13 WR, 65.5--69.5 cm	93.22	92.11	93.26	92.146	910CELL	2
C9033A-12H-2 WR, 0.0--4.0 cm	93.525	93.285	93.565	93.316	910CELL	2
C9033A-12H-2 WR, 136.5--140.5 cm	94.89	94.33	94.93	94.361	910CELL	2
C9033A-12H-4 WR, 128.5--132.5 cm	96.285	95.398	96.325	95.429	910CELL	2
C9033A-12H-6 WR, 3.0--7.0 cm	97.68	96.466	97.72	96.497	910CELL	2
C9033A-12H-7 WR, 109.5--113.5 cm	98.815	97.335	98.855	97.366	910CELL	2
C9033A-12H-8 WR, 126.5--130.5 cm	100.12	98.335	100.16	98.365	910CELL	2
C9033A-12H-9 WR, 82.5--86.5 cm	100.985	98.997	101.025	99.028	910CELL	2
C9033A-12H-11 WR, 40.5--44.5 cm	101.5	99.391	101.54	99.422	910CELL	2
C9033A-1H-1 WR, 0.0--4.0 cm	0	0	0.04	0.04	910VIRC	1
C9033B-1H-1 WR, 0.0--4.0 cm	0	0	0.04	0.039	910VIRC	1
C9033B-1H-1 WR, 136.5--140.5 cm	1.365	1.313	1.405	1.351	910VIRC	1
C9033A-1H-2 WR, 21.0--25.0 cm	1.605	1.605	1.645	1.645	910VIRC	1
C9033B-1H-2 WR, 96.5--100.5 cm	2.37	2.279	2.41	2.317	910VIRC	1

C9033B-1H-3 WR, 137.5--141.5 cm	3.785	3.639	3.825	3.678	910VIRC	1
C9033A-2H-2 WR, 0.0--4.0 cm	3.9	3.823	3.94	3.861	910VIRC	1
C9033B-1H-4 WR, 95.5--99.5 cm	4.78	4.596	4.82	4.635	910VIRC	1
C9033A-2H-4 WR, 0.0--4.0 cm	5.38	5.222	5.42	5.26	910VIRC	1
C9033B-1H-5 WR, 96.5--100.5 cm	5.785	5.563	5.825	5.601	910VIRC	1
C9033A-2H-6 WR, 0.0--4.0 cm	6.845	6.607	6.885	6.645	910VIRC	1
C9033B-1H-6 WR, 106.0--110.0 cm	6.885	6.62	6.925	6.659	910VIRC	1
C9033A-2H-7 WR, 0.0--4.0 cm	8.25	7.935	8.29	7.973	910VIRC	1
C9033A-2H-9 WR, 0.0--4.0 cm	9.75	9.353	9.79	9.391	910VIRC	1
C9033A-2H-10 WR, 0.0--4.0 cm	11.165	10.691	11.205	10.729	910VIRC	1
C9033A-2H-10 WR, 111.0--115.0 cm	12.275	11.74	12.315	11.778	910VIRC	1
C9033A-3H-1 WR, 106.5--110.5 cm	13.065	12.975	13.105	13.012	910VIRC	1
C9033A-3H-3 WR, 128.5--132.5 cm	14.45	14.243	14.49	14.28	910VIRC	1
C9033A-3H-4 WR, 96.5--100.5 cm	15.455	15.163	15.495	15.2	910VIRC	1
C9033A-3H-6 WR, 118.5--122.5 cm	16.74	16.34	16.78	16.376	910VIRC	1
C9033A-3H-7 WR, 119.0--123.0 cm	17.97	17.466	18.01	17.503	910VIRC	1
C9033A-3H-8 WR, 116.0--120.0 cm	19.17	18.565	19.21	18.601	910VIRC	1
C9033A-3H-9 WR, 116.5--120.5 cm	20.375	19.668	20.415	19.705	910VIRC	1
C9033A-3H-11 WR, 91.5--95.5 cm	21.39	20.597	21.43	20.634	910VIRC	1
C9033A-4H-2 WR, 127.0--131.0 cm	23.67	23.384	23.71	23.42	910VIRC	1
C9033A-4H-4 WR, 134.0--138.0 cm	25.11	24.67	25.15	24.705	910VIRC	1
C9033A-4H-5 WR, 129.0--133.0 cm	26.44	25.857	26.48	25.893	910VIRC	1
C9033A-4H-7 WR, 128.0--132.0 cm	27.82	27.089	27.86	27.125	910VIRC	1
C9033A-4H-9 WR, 127.0--131.0 cm	29.355	28.46	29.395	28.496	910VIRC	1
C9033A-4H-11 WR, 127.0--131.0 cm	30.725	29.683	30.765	29.719	910VIRC	1
C9033A-4H-12 WR, 48.0--52.0 cm	31.245	30.147	31.285	30.183	910VIRC	1
C9033A-5H-1 WR, 93.5--97.5 cm	31.435	31.295	31.475	31.329	910VIRC	1
C9033A-5H-2 WR, 119.0--123.0 cm	32.665	32.342	32.705	32.376	910VIRC	1
C9033A-5H-4 WR, 122.0--126.0 cm	33.985	33.465	34.025	33.499	910VIRC	1
C9033A-5H-6 WR, 117.0--121.0 cm	35.415	34.681	35.455	34.715	910VIRC	1
C9033A-5H-7 WR, 122.0--126.0 cm	36.675	35.753	36.715	35.787	910VIRC	1
C9033A-5H-8 WR, 116.0--120.0 cm	37.875	36.774	37.915	36.808	910VIRC	1
C9033A-5H-10 WR, 112.0--116.0 cm	39.095	37.811	39.135	37.846	910VIRC	1
C9033A-5H-11 WR, 110.0--114.0 cm	40.235	38.781	40.275	38.815	910VIRC	1
C9033A-6H-3 WR, 116.5--120.5 cm	41.765	41.566	41.805	41.603	910VIRC	1
C9033A-6H-5 WR, 117.0--121.0 cm	43.035	42.724	43.075	42.761	910VIRC	1
C9033A-6H-6 WR, 116.0--120.0 cm	44.235	43.819	44.275	43.856	910VIRC	1
C9033A-6H-7 WR, 116.5--120.5 cm	45.44	44.918	45.48	44.955	910VIRC	1
C9033A-6H-8 WR, 87.0--91.0 cm	46.35	45.748	46.39	45.785	910VIRC	1
C9033A-6H-10 WR, 116.0--120.0 cm	47.61	46.898	47.65	46.934	910VIRC	1
C9033A-6H-11 WR, 117.0--121.0 cm	48.82	48.001	48.86	48.038	910VIRC	1
C9033A-6H-13 WR, 48.5--52.5 cm	49.405	48.535	49.445	48.571	910VIRC	1
C9033A-7H-2 WR, 90.0--94.0 cm	50.25	50.174	50.29	50.212	910VIRC	1
C9033A-7H-3 WR, 96.0--100.0 cm	51.25	51.113	51.29	51.151	910VIRC	1
C9033A-7H-4 WR, 117.0--121.0 cm	52.46	52.25	52.5	52.287	910VIRC	1
C9033A-7H-6 WR, 112.0--116.0 cm	53.68	53.396	53.72	53.433	910VIRC	1
C9033A-7H-7 WR, 117.0--121.0 cm	54.89	54.532	54.93	54.57	910VIRC	1
C9033A-8H-2 WR, 66.0--70.0 cm	57.67	57.5	57.71	57.534	910VIRC	1
C9033A-8H-4 WR, 122.5--126.5 cm	59.015	58.65	59.055	58.684	910VIRC	1
C9033A-8H-5 WR, 116.5--120.5 cm	60.22	59.68	60.26	59.714	910VIRC	1
C9033A-8H-6 WR, 116.5--120.5 cm	61.425	60.709	61.465	60.744	910VIRC	1
C9033A-8H-8 WR, 117.0--121.0 cm	62.705	61.803	62.745	61.838	910VIRC	1
C9033A-8H-9 WR, 114.0--118.0 cm	63.89	62.816	63.93	62.85	910VIRC	1
C9033A-8H-10 WR, 116.0--120.0 cm	65.095	63.846	65.135	63.88	910VIRC	1
C9033A-8H-12 WR, 127.0--131.0 cm	66.475	65.026	66.515	65.06	910VIRC	1
C9033A-9H-2 WR, 69.0--73.0 cm	66.7	66.526	66.74	66.56	910VIRC	1
C9033A-9H-4 WR, 126.0--130.0 cm	68.1	67.723	68.14	67.758	910VIRC	1
C9033A-9H-5 WR, 126.0--130.0 cm	69.405	68.839	69.445	68.873	910VIRC	1
C9033A-9H-6 WR, 27.0--31.0 cm	69.715	69.104	69.755	69.139	910VIRC	1
C9033A-9H-8 WR, 126.0--130.0 cm	71.12	70.306	71.16	70.34	910VIRC	1
C9033A-9H-9 WR, 126.0--130.0 cm	72.425	71.422	72.465	71.456	910VIRC	1
C9033A-9H-11 WR, 126.0--130.0 cm	73.8	72.597	73.84	72.632	910VIRC	1
C9033A-9H-12 WR, 93.0--97.0 cm	74.775	73.431	74.815	73.465	910VIRC	1
C9033A-9H-13 WR, 76.0--80.0 cm	75.575	74.115	75.615	74.149	910VIRC	1
C9033A-10H-2 WR, 103.0--107.0 cm	75.855	75.639	75.895	75.673	910VIRC	1
C9033A-10H-4 WR, 126.0--130.0 cm	77.225	76.791	77.265	76.825	910VIRC	1
C9033A-10H-5 WR, 126.0--130.0 cm	78.525	77.884	78.565	77.918	910VIRC	1
C9033A-10H-7 WR, 126.5--130.5 cm	79.9	79.04	79.94	79.074	910VIRC	1
C9033A-10H-8 WR, 116.0--120.0 cm	81.1	80.049	81.14	80.082	910VIRC	1

C9033A-10H-10 WR, 126.5--130.5 cm	82.475	81.205	82.515	81.238	910VIRC	1
C9033A-10H-11 WR, 41.5--45.5 cm	82.93	81.587	82.97	81.621	910VIRC	1
C9033A-10H-12 WR, 134.0--138.0 cm	84.31	82.748	84.35	82.781	910VIRC	1
C9033A-11H-3 WR, 0.0--4.0 cm	84.39	84.288	84.43	84.324	910VIRC	1
C9033A-11H-3 WR, 83.0--87.0 cm	85.22	85.024	85.26	85.059	910VIRC	1
C9033A-11H-4 WR, 137.5--141.5 cm	86.635	86.277	86.675	86.313	910VIRC	1
C9033A-11H-6 WR, 101.0--104.0 cm	87.755	87.269	87.785	87.296	910VIRC	1
C9033A-11H-7 WR, 126.5--130.5 cm	89.06	88.425	89.1	88.461	910VIRC	1
C9033A-11H-9 WR, 116.0--120.0 cm	90.33	89.55	90.37	89.586	910VIRC	1
C9033A-11H-10 WR, 116.0--120.0 cm	91.53	90.613	91.57	90.649	910VIRC	1
C9033A-11H-11 WR, 88.5--92.5 cm	92.455	91.433	92.495	91.468	910VIRC	1
C9033A-11H-13 WR, 65.5--69.5 cm	93.22	92.11	93.26	92.146	910VIRC	1
C9033A-12H-2 WR, 0.0--4.0 cm	93.525	93.285	93.565	93.316	910VIRC	1
C9033A-12H-2 WR, 136.5--140.5 cm	94.89	94.33	94.93	94.361	910VIRC	1
C9033A-12H-4 WR, 128.5--132.5 cm	96.285	95.398	96.325	95.429	910VIRC	1
C9033A-12H-6 WR, 3.0--7.0 cm	97.68	96.466	97.72	96.497	910VIRC	1
C9033A-12H-7 WR, 109.5--113.5 cm	98.815	97.335	98.855	97.366	910VIRC	1
C9033A-12H-8 WR, 126.5--130.5 cm	100.12	98.335	100.16	98.365	910VIRC	1
C9033A-12H-9 WR, 82.5--86.5 cm	100.985	98.997	101.025	99.028	910VIRC	1
C9033A-12H-11 WR, 40.5--44.5 cm	101.5	99.391	101.54	99.422	910VIRC	1
C9033A-1H-1 WR, 135.0--139.5 cm	1.35	1.35	1.395	1.395	910WTW	10
C9033A-2H-6 WR, 135.0--140.0 cm	8.195	7.883	8.245	7.931	910WTW	10
C9033A-2H-9 WR, 136.0--141.0 cm	11.11	10.639	11.16	10.686	910WTW	10
C9033A-3H-7 WR, 69.0--74.0 cm	17.47	17.008	17.52	17.054	910WTW	10
C9033A-3H-11 WR, 0.0--5.0 cm	20.475	19.759	20.525	19.805	910WTW	10
C9033A-4H-5 WR, 118.0--123.0 cm	26.33	25.759	26.38	25.804	910WTW	10
C9033A-4H-9 WR, 85.0--90.0 cm	28.935	28.085	28.985	28.13	910WTW	10
C9033A-5H-4 WR, 60.0--65.0 cm	33.365	32.937	33.415	32.98	910WTW	10
C9033A-5H-10 WR, 25.0--30.0 cm	38.225	37.071	38.275	37.114	910WTW	10
C9033A-6H-5 WR, 0.0--5.0 cm	41.865	41.657	41.915	41.703	910WTW	10
C9033A-6H-7 WR, 30.0--35.0 cm	44.575	44.129	44.625	44.175	910WTW	10
C9033A-6H-13 WR, 0.0--5.0 cm	48.92	48.092	48.97	48.138	910WTW	10
C9033A-7H-4 WR, 85.0--90.0 cm	52.14	51.949	52.19	51.996	910WTW	10
C9033A-7H-7 WR, 15.0--20.0 cm	53.87	53.574	53.92	53.621	910WTW	10
C9033A-8H-4 WR, 55.0--60.0 cm	58.34	58.073	58.39	58.115	910WTW	10
C9033A-8H-12 WR, 0.0--5.0 cm	65.205	63.94	65.255	63.983	910WTW	10
C9033A-9H-4 WR, 0.0--5.0 cm	66.84	66.646	66.89	66.689	910WTW	10
C9033A-9H-5 WR, 0.0--5.0 cm	68.145	67.762	68.195	67.805	910WTW	10
C9033A-9H-9 WR, 0.0--5.0 cm	71.165	70.344	71.215	70.387	910WTW	10
C9033A-10H-5 WR, 95.0--100.0 cm	78.215	77.623	78.265	77.665	910WTW	10
C9033A-10H-10 WR, 35.0--40.0 cm	81.56	80.436	81.61	80.478	910WTW	10
C9033A-11H-3 WR, 25.0--30.0 cm	84.64	84.51	84.69	84.554	910WTW	10
C9033A-11H-10 WR, 30.0--35.0 cm	90.67	89.851	90.72	89.896	910WTW	10
C9033A-12H-11 WR, 0.0--5.0 cm	101.095	99.081	101.145	99.119	910WTW	10
C9033A-1H-1 WR, 135.0--139.5 cm	1.35	1.35	1.395	1.395	910WTX	2
C9033A-2H-6 WR, 135.0--140.0 cm	8.195	7.883	8.245	7.931	910WTX	2
C9033A-2H-9 WR, 95.0--110.0 cm	10.7	10.251	10.85	10.393	910WTX	2
C9033A-2H-9 WR, 136.0--141.0 cm	11.11	10.639	11.16	10.686	910WTX	2
C9033A-3H-7 WR, 69.0--74.0 cm	17.47	17.008	17.52	17.054	910WTX	2
C9033A-3H-11 WR, 0.0--5.0 cm	20.475	19.759	20.525	19.805	910WTX	2
C9033A-4H-5 WR, 118.0--123.0 cm	26.33	25.759	26.38	25.804	910WTX	2
C9033A-5H-4 WR, 60.0--65.0 cm	33.365	32.937	33.415	32.98	910WTX	2
C9033A-5H-10 WR, 25.0--30.0 cm	38.225	37.071	38.275	37.114	910WTX	2
C9033A-6H-5 WR, 0.0--5.0 cm	41.865	41.657	41.915	41.703	910WTX	10
C9033A-6H-7 WR, 30.0--35.0 cm	44.575	44.129	44.625	44.175	910WTX	2
C9033A-7H-4 WR, 85.0--90.0 cm	52.14	51.949	52.19	51.996	910WTX	2
C9033A-7H-7 WR, 85.0--90.0 cm	54.57	54.232	54.62	54.279	910WTX	2
C9033A-8H-4 WR, 55.0--60.0 cm	58.34	58.073	58.39	58.115	910WTX	2
C9033A-8H-12 WR, 0.0--5.0 cm	65.205	63.94	65.255	63.983	910WTX	2
C9033A-9H-4 WR, 0.0--5.0 cm	66.84	66.646	66.89	66.689	910WTX	2
C9033A-9H-5 WR, 60.0--65.0 cm	68.745	68.275	68.795	68.318	910WTX	2
C9033A-9H-9 WR, 0.0--5.0 cm	71.165	70.344	71.215	70.387	910WTX	2
C9033A-10H-5 WR, 90.0--95.0 cm	78.165	77.581	78.215	77.623	910WTX	2
C9033A-10H-10 WR, 35.0--40.0 cm	81.56	80.436	81.61	80.478	910WTX	2
C9033A-11H-3 WR, 25.0--30.0 cm	84.64	84.51	84.69	84.554	910WTX	2
C9033A-11H-10 WR, 30.0--35.0 cm	90.67	89.851	90.72	89.896	910WTX	2
C9033A-12H-11 WR, 0.0--5.0 cm	101.095	99.081	101.145	99.119	910WTX	2
C9033A-1H-3 WR, 0.0--7.0 cm	1.645	1.645	1.715	1.715	HS	5
C9033A-2H-2 WR, 0.0--7.0 cm	3.9	3.823	3.97	3.89	HS	5

C9033A-2H-5 WR, 0.0--6.0 cm	6.785	6.551	6.845	6.607	HS	5
C9033A-2H-8 WR, 0.0--6.0 cm	9.69	9.297	9.75	9.353	HS	5
C9033A-3H-2 WR, 0.0--6.0 cm	13.105	13.012	13.165	13.067	HS	5
C9033A-3H-5 WR, 0.0--6.0 cm	15.495	15.2	15.555	15.255	HS	5
C9033A-3H-10 WR, 0.0--6.0 cm	20.415	19.705	20.475	19.759	HS	5
C9033A-4H-3 WR, 0.0--6.0 cm	23.71	23.42	23.77	23.473	HS	5
C9033A-4H-6 WR, 0.0--6.0 cm	26.48	25.893	26.54	25.946	HS	5
C9033A-4H-10 WR, 0.0--6.0 cm	29.395	28.496	29.455	28.549	HS	5
C9033A-5H-3 WR, 0.0--6.0 cm	32.705	32.376	32.765	32.427	HS	5
C9033A-5H-5 WR, 0.0--22.0 cm	34.025	33.499	34.245	33.686	HS	5
C9033A-5H-9 WR, 0.0--6.0 cm	37.915	36.808	37.975	36.859	HS	5
C9033A-6H-4 WR, 0.0--6.0 cm	41.805	41.603	41.865	41.657	HS	5
C9033A-6H-9 WR, 0.0--6.0 cm	46.39	45.785	46.45	45.839	HS	5
C9033A-6H-12 WR, 0.0--6.0 cm	48.86	48.038	48.92	48.092	HS	5
C9033A-7H-5 WR, 0.0--6.0 cm	52.5	52.287	52.56	52.344	HS	5
C9033A-7H-8 WR, 0.0--6.0 cm	54.93	54.57	54.99	54.626	HS	5
C9033A-8H-3 WR, 0.0--8.0 cm	57.71	57.534	57.79	57.603	HS	5
C9033A-8H-7 WR, 0.0--7.0 cm	61.465	60.744	61.535	60.803	HS	5
C9033A-8H-11 WR, 0.0--7.0 cm	65.135	63.88	65.205	63.94	HS	5
C9033A-9H-3 WR, 0.0--10.0 cm	66.74	66.56	66.84	66.646	HS	5
C9033A-9H-7 WR, 0.0--10.0 cm	69.76	69.143	69.86	69.228	HS	5
C9033A-9H-10 WR, 0.0--7.0 cm	72.47	71.46	72.54	71.52	HS	5
C9033A-10H-3 WR, 0.0--7.0 cm	75.895	75.673	75.965	75.732	HS	5
C9033A-10H-6 WR, 0.0--7.0 cm	78.565	77.918	78.635	77.976	HS	5
C9033A-10H-9 WR, 0.0--7.0 cm	81.14	80.082	81.21	80.141	HS	5
C9033A-11H-5 WR, 0.0--7.0 cm	86.675	86.313	86.745	86.375	HS	5
C9033A-11H-8 WR, 0.0--7.0 cm	89.1	88.461	89.17	88.523	HS	5
C9033A-11H-12 WR, 0.0--7.0 cm	92.495	91.468	92.565	91.53	HS	5
C9033A-12H-3 WR, 0.0--7.0 cm	94.93	94.361	95	94.414	HS	5
C9033A-12H-6 WR, 0.0--7.0 cm	97.65	96.443	97.72	96.497	HS	5
C9033A-12H-10 WR, 0.0--7.0 cm	101.025	99.028	101.095	99.081	HS	5
C9033A-1H-3 WR, 0.0--7.0 cm	1.645	1.645	1.715	1.715	HSH2	5
C9033A-2H-2 WR, 0.0--7.0 cm	3.9	3.823	3.97	3.89	HSH2	5
C9033A-2H-5 WR, 0.0--6.0 cm	6.785	6.551	6.845	6.607	HSH2	5
C9033A-2H-8 WR, 0.0--6.0 cm	9.69	9.297	9.75	9.353	HSH2	5
C9033A-3H-2 WR, 0.0--6.0 cm	13.105	13.012	13.165	13.067	HSH2	5
C9033A-3H-5 WR, 0.0--6.0 cm	15.495	15.2	15.555	15.255	HSH2	5
C9033A-3H-10 WR, 0.0--6.0 cm	20.415	19.705	20.475	19.759	HSH2	5
C9033A-4H-3 WR, 0.0--6.0 cm	23.71	23.42	23.77	23.473	HSH2	5
C9033A-4H-6 WR, 0.0--6.0 cm	26.48	25.893	26.54	25.946	HSH2	5
C9033A-4H-10 WR, 0.0--6.0 cm	29.395	28.496	29.455	28.549	HSH2	5
C9033A-5H-3 WR, 0.0--6.0 cm	32.705	32.376	32.765	32.427	HSH2	5
C9033A-5H-5 WR, 0.0--22.0 cm	34.025	33.499	34.245	33.686	HSH2	5
C9033A-5H-9 WR, 0.0--6.0 cm	37.915	36.808	37.975	36.859	HSH2	5
C9033A-6H-4 WR, 0.0--6.0 cm	41.805	41.603	41.865	41.657	HSH2	5
C9033A-6H-9 WR, 0.0--6.0 cm	46.39	45.785	46.45	45.839	HSH2	5
C9033A-6H-12 WR, 0.0--6.0 cm	48.86	48.038	48.92	48.092	HSH2	5
C9033A-7H-5 WR, 0.0--6.0 cm	52.5	52.287	52.56	52.344	HSH2	5
C9033A-7H-8 WR, 0.0--6.0 cm	54.93	54.57	54.99	54.626	HSH2	5
C9033A-8H-3 WR, 0.0--8.0 cm	57.71	57.534	57.79	57.603	HSH2	5
C9033A-8H-7 WR, 0.0--7.0 cm	61.465	60.744	61.535	60.803	HSH2	5
C9033A-8H-11 WR, 0.0--7.0 cm	65.135	63.88	65.205	63.94	HSH2	5
C9033A-9H-3 WR, 0.0--10.0 cm	66.74	66.56	66.84	66.646	HSH2	5
C9033A-9H-7 WR, 0.0--10.0 cm	69.76	69.143	69.86	69.228	HSH2	5
C9033A-9H-10 WR, 0.0--7.0 cm	72.47	71.46	72.54	71.52	HSH2	5
C9033A-10H-3 WR, 0.0--7.0 cm	75.895	75.673	75.965	75.732	HSH2	5
C9033A-10H-6 WR, 0.0--7.0 cm	78.565	77.918	78.635	77.976	HSH2	5
C9033A-10H-9 WR, 0.0--7.0 cm	81.14	80.082	81.21	80.141	HSH2	5
C9033A-11H-5 WR, 0.0--7.0 cm	86.675	86.313	86.745	86.375	HSH2	5
C9033A-11H-8 WR, 0.0--7.0 cm	89.1	88.461	89.17	88.523	HSH2	5
C9033A-11H-12 WR, 0.0--7.0 cm	92.495	91.468	92.565	91.53	HSH2	5
C9033A-12H-3 WR, 0.0--7.0 cm	94.93	94.361	95	94.414	HSH2	5
C9033A-12H-6 WR, 0.0--7.0 cm	97.65	96.443	97.72	96.497	HSH2	5
C9033A-12H-10 WR, 0.0--7.0 cm	101.025	99.028	101.095	99.081	HSH2	5
C9033A-1H-1 WR, 135.0--139.5 cm	1.35	1.35	1.395	1.395	PP	10
C9033A-2H-6 WR, 135.0--140.0 cm	8.195	7.883	8.245	7.931	PP	10
C9033A-2H-9 WR, 136.0--141.0 cm	11.11	10.639	11.16	10.686	PP	10
C9033A-3H-7 WR, 69.0--74.0 cm	17.47	17.008	17.52	17.054	PP	10
C9033A-3H-11 WR, 0.0--6.0 cm	20.475	19.759	20.535	19.814	PP	10

C9033A-4H-5 WR, 118.0--123.0 cm	26.33	25.759	26.38	25.804	PP	10
C9033A-4H-9 WR, 85.0--90.0 cm	28.935	28.085	28.985	28.13	PP	10
C9033A-5H-4 WR, 60.0--65.0 cm	33.365	32.937	33.415	32.98	PP	10
C9033A-5H-10 WR, 25.0--30.0 cm	38.225	37.071	38.275	37.114	PP	10
C9033A-6H-5 WR, 0.0--6.0 cm	41.865	41.657	41.925	41.712	PP	10
C9033A-6H-7 WR, 30.0--35.0 cm	44.575	44.129	44.625	44.175	PP	10
C9033A-6H-13 WR, 0.0--5.0 cm	48.92	48.092	48.97	48.138	PP	10
C9033A-7H-4 WR, 85.0--90.0 cm	52.14	51.949	52.19	51.996	PP	10
C9033A-7H-7 WR, 15.0--20.0 cm	53.87	53.574	53.92	53.621	PP	10
C9033A-8H-4 WR, 55.0--60.0 cm	58.34	58.073	58.39	58.115	PP	10
C9033A-8H-12 WR, 0.0--5.0 cm	65.205	63.94	65.255	63.983	PP	10
C9033A-9H-4 WR, 0.0--5.0 cm	66.84	66.646	66.89	66.689	PP	10
C9033A-9H-5 WR, 0.0--5.0 cm	68.145	67.762	68.195	67.805	PP	10
C9033A-9H-9 WR, 0.0--5.0 cm	71.165	70.344	71.215	70.387	PP	10
C9033A-10H-5 WR, 95.0--100.0 cm	78.215	77.623	78.265	77.665	PP	10
C9033A-10H-10 WR, 34.0--40.0 cm	81.55	80.427	81.61	80.478	PP	10
C9033A-11H-3 WR, 25.0--31.0 cm	84.64	84.51	84.7	84.563	PP	10
C9033A-11H-10 WR, 29.0--35.0 cm	90.66	89.843	90.72	89.896	PP	10
C9033A-12H-11 WR, 0.0--6.0 cm	101.095	99.081	101.155	99.127	PP	10
C9033A-4H-2 WR, 6.0 cm	22.46	22.304	22.46	22.304	VAC	100
C9033A-4H-11 WR, 26.0 cm	29.715	28.781	29.715	28.781	VAC	100
C9033A-5H-5 WR, 22.0 cm	34.245	33.686	34.245	33.686	VAC	100
C9033A-5H-11 WR, 34.0 cm	39.475	38.135	39.475	38.135	VAC	100
C9033A-6H-2 WR, 97.5 cm	40.6	40.503	40.6	40.503	VAC	100
C9033A-6H-11 WR, 68.0 cm	48.33	47.554	48.33	47.554	VAC	100
C9033A-7H-3 WR, 31.0 cm	50.6	50.503	50.6	50.503	VAC	100
C9033A-7H-9 WR, 10.0 cm	55.09	54.72	55.09	54.72	VAC	100
C9033A-8H-4 WR, 75.0 cm	58.54	58.244	58.54	58.244	VAC	100
C9033A-8H-10 WR, 107.0 cm	65.005	63.769	65.005	63.769	VAC	100
C9033A-9H-4 WR, 102.0 cm	67.86	67.518	67.86	67.518	VAC	100
C9033A-9H-12 WR, 59.5 cm	74.44	73.145	74.44	73.145	VAC	100
C9033A-10H-4 WR, 0.0 cm	75.965	75.732	75.965	75.732	VAC	100
C9033A-10H-12 WR, 64.0 cm	83.61	82.159	83.61	82.159	VAC	100
C9033A-11H-3 WR, 87.0 cm	85.26	85.059	85.26	85.059	VAC	100
C9033A-11H-11 WR, 69.0 cm	92.26	91.26	92.26	91.26	VAC	100
C9033A-12H-2 WR, 95.0 cm	94.475	94.012	94.475	94.012	VAC	100
C9033A-12H-9 WR, 47.0 cm	100.63	98.725	100.63	98.725	VAC	100

Hole	Core	Type	Sec.	Top(cm)	Bottom (cm)	Interval (cm)	IWIC (mL)	910VFA (mL)	910DIC (mL)	910H2O (mL)	910OM (mL)	910FTMS (mL)	910HTIW (mL)
A	1	H	1	55	70	15	3	5	1.5	3	1.5		120
A	2	H	3	25	40	15	3	5	1.5	3	1.5		90
A	2	H	6	25	40	15	3	5	1.5	3	1.5		70
A	2	H	9	25	40	15	3	5	1.5	3	1.5		50
A	3	H	4	55	75	20	3	5	1.5	3	1.5	30	30
A	3	H	7	90	105	15	3	5	1.5	3	1.5		30
A	3	H	9	65	80	15	3	5	1.5	3	1.5		30
A	4	H	2	90	105	15	3	5	1.5	3	1.5		30
A	4	H	5	15	30	15	3	5	1.5	3	1.5		30
A	4	H	9	100	115	15	3	5	1.5	3	1.5		30
A	5	H	2	75	95	20	3	5	1.5	3	1.5	30	30
A	5	H	6	90	104	14	3	5	1.5	3	1.5		30
A	5	H	10	75	90	15	3	5	1.5	3	1.5		30
A	6	H	3	80	95	15	3	5	1.5	3	1.5		30
A	6	H	7	90	105	15	3	5	1.5	3	1.5		30
A	6	H	11	15	35	20	3	5	1.5	3	1.5	30	30
A	7	H	7	85	106	21	3	5	1.5	3	1.5	30	30
A	7	H	4	85	105	20	3	5	1.5	3	1.5	30	30
A	7	H	9	75	95	20	3	5	1.5	3	1.5	30	30
A	8	H	5	30	50	20	3	5	1.5	3	1.5	30	30
A	8	H	8	20	40	20	3	10	1.5	3	1.5	30	30
A	8	H	12	90	105	15	3	10	1.5	3	1.5		30
A	9	H	4	31	46	15	3	10	1.5	3	1.5		30
A	9	H	9	24	44	20	3	10	1.5	3	1.5	30	30
A	9	H	13	35	55	20	3	10	1.5	3	1.5	30	30
A	10	H	5	0	20	20	3	10	1.5	3	1.5	30	30
A	10	H	8	75	95	20	3	10	1.5	3	1.5	30	30
A	10	H	12	103	123	20	3	10	1.5	3	1.5	30	30
A	11	H	3	0	25	25	3	5	1.5	3	1.5	30	30
A	11	H	9	45	65	20	3	5	1.5	3	1.5	30	30
A	11	H	13	25	45	20	3	5	1.5	3	1.5	30	30
A	12	H	8	80	100	20	3	5	1.5	3	1.5	30	30
B	1	H	1	20	-	-	3.5	2	1.5	1			1
B	1	H	1	70	-	-	3.5	2	1.5	1			3
B	1	H	1	120	-	-	3.5	2	1.5	1			1
B	1	H	2	30	-	-	3.5	2	1.5	1			2
B	1	H	2	80	-	-	3.5	2	1.5	1			1
B	1	H	3	50	-	-	3.5	2	1.5	1			3
B	1	H	3	100	-	-	3.5	2	1.5	1			3
B	1	H	4	10	-	-	3.5	2	1.5	1			3
B	1	H	4	60	-	-	3.5	2	1.5	1			3
B	1	H	5	10	-	-	3.5	2	1.5	1			3
B	1	H	5	80	-	-	3.5	2	1.5	1			3
B	1	H	6	30	-	-	3.5	2	1.5	1			1
B	1	H	6	80	-	-	3.5	2	1.5	1			2

Appendix Figure: Visual core description sheets of core sections.

C9033A_1H_1

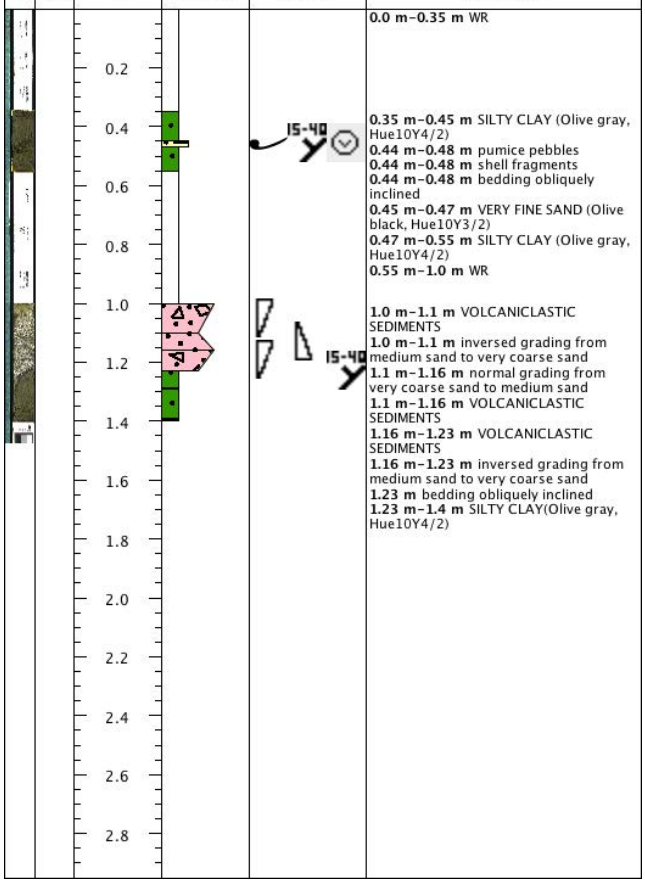

C9033A_1H_2

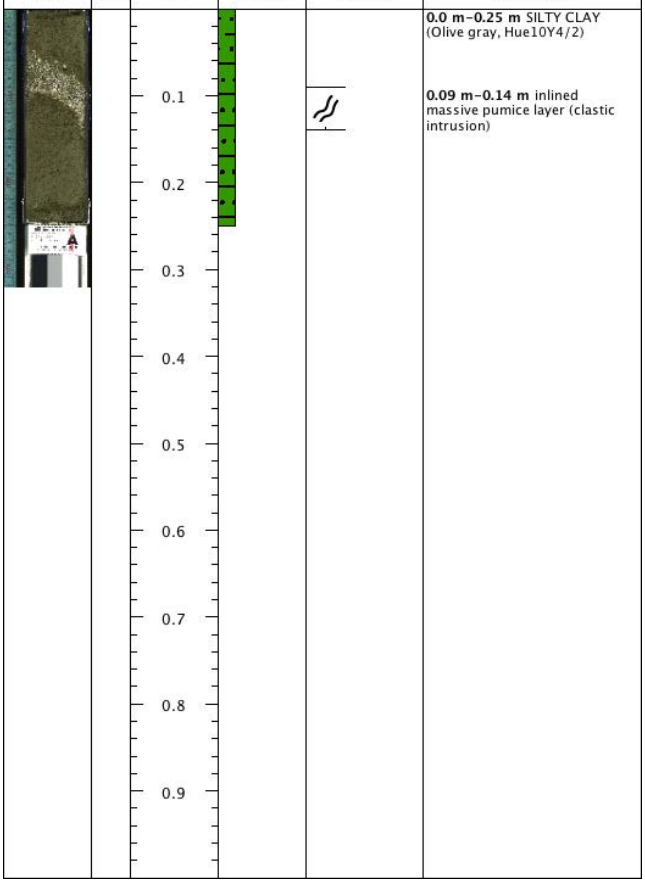

C9033A_1H_CC

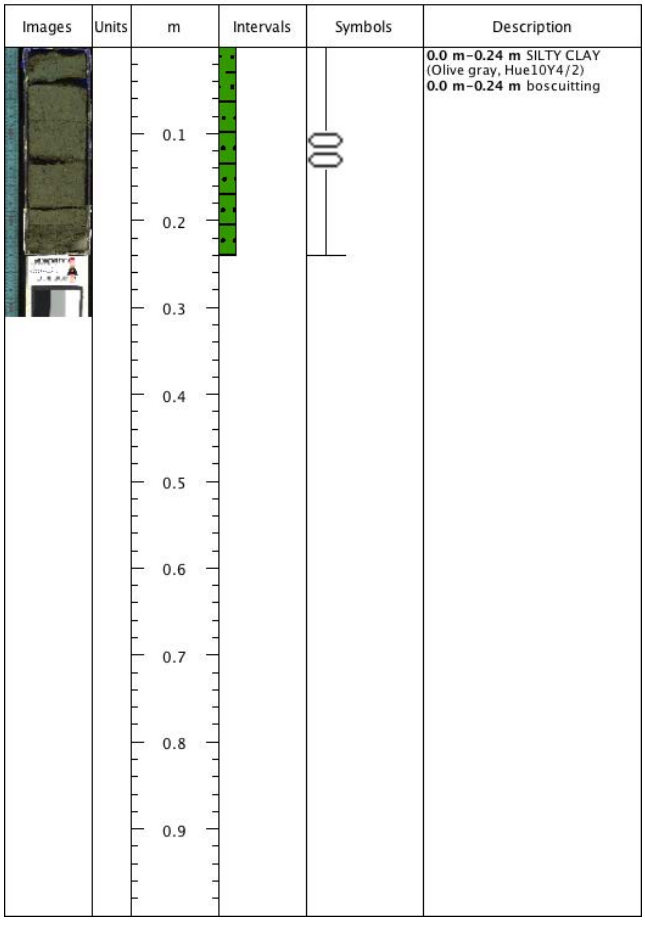

C9033A_2H_1

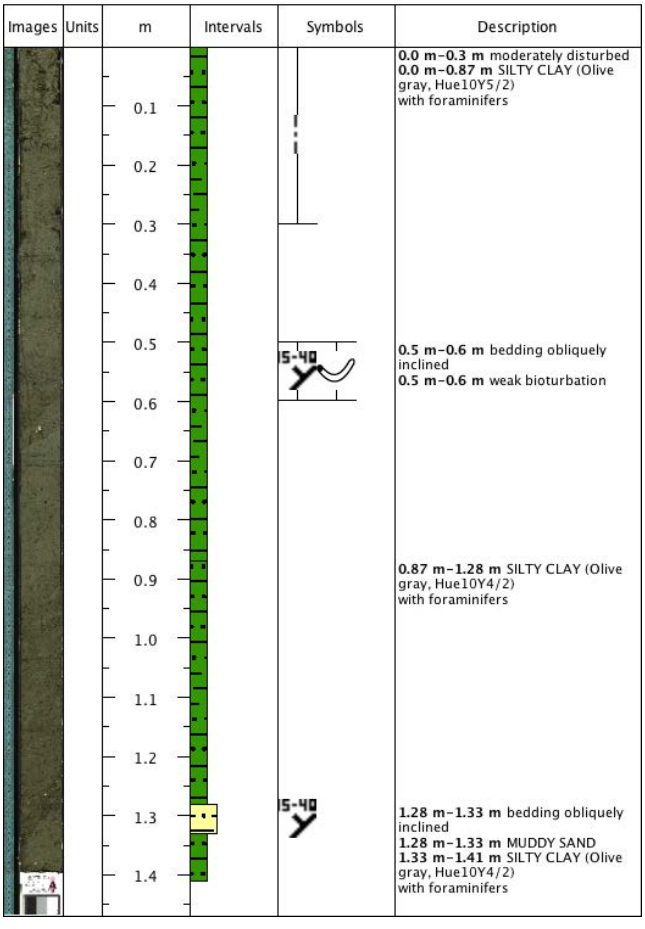

C9033A_2H_3

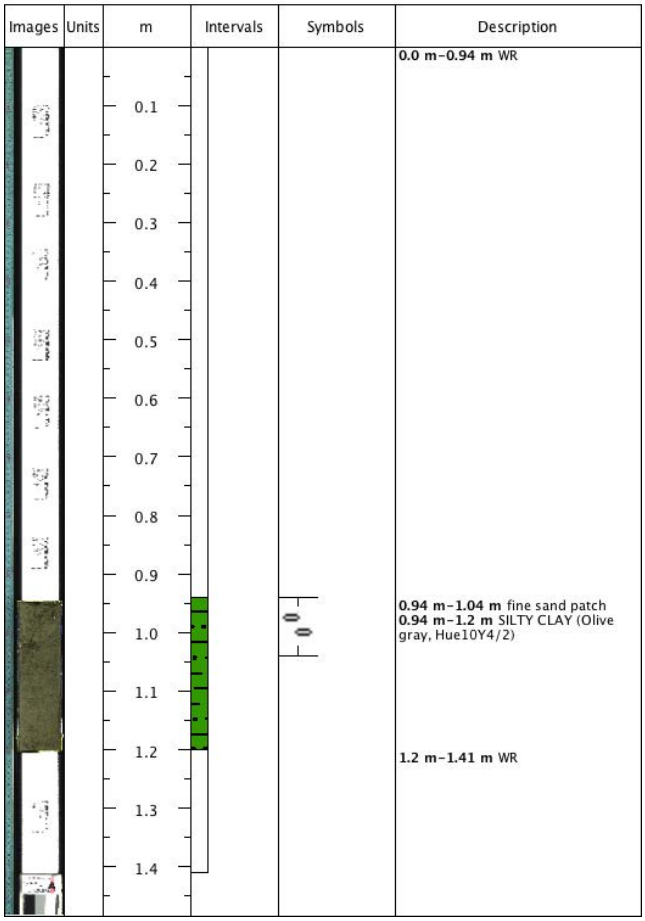

C9033A_2H_4

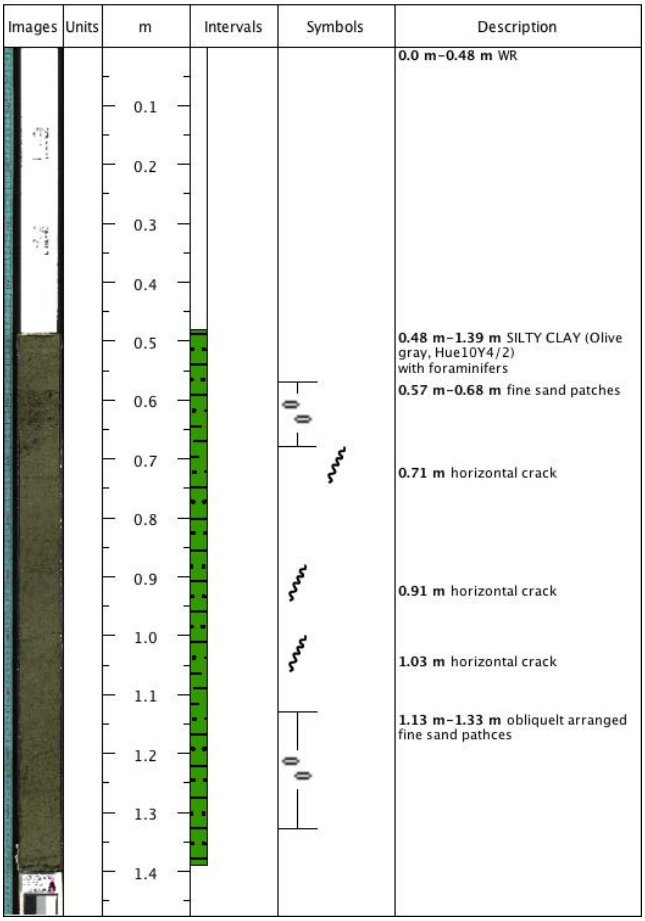

C9033A_2H_6

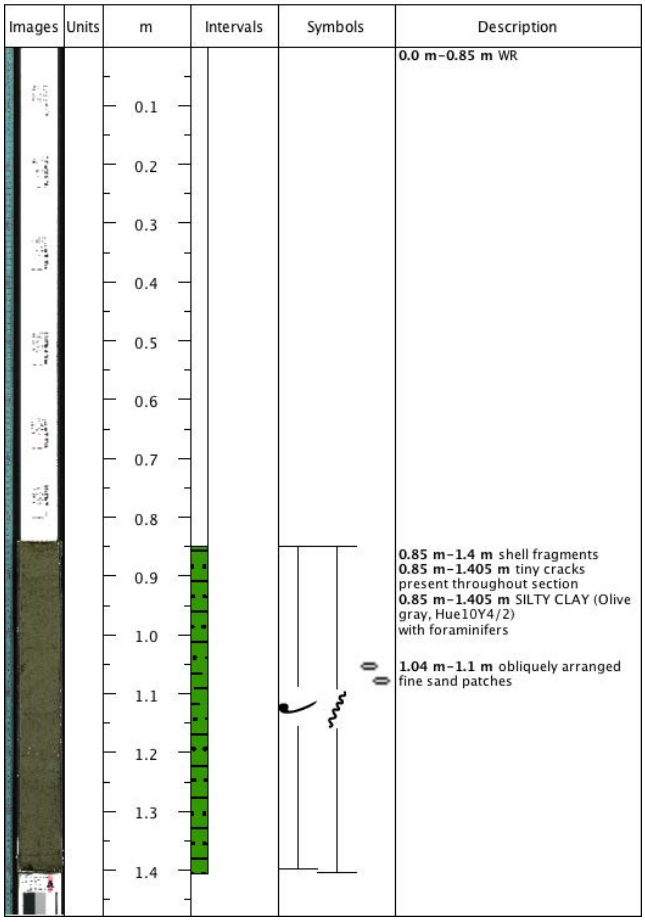

C9033A_2H_7

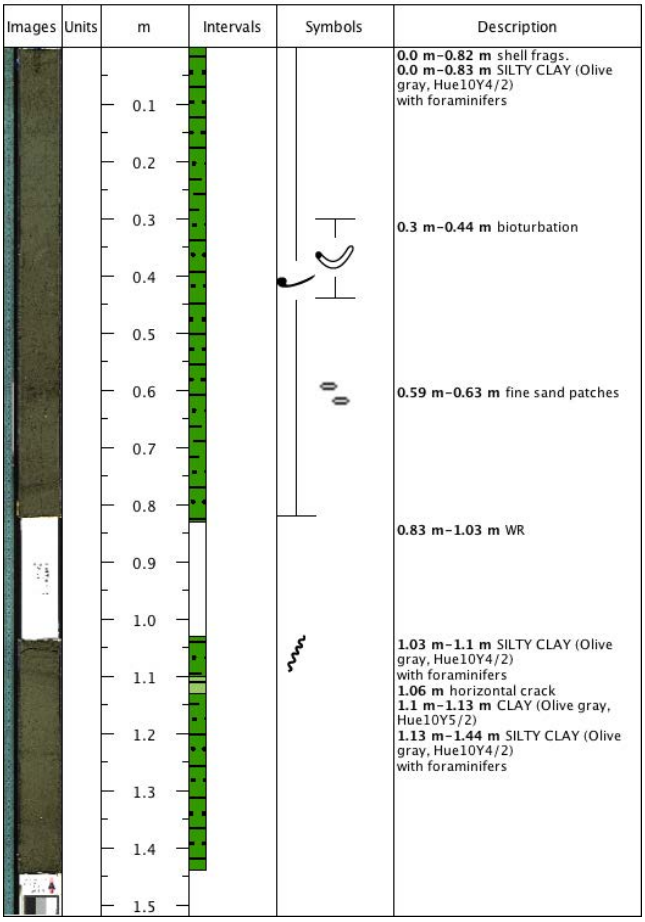

C9033A_2H_9

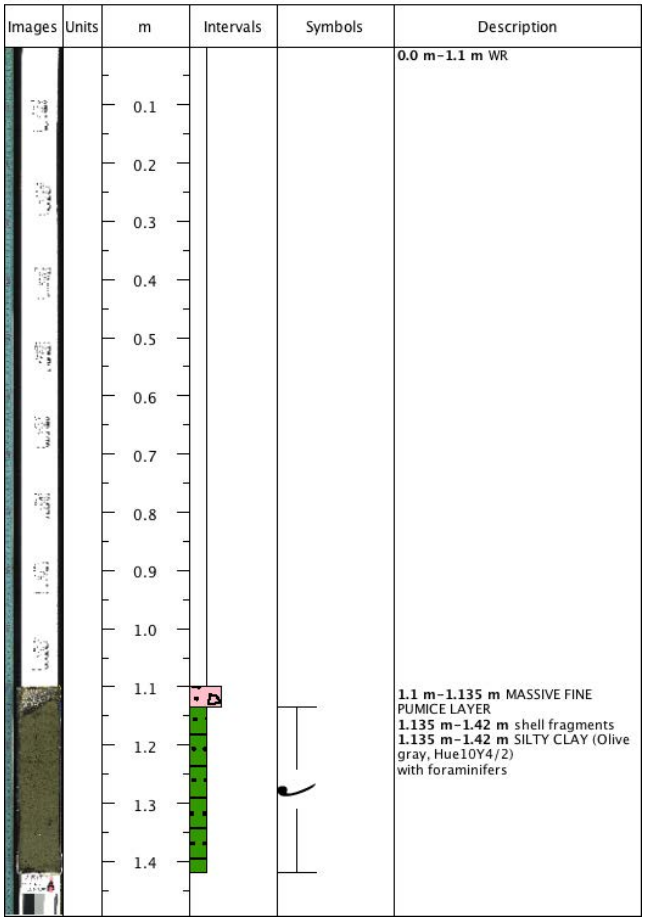

C9033A_2H_10

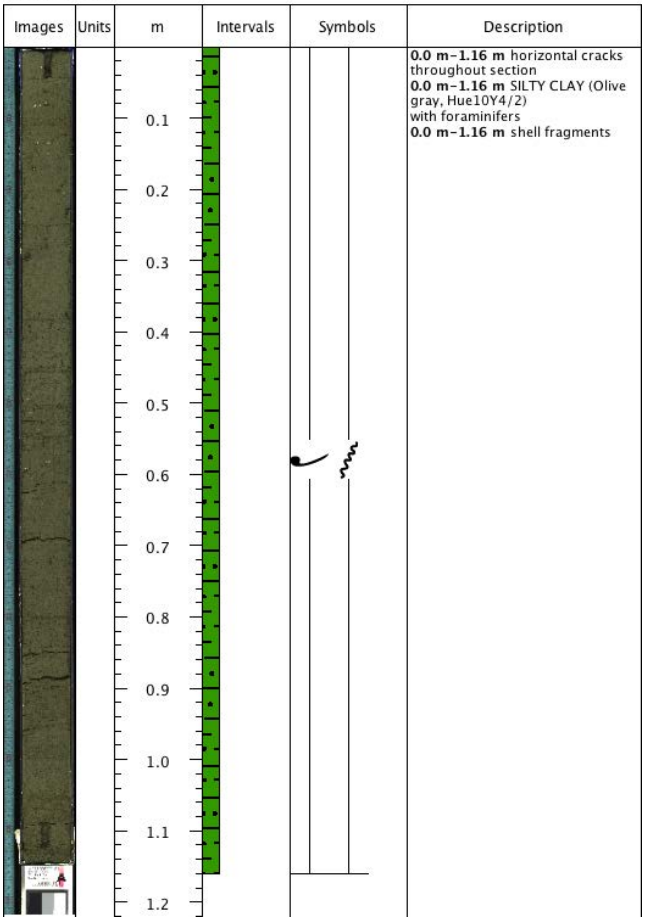

C9033A_2H_CC

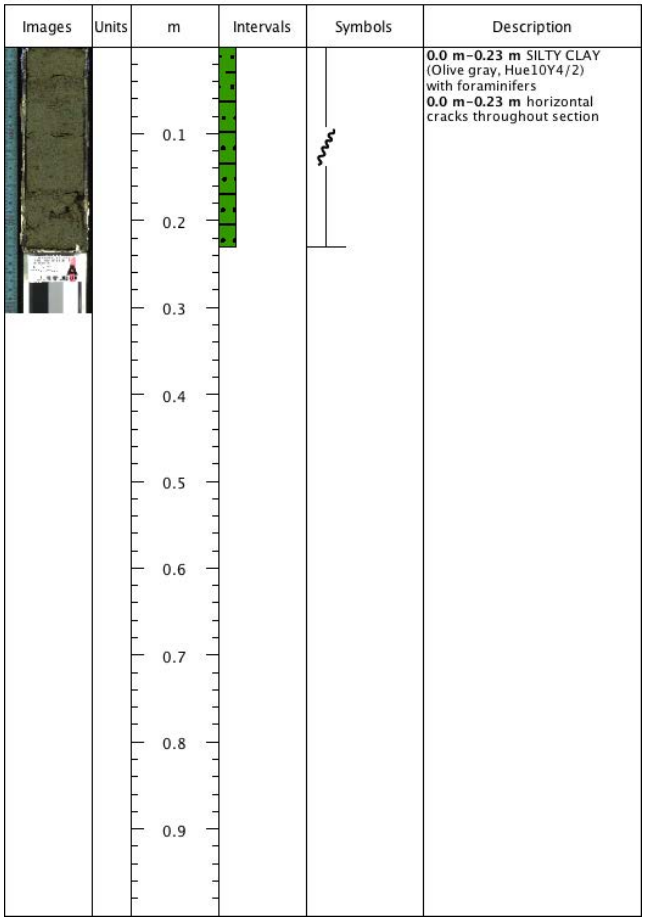

C9033A_3H_1

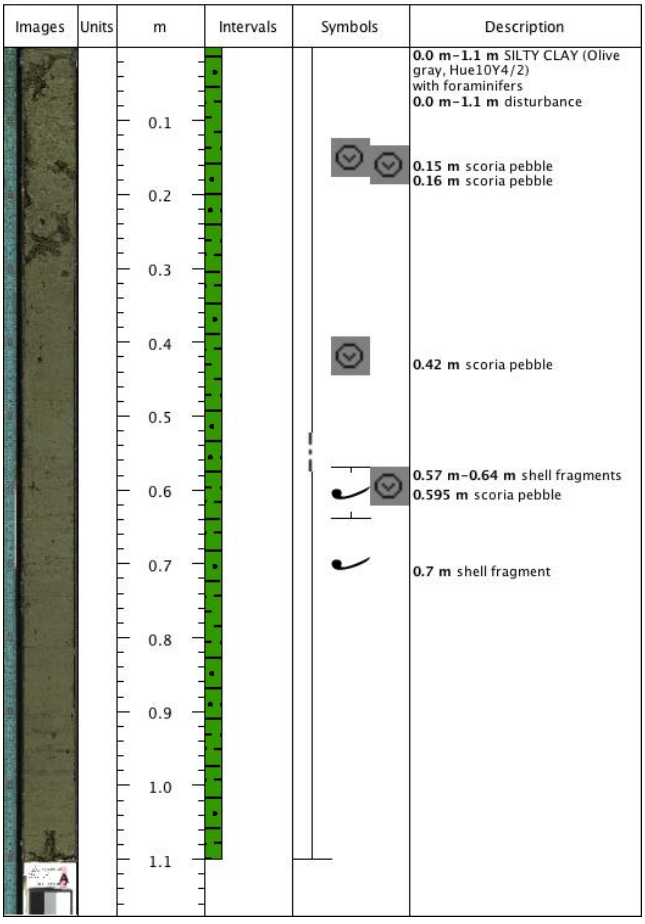

C9033A_3H_3

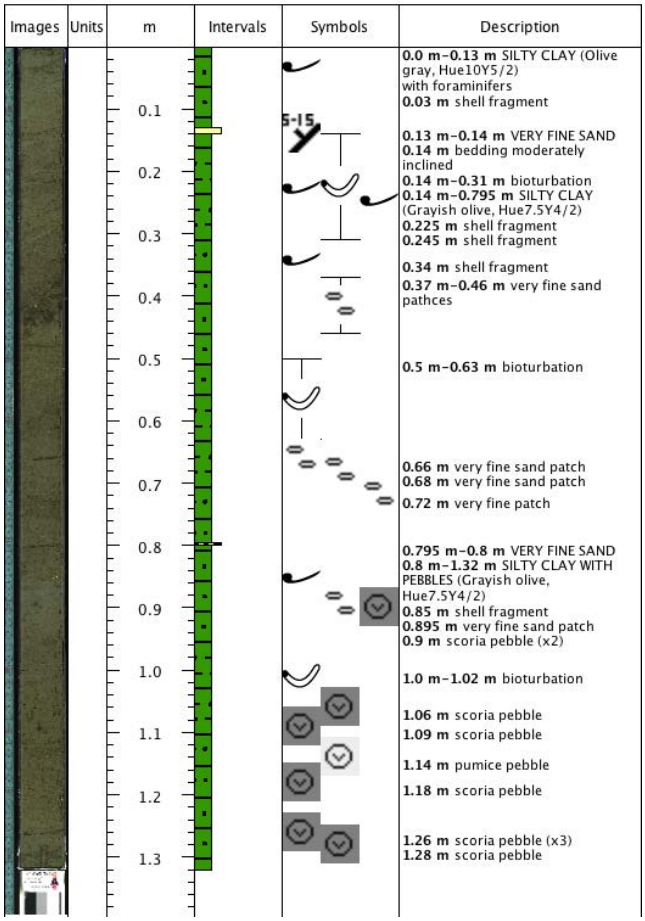

C9033A_3H_6

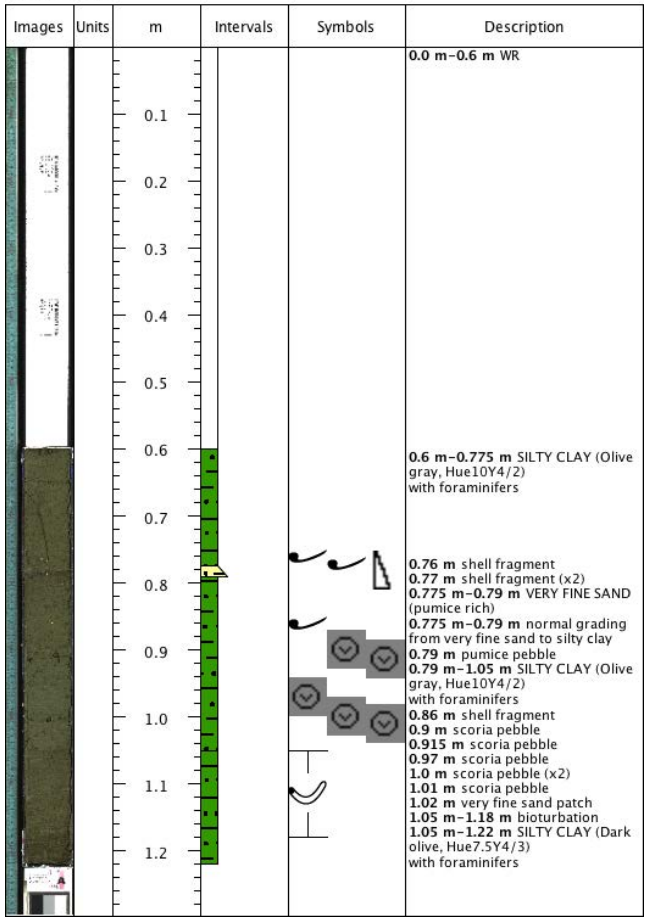

C9033A_3H_7

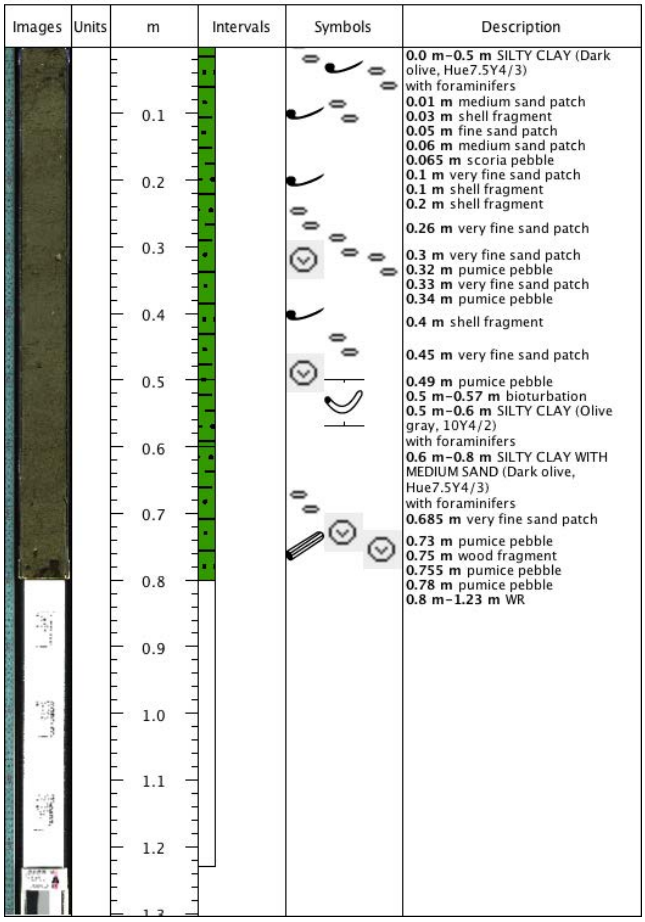

C9033A_3H_8

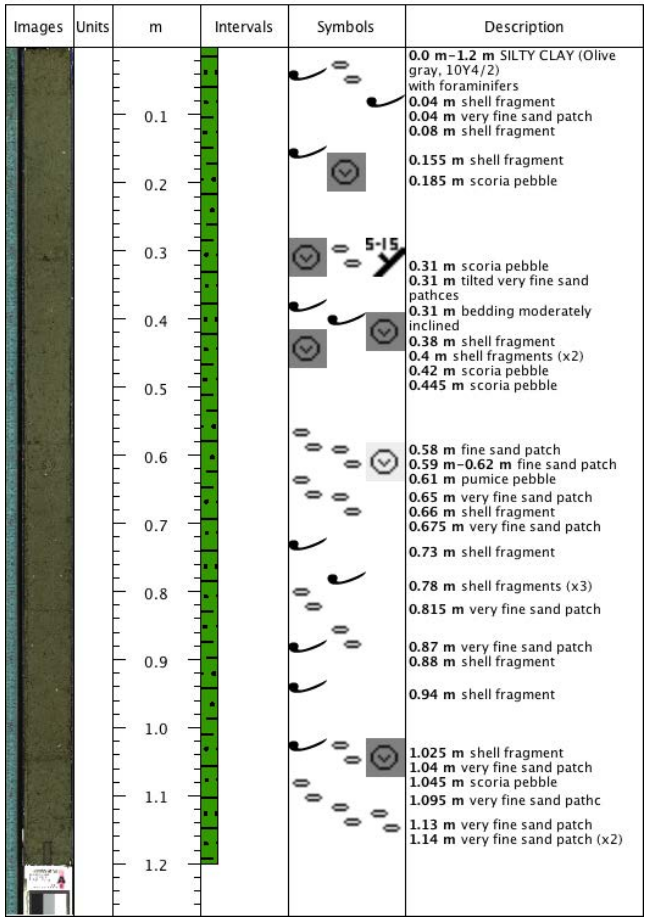

C9033A_3H_11

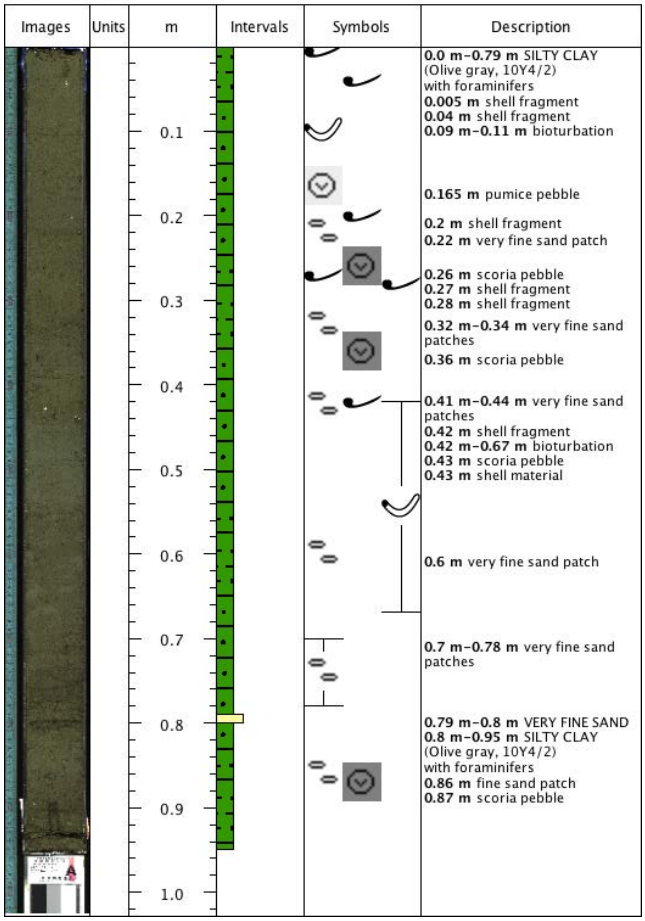

C9033A_3H_CC

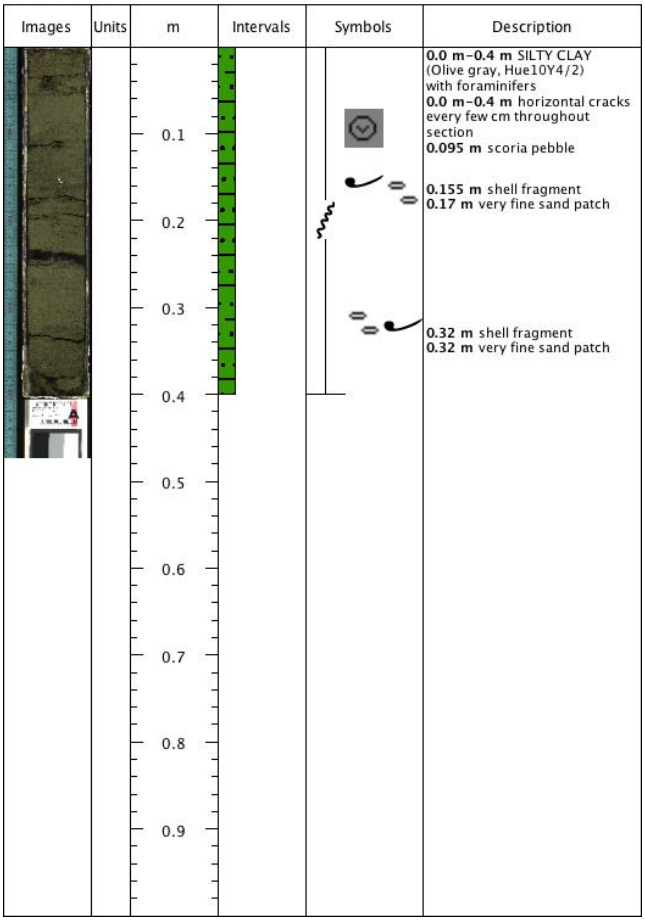

C9033A_4H_1

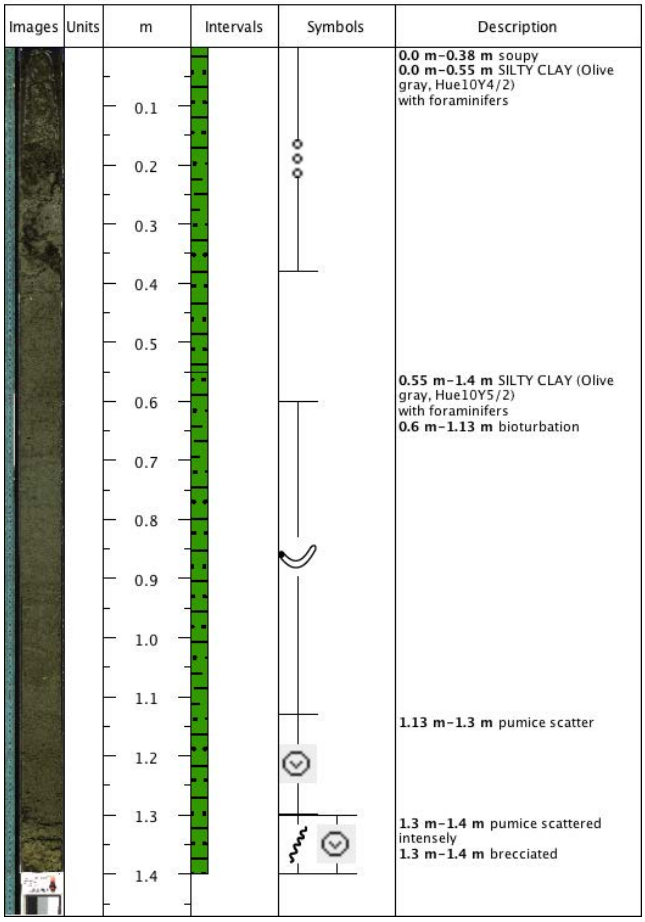

C9033A_4H_2

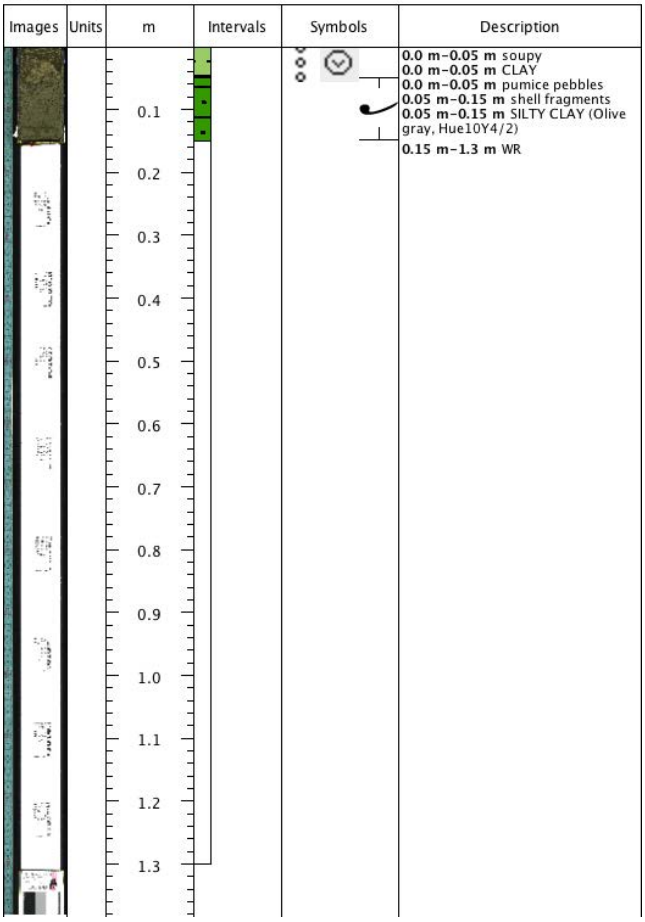

C9033A_4H_4

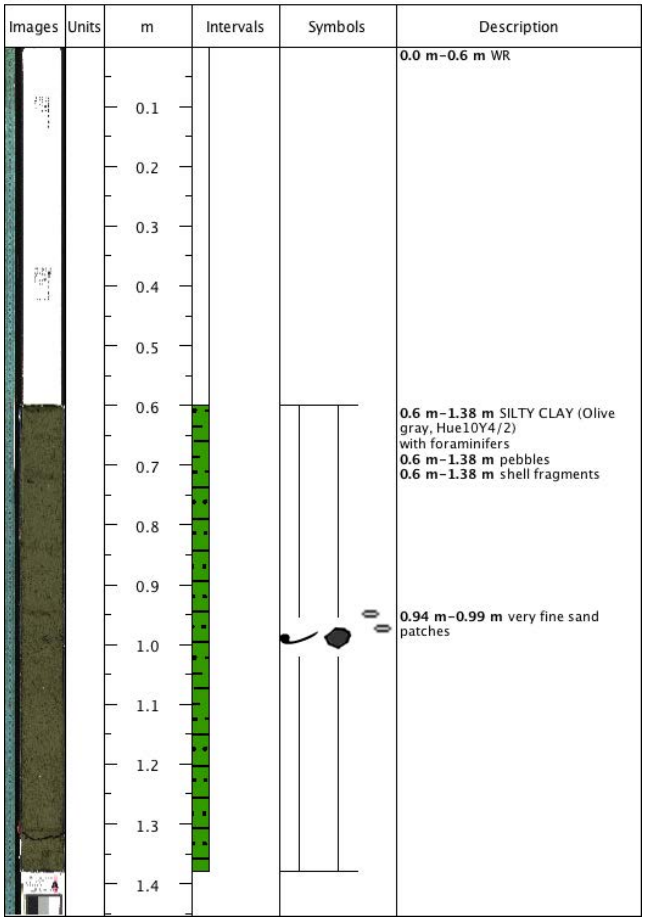

C9033A_4H_5

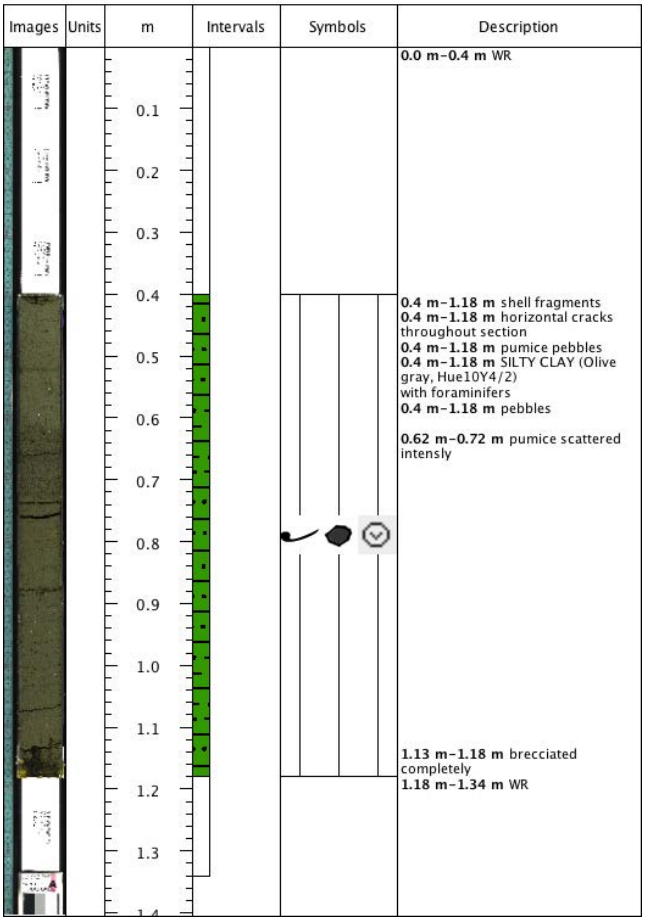

C9033A_4H_7

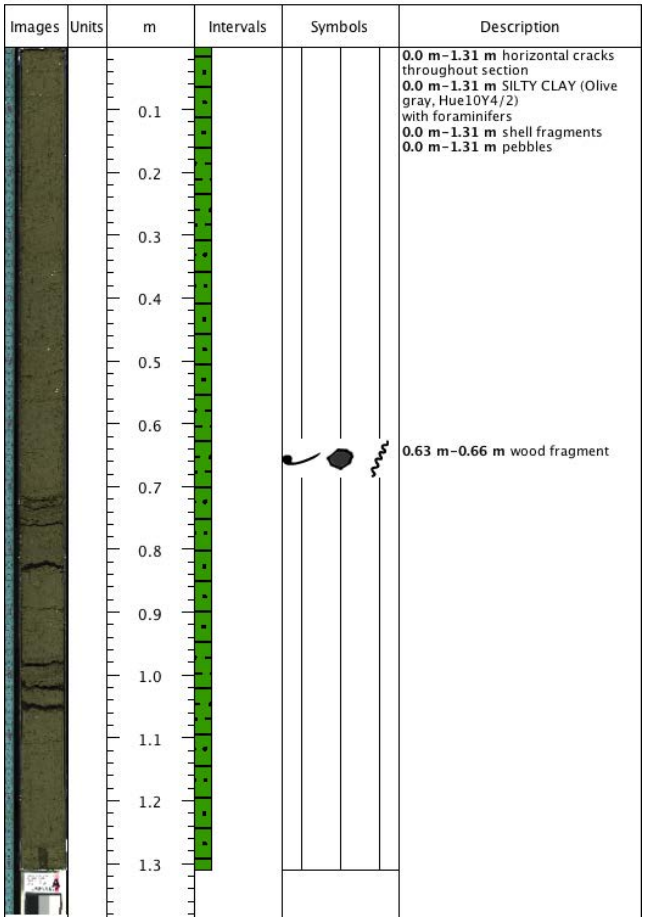

C9033A_4H_8

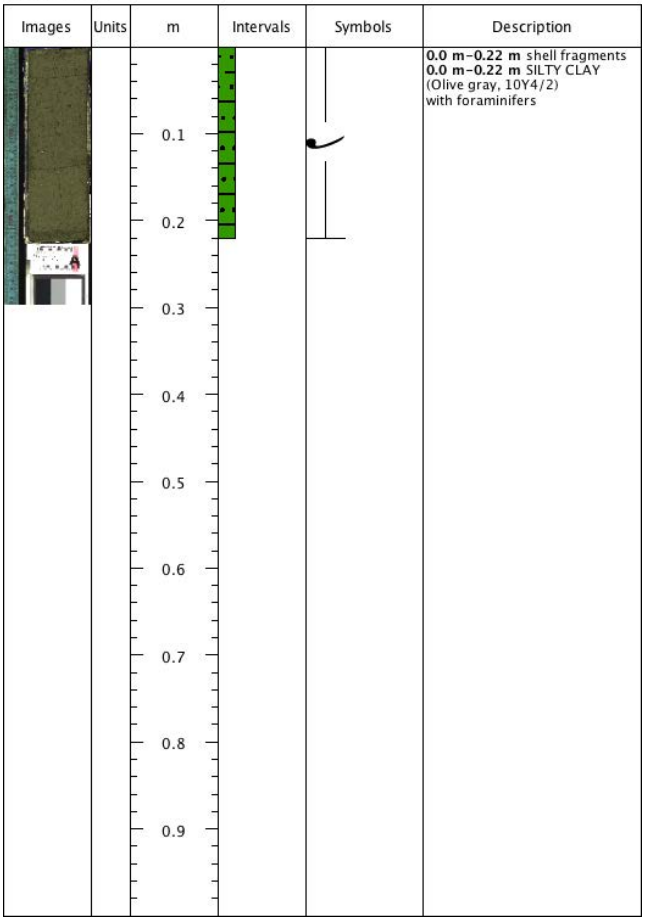

C9033A_4H_9

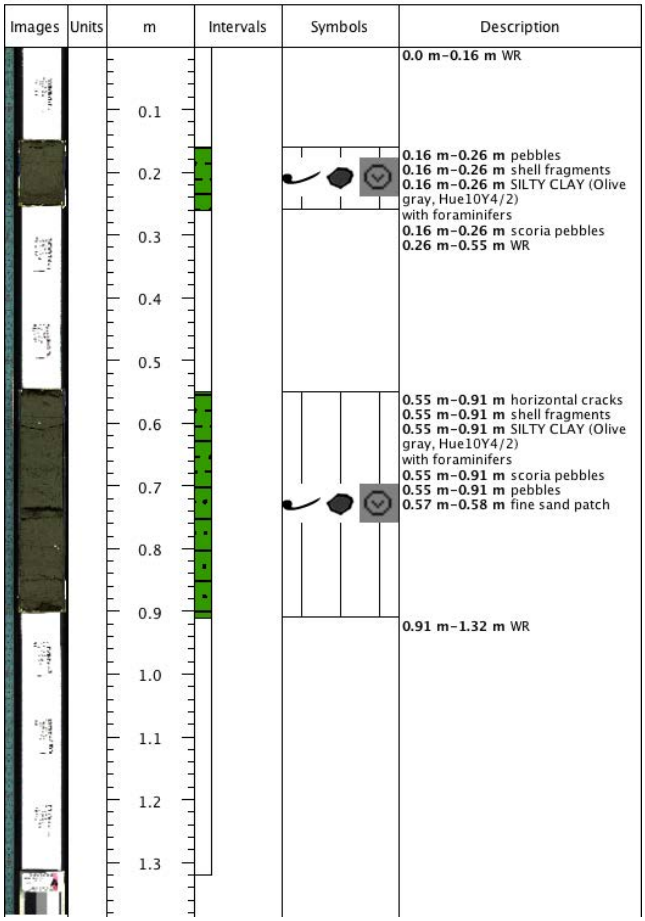

C9033A_4H_11

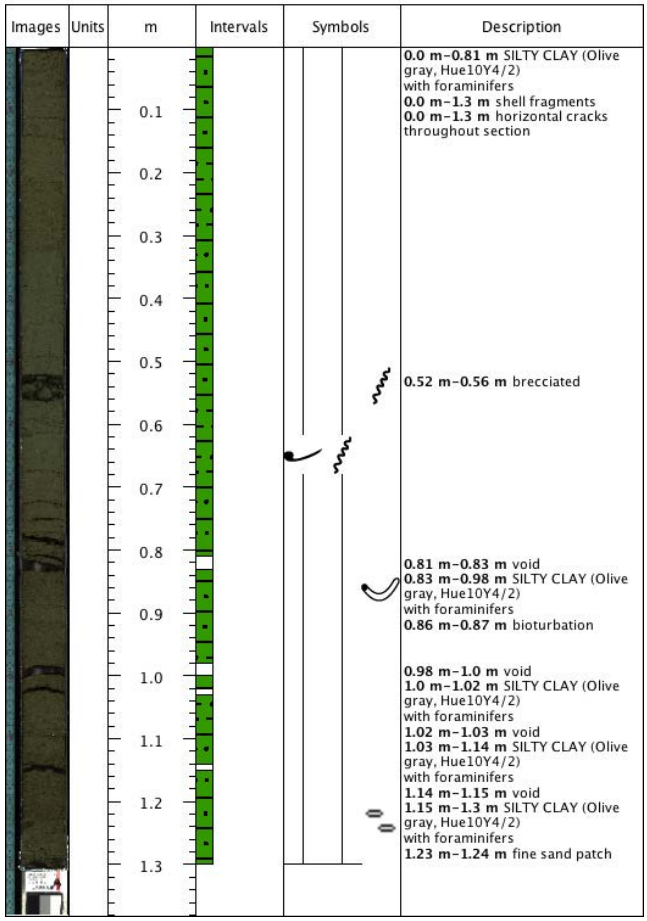

C9033A_4H_12

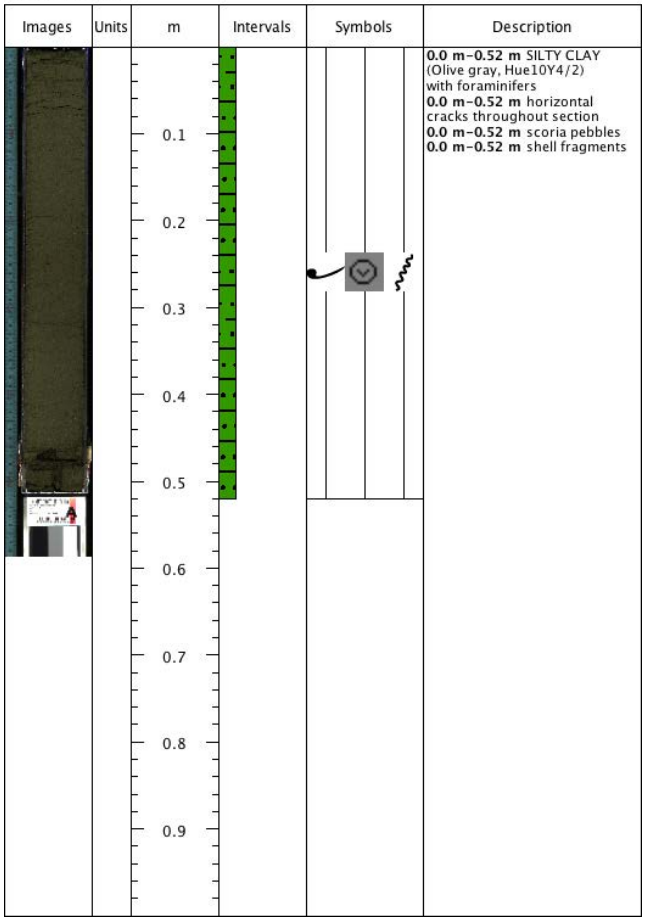

C9033A_4H_CC

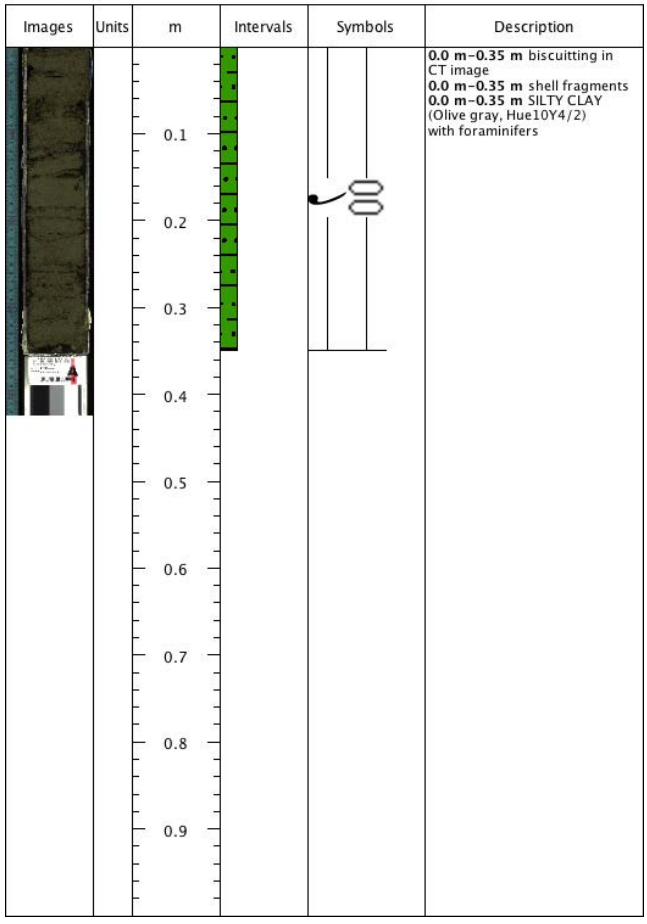

C9033A_5H_1

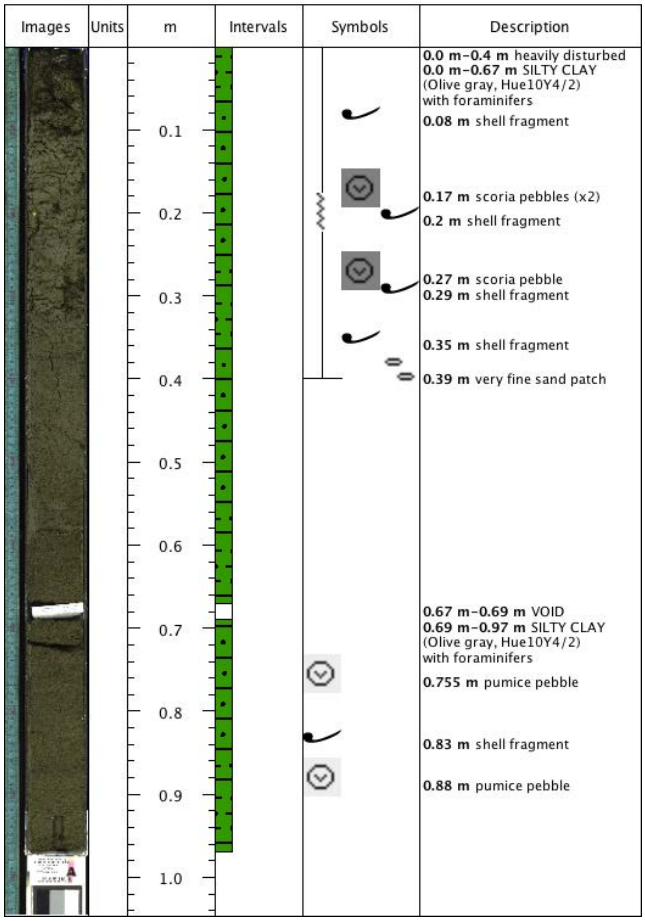

C9033A_5H_4

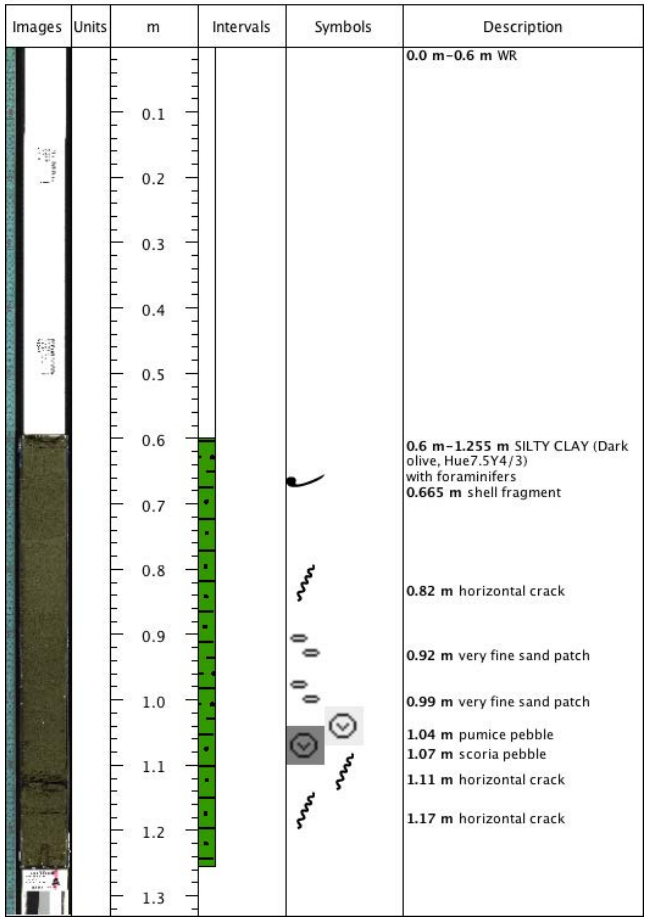

C9033A_5H_6

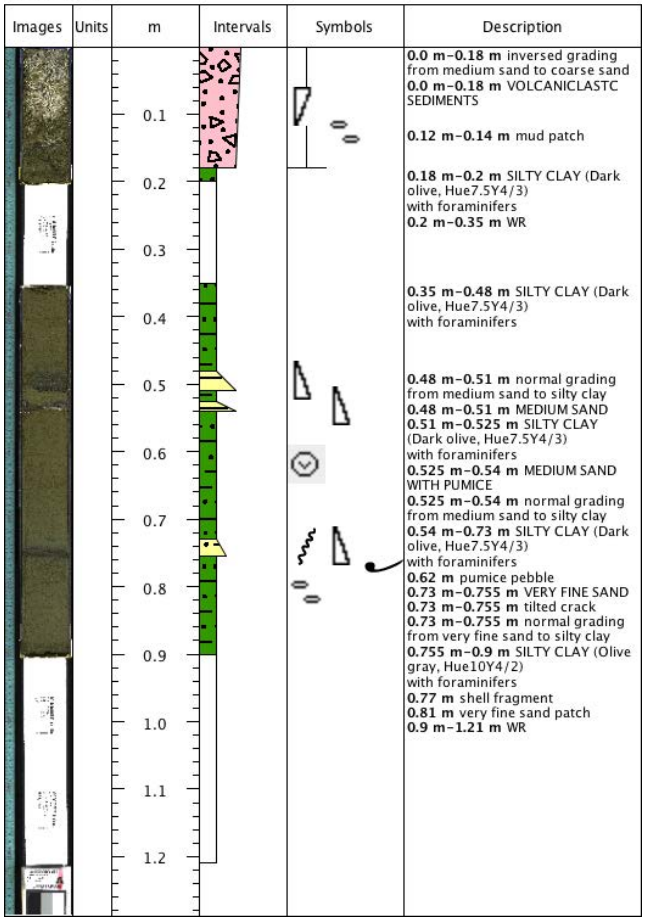

C9033A_5H_7

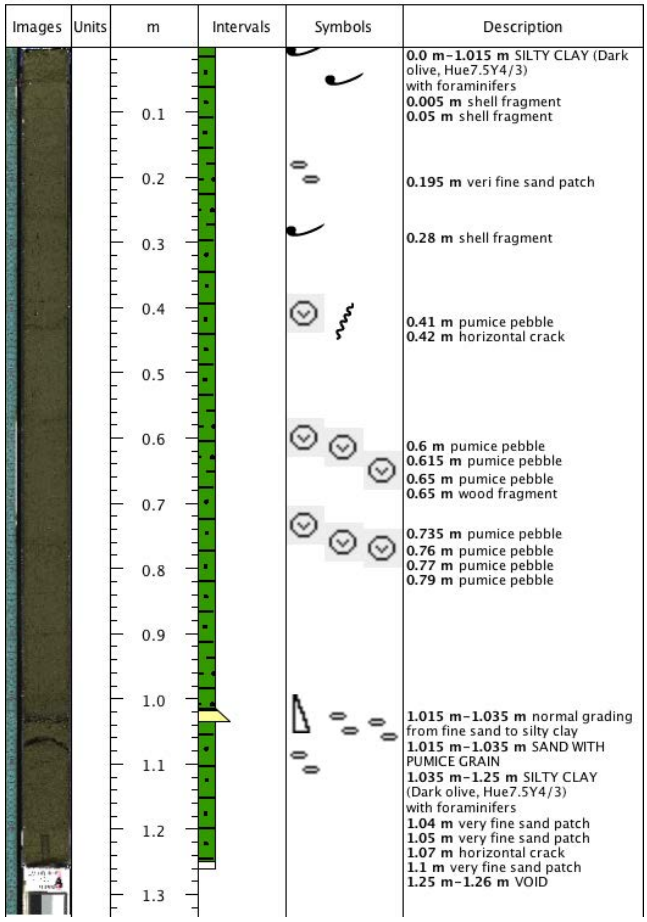

C9033A_5H_8

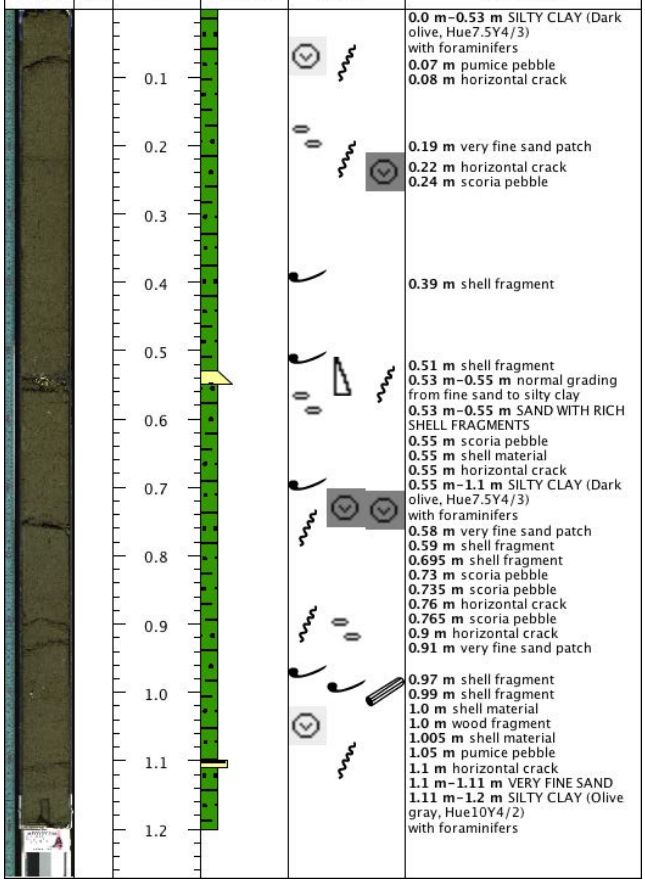

C9033A_5H_10

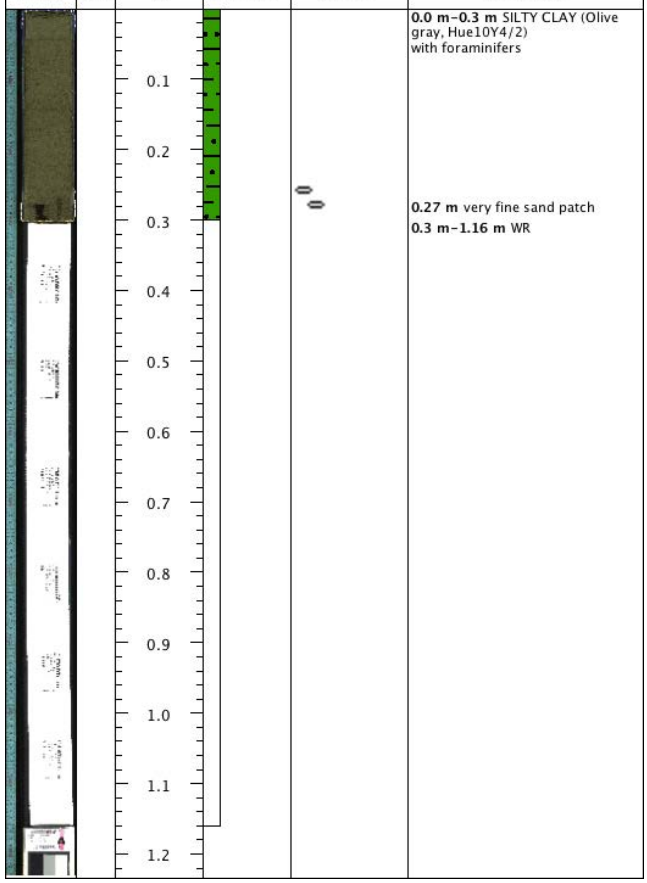

C9033A_5H_11

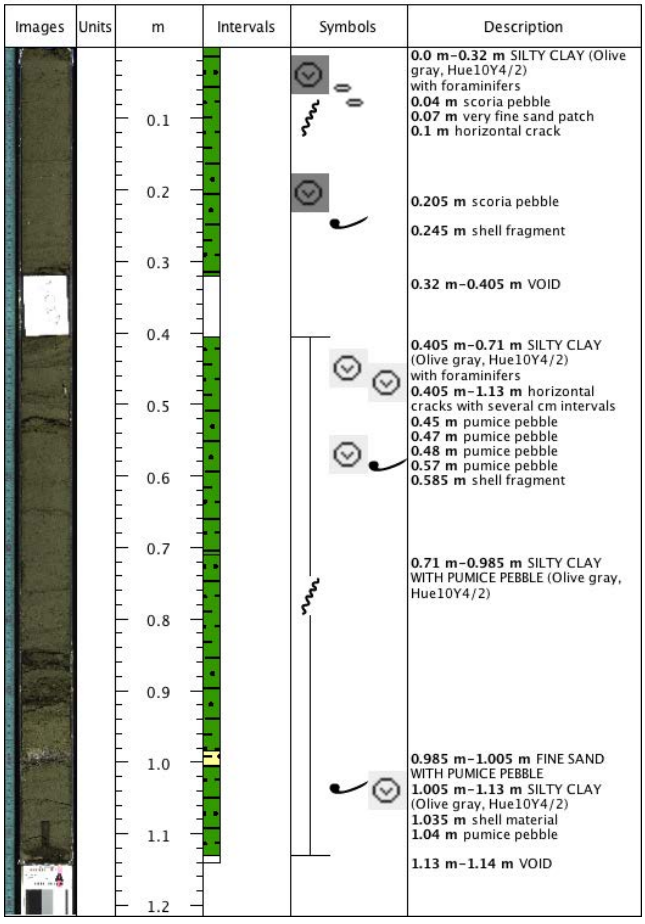

C9033A_5H_CC

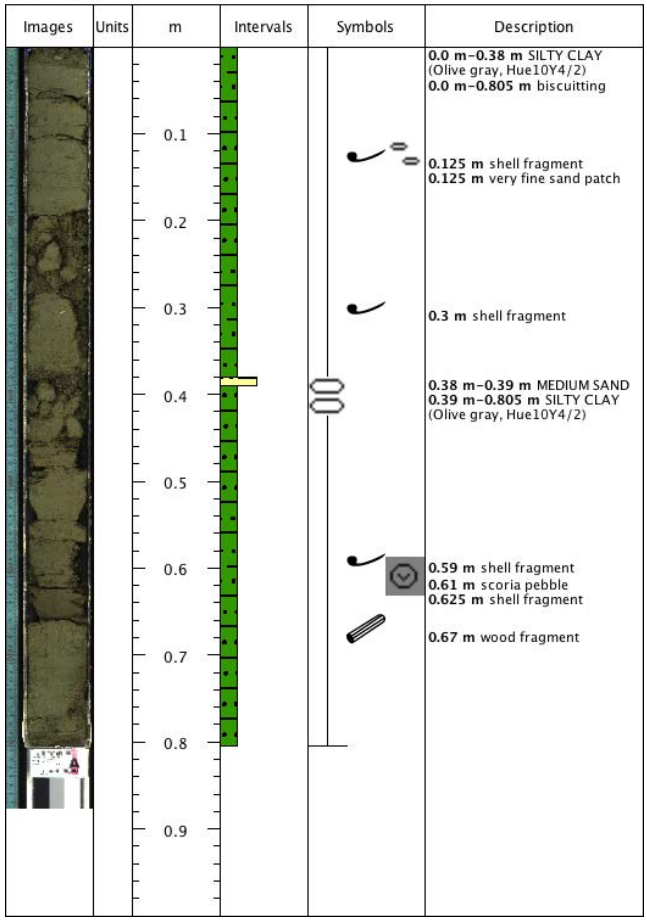

C9033A_6H_1

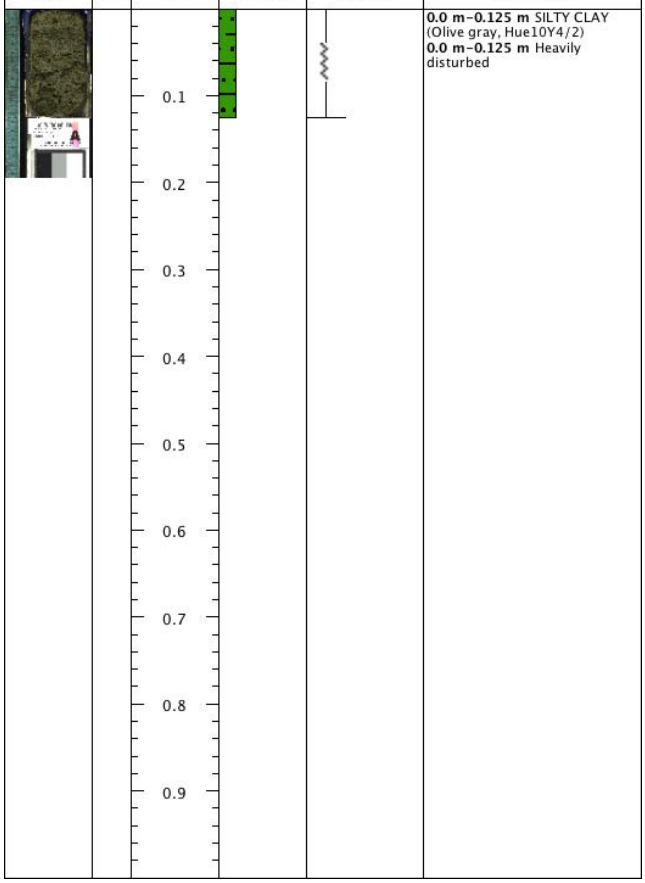

C9033A_6H_2

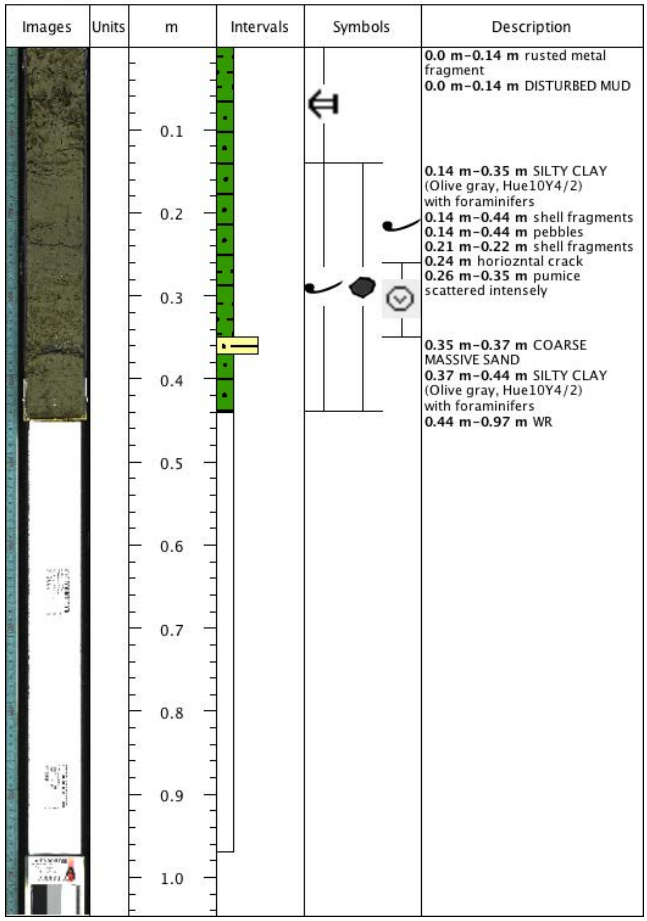

C9033A_6H_3

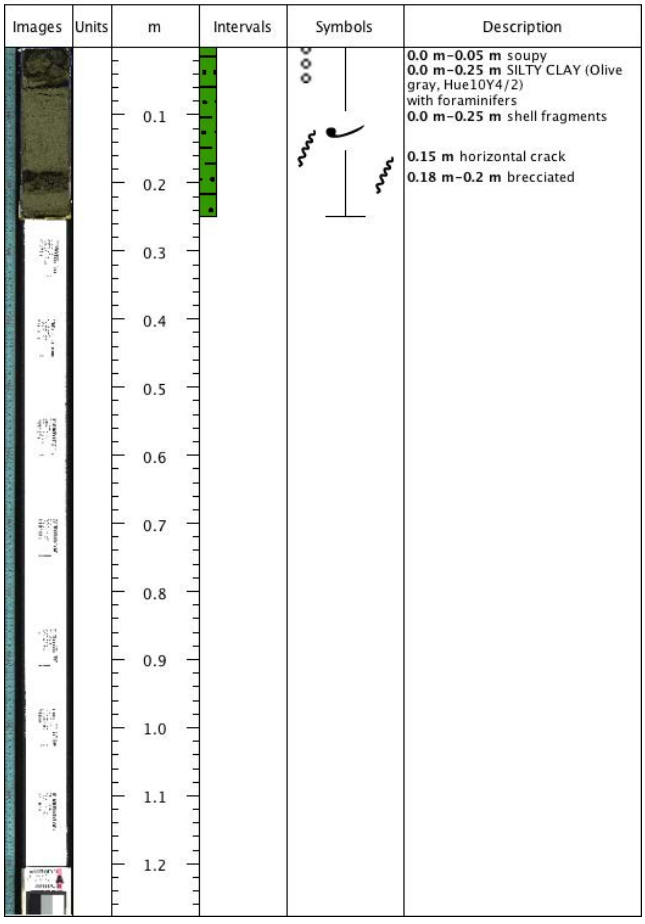

C9033A_6H_5

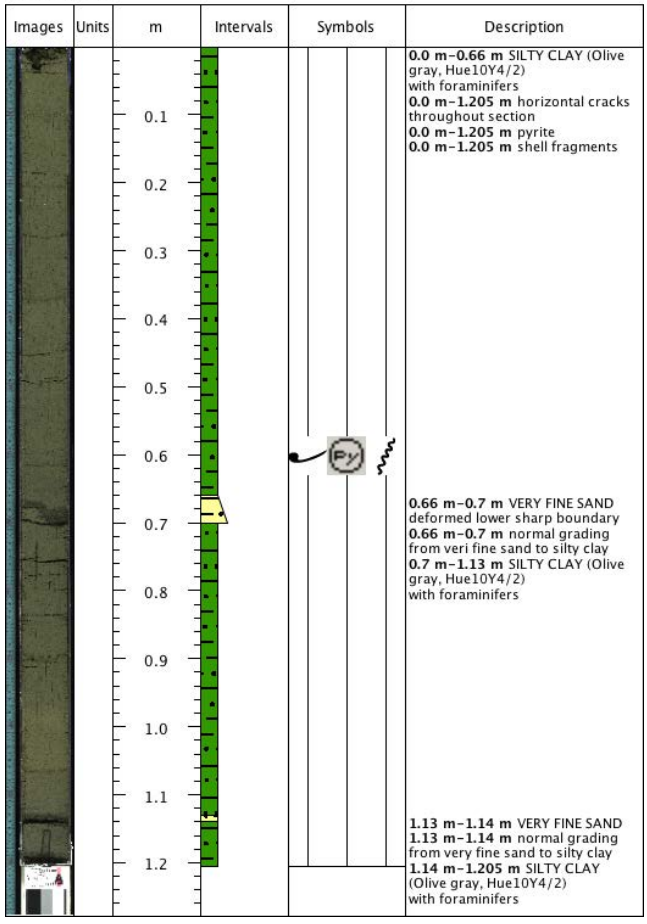

C9033A_6H_6

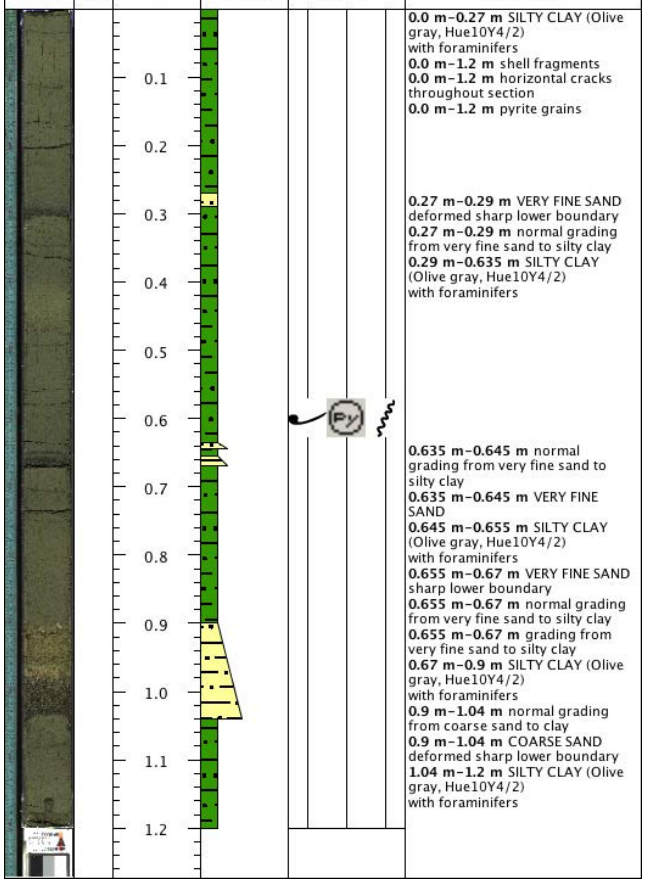

C9033A_6H_7

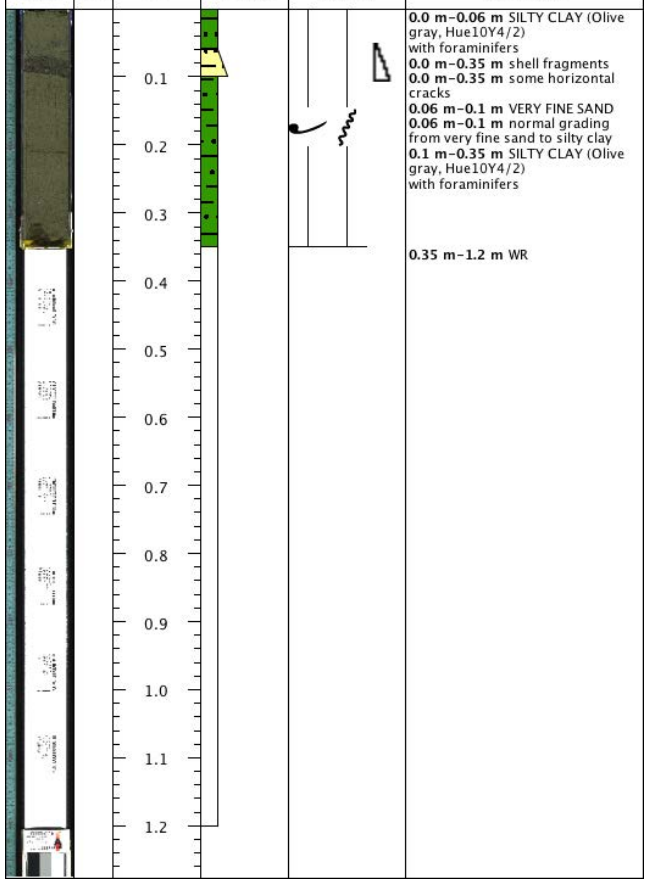

C9033A_6H_8

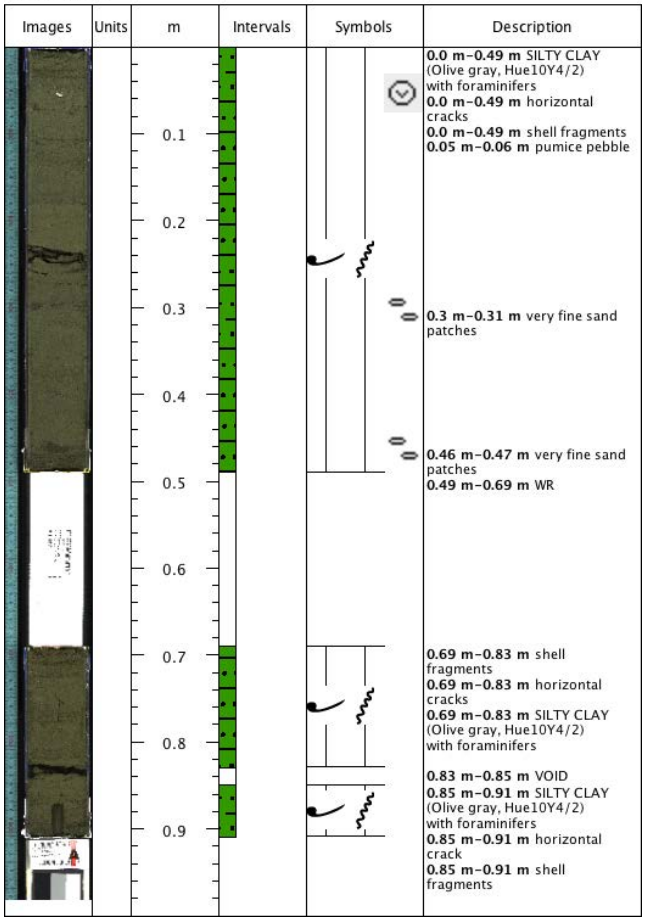

C9033A_6H_11

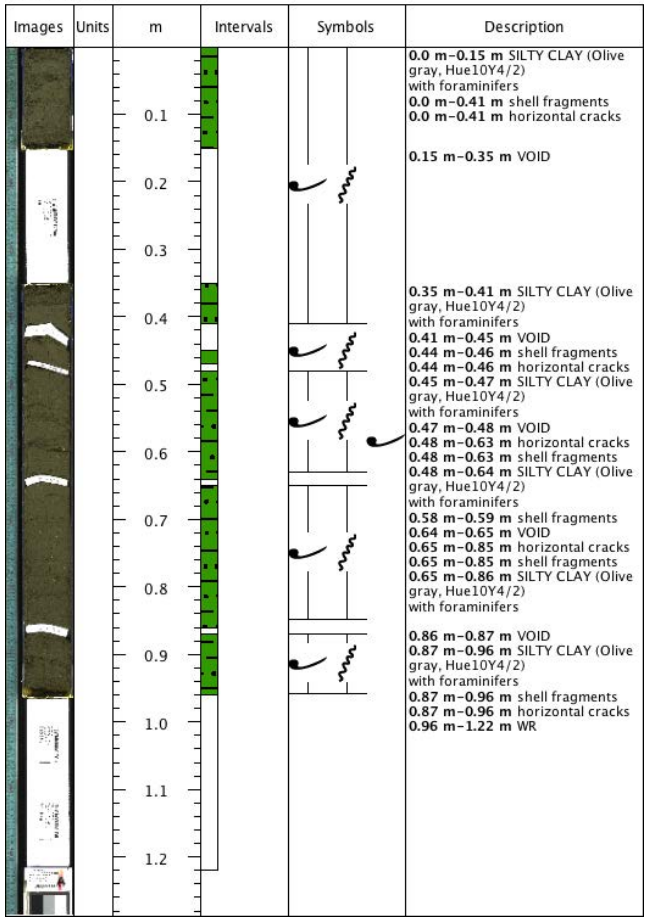

C9033A_6H_13

Units	m	Intervals	Symbols	Description
	0.1			**0.0 m–0.16 m** SILTY CLAY (Olive gray, Hue10Y4/2) with foraminifers **0.0 m–0.3 m** some horizontal cracks **0.0 m–0.3 m** shell fragments
	0.2		15-40	**0.16 m–0.19 m** CLAY bottom depth 16–20 cm inclined **0.19 m–0.3 m** SILTY CLAY (Olive gray, Hue10Y4/2) **0.2 m** bedding obliquely inclined
	0.3			**0.3 m–0.38 m** VERY FINE SAND
	0.4			
	0.5			
	0.6			
	0.7			
	0.8			
	0.9			

C9033A_6H_CC

Units	m	Intervals	Symbols	Description
	0.1			**0.0 m–0.47 m** biscutting in CT image **0.0 m–0.47 m** SILTY CLAY (Olive gray, Hue10Y4/2)
	0.2			
	0.3			
	0.4			
	0.5			
	0.6			
	0.7			
	0.8			
	0.9			

C9033A_7H_1

Units	m	Intervals	Symbols	Description
	0.1			**0.0 m–0.15 m** moderately disturbed **0.0 m–0.15 m** DISTURBED MUD
	0.2			**0.105 m** scoria pebble **0.12 m** scoria pebble
	0.3			**0.15 m–0.35 m** horizontal cracks **0.15 m–0.35 m** SILTY CLAY (Olive gray, Hue10Y4/2) with foraminifers **0.19 m** very fine sand patches **0.26 m** medium sand patch **0.27 m** medium sand patch
	0.4			
	0.5			
	0.6			
	0.7			
	0.8			
	0.9			

C9033A_7H_2

Units	m	Intervals	Symbols	Description
	0.1			**0.0 m–0.09 m** SILTY CLAY (Olive gray, Hue10Y4/2) with foraminifers **0.0 m–0.94 m** horizontal cracks with several cm intervals **0.04 m** very fine sand patch **0.07 m** shell fragment **0.09 m–0.1 m** SILTY CLAY (Grayish olive, Hue7.5Y5/3) **0.1 m** bedding moderately inclined
	0.2		5-15	**0.1 m–0.18 m** SILTY CLAY (Olive gray, Hue10Y4/2) with foraminifers **0.14 m** very fine sand patch **0.18 m–0.2 m** VOID **0.2 m–0.24 m** SILTY CLAY (Olive gray, Hue10Y4/2) with foraminifers **0.24 m–0.28 m** VOID **0.28 m–0.35 m** SILTY CLAY (Olive gray, Hue10Y4/2) with foraminifers **0.35 m–0.355 m** SILTY CLAY (Grayish olive, Hue7.5Y5/3) **0.355 m–0.4 m** SILTY CLAY (Olive gray, Hue10Y4/2) with foraminifers
	0.3			**0.36 m** very fine sand patch **0.4 m–0.415 m** normal grading from very fine sand to silty clay **0.4 m–0.415 m** VERY FINE SAND **0.415 m–0.56 m** SILTY CLAY (Olive gray, Hue10Y4/2) with foraminifers **0.52 m–0.57 m** bedding obliquely inclined **0.56 m–0.57 m** VERY FINE SAND **0.57 m–0.94 m** SILTY CLAY (Olive gray, Hue10Y4/2) with foraminifers **0.75 m** mud patch
	0.4			
	0.5		15-40	
	0.6			
	0.7			
	0.8			
	0.9			**0.87 m** very fine sand patch
	1.0			

C9033A_7H_3

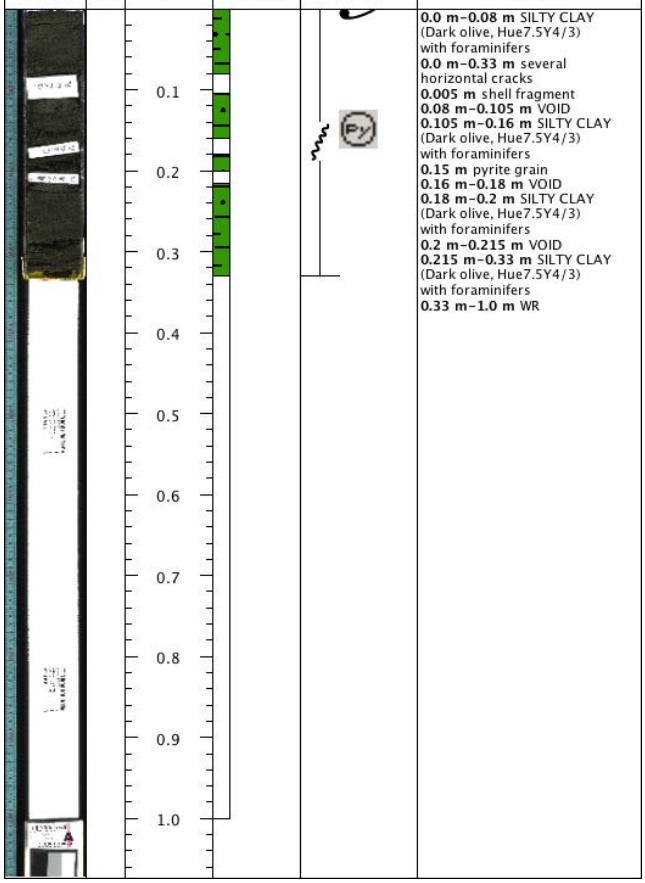

C9033A_7H_4

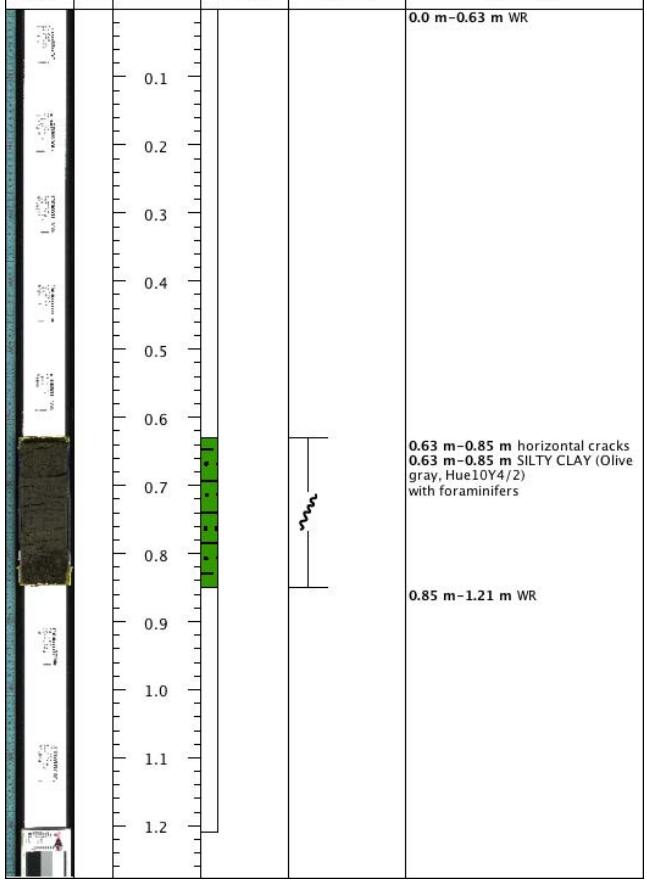

C9033A_7H_6

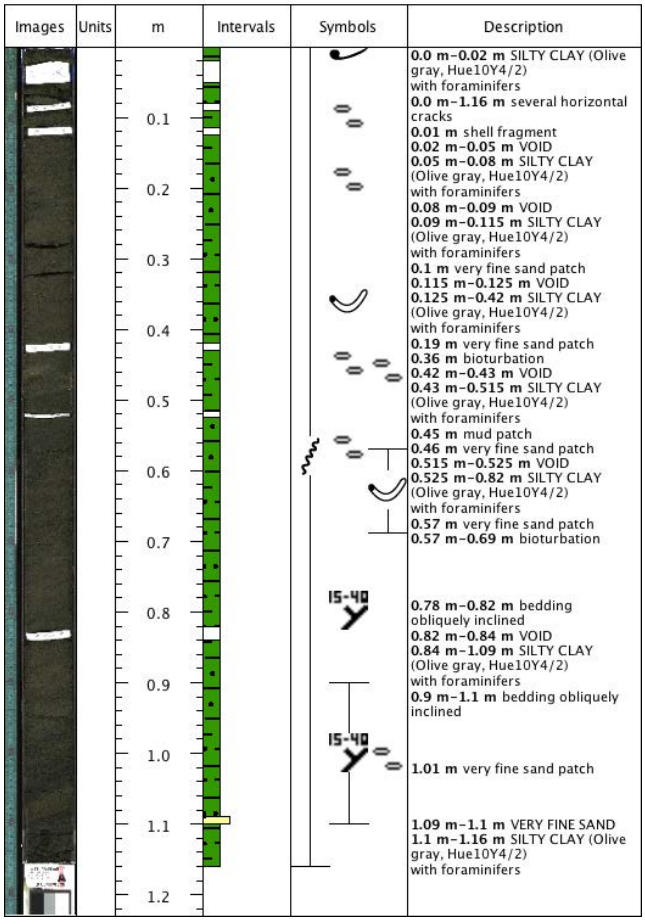

C9033A_7H_7

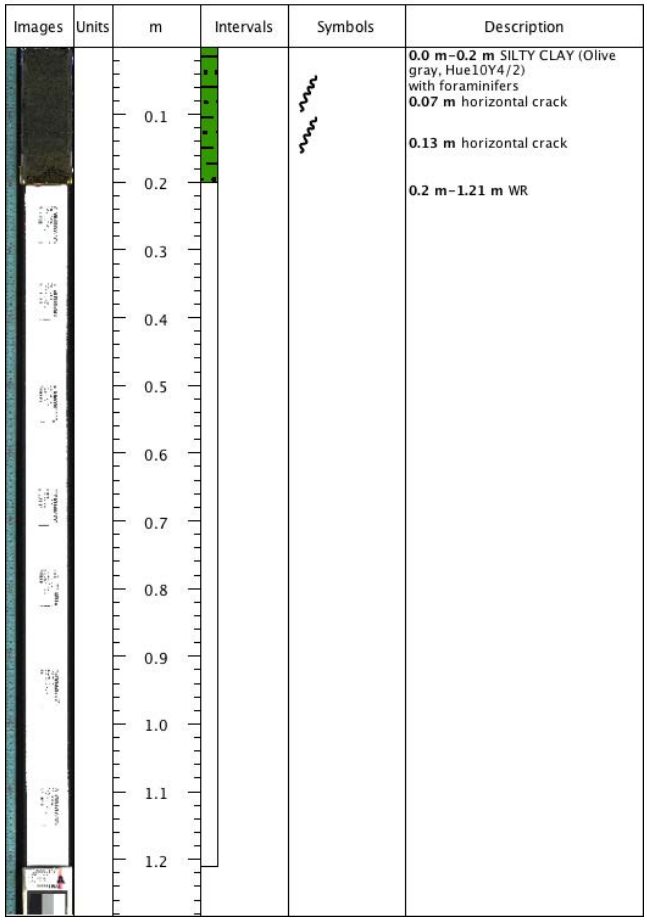

C9033A_7H_9

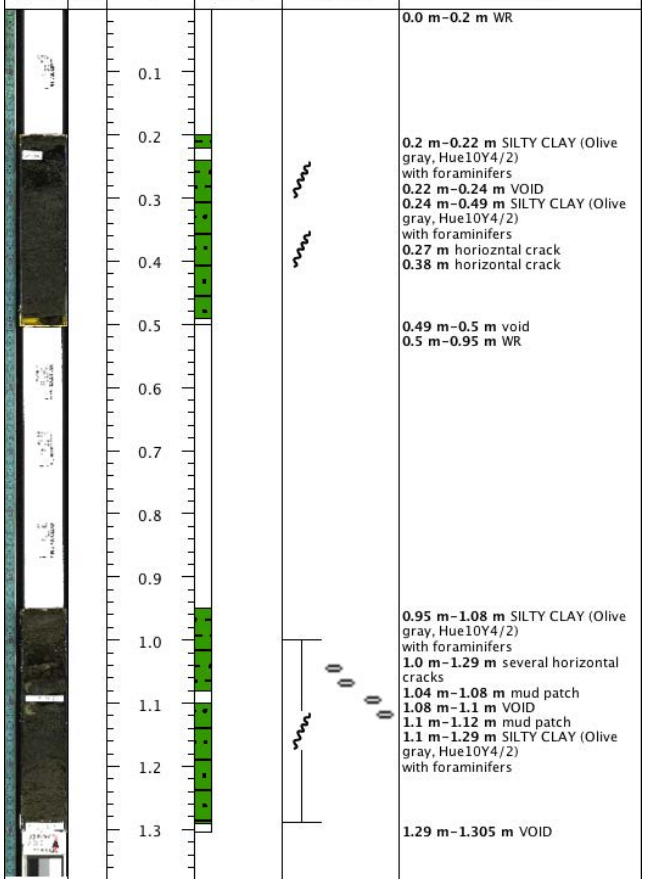

C9033A_7H_CC

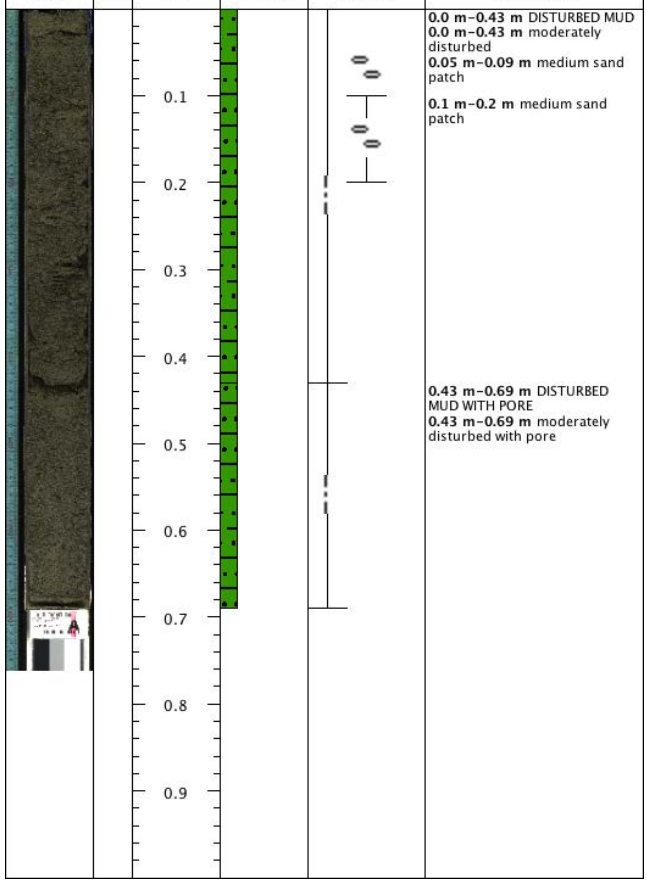

C9033A_8H_1

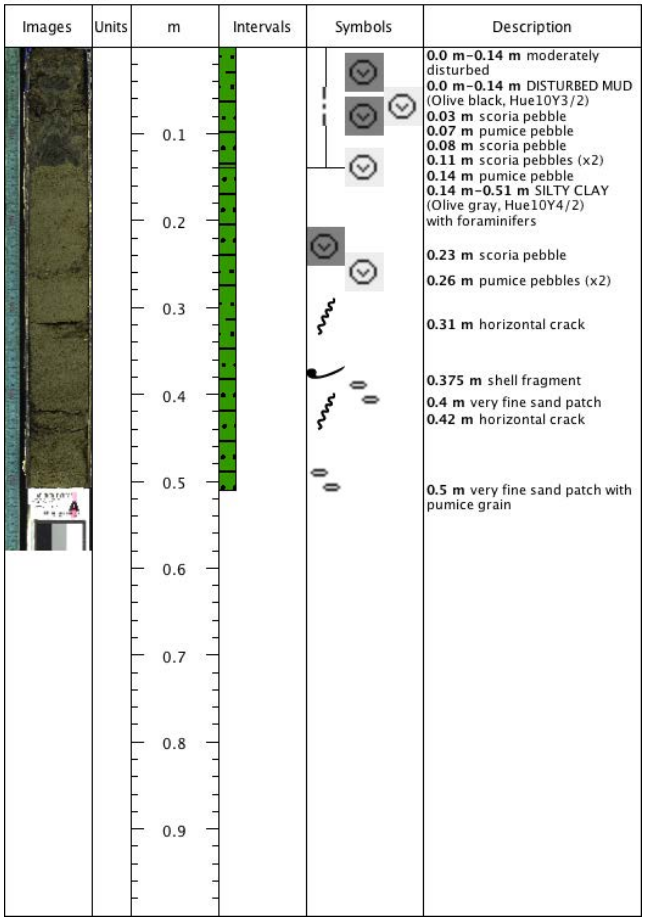

C9033A_8H_2

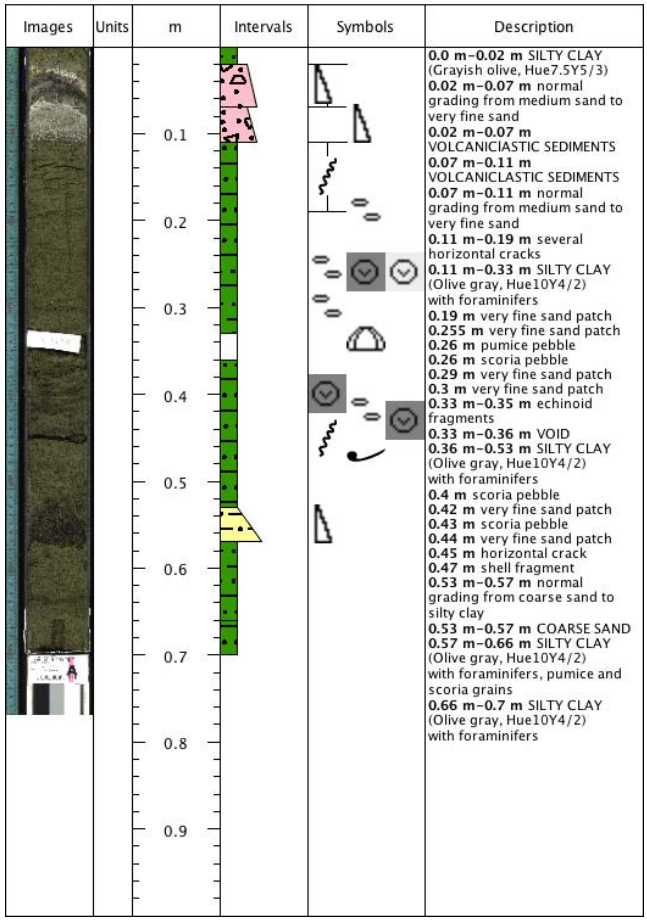

C9033A_8H_4

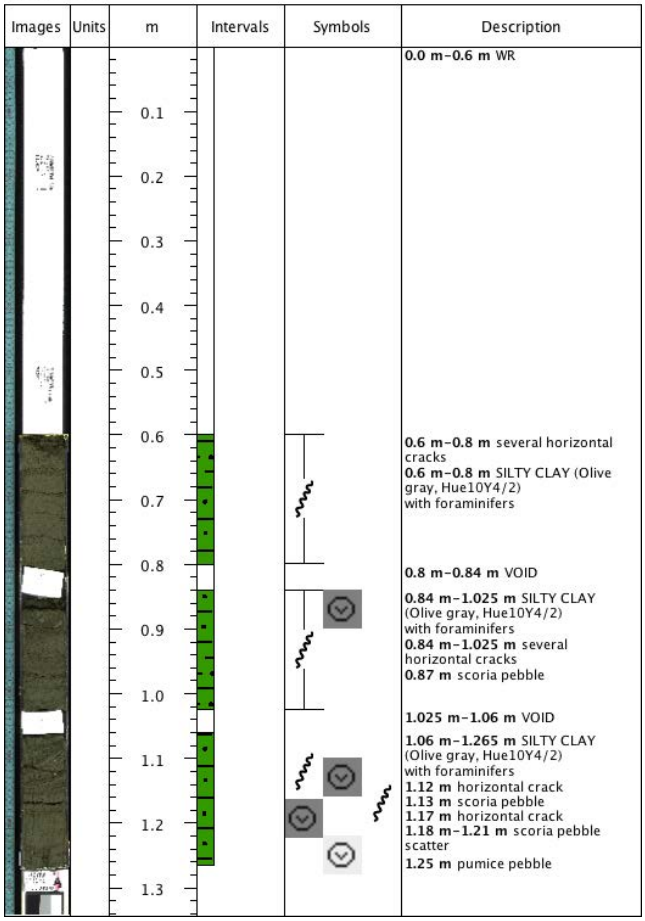

C9033A_8H_6

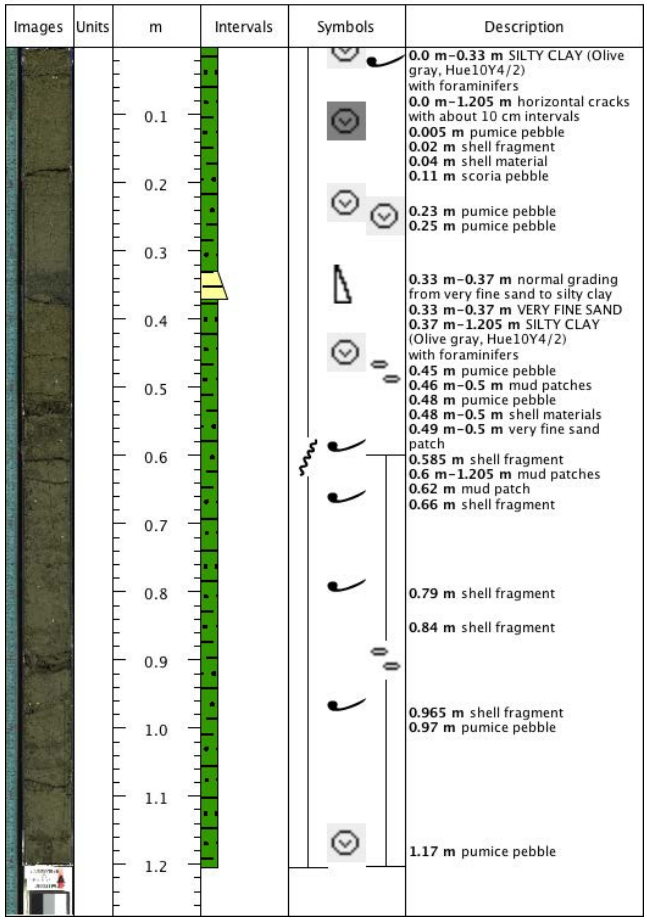

C9033A_8H_9

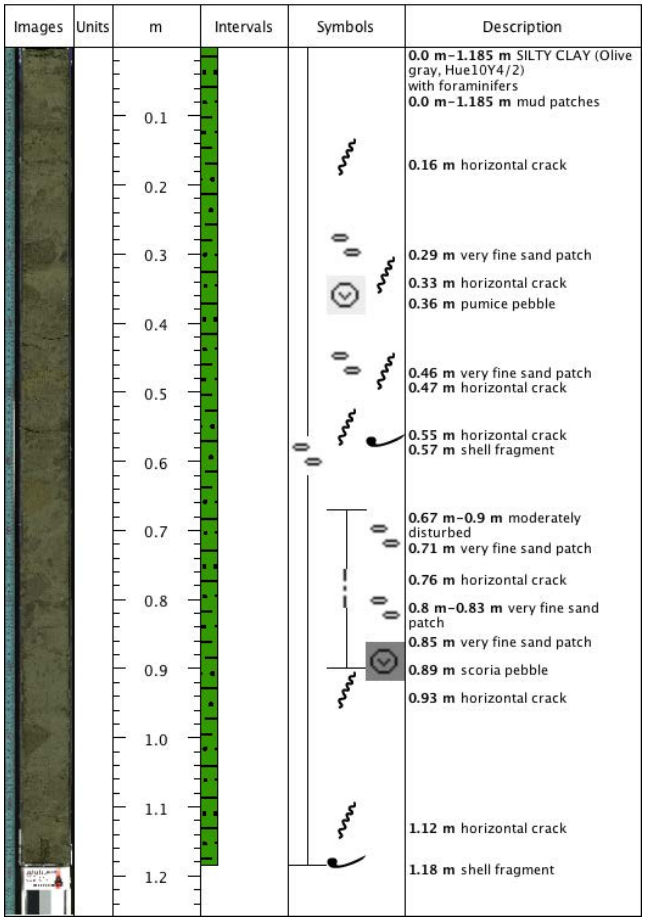

C9033A_8H_10

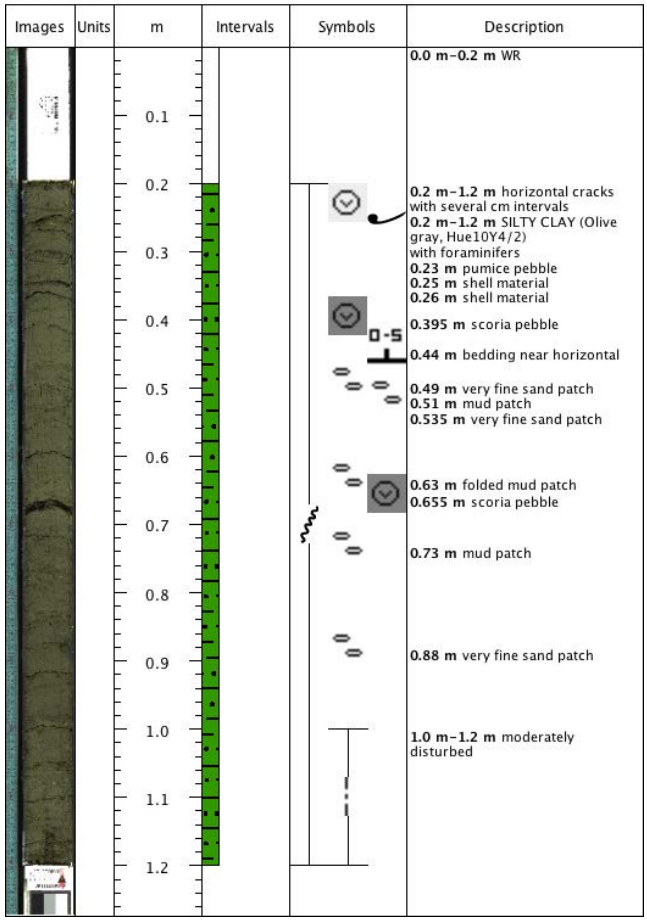

C9033A_8H_12

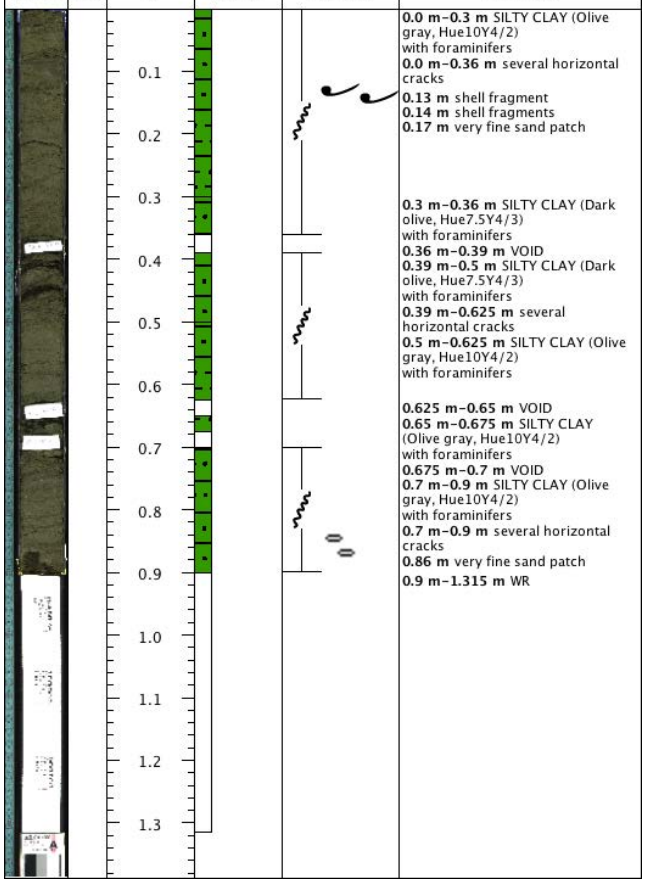

C9033A_8H_CC

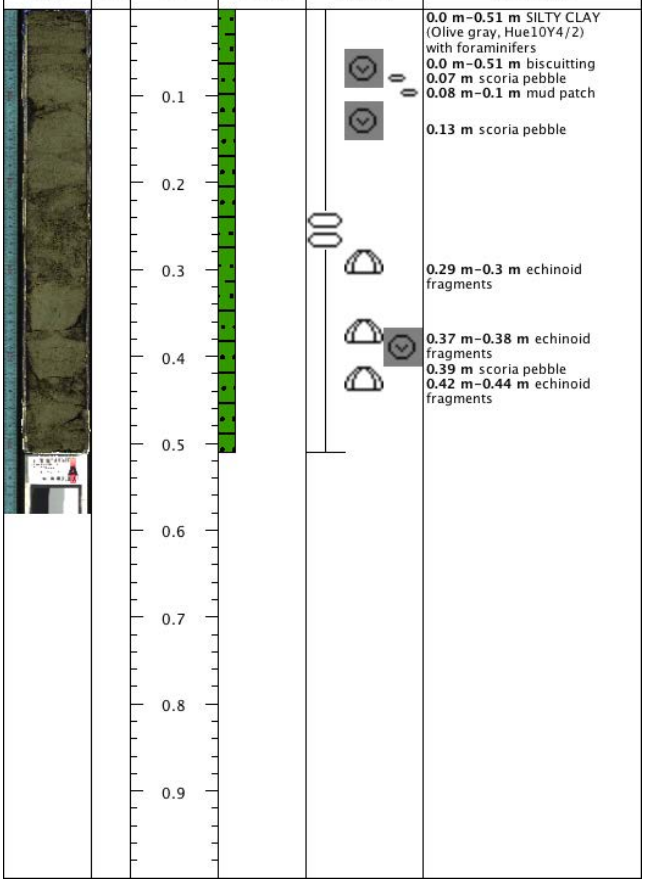

C9033A_9H_1

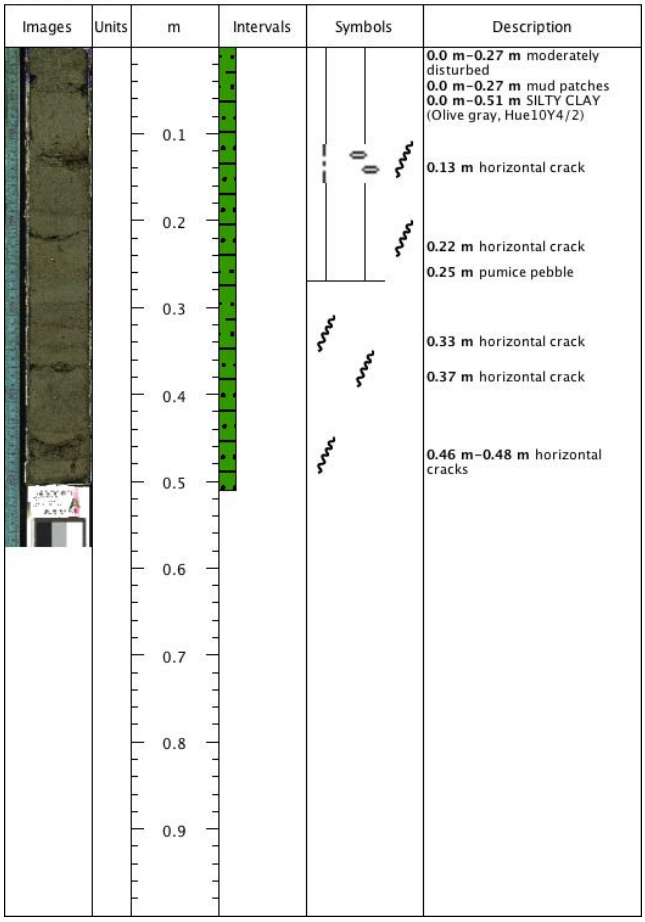

C9033A_9H_2

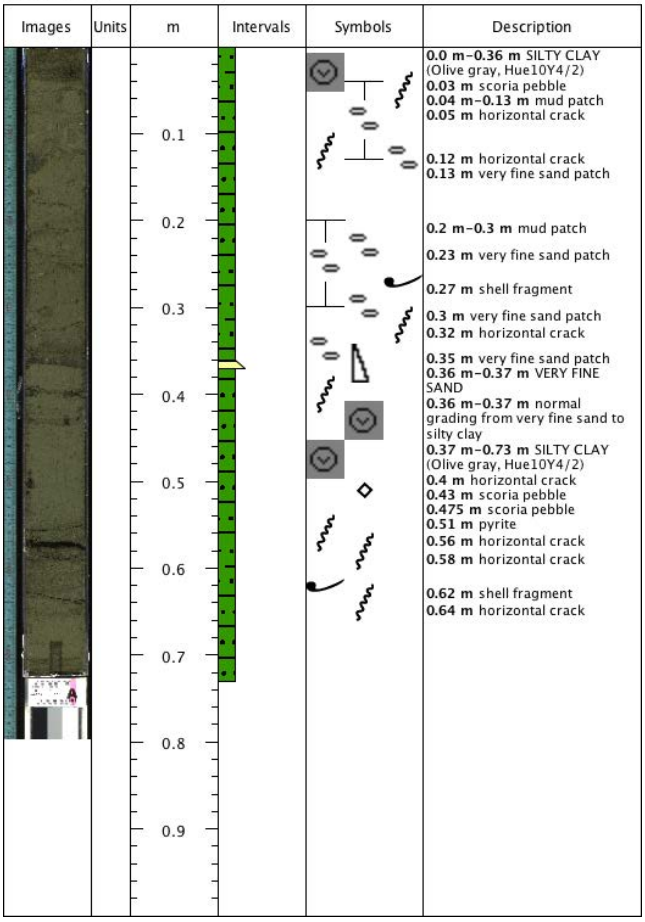

C9033A_9H_4

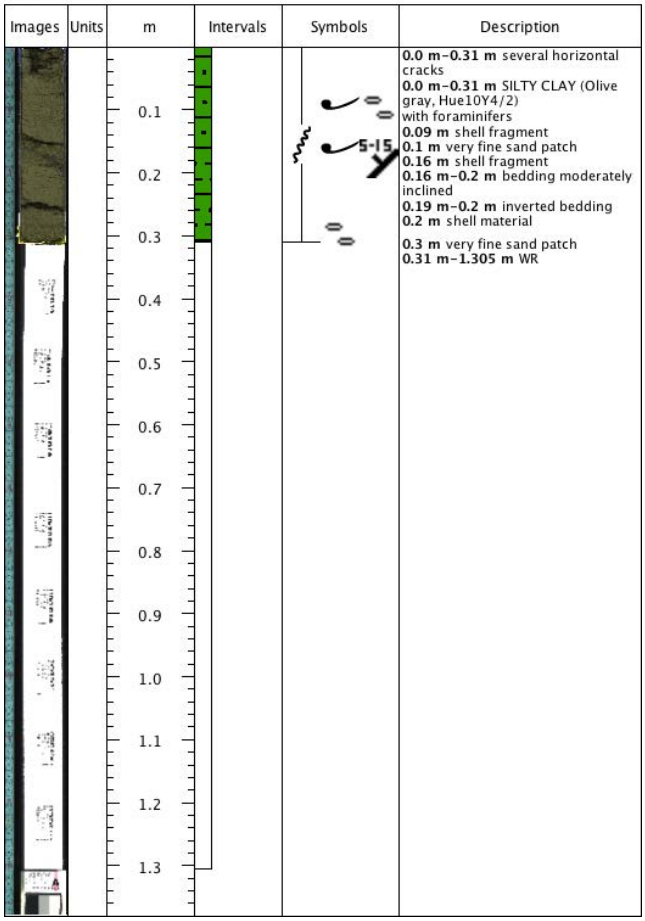

C9033A_9H_5

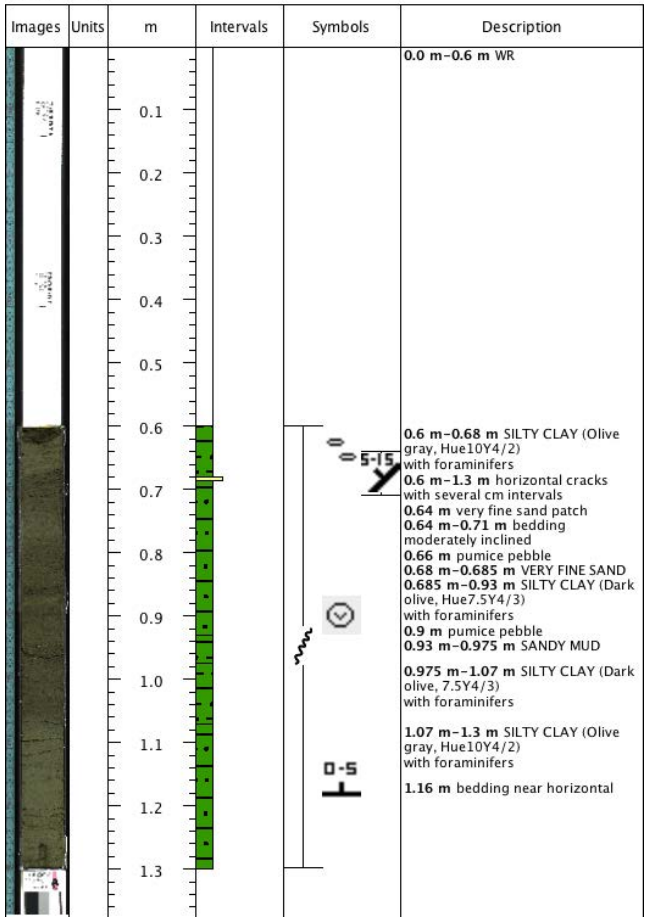

C9033A_9H_6

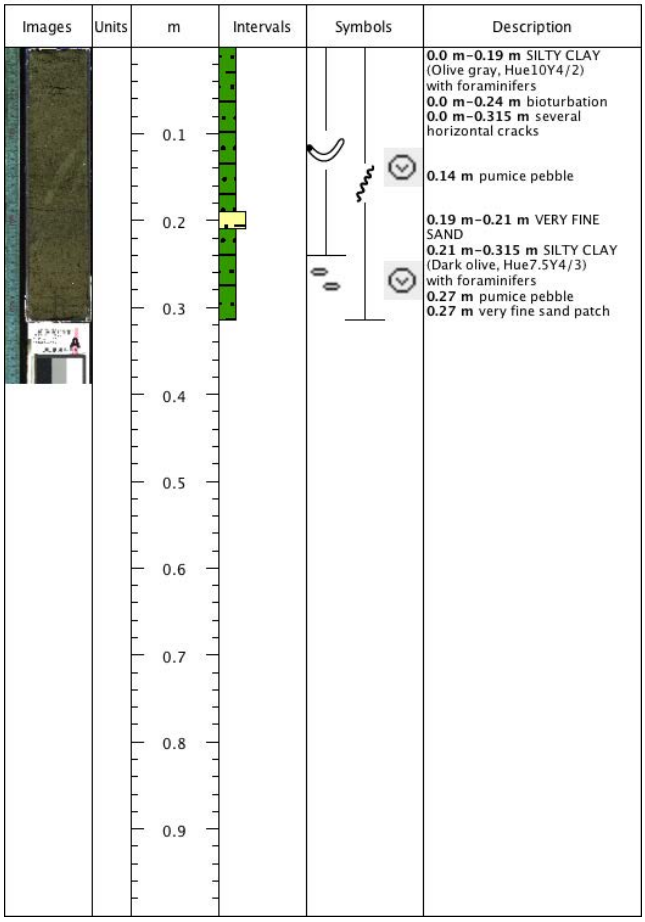

C9033A_9H_8

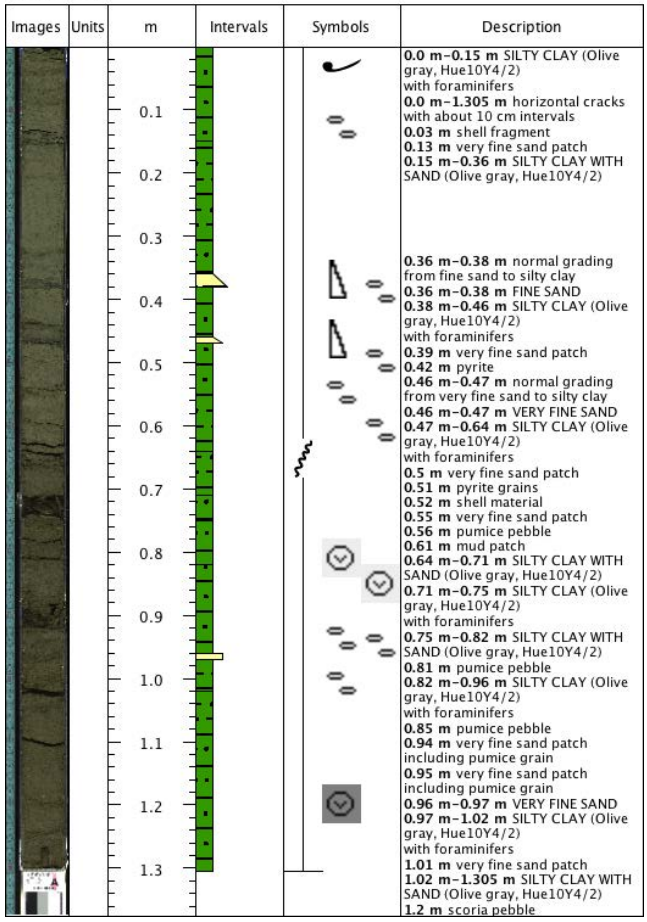

C9033A_9H_9

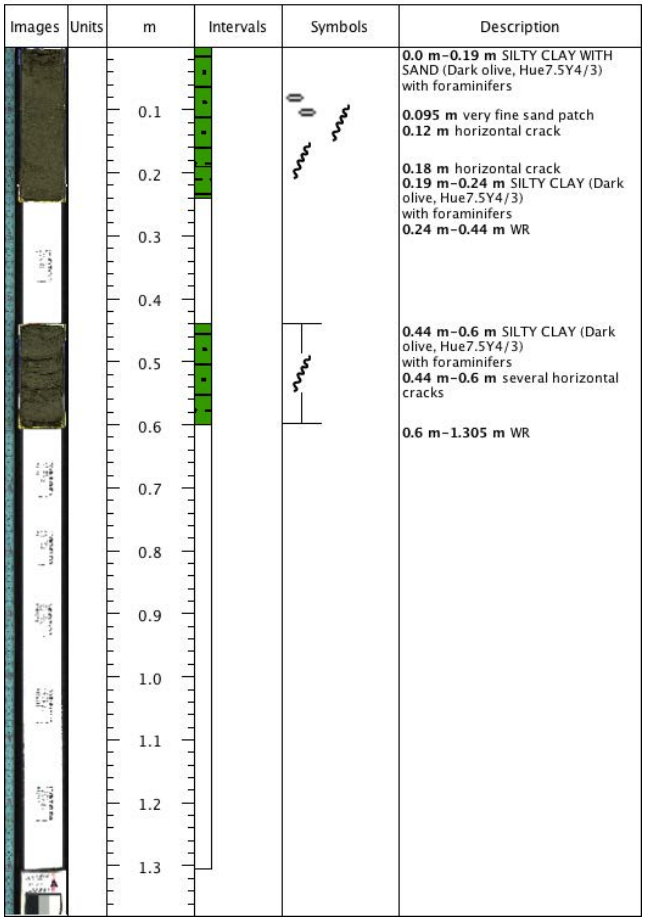

C9033A_9H_11

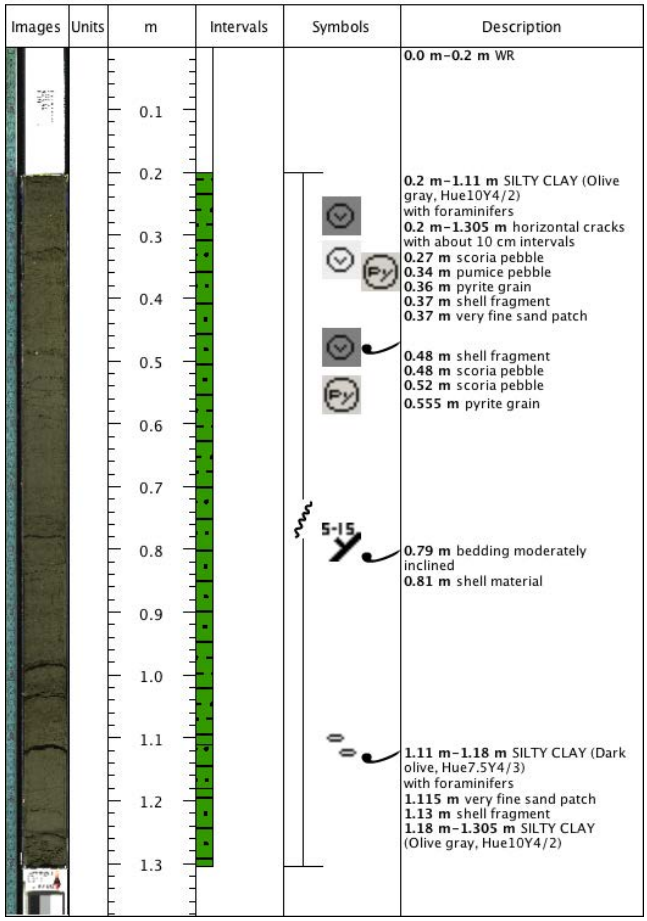

C9033A_9H_12

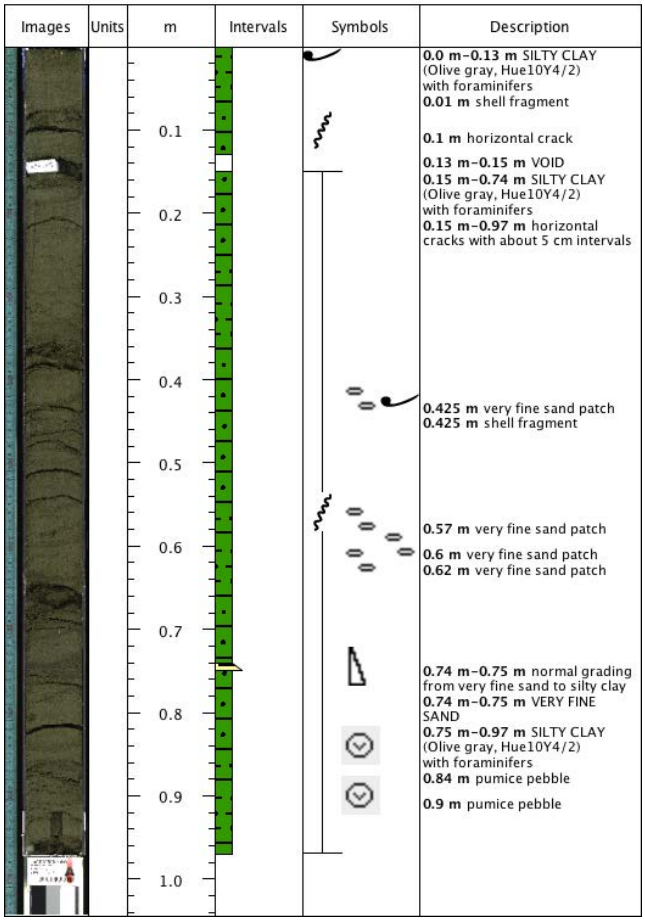

C9033A_9H_13

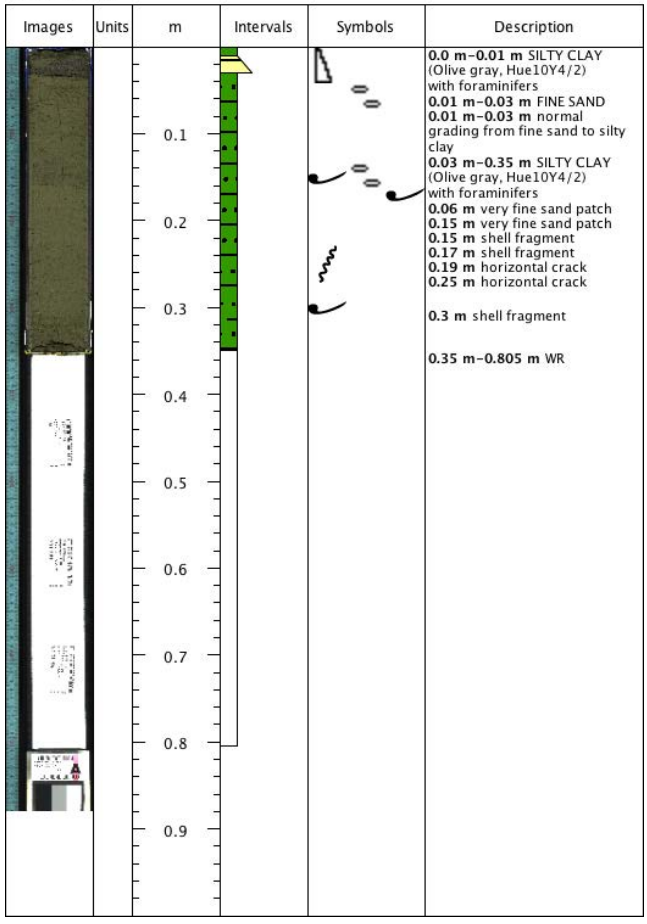

C9033A_9H_CC

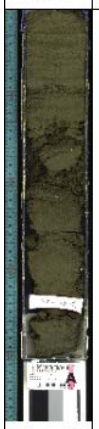

m	Intervals	Symbols	Description
0.1			**0.0 m–0.33 m** SILTY CLAY (Olive gray, Hue10Y4/2) with foraminifers
			0.07 m pumice pebble
			0.1 m–0.405 m biscuitting
0.2			**0.16 m** pumice pebble
0.3			**0.3 m** shell fragment
			0.33 m shell fragment
			0.33 m–0.35 m VOID
			0.35 m–0.405 m SILTY CLAY (Olive gray, Hue10Y4/2)
0.4			**0.4 m** very fine sand patch
0.5			
0.6			
0.7			
0.8			
0.9			

C9033A_10H_1

m	Intervals	Symbols	Description
0.1			**0.0 m–0.09 m** moderately disturbed with pore
			0.0 m–0.15 m DISTURBED MUD
			0.07 m–0.1 m mudstone pebble
0.2			**0.14 m** horizontal crack
			0.15 m–0.18 m bioturbation
			0.15 m–0.32 m SILTY CLAY (Olive gray, Hue10Y4/2) with foraminifers
0.3			**0.26 m** horizontal crack
			0.29 m pumice pebble
0.4			
0.5			
0.6			
0.7			
0.8			
0.9			

C9033A_10H_2

m	Intervals	Symbols	Description
0.1			**0.0 m–0.63 m** SILTY CLAY (Olive gray, Hue10Y4/2) with foraminifers
0.2			**0.18 m** very fine sand patch
			0.24 m horizontal crack
0.3			**0.3 m** horizontal crack
0.4			**0.4 m** horizontal crack
0.5			**0.49 m** very fine sand patch
			0.51 m horizontal crack
			0.53 m very fine sand patch
0.6			**0.58 m** horizontal crack
			0.63 m–0.64 m VOID
			0.64 m–0.91 m SILTY CLAY (Olive gray, Hue10Y4/2) with foraminifers
0.7			**0.64 m–0.91 m** several horizontal cracks
0.8			
0.9			**0.86 m** pumice pebble
			0.91 m–0.93 m VOID
			0.93 m–1.07 m SILTY CLAY (Olive gray, Hue10Y4/2) with foraminifers
1.0			
1.1			

C9033A_10H_4

m	Intervals	Symbols	Description
0.1			**0.0 m–0.345 m** SILTY CLAY (Olive gray, Hue10Y4/2) with foraminifers
			0.0 m–1.3 m horizontal cracks with about 10 cm intervals
0.2			**0.2 m** pumice pebble
			0.205 m shell fragment
0.3			**0.28 m** very fine sand patch
			0.305 m very fine sand patch
0.4			**0.345 m–0.35 m** VERY FINE SAND
			0.345 m–0.35 m normal grading from very fine sand to silty clay
			0.35 m–0.43 m SILTY CLAY (Drak olive, Hue7.5Y4/3) with foraminifers
0.5			**0.365 m** very fine sand patch
			0.37 m fine sand patch including pumice grain
			0.42 m shell fragment
0.6			**0.43 m–0.44 m** inverted bedding showing grading
			0.43 m–0.44 m VERY FINE SAND (sharp top boundary)
0.7			**0.44 m–1.3 m** SILTY CLAY (Olive gray, Hue10Y4/2) with foraminifers
0.8			**0.45 m–0.57 m** very fine sand patches
			0.63 m very fine sand patch
0.9			**0.68 m–0.75 m** very fine sand patches
			0.79 m very fine sand patch
			0.88 m–0.93 m very fine sand patches
1.0			
			1.045 m pumice pebble
1.1			
1.2			
1.3			

C9033A_10H_5

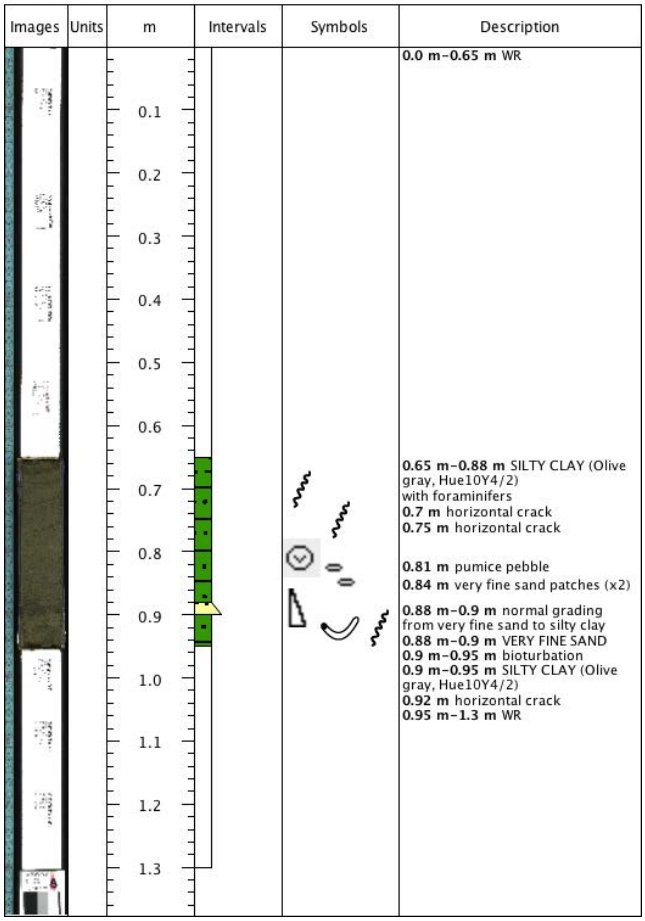

C9033A_10H_7

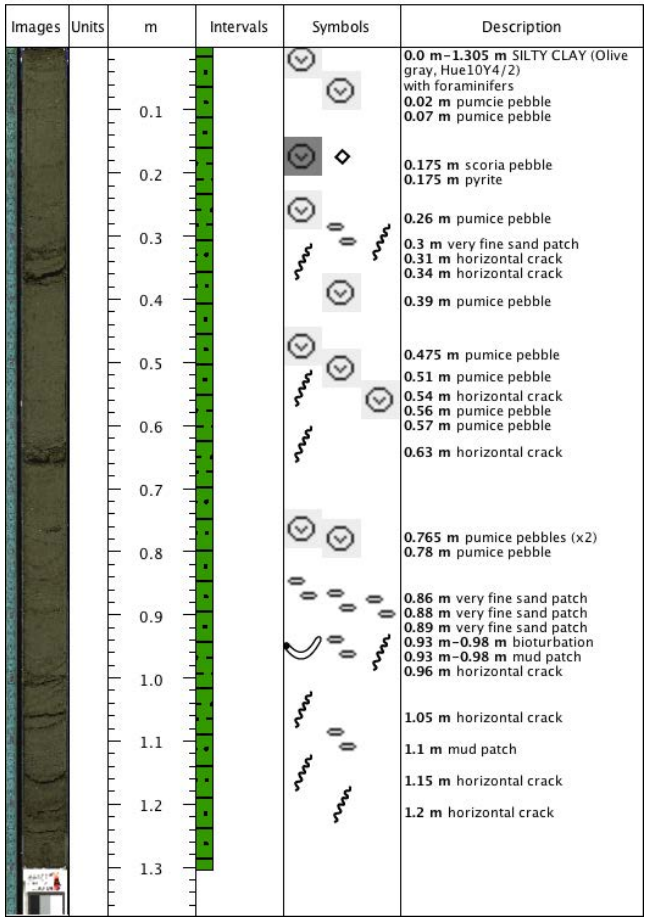

C9033A_10H_10

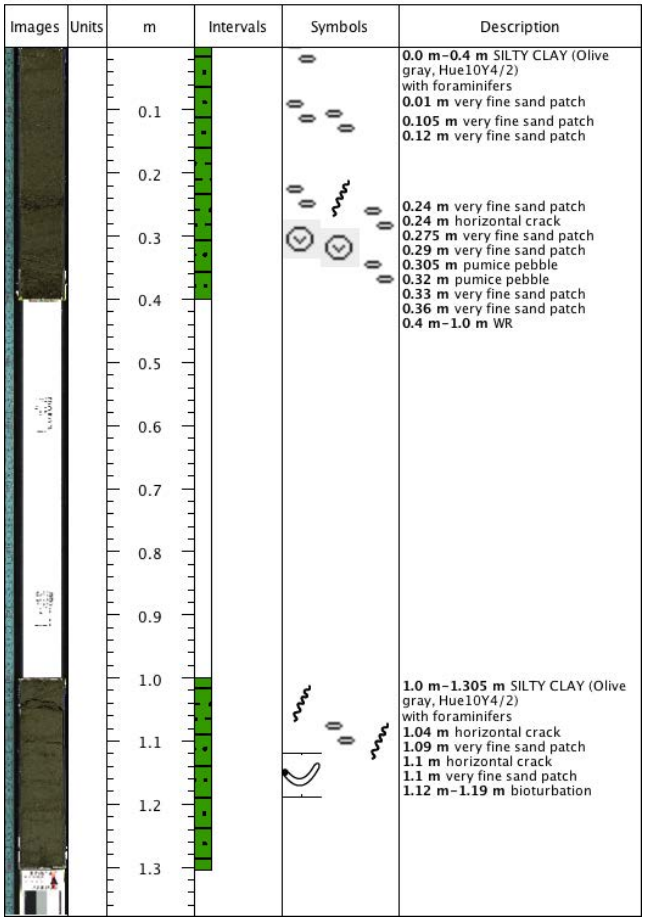

C9033A_10H_11

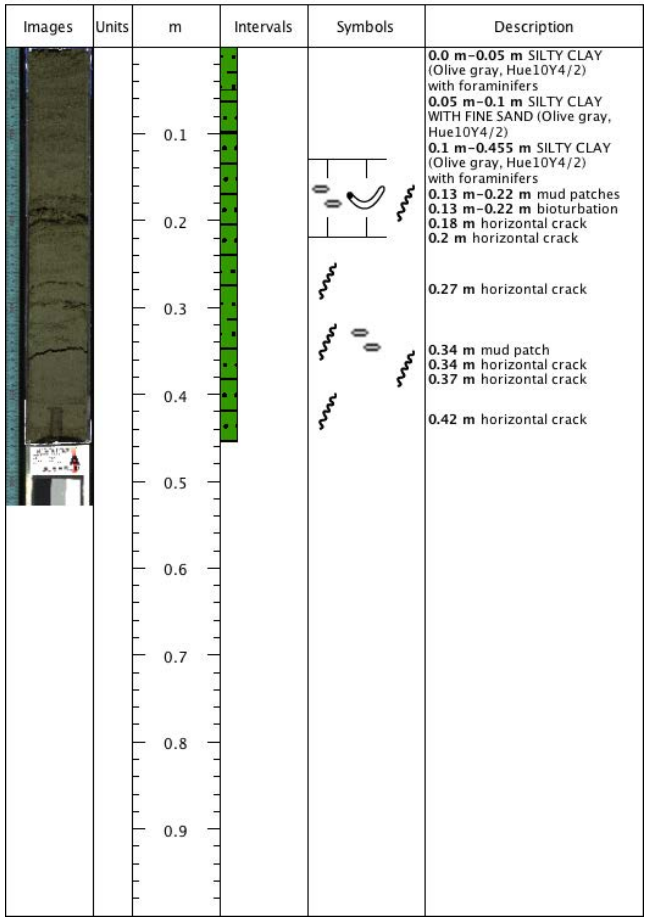

C9033A_10H_12

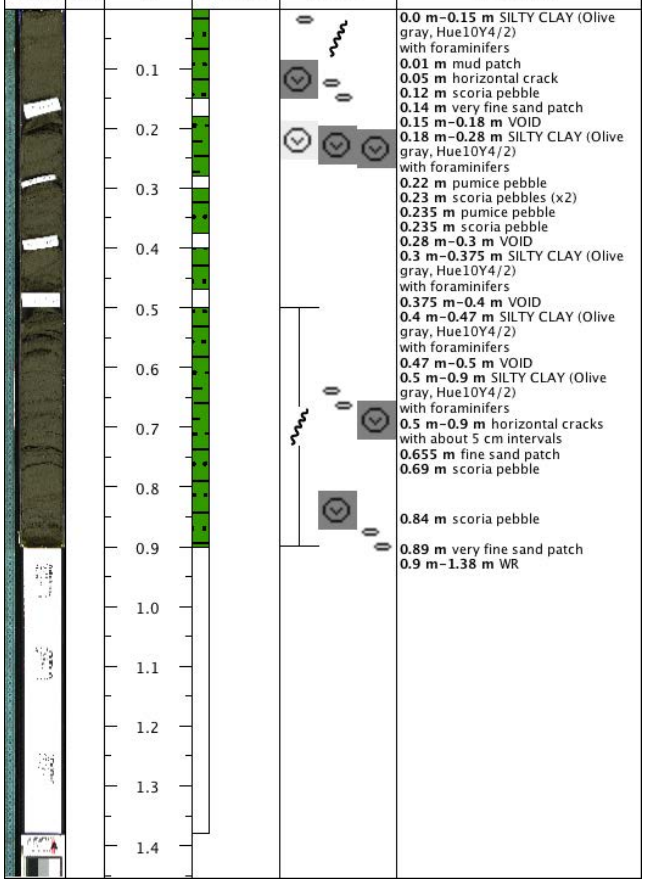

C9033A_10H_CC

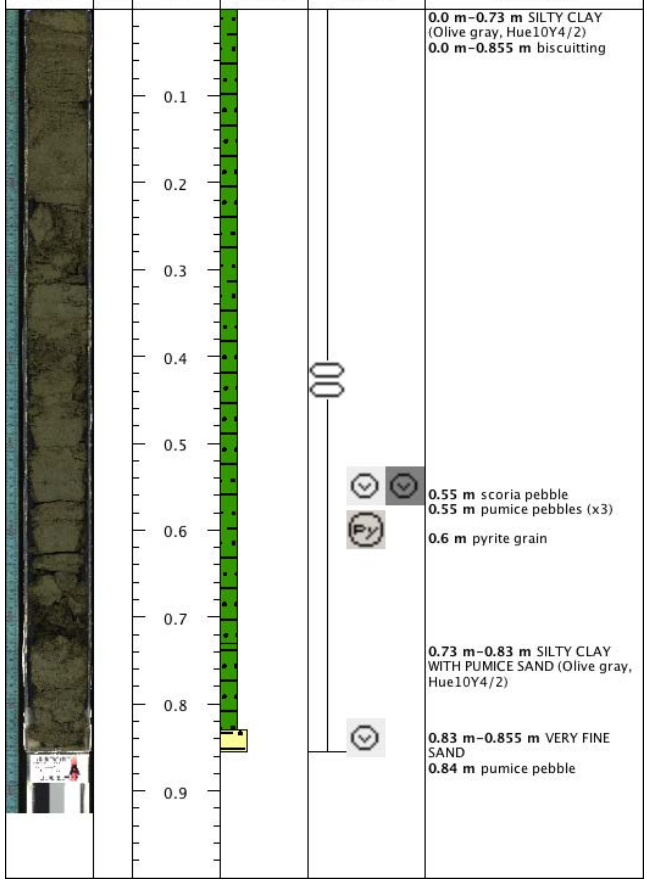

C9033A_11H_1

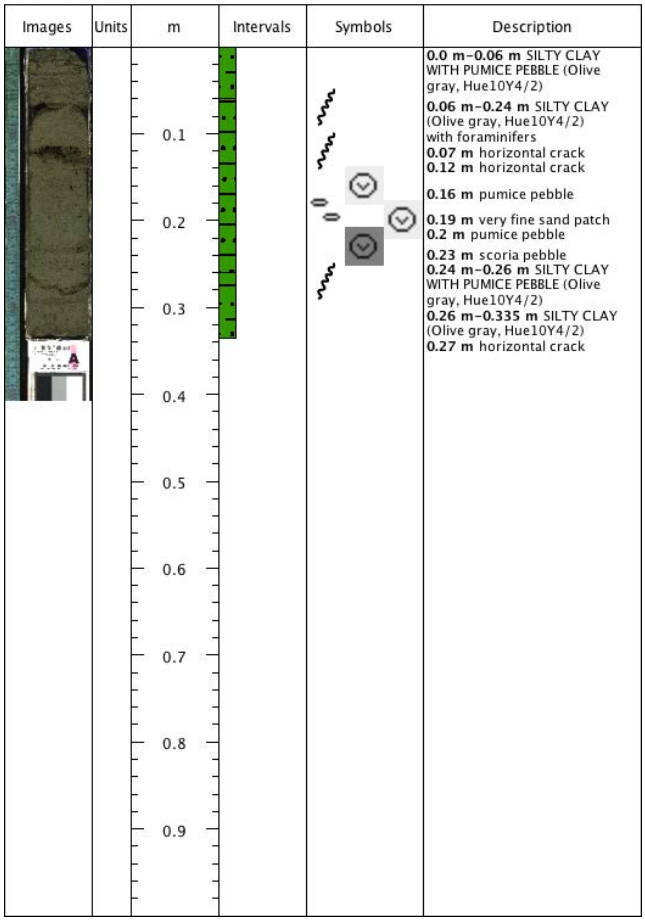

C9033A_11H_2

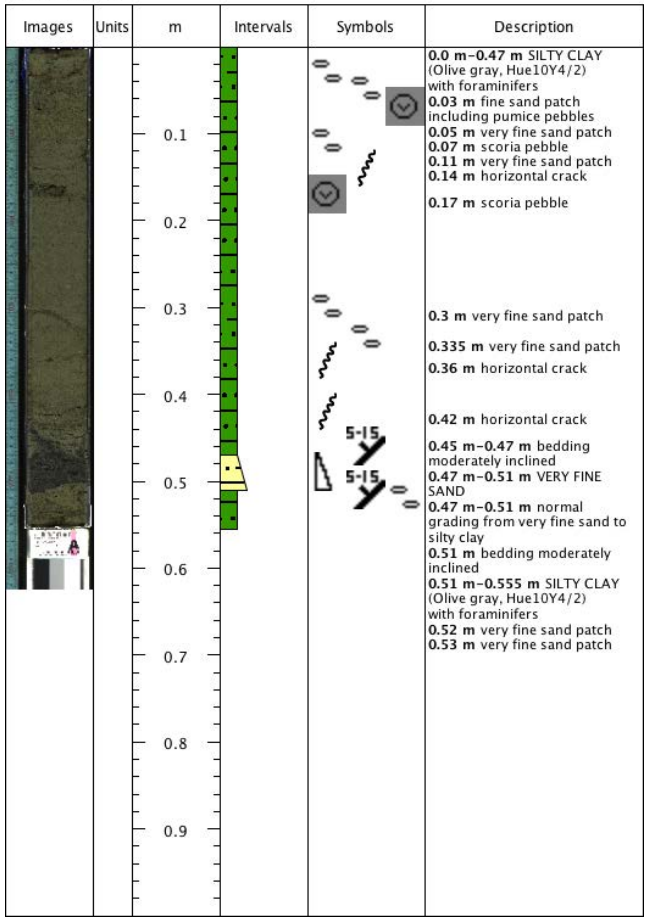

C9033A_11H_3

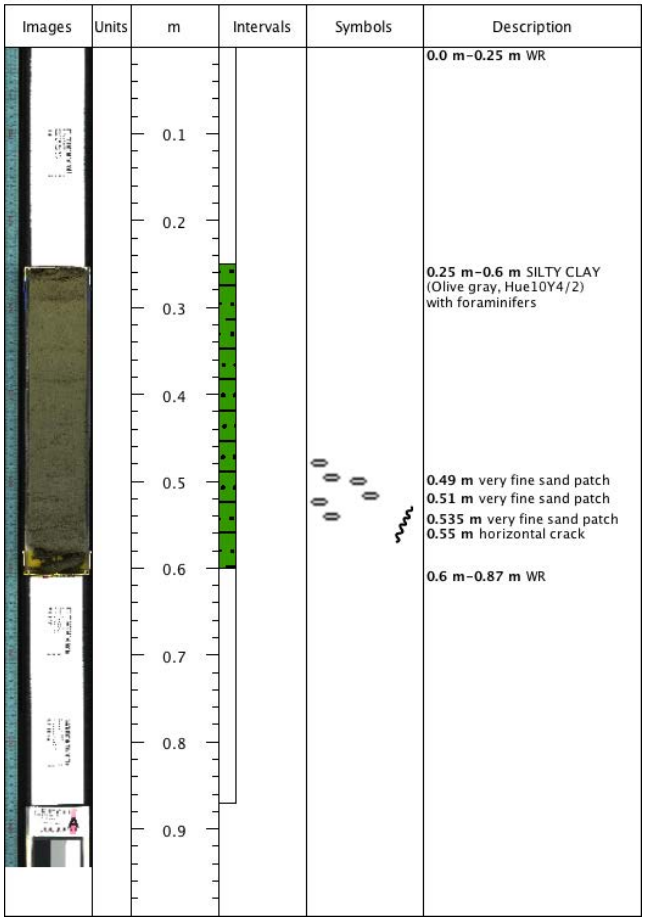

C9033A_11H_4

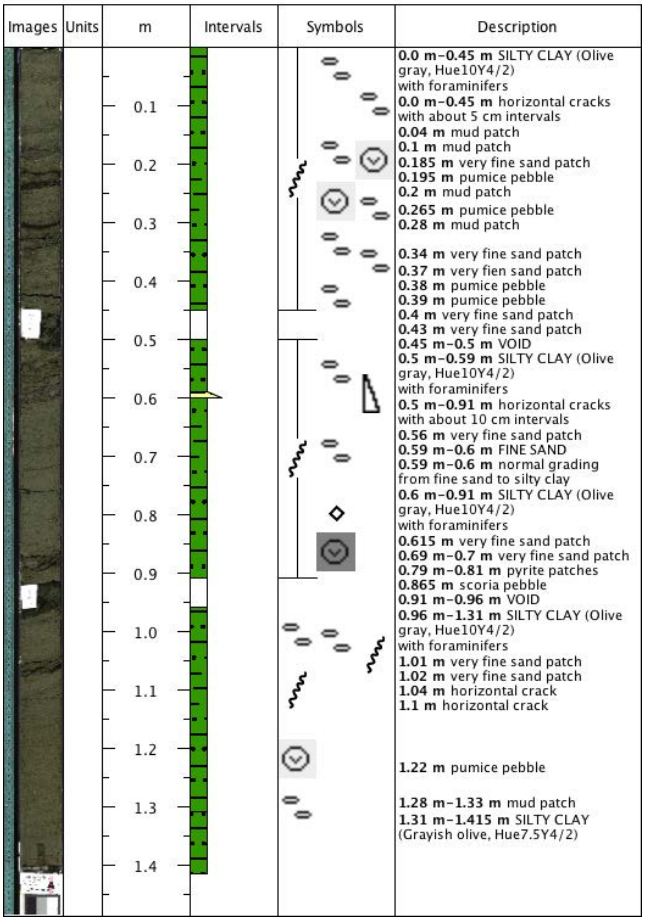

C9033A_11H_6

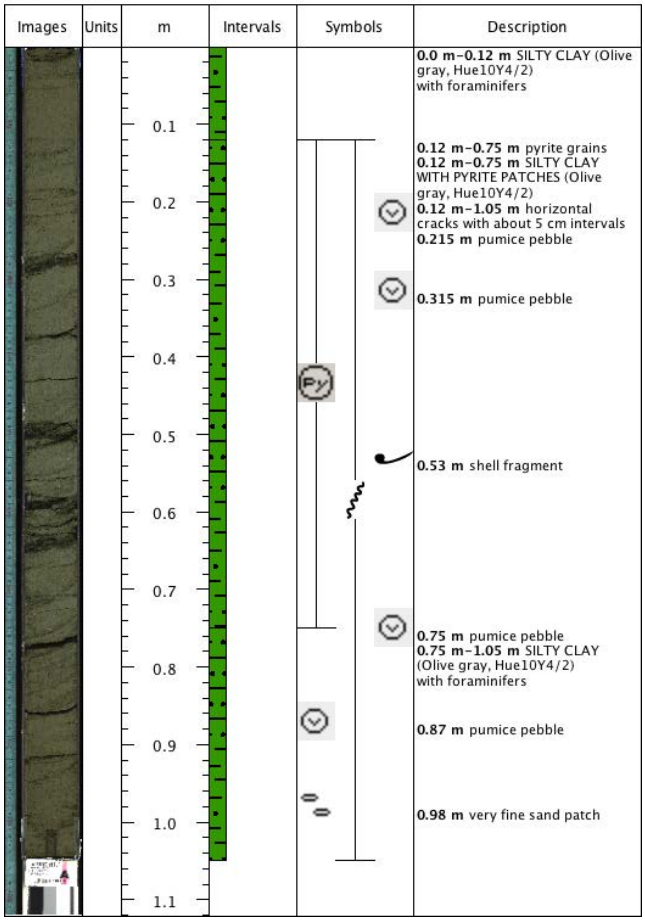

C9033A_11H_7

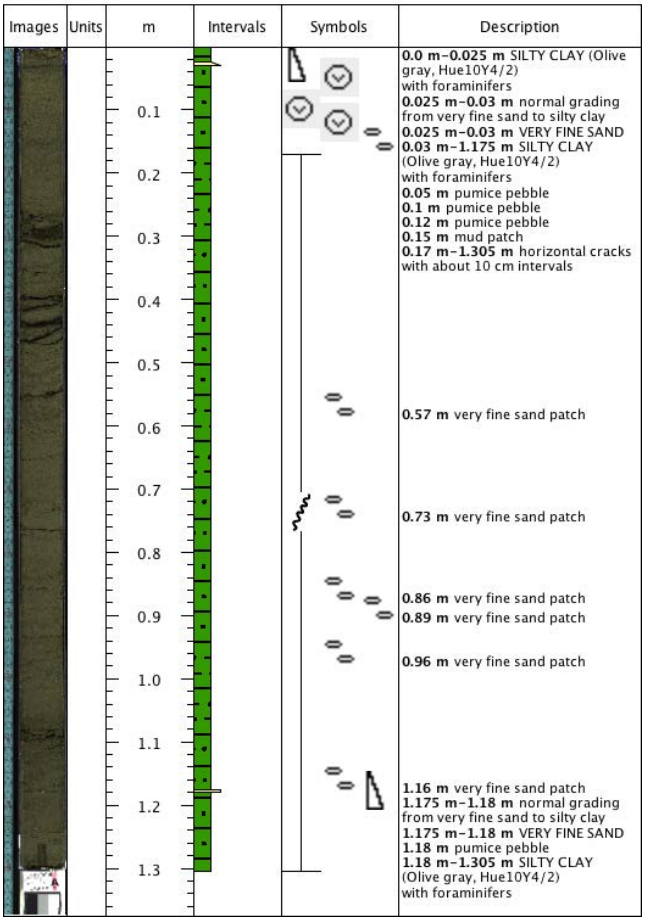

C9033A_11H_10

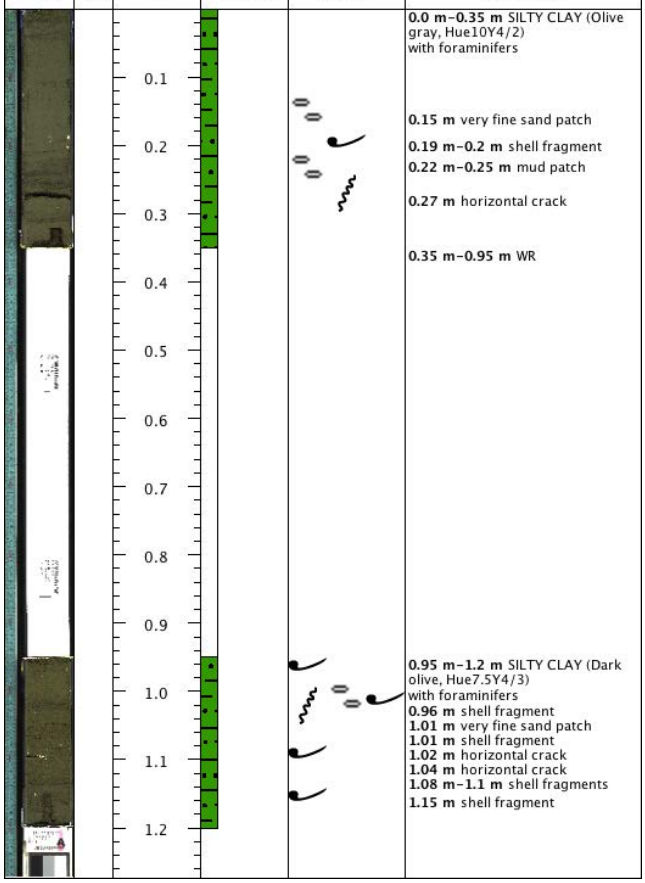

C9033A_11H_11

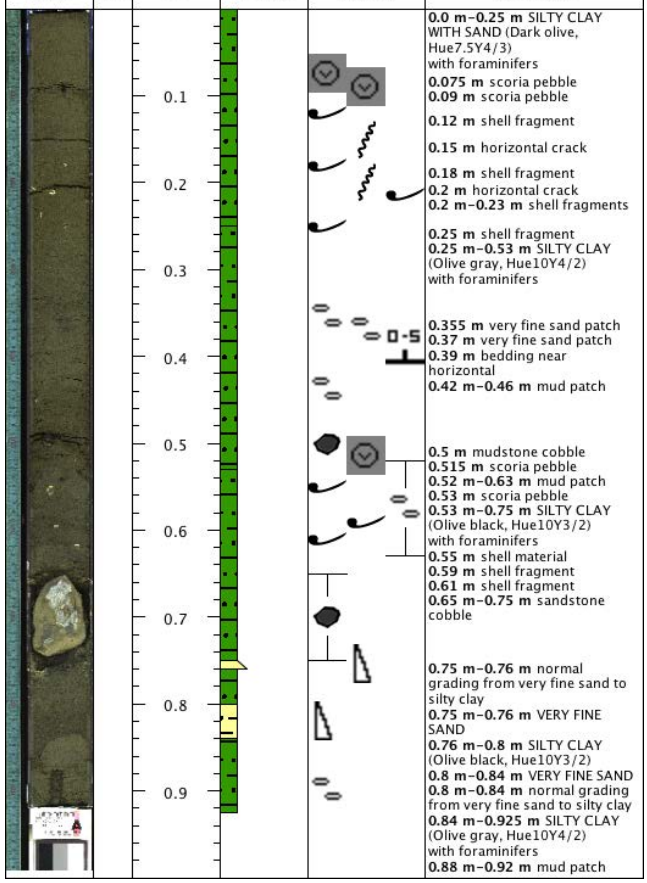

C9033A_11H_CC

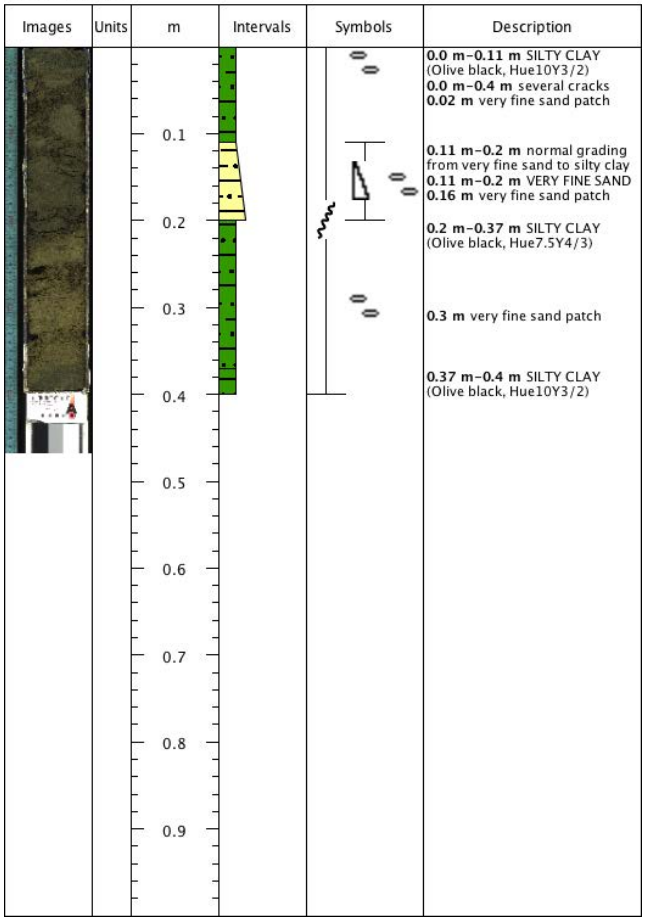

C9033A_12H_1

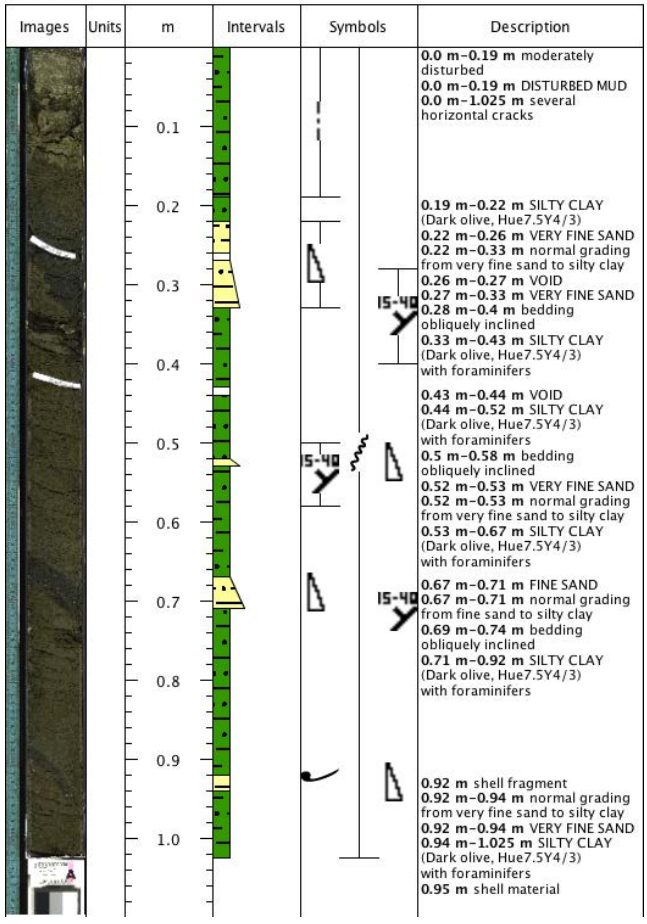

C9033A_12H_2

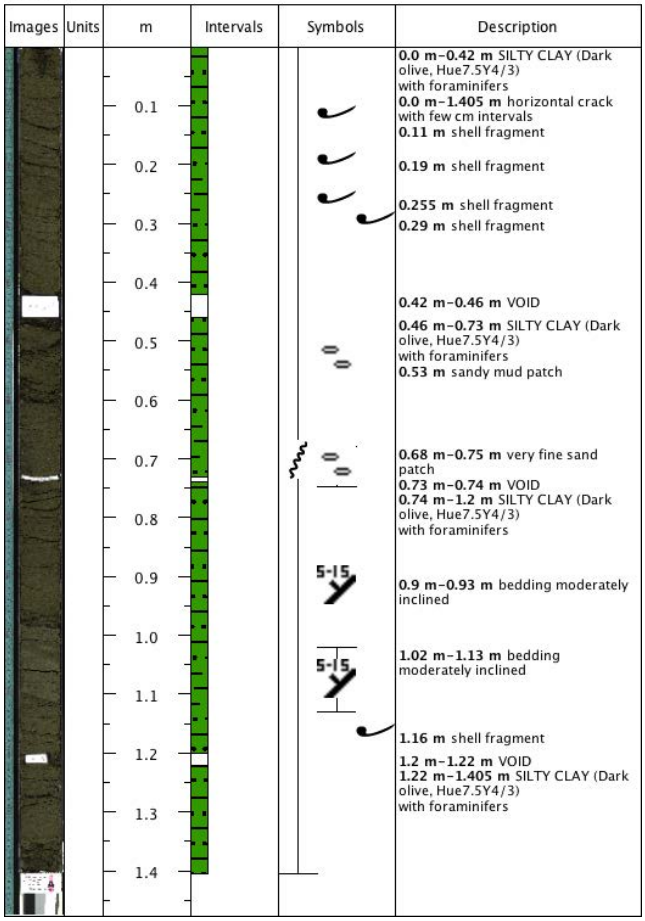

C9033A_12H_4

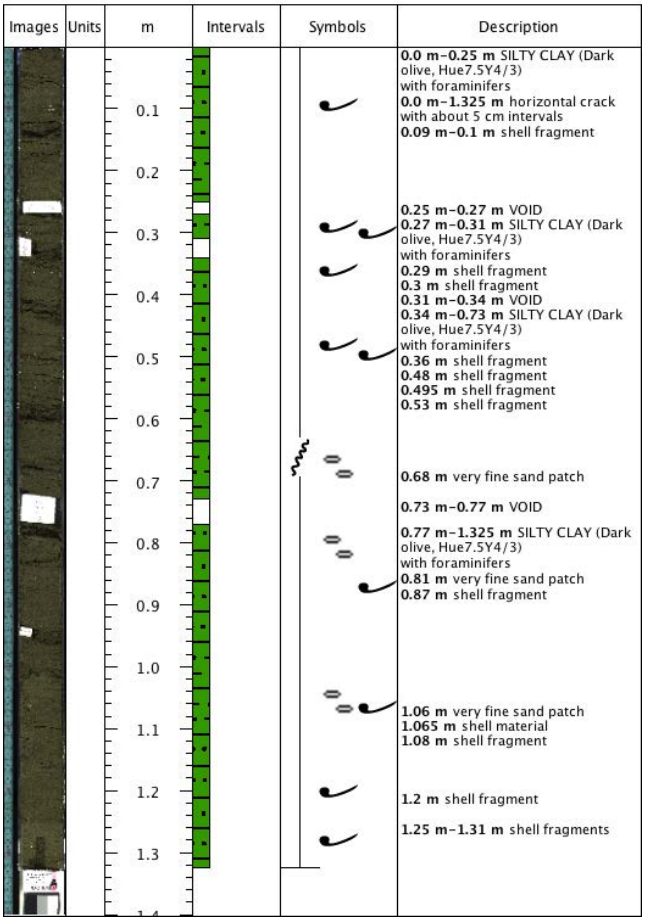

C9033A_12H_5

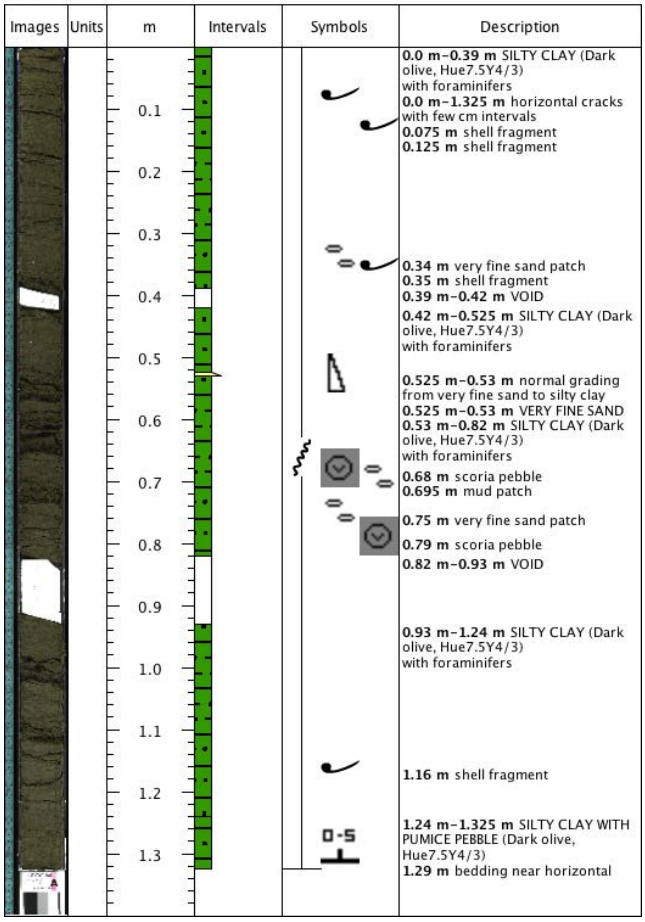

C9033A_12H_7

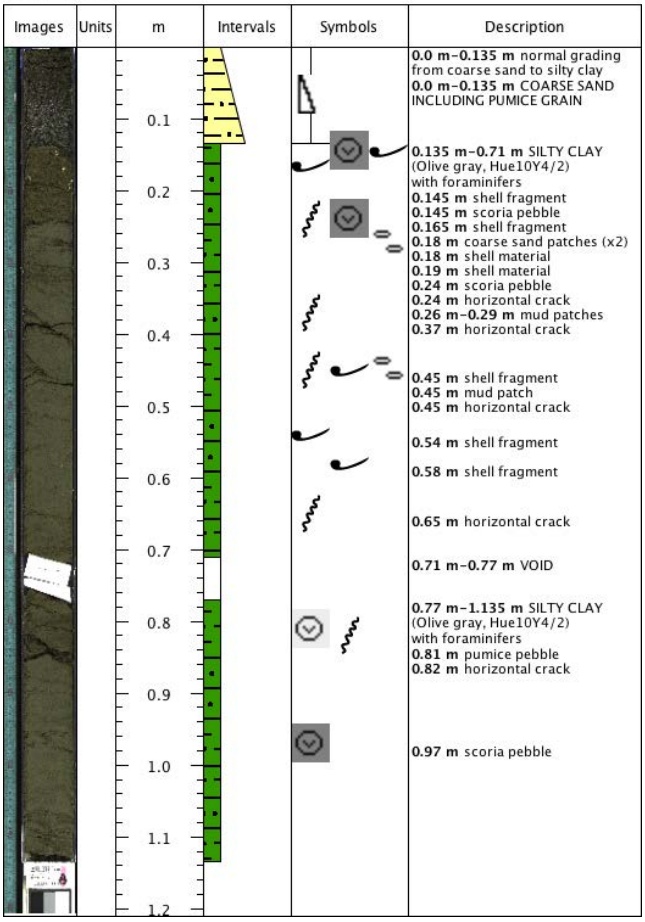

C9033A_12H_9

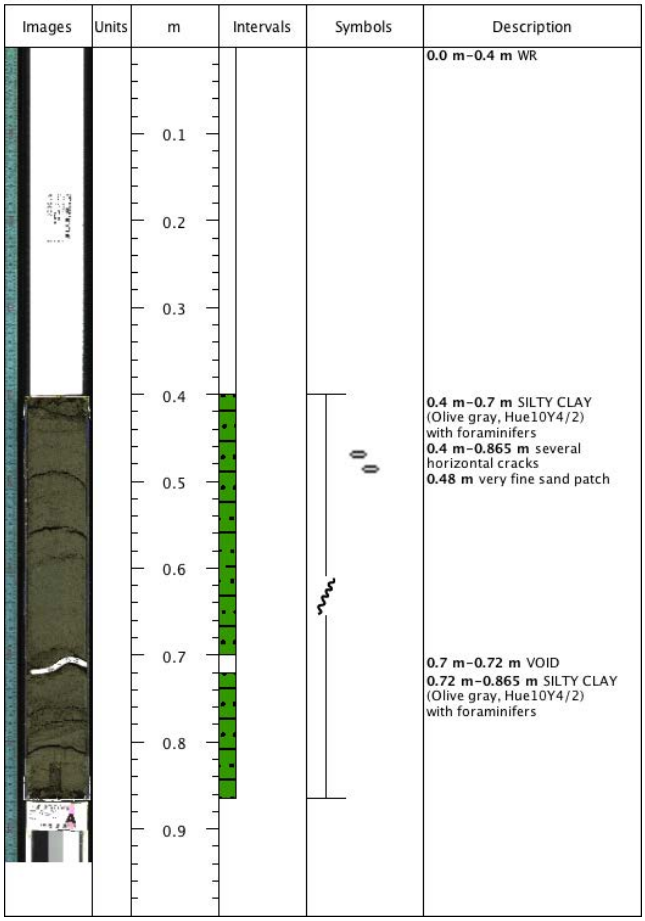

C9033A_12H_11

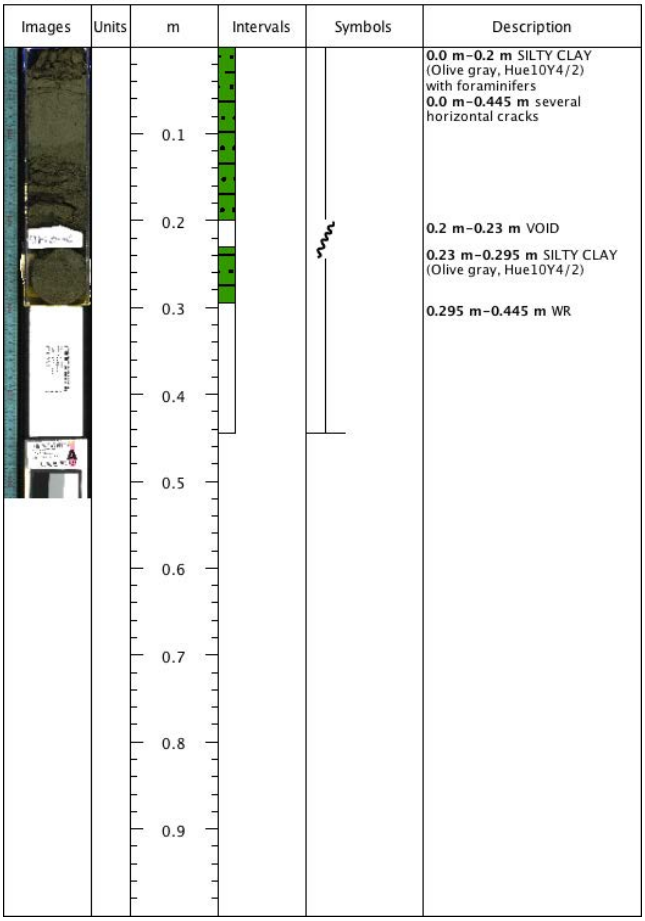

C9033A_12H_CC

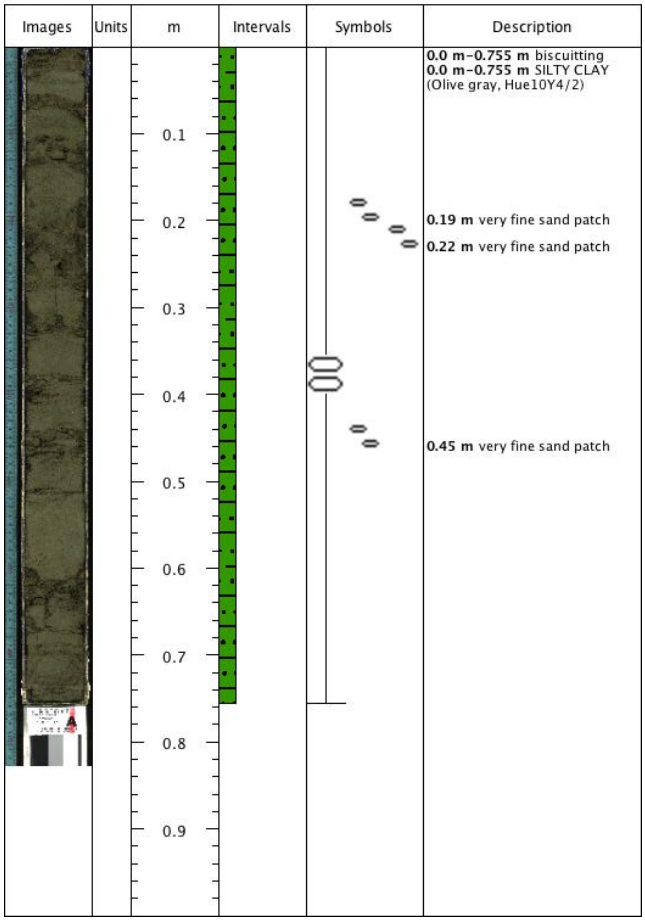

C9033C_1H_1

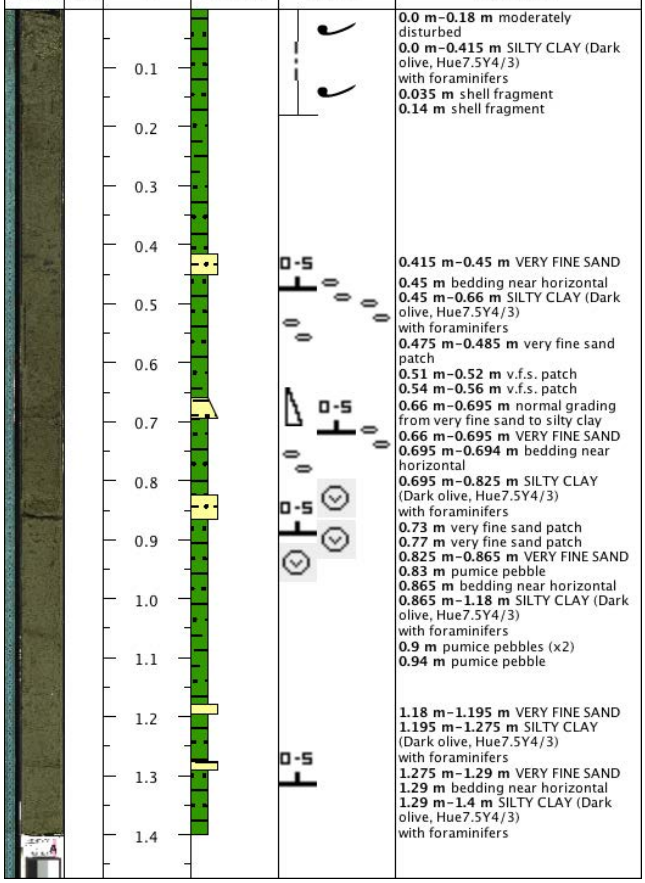

C9033C_1H_2

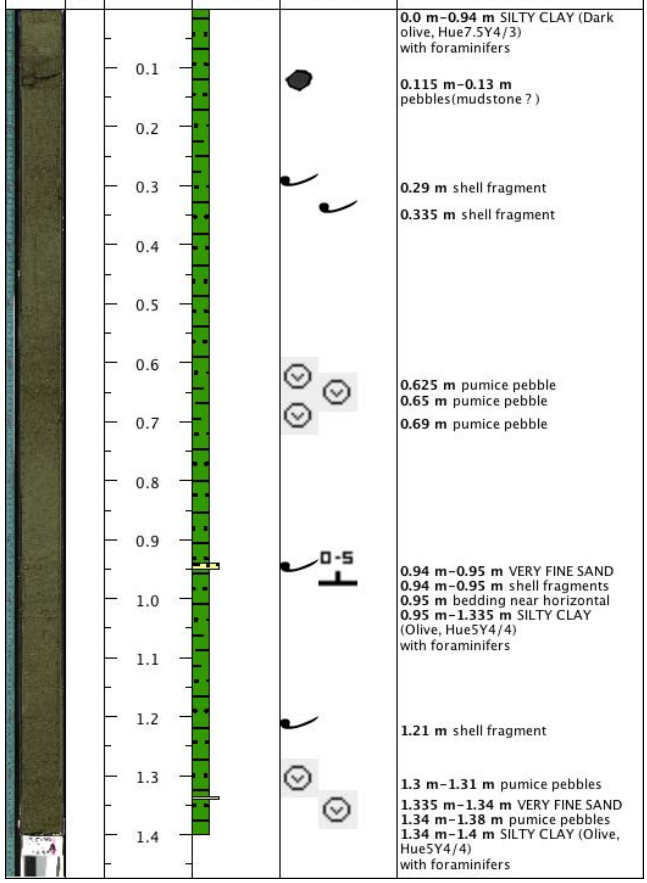

C9033C_1H_3

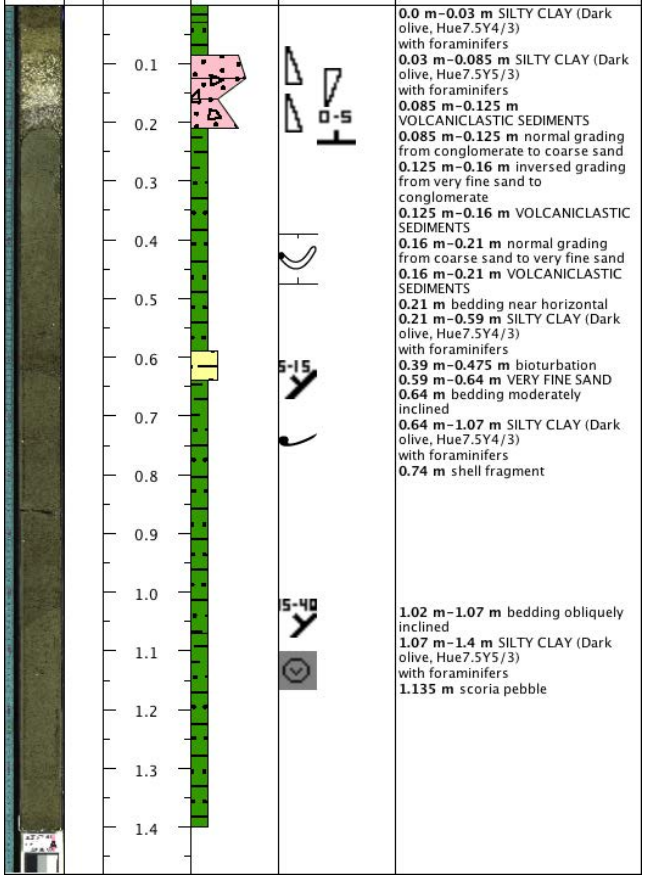

C9033C_1H_4

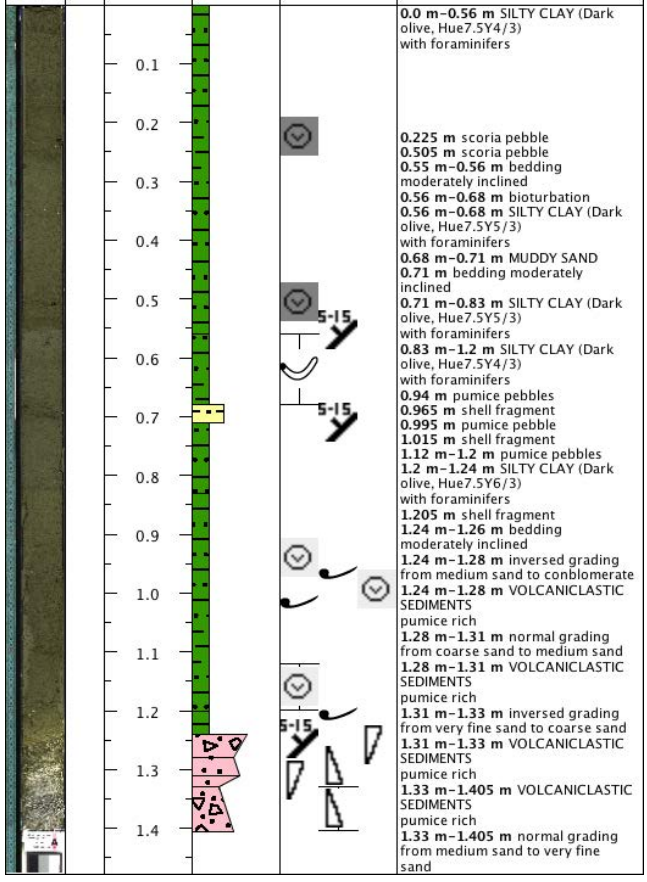

C9033C_1H_5

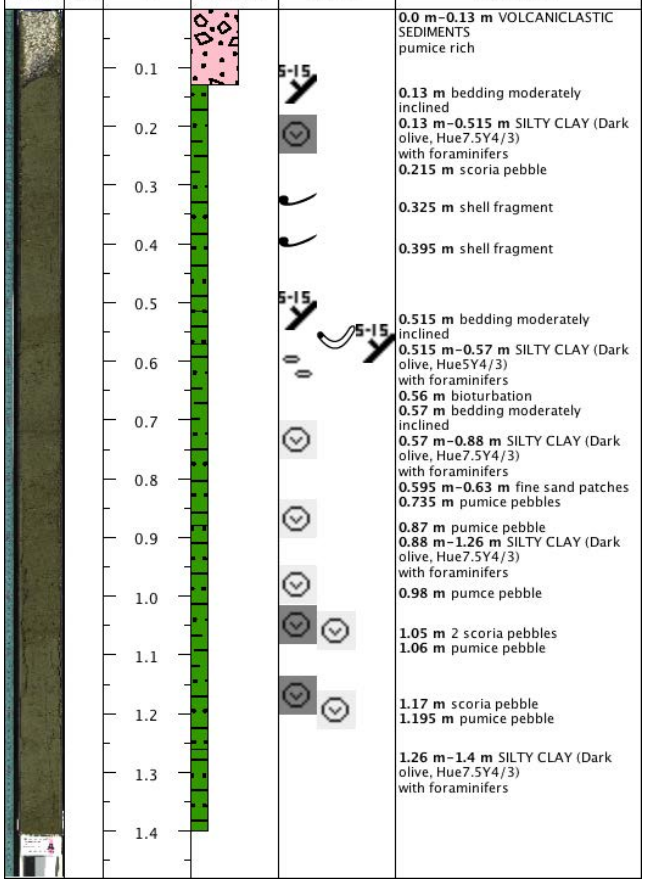

C9033C_1H_6

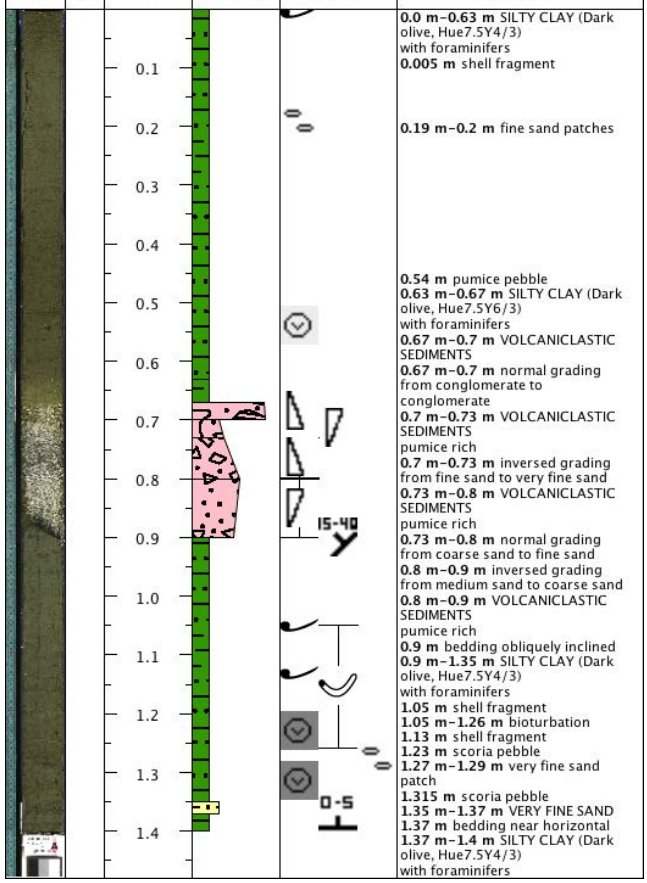

C9033C_1H_7

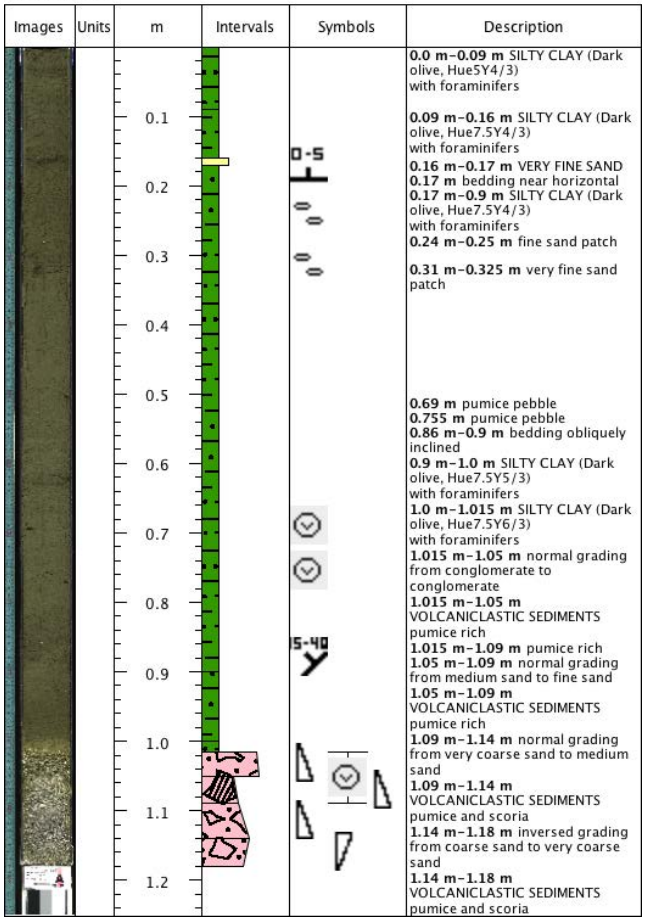

C9033C_1H_CC

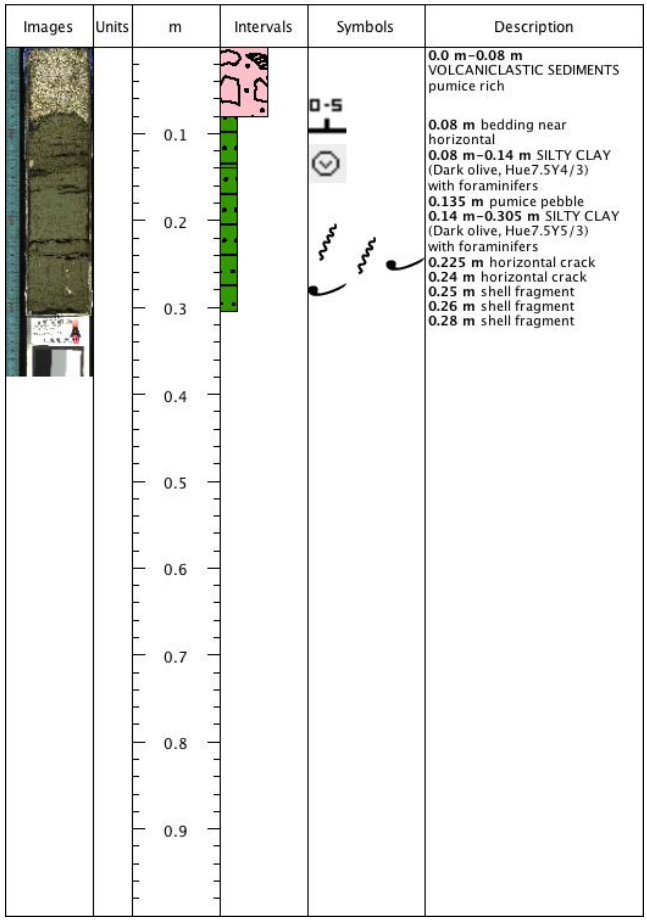

C9033C_2H_1

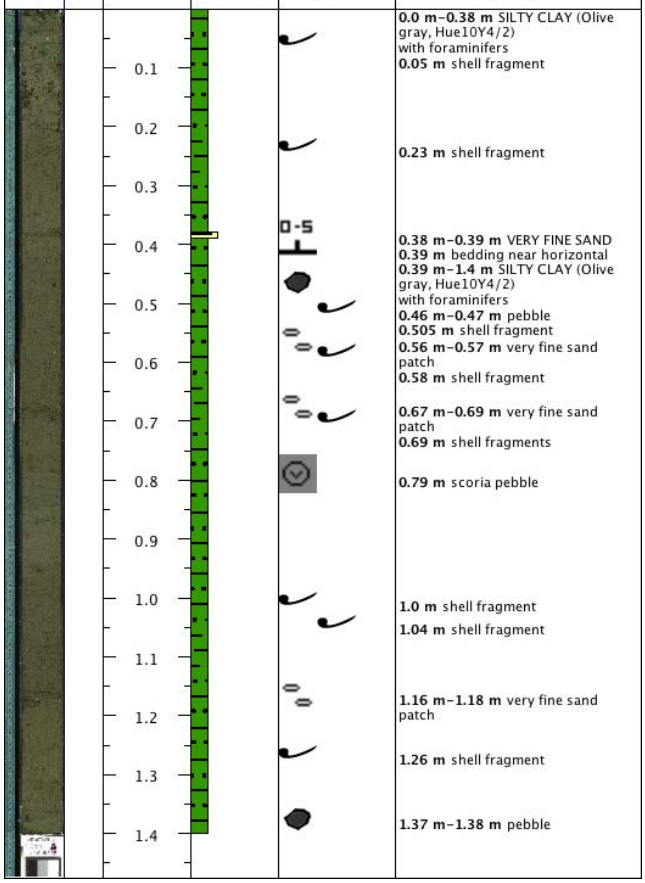

C9033C_2H_2

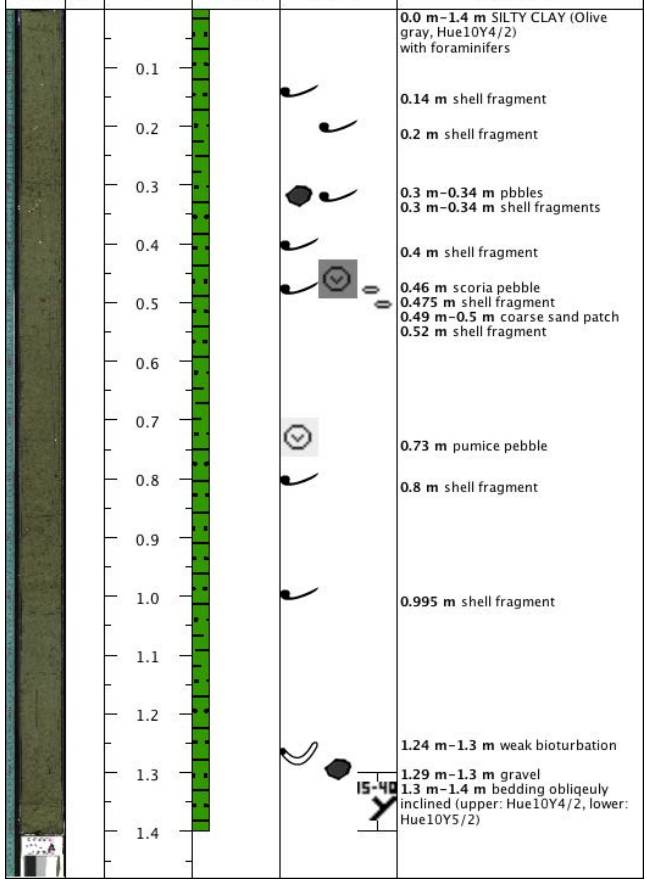

C9033C_2H_3

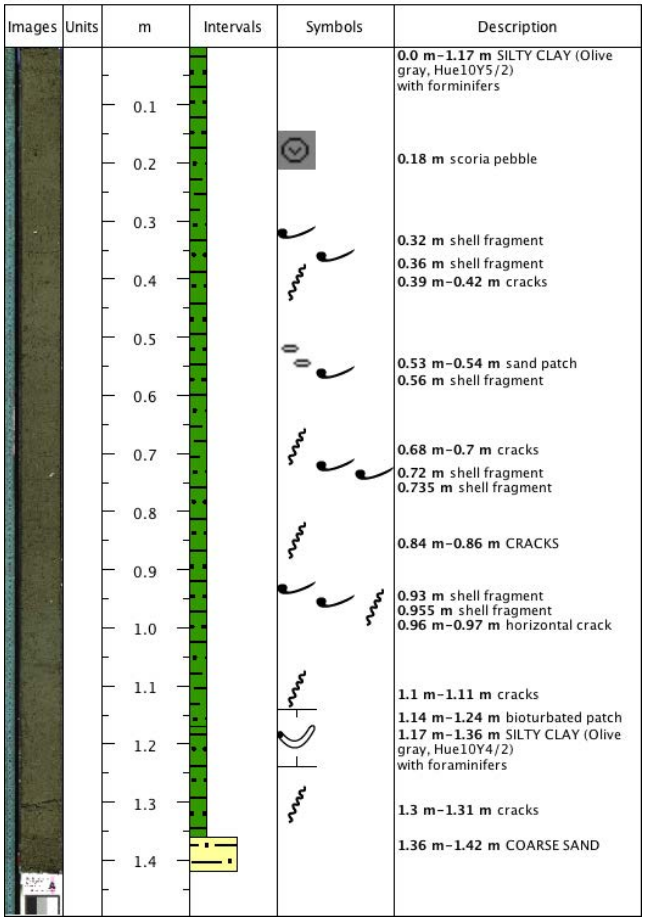

C9033C_2H_4

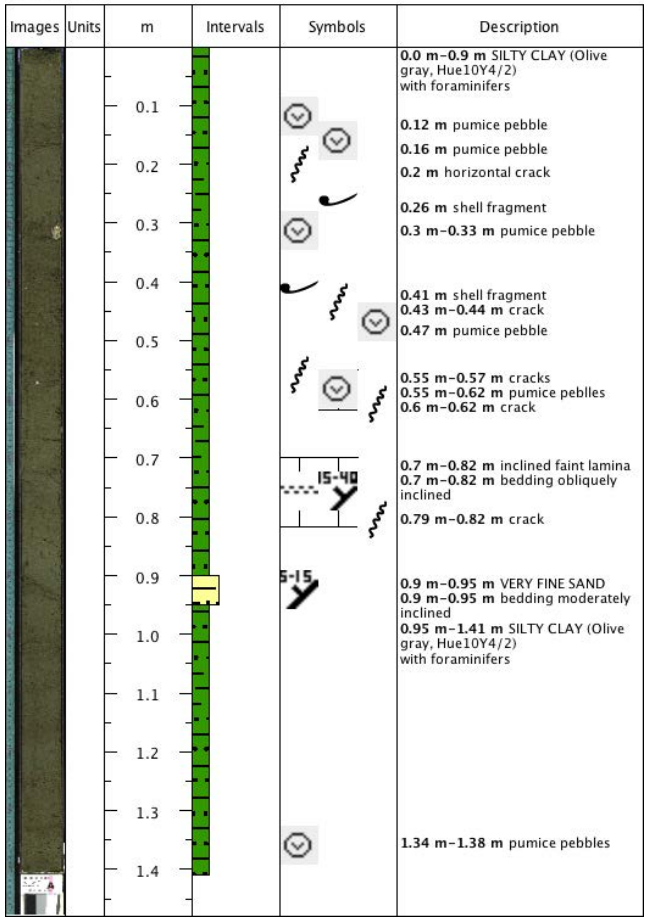

C9033C_2H_5

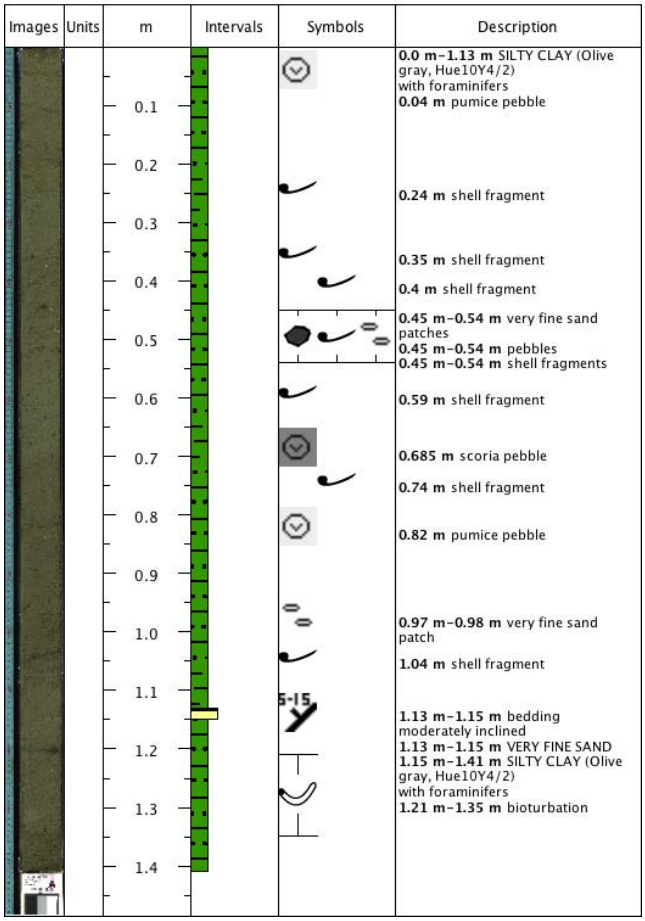

C9033C_2H_6

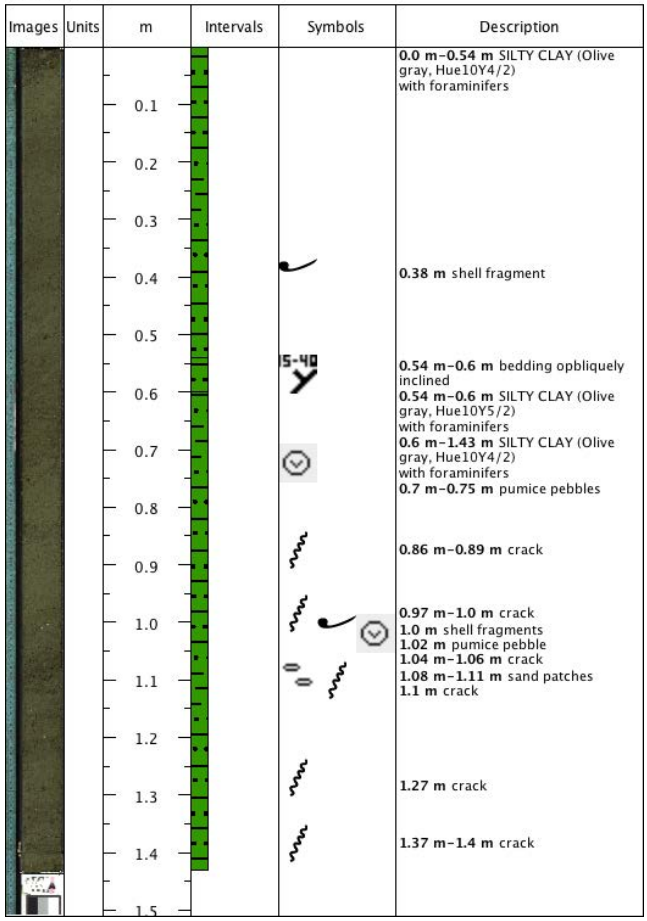

C9033C_2H_7

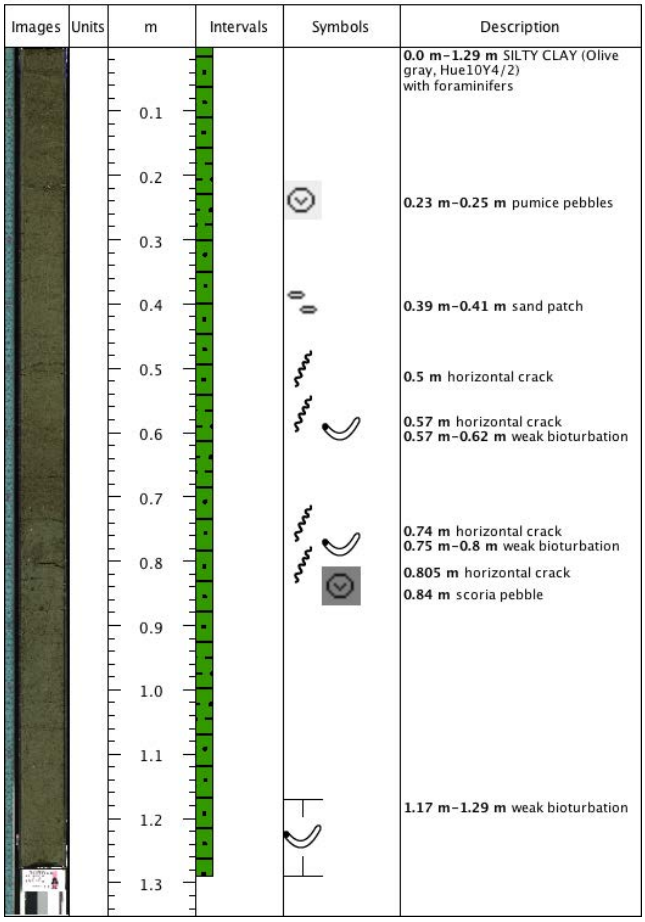

C9033C_2H_CC

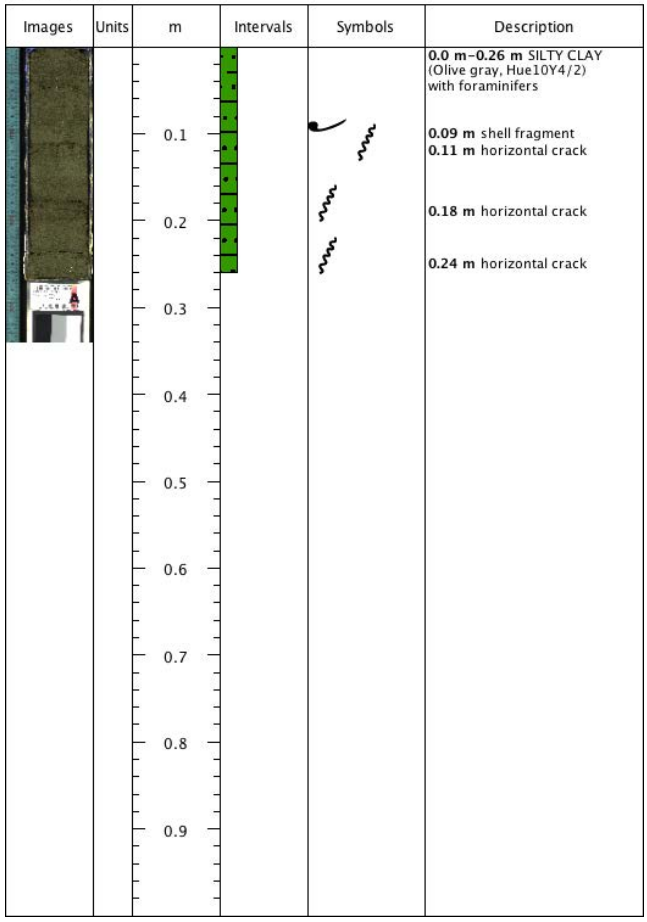

C9033C_3H_1

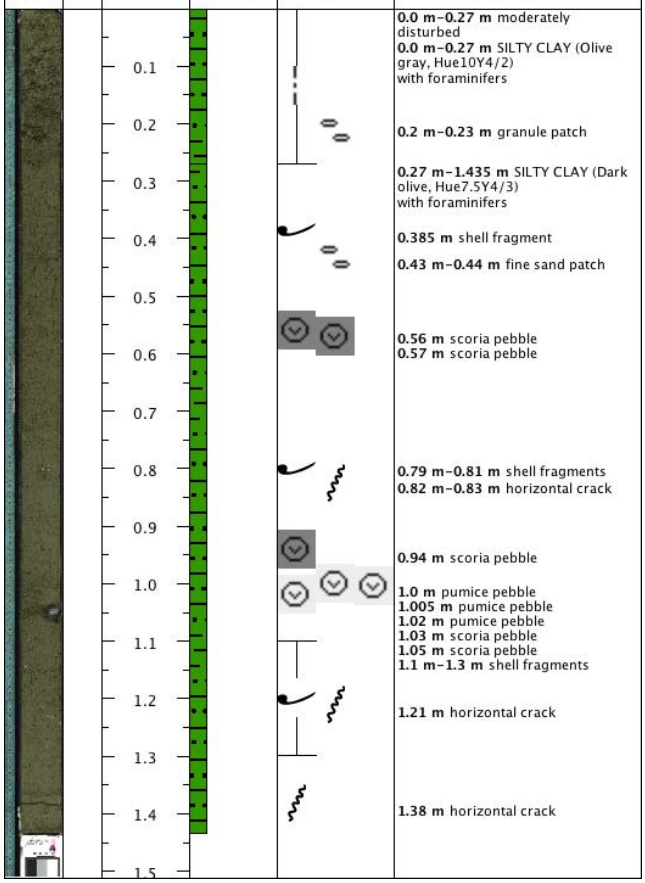

C9033C_3H_2

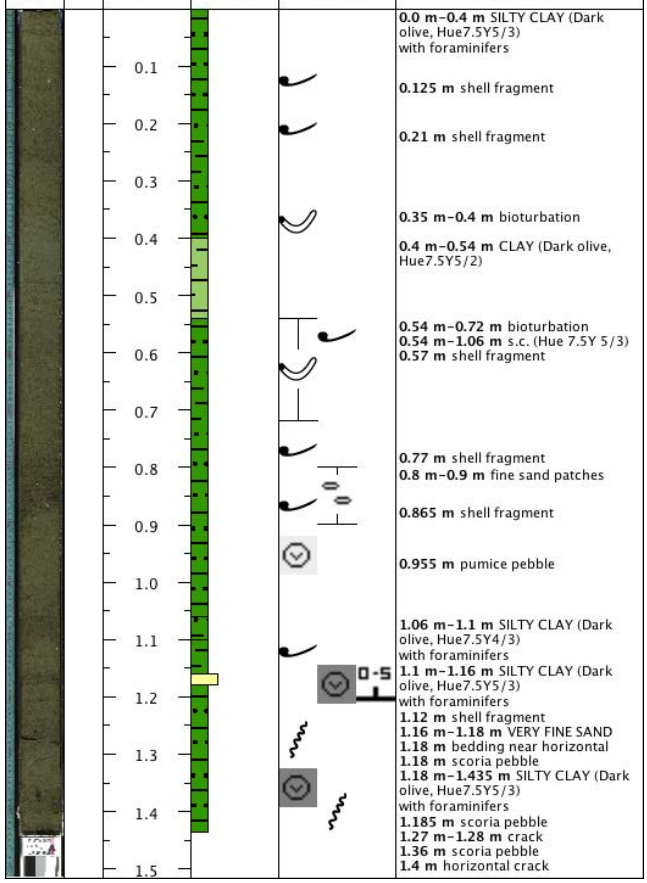

C9033C_3H_3

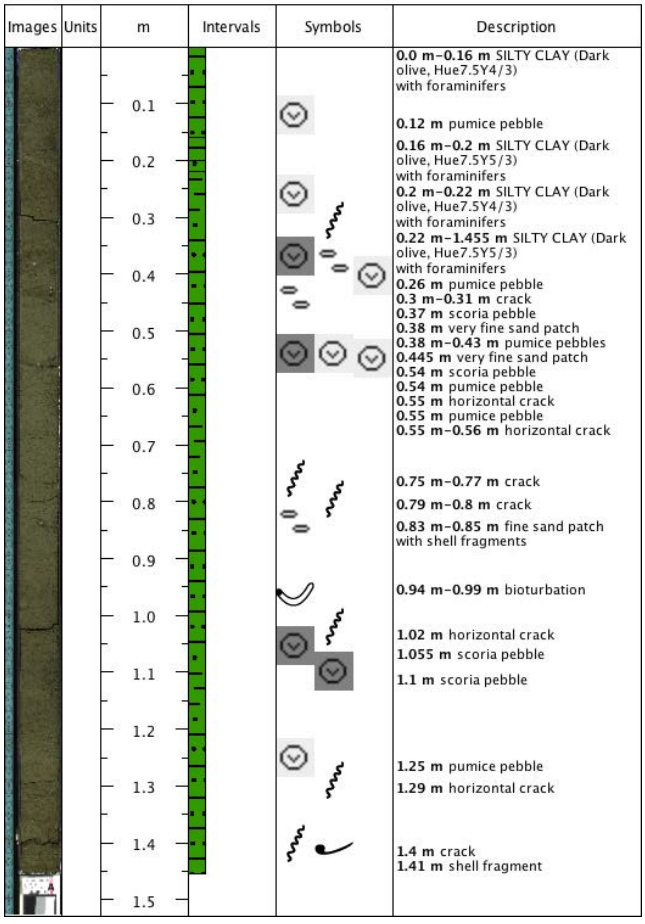

C9033C_3H_4

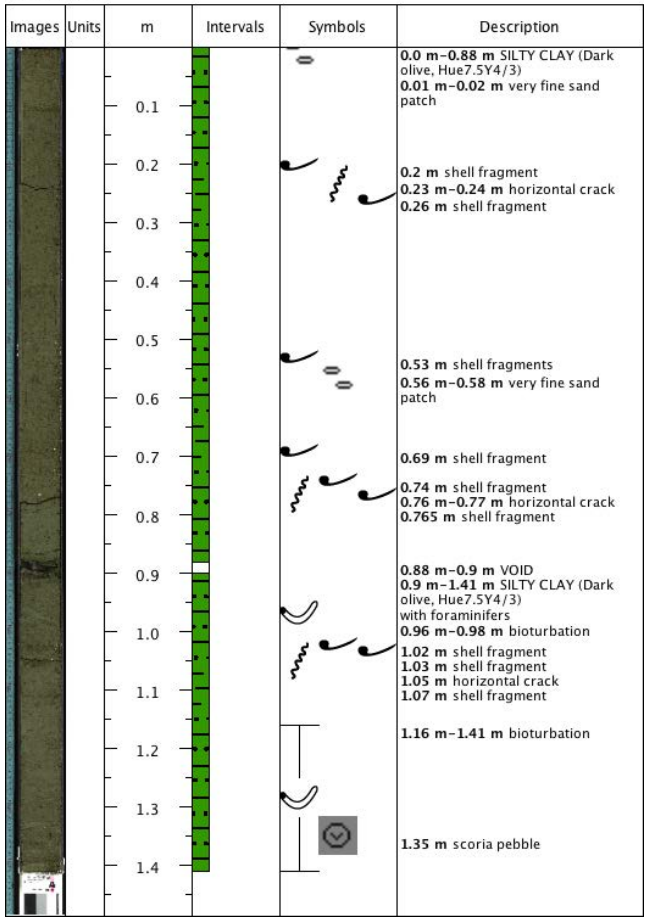

C9033C_3H_5

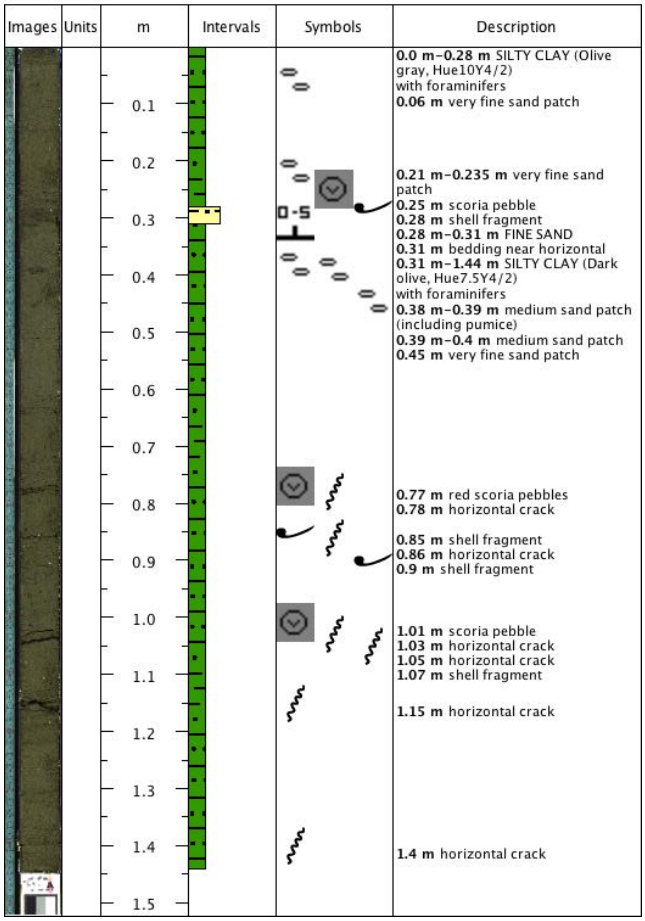

C9033C_3H_6

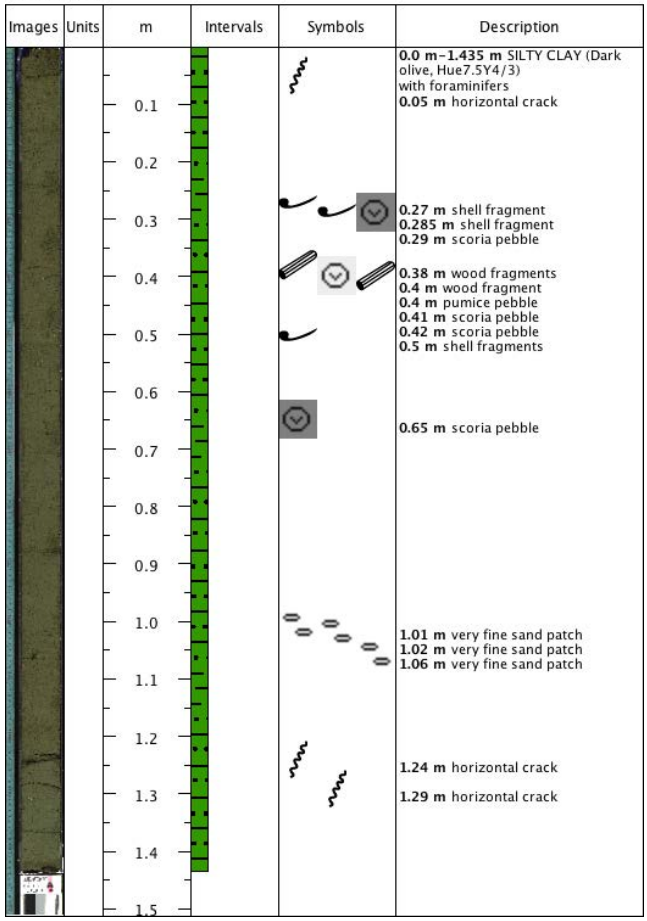

C9033C_3H_7

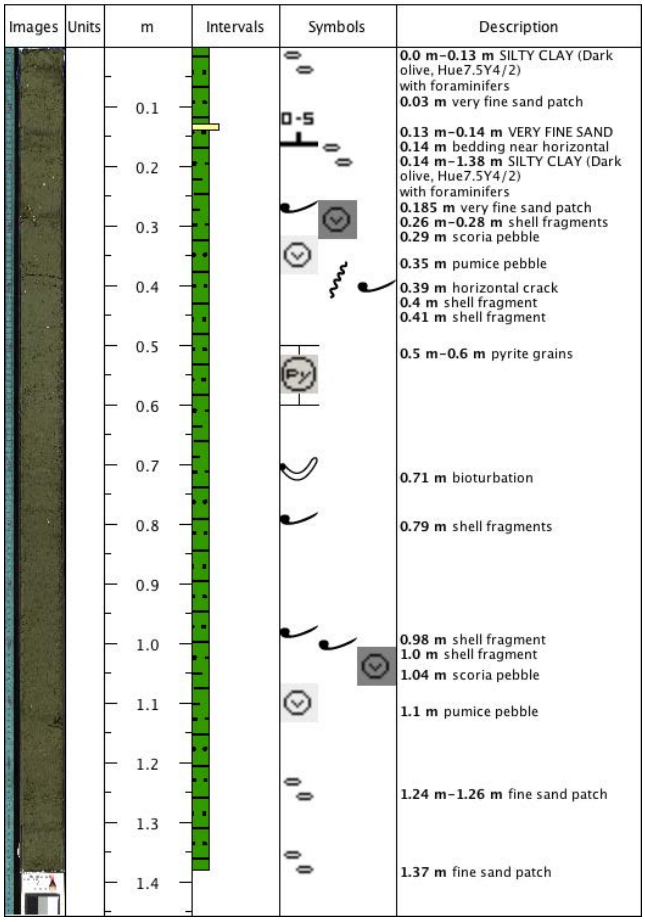

C9033C_3H_CC

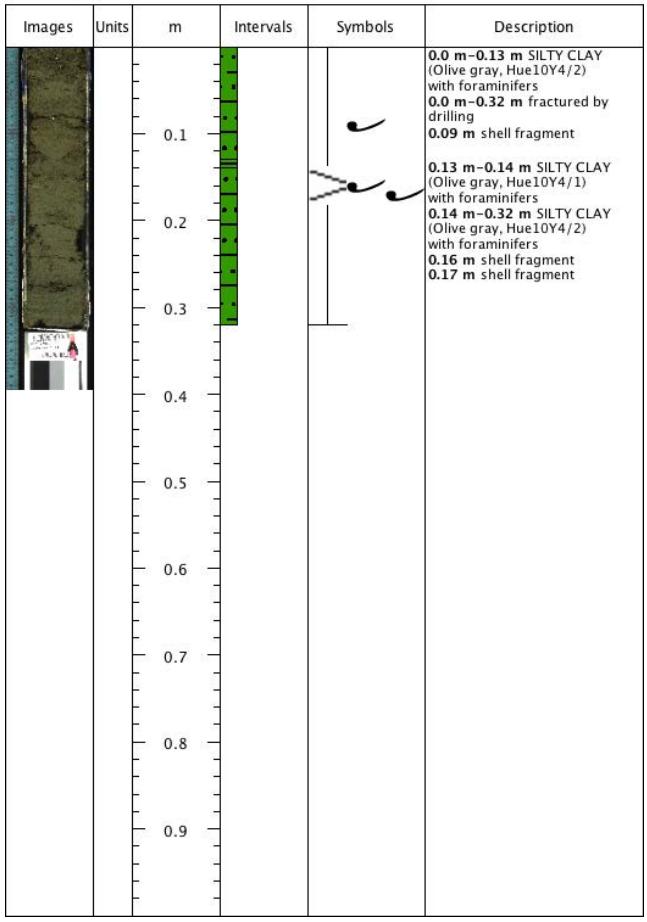

C9033C_4H_1

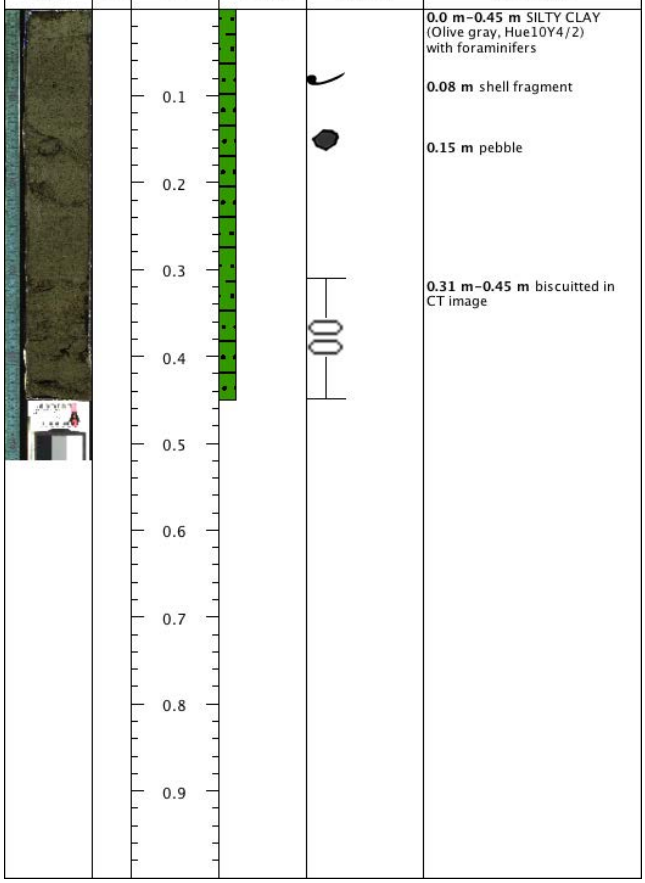

C9033C_4H_2

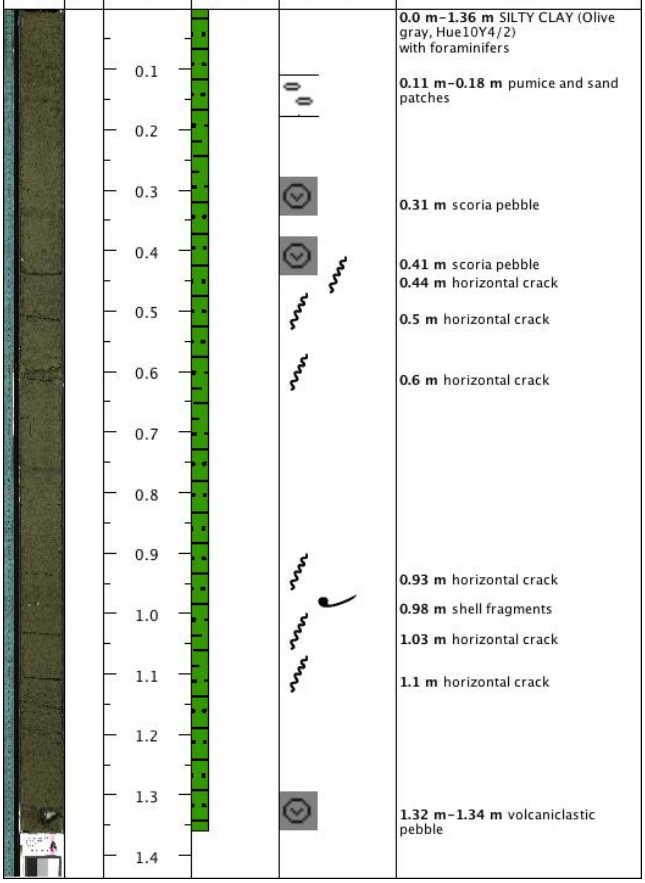

C9033C_4H_3

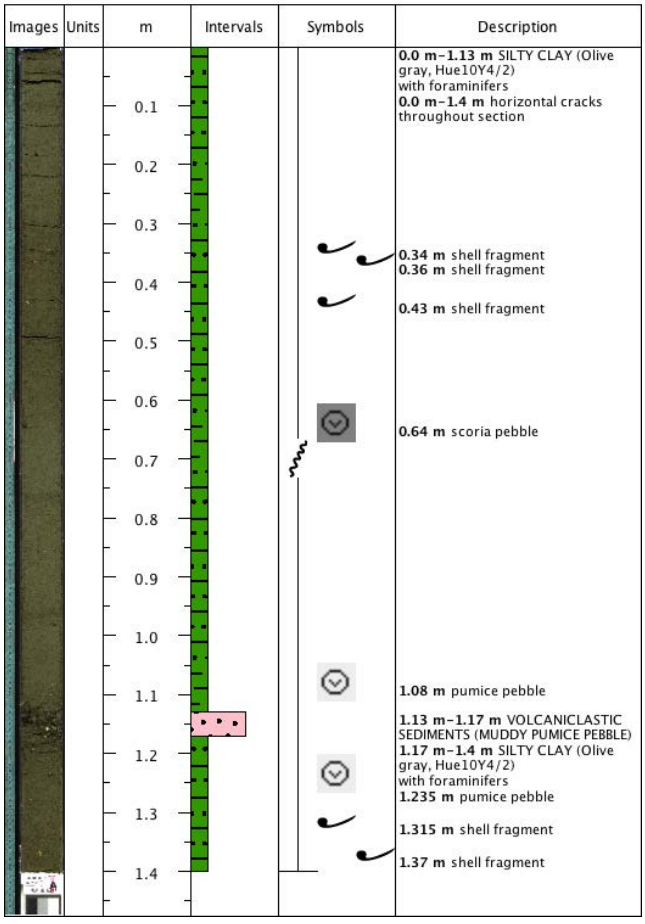

C9033C_4H_4

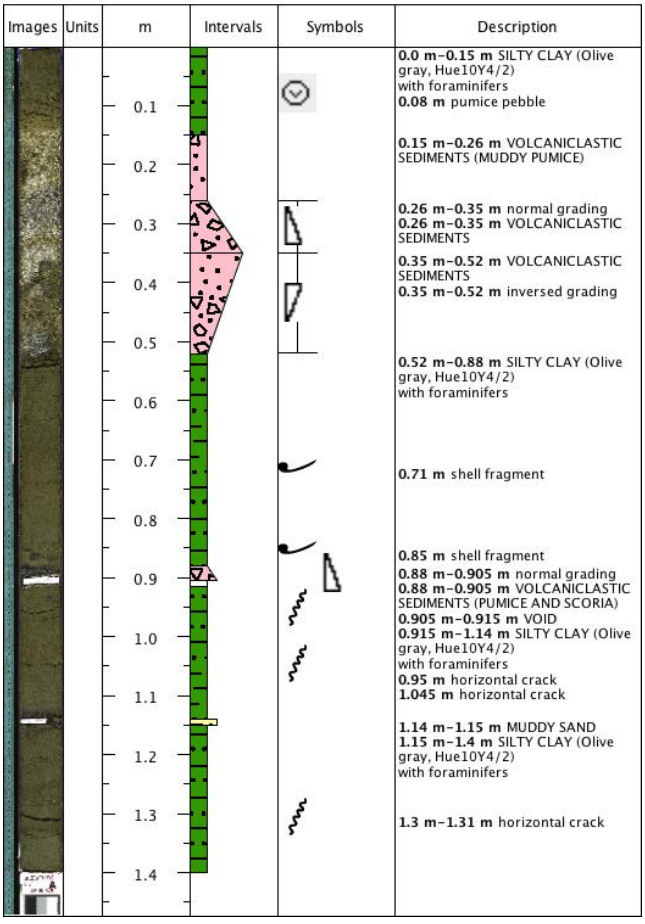

C9033C_4H_5

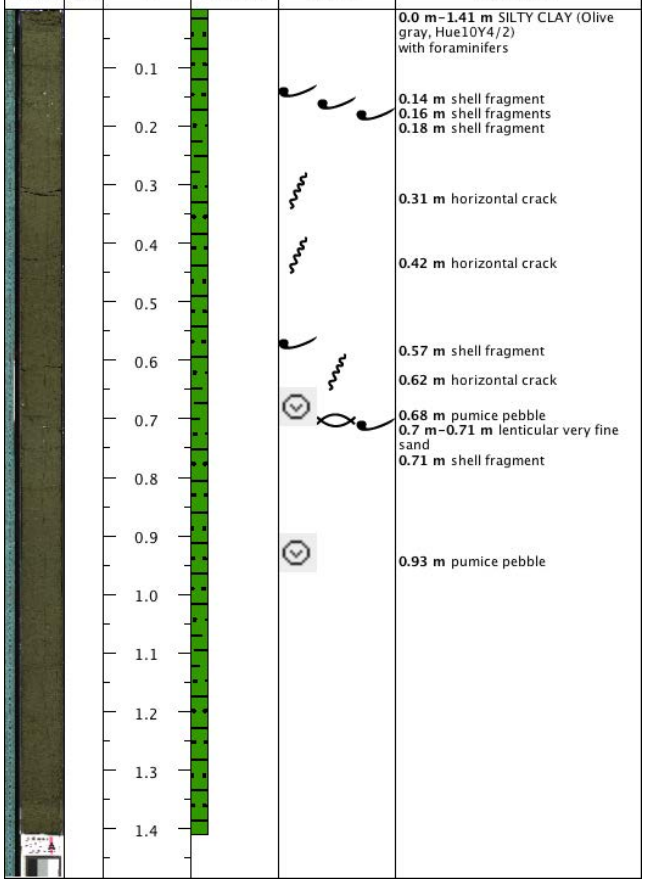

C9033C_4H_6

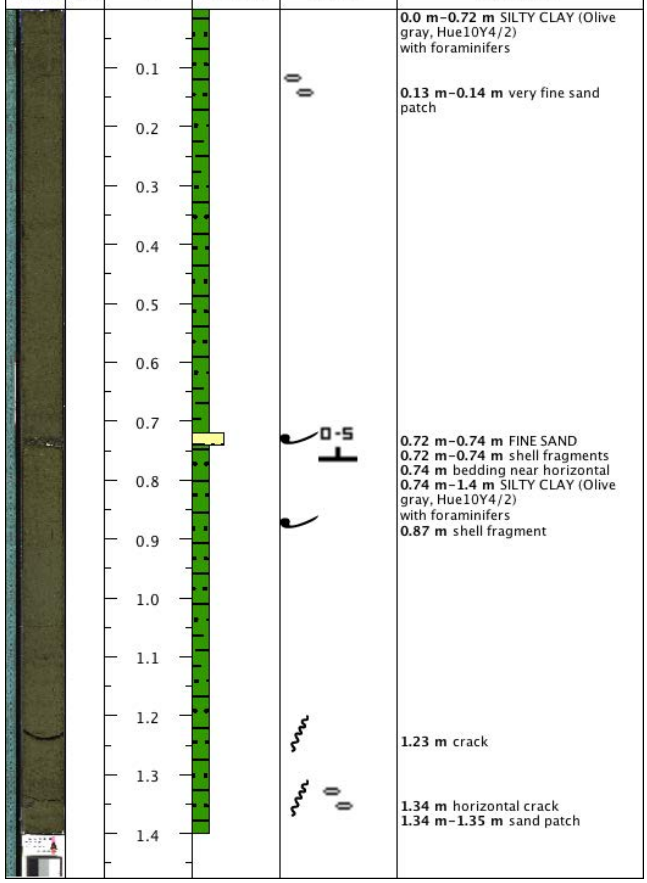

C9033C_4H_7

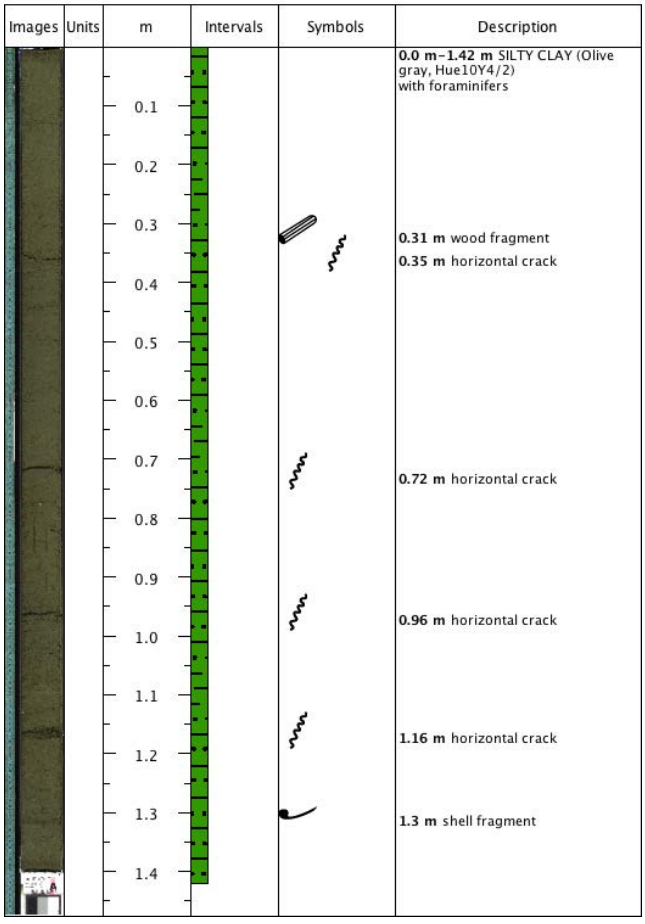

C9033C_4H_8

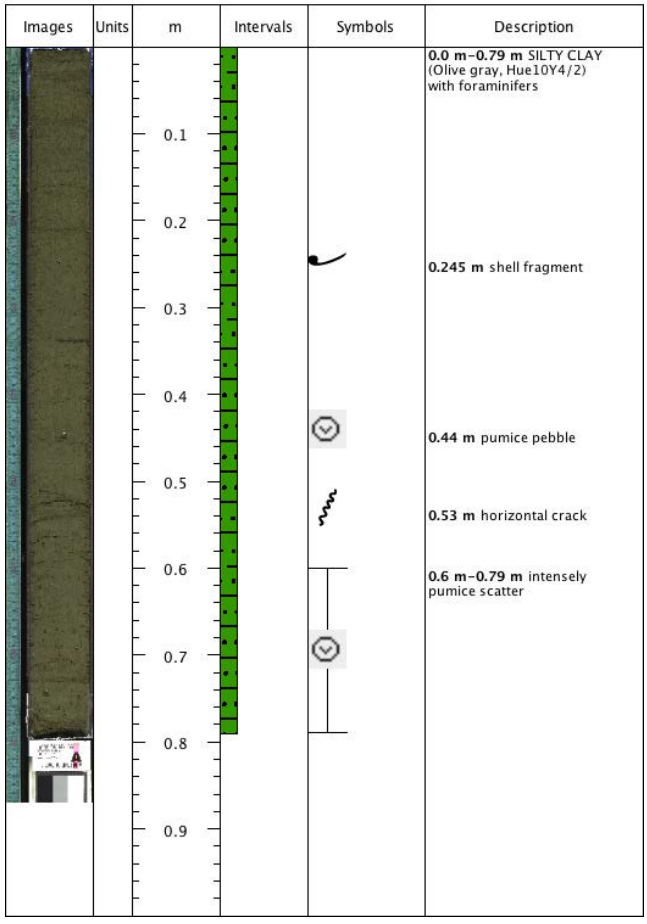

C9033C_4H_9

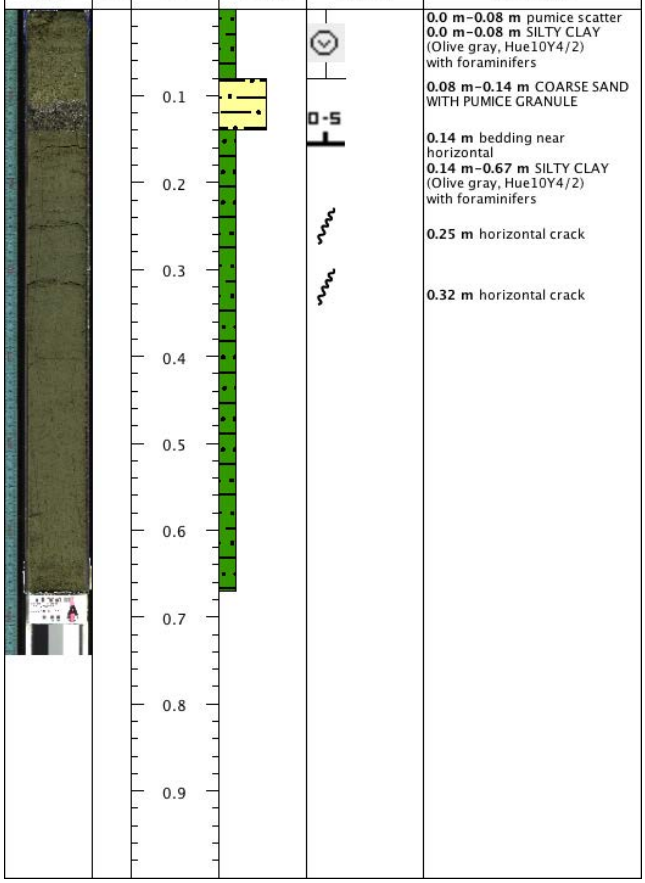

C9033C_4H_CC

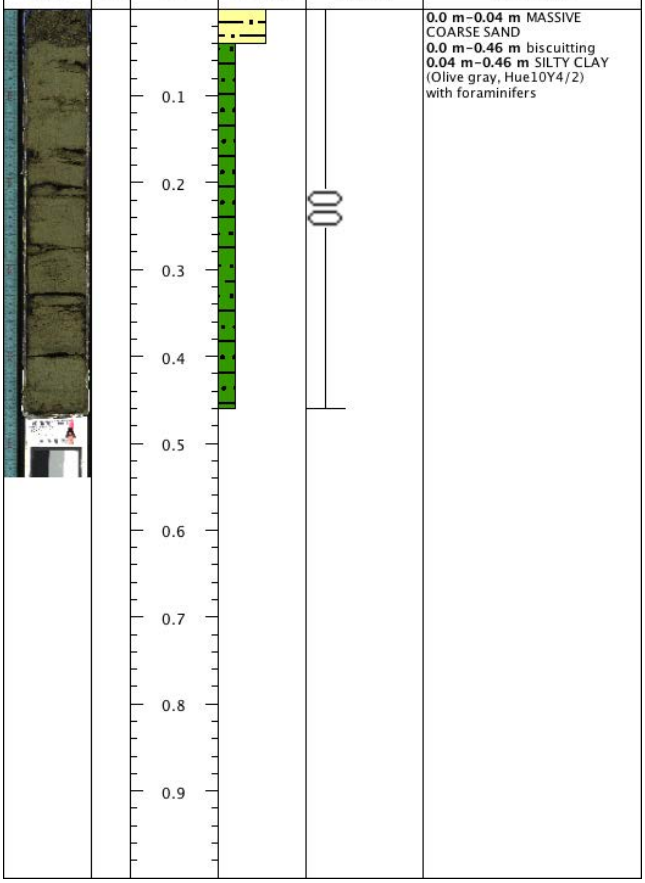

C9033C_5H_1

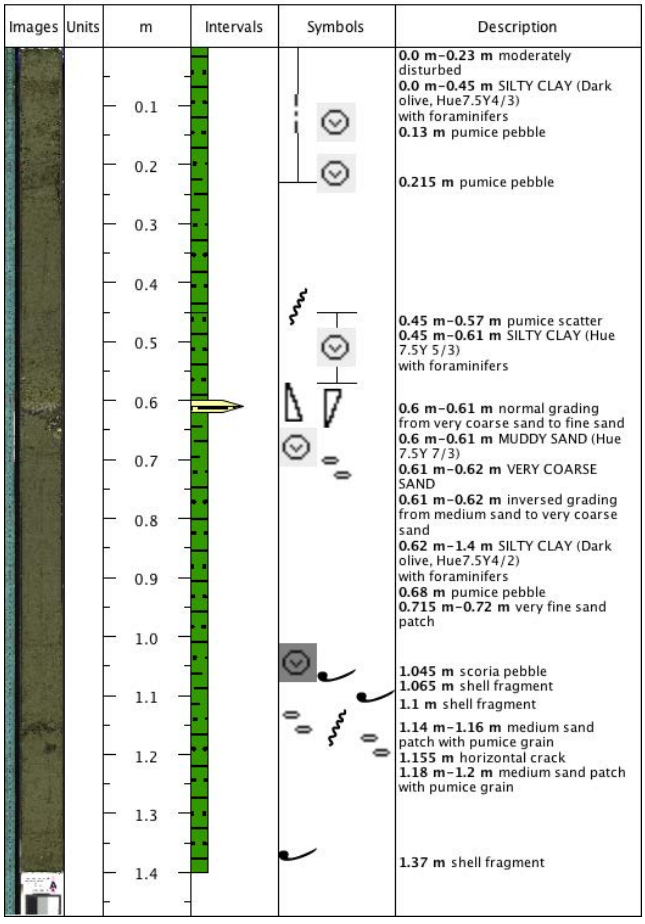

C9033C_5H_2

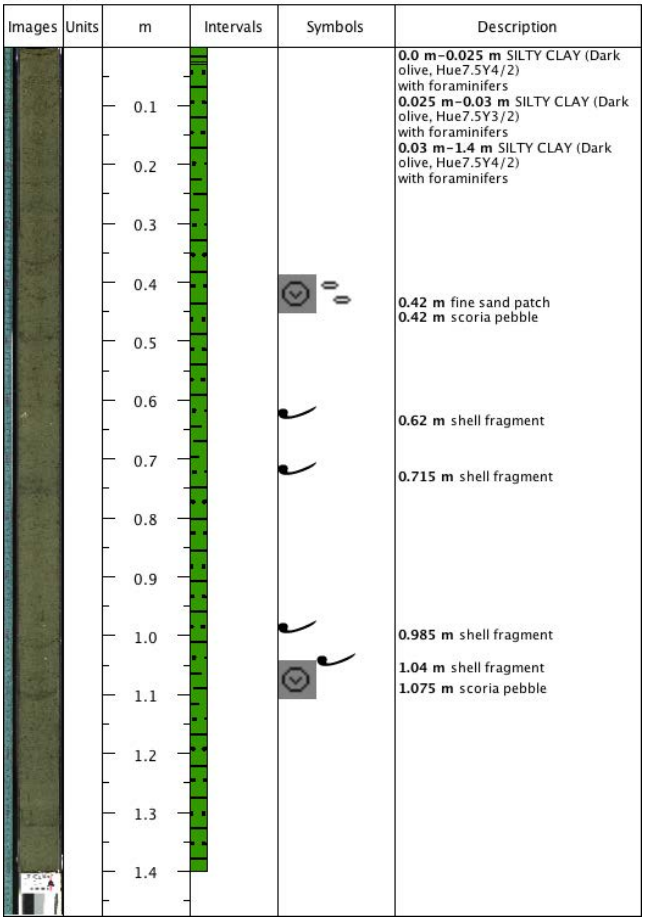

C9033C_5H_3

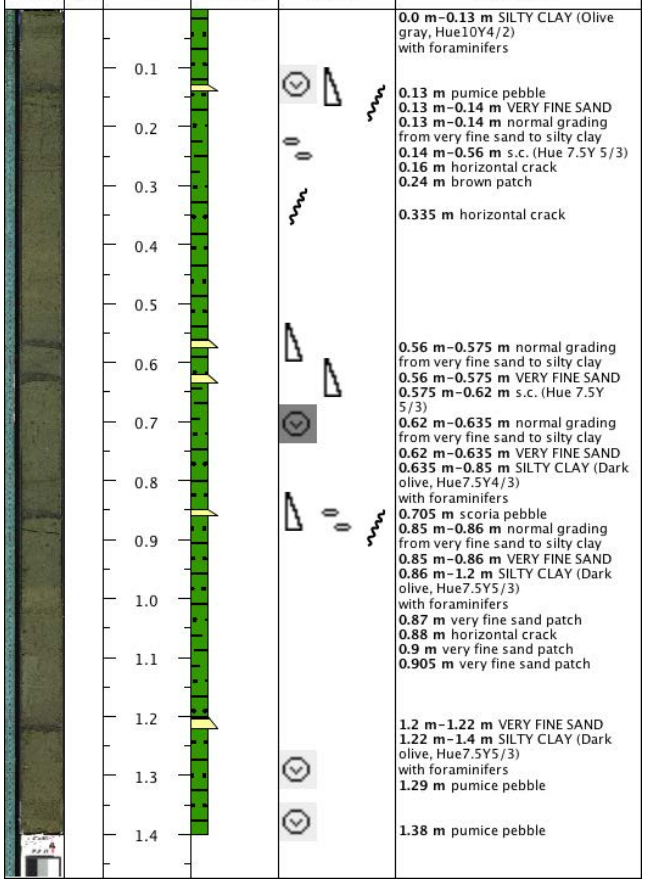

Images	Units	m	Intervals	Symbols	Description
					0.0 m–0.13 m SILTY CLAY (Olive gray, Hue10Y4/2) with foraminifers
		0.1			**0.13 m** pumice pebble **0.13 m–0.14 m** VERY FINE SAND **0.13 m–0.14 m** normal grading from very fine sand to silty clay **0.14 m–0.56 m** s.c. (Hue 7.5Y 5/3) **0.16 m** horizontal crack **0.24 m** brown patch
		0.2			
		0.3			**0.335 m** horizontal crack
		0.4			
		0.5			
		0.6			**0.56 m–0.575 m** normal grading from very fine sand to silty clay **0.56 m–0.575 m** VERY FINE SAND **0.575 m–0.62 m** s.c. (Hue 7.5Y 5/3)
		0.7			**0.62 m–0.635 m** normal grading from very fine sand to silty clay **0.62 m–0.635 m** VERY FINE SAND **0.635 m–0.85 m** SILTY CLAY (Dark olive, Hue7.5Y4/3) with foraminifers **0.705 m** scoria pebble
		0.8			
		0.9			**0.85 m–0.86 m** normal grading from very fine sand to silty clay **0.85 m–0.86 m** VERY FINE SAND **0.86 m–1.2 m** SILTY CLAY (Dark olive, Hue7.5Y5/3) with foraminifers **0.87 m** very fine sand patch **0.88 m** horizontal crack **0.9 m** very fine sand patch **0.905 m** very fine sand patch
		1.0			
		1.1			
		1.2			**1.2 m–1.22 m** VERY FINE SAND **1.22 m–1.4 m** SILTY CLAY (Dark olive, Hue7.5Y5/3) with foraminifers **1.29 m** pumice pebble
		1.3			
		1.4			**1.38 m** pumice pebble

C9033C_5H_4

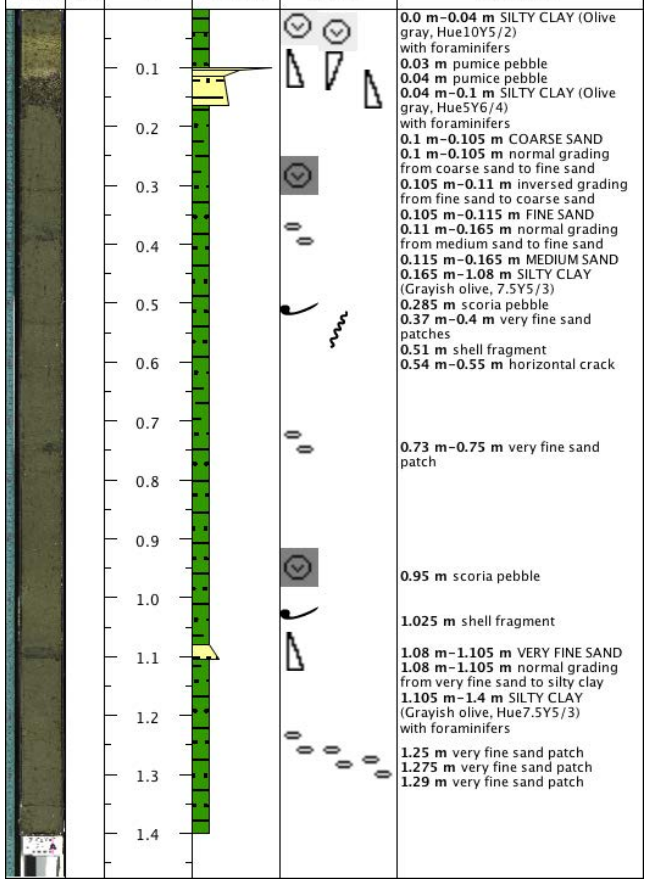

Images	Units	m	Intervals	Symbols	Description
					0.0 m–0.04 m SILTY CLAY (Olive gray, Hue10Y5/2) with foraminifers **0.03 m** pumice pebble **0.04 m** pumice pebble **0.04 m–0.1 m** SILTY CLAY (Olive gray, Hue5Y6/4) with foraminifers **0.1 m–0.105 m** COARSE SAND **0.1 m–0.105 m** normal grading from coarse sand to fine sand **0.105 m–0.11 m** inversed grading from fine sand to coarse sand **0.105 m–0.115 m** FINE SAND **0.11 m–0.165 m** normal grading from medium sand to fine sand **0.115 m–0.165 m** MEDIUM SAND **0.165 m–1.08 m** SILTY CLAY (Grayish olive, 7.5Y5/3) **0.285 m** scoria pebble **0.37 m–0.4 m** very fine sand patches **0.51 m** shell fragment **0.54 m–0.55 m** horizontal crack
		0.1			
		0.2			
		0.3			
		0.4			
		0.5			
		0.6			
		0.7			**0.73 m–0.75 m** very fine sand patch
		0.8			
		0.9			**0.95 m** scoria pebble
		1.0			**1.025 m** shell fragment
		1.1			**1.08 m–1.105 m** VERY FINE SAND **1.08 m–1.105 m** normal grading from very fine sand to silty clay **1.105 m–1.4 m** SILTY CLAY (Grayish olive, Hue7.5Y5/3) with foraminifers
		1.2			
		1.3			**1.25 m** very fine sand patch **1.275 m** very fine sand patch **1.29 m** very fine sand patch
		1.4			

C9033C_5H_5

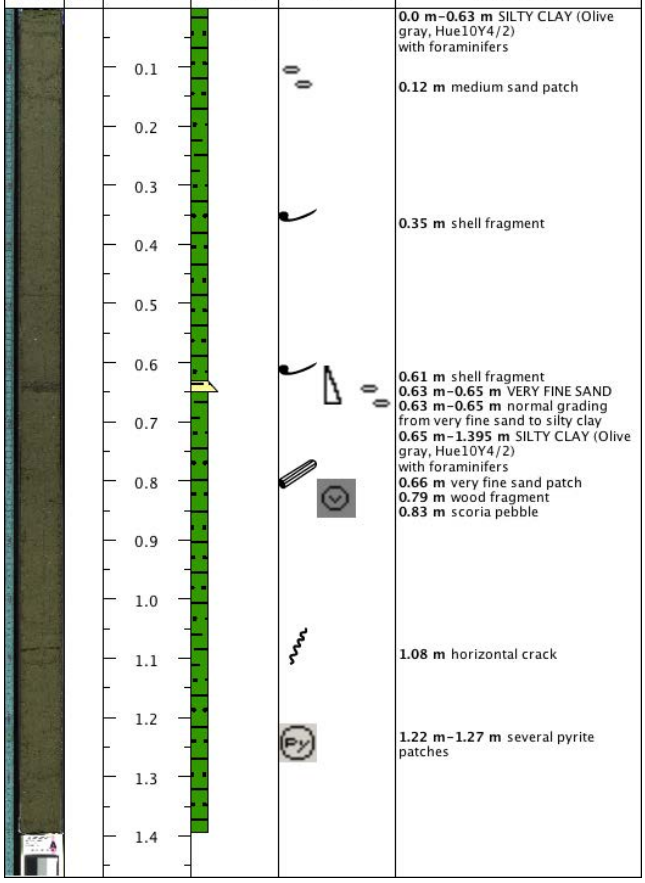

Images	Units	m	Intervals	Symbols	Description
					0.0 m–0.63 m SILTY CLAY (Olive gray, Hue10Y4/2) with foraminifers
		0.1			**0.12 m** medium sand patch
		0.2			
		0.3			**0.35 m** shell fragment
		0.4			
		0.5			
		0.6			**0.61 m** shell fragment **0.63 m–0.65 m** VERY FINE SAND **0.63 m–0.65 m** normal grading from very fine sand to silty clay **0.65 m–1.395 m** SILTY CLAY (Olive gray, Hue10Y4/2) with foraminifers **0.66 m** very fine sand patch **0.79 m** wood fragment **0.83 m** scoria pebble
		0.7			
		0.8			
		0.9			
		1.0			
		1.1			**1.08 m** horizontal crack
		1.2		Py	**1.22 m–1.27 m** several pyrite patches
		1.3			
		1.4			

C9033C_5H_6

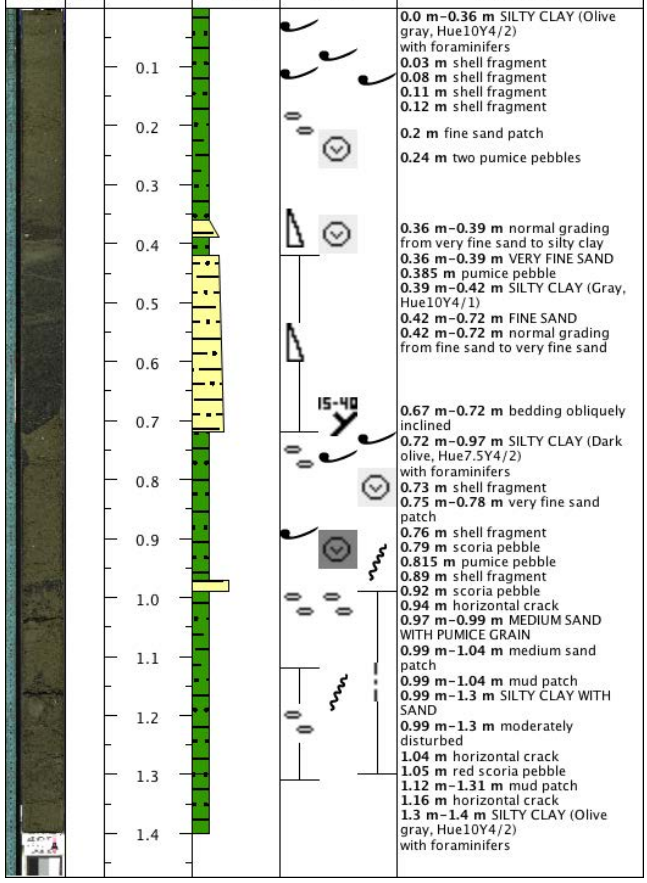

Images	Units	m	Intervals	Symbols	Description
					0.0 m–0.36 m SILTY CLAY (Olive gray, Hue10Y4/2) with foraminifers **0.03 m** shell fragment **0.08 m** shell fragment **0.11 m** shell fragment **0.12 m** shell fragment
		0.1			
		0.2			**0.2 m** fine sand patch **0.24 m** two pumice pebbles
		0.3			
		0.4			**0.36 m–0.39 m** normal grading from very fine sand to silty clay **0.36 m–0.39 m** VERY FINE SAND **0.385 m** pumice pebble **0.39 m–0.42 m** SILTY CLAY (Gray, Hue10Y4/1) **0.42 m–0.72 m** FINE SAND **0.42 m–0.72 m** normal grading from fine sand to very fine sand
		0.5			
		0.6			
		0.7			**0.67 m–0.72 m** bedding obliquely inclined **0.72 m–0.97 m** SILTY CLAY (Dark olive, Hue7.5Y4/2) with foraminifers **0.73 m** shell fragment **0.75 m–0.78 m** very fine sand patch **0.76 m** shell fragment **0.79 m** scoria pebble **0.815 m** pumice pebble **0.89 m** shell fragment **0.92 m** scoria pebble **0.94 m** horizontal crack **0.97 m–0.99 m** MEDIUM SAND WITH PUMICE GRAIN **0.99 m–1.04 m** medium sand patch **0.99 m–1.04 m** mud patch **0.99 m–1.3 m** SILTY CLAY WITH SAND **0.99 m–1.3 m** moderately disturbed **1.04 m** horizontal crack **1.05 m** red scoria pebble **1.12 m–1.31 m** mud patch **1.16 m** horizontal crack **1.3 m–1.4 m** SILTY CLAY (Olive gray, Hue10Y4/2) with foraminifers
		0.8			
		0.9			
		1.0			
		1.1			
		1.2			
		1.3			
		1.4			

C9033C_5H_7

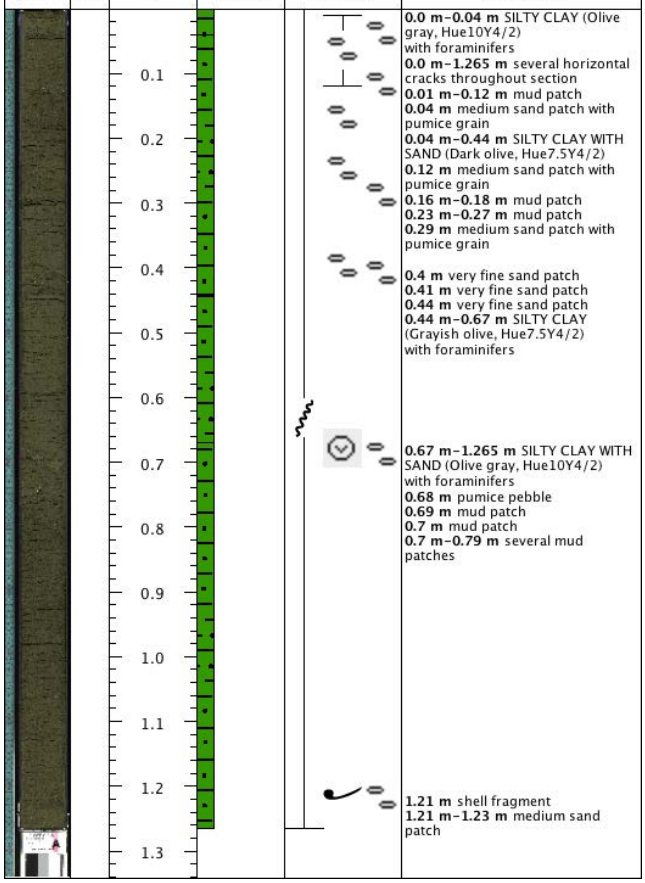

C9033C_5H_CC

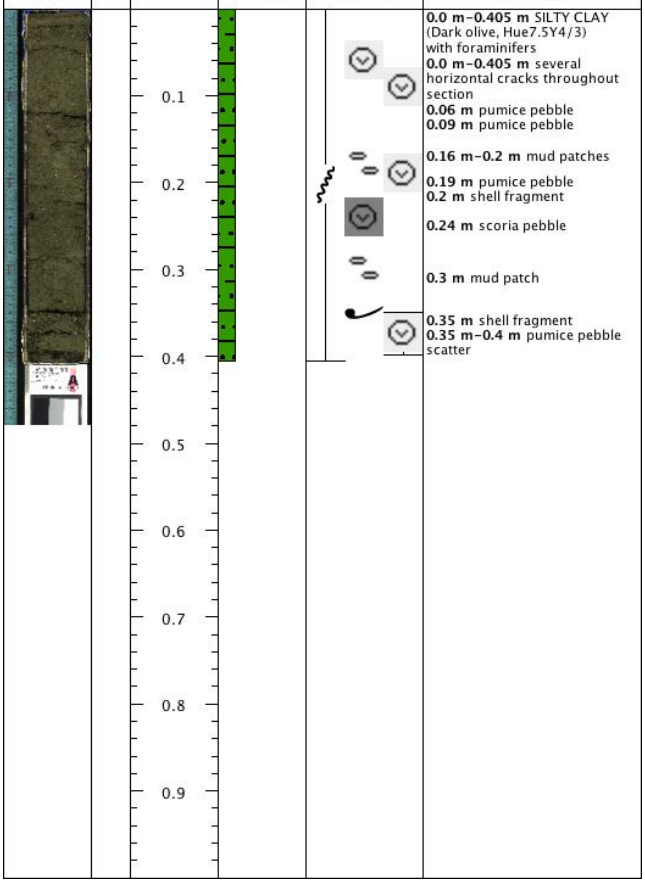

C9033C_6H_1

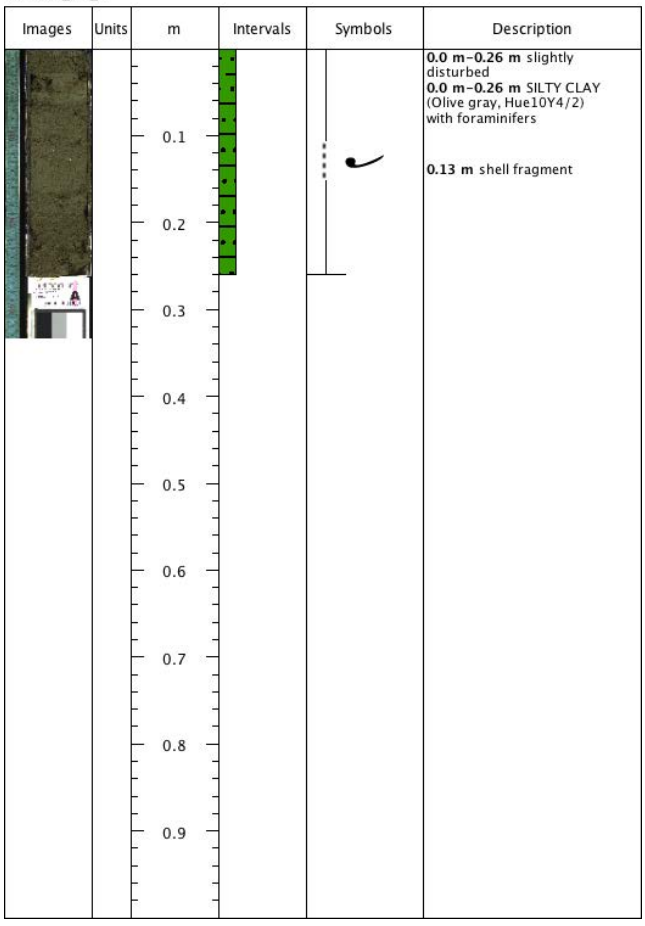

C9033C_6H_2

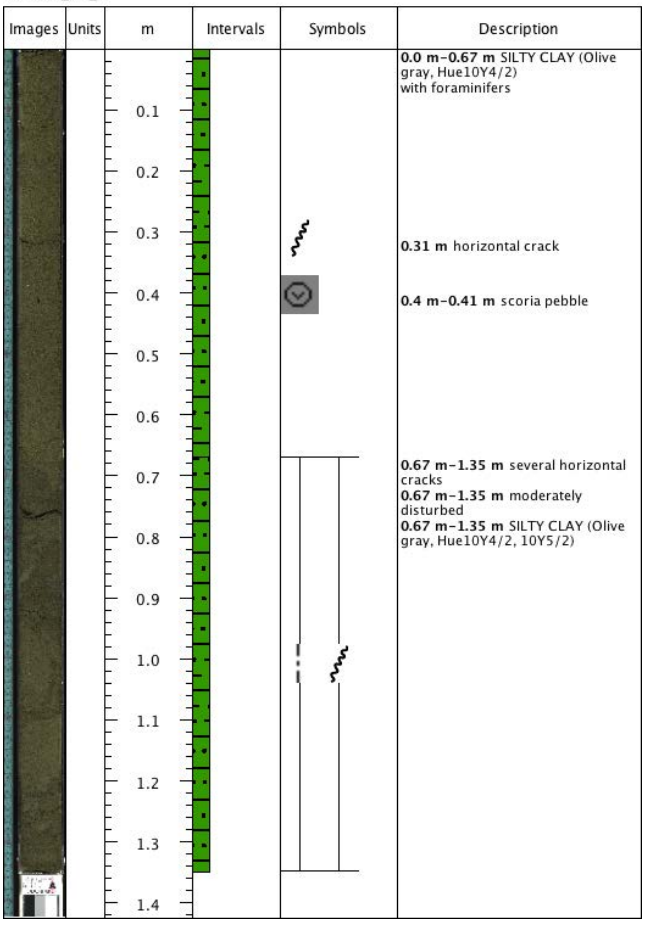

C9033C_6H_3

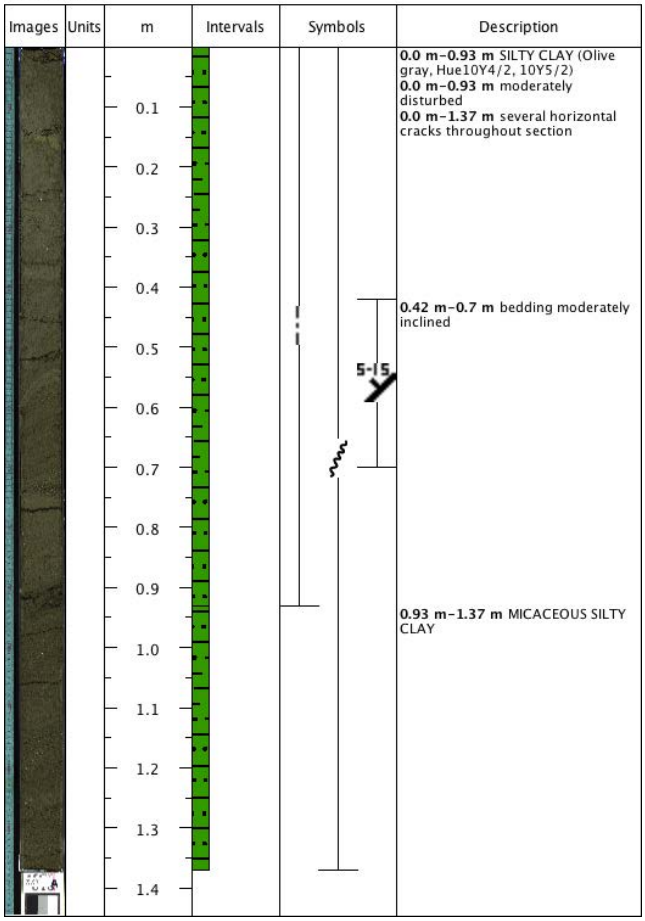

C9033C_6H_4

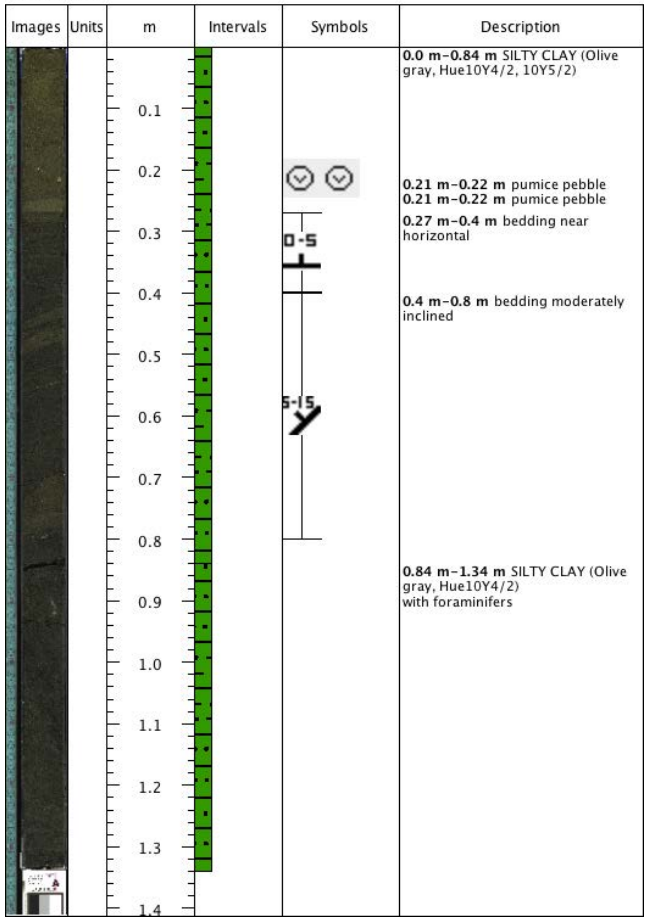

C9033C_6H_5

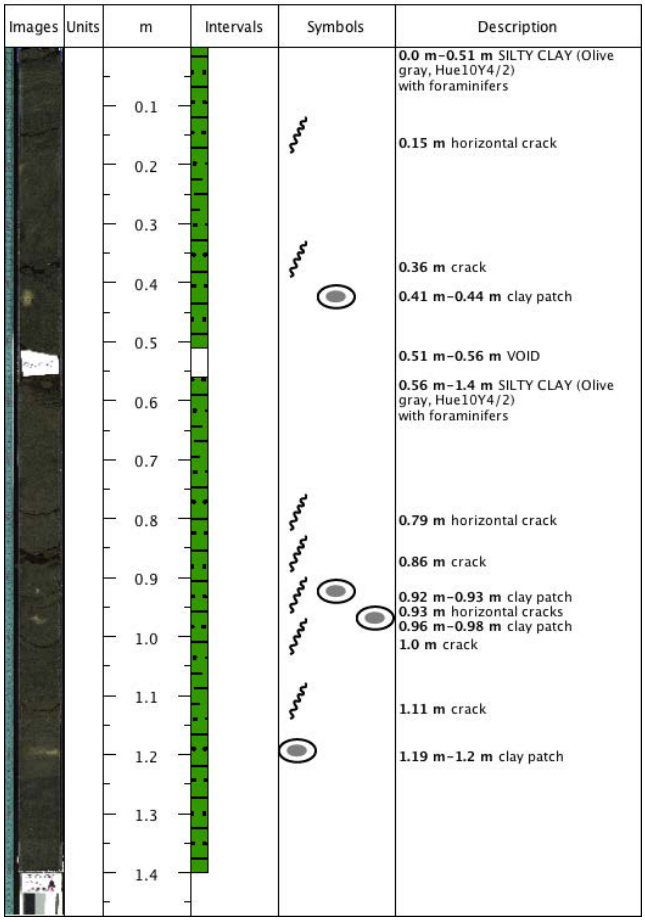

C9033C_6H_6

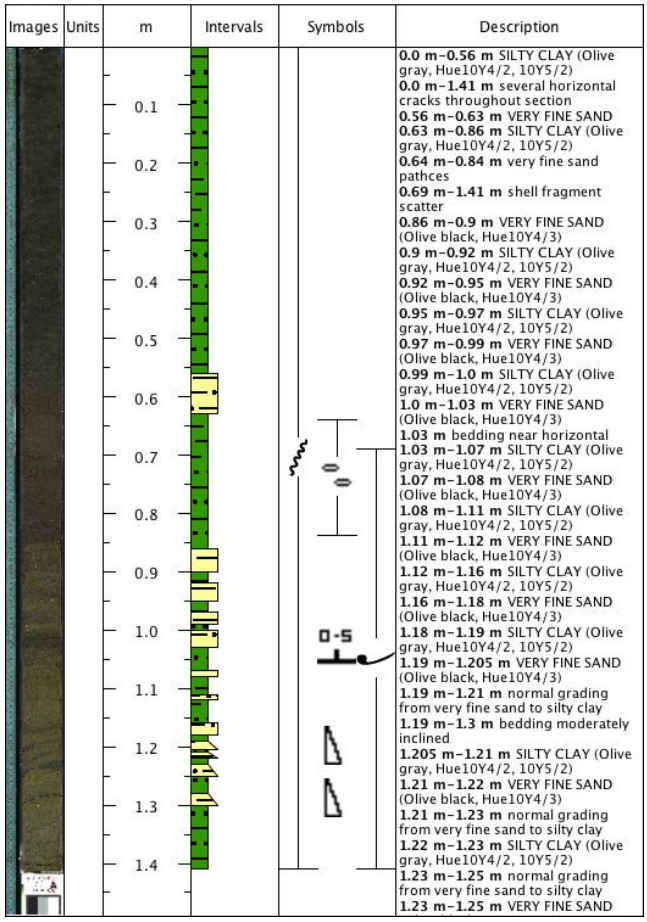

C9033C_6H_7

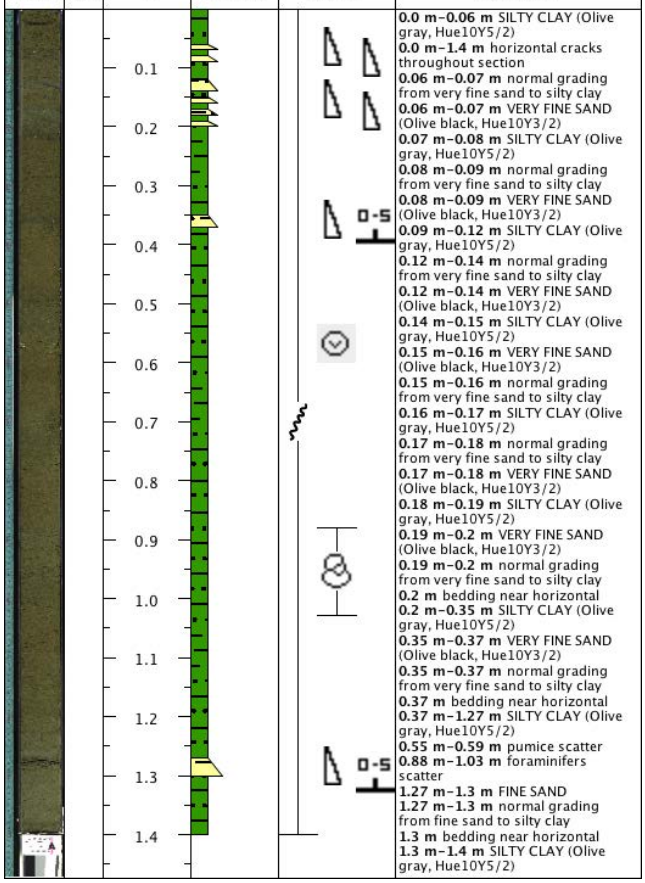

C9033C_6H_8

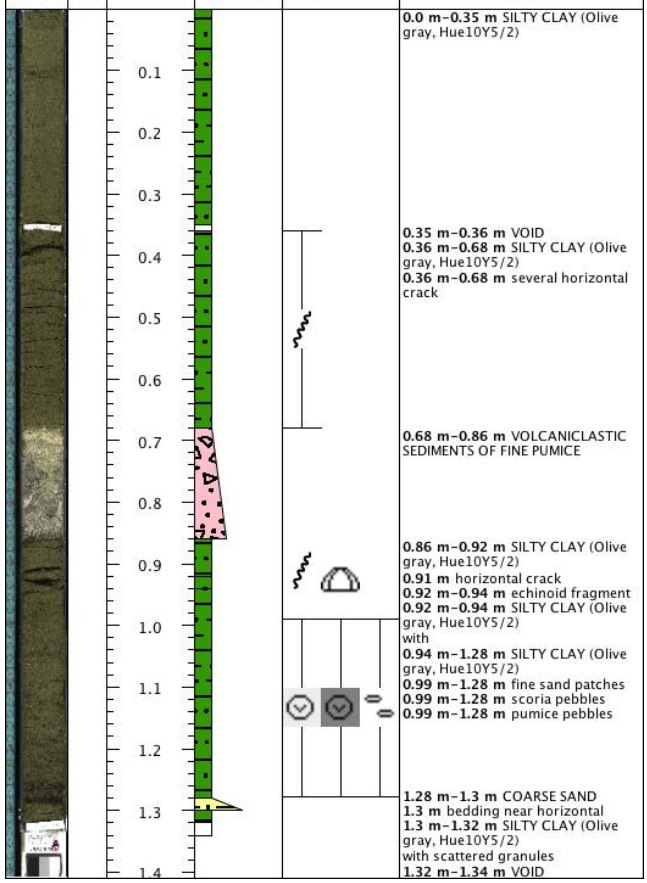

C9033C_6H_CC

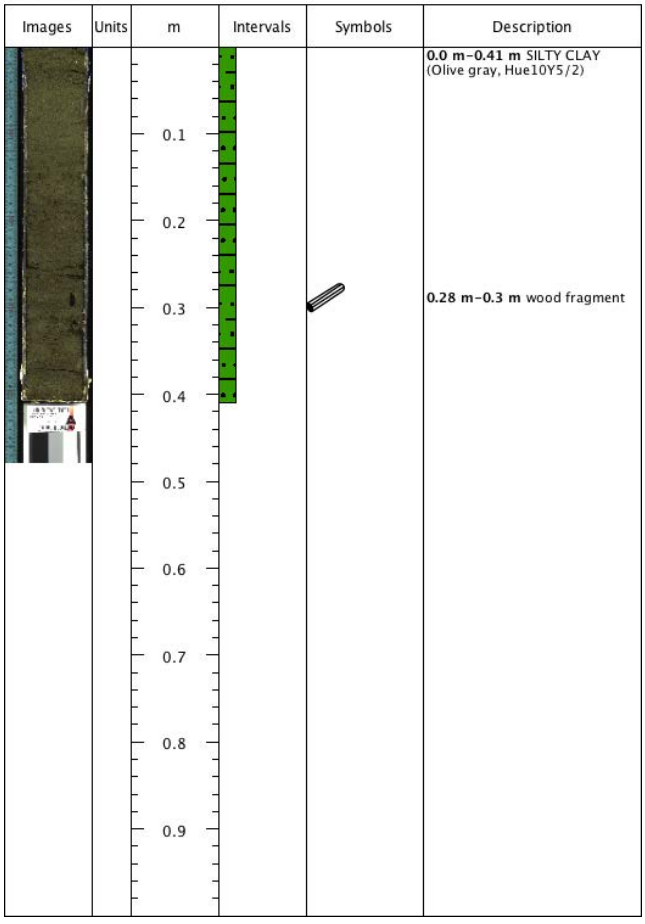

C9033C_7H_1

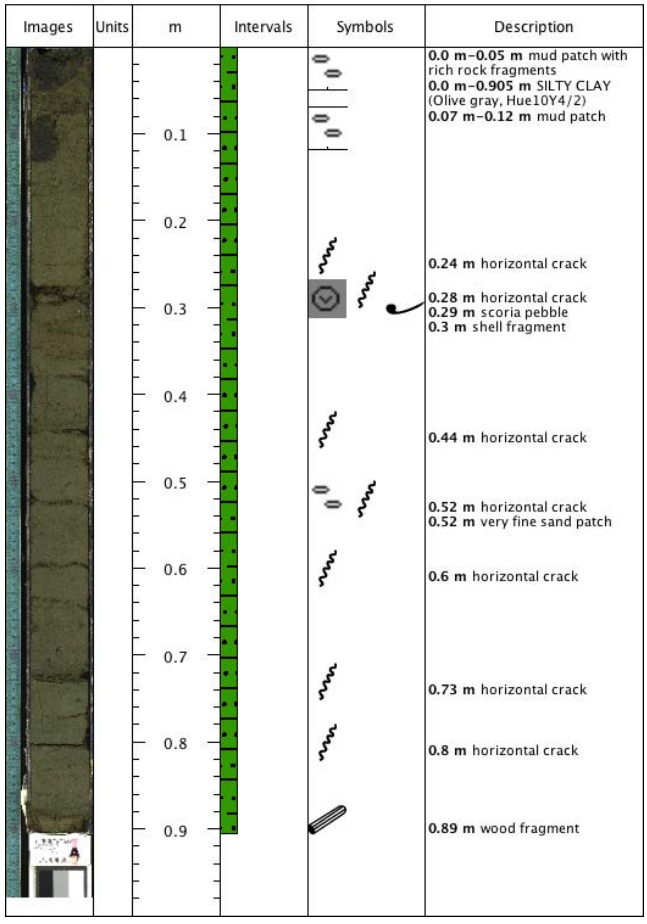

C9033C_7H_2

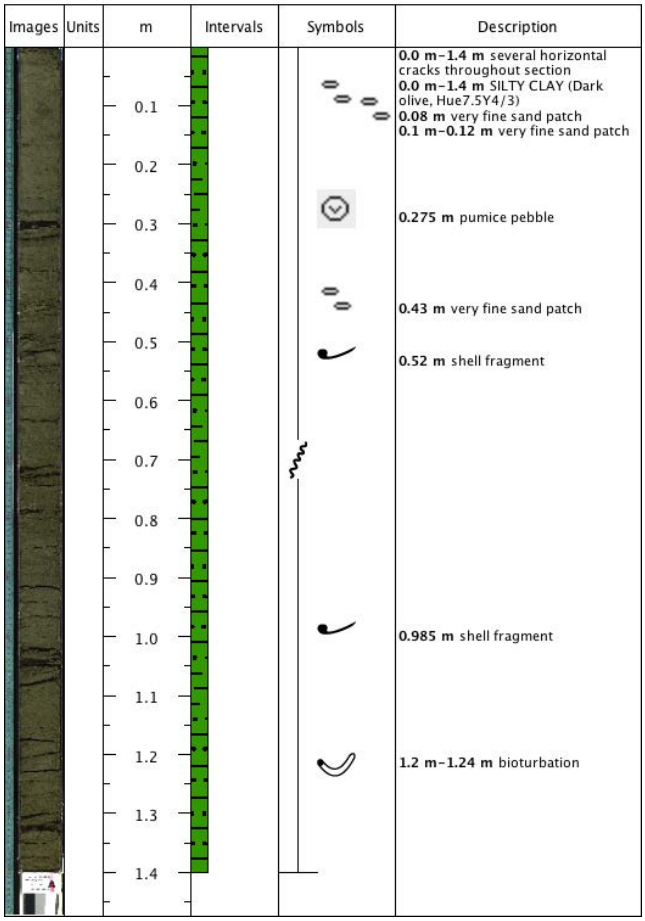

C9033C_7H_3

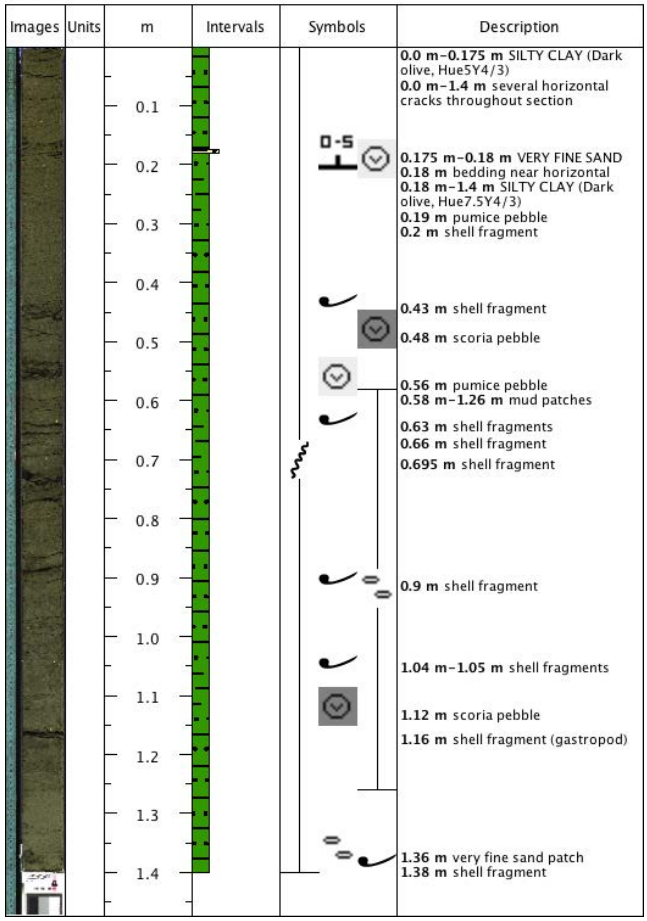

C9033C_7H_4

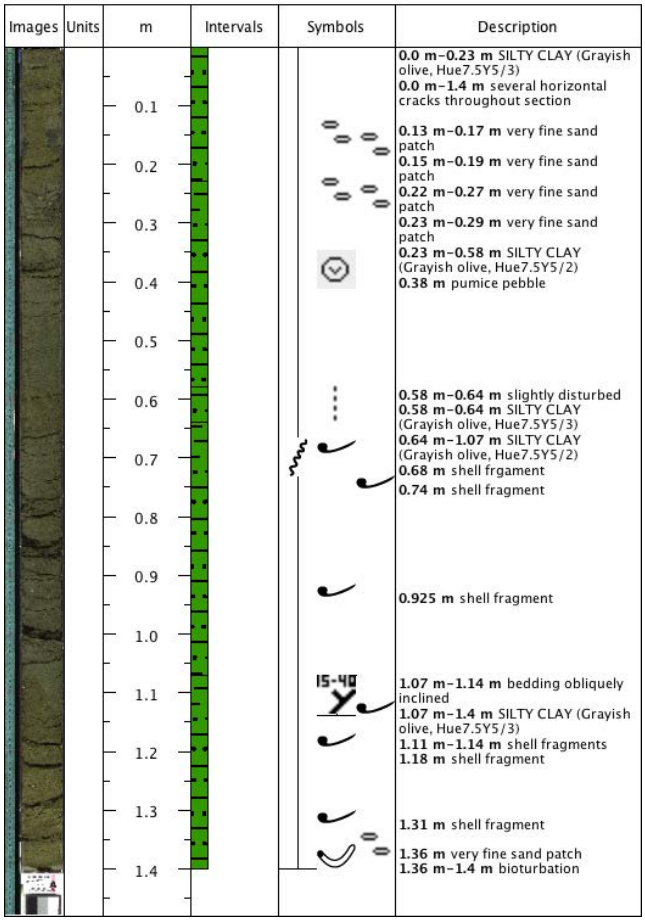

C9033C_7H_5

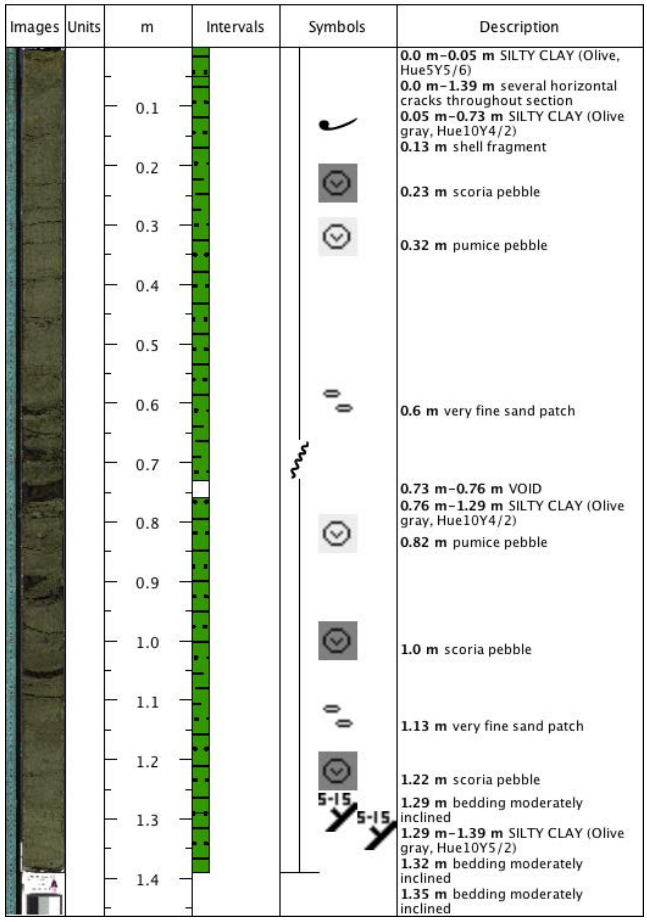

C9033C_7H_6

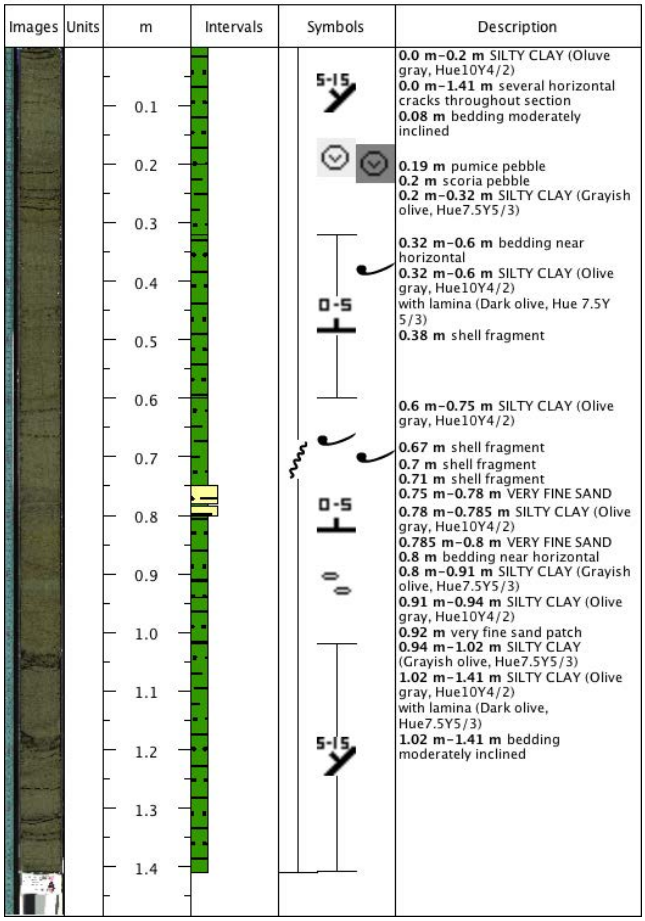

C9033C_7H_7

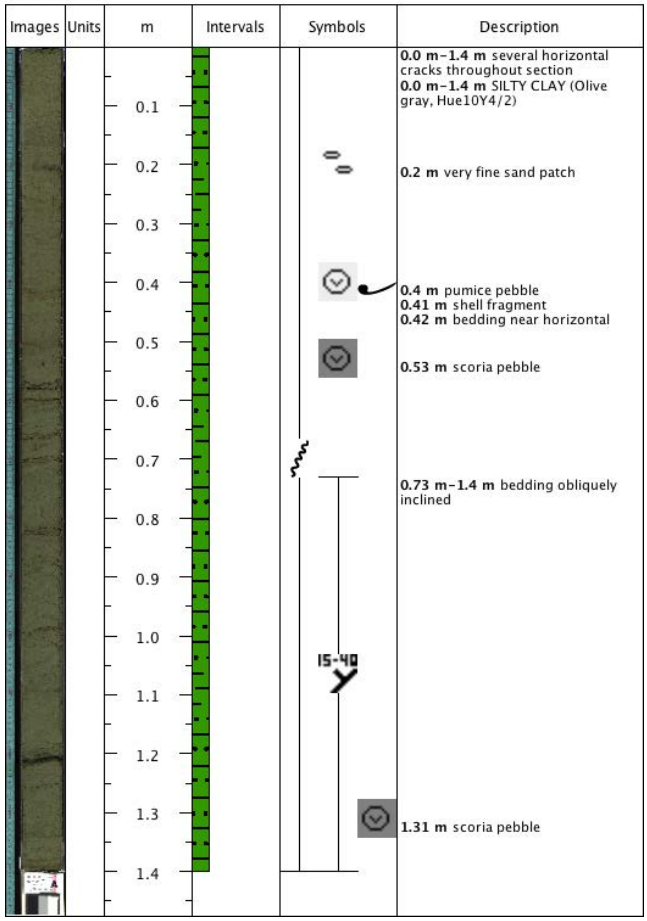

C9033C_7H_8

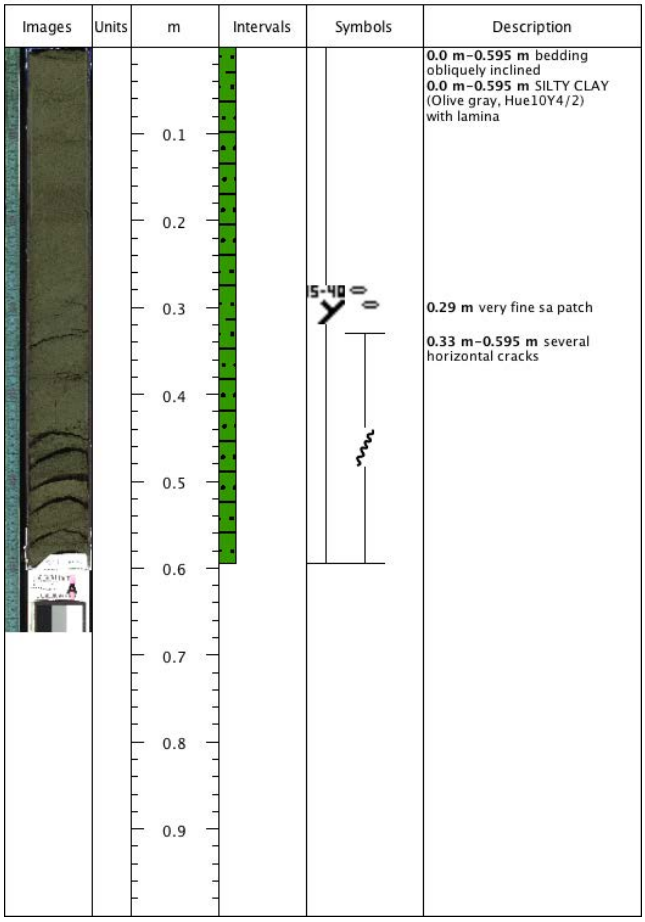

C9033C_7H_9

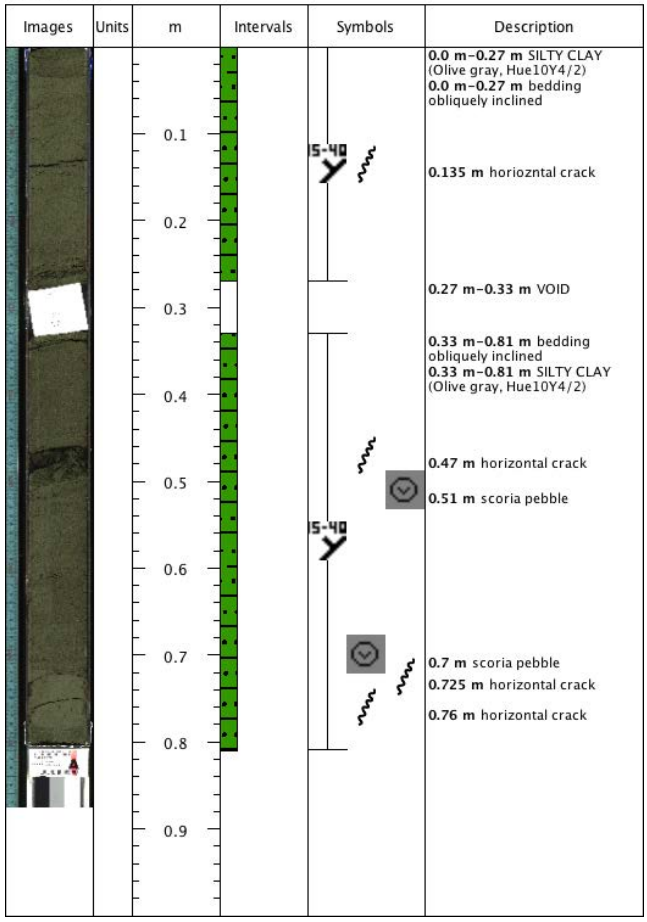

C9033C_7H_CC

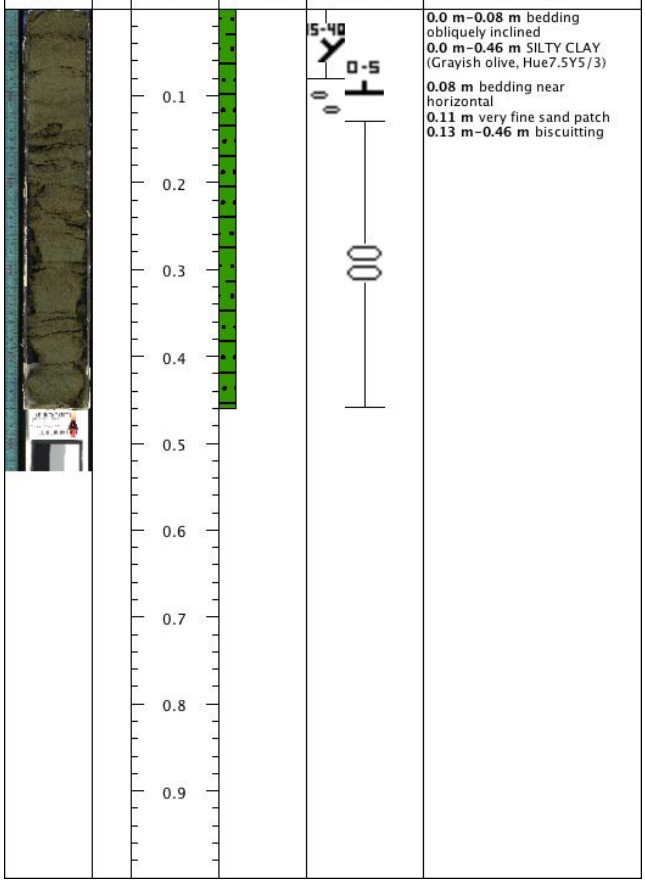

C9033C_8H_1

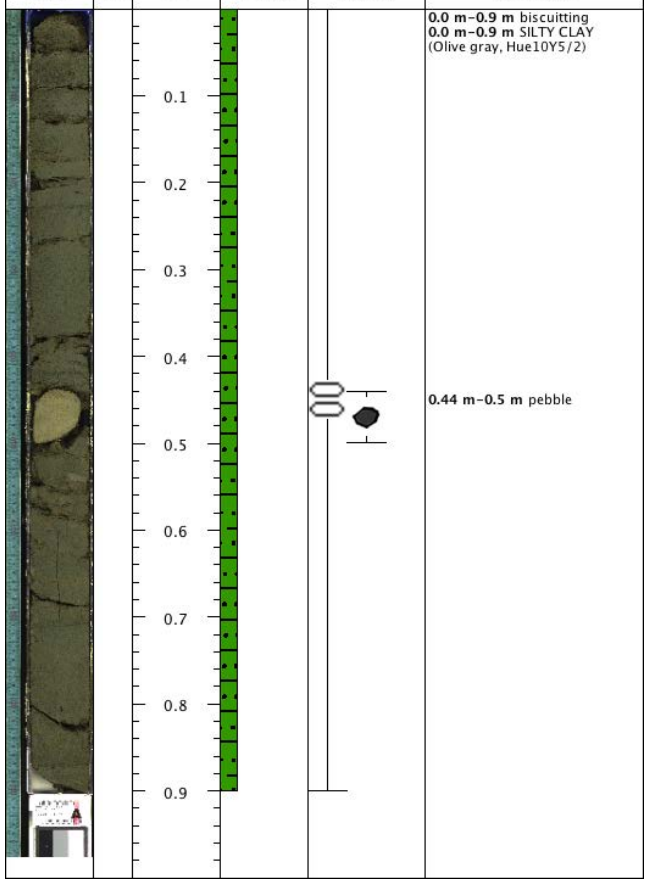

C9033C_8H_2

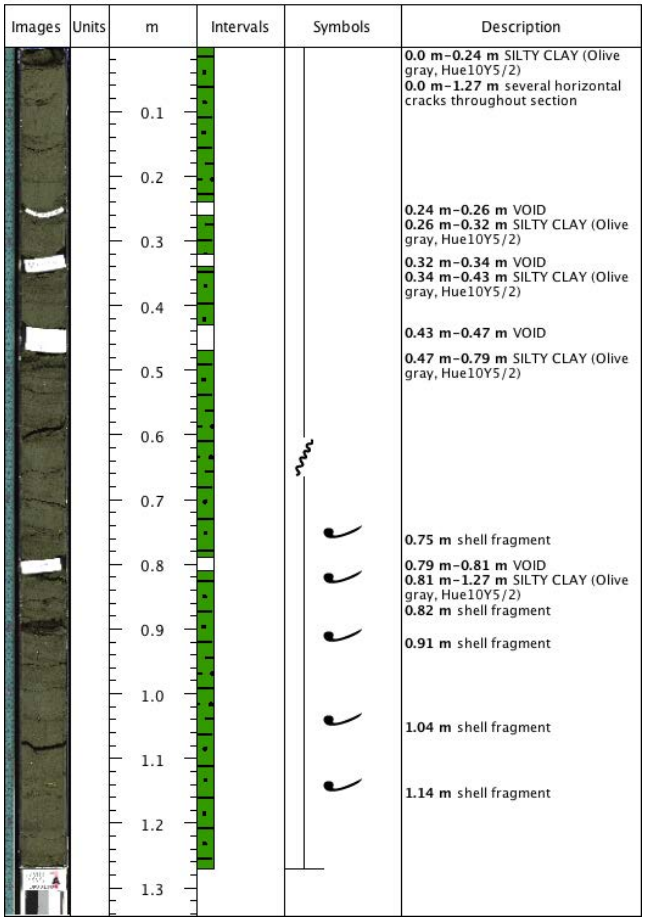

C9033C_8H_3

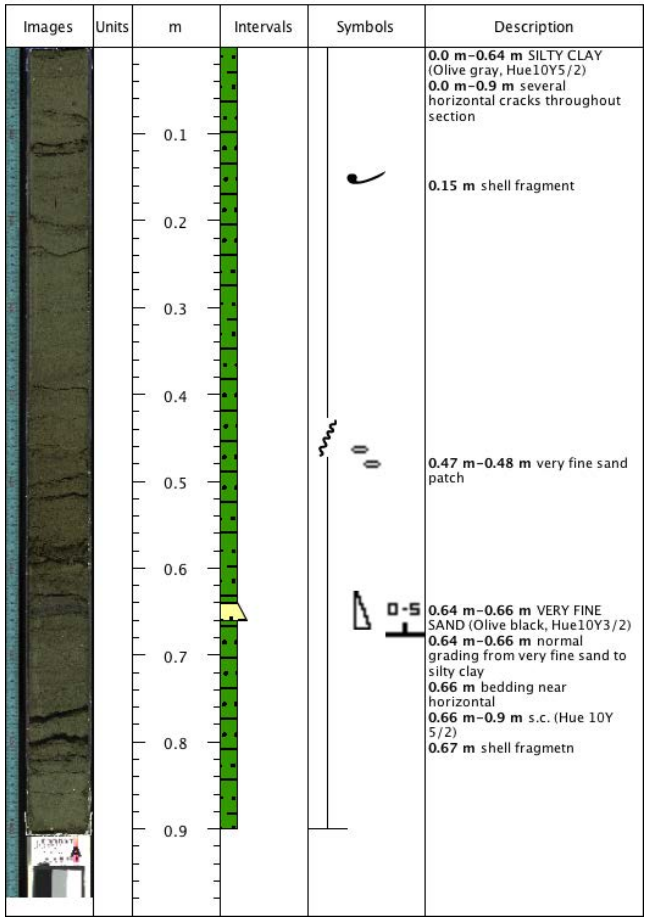

C9033C_8H_4

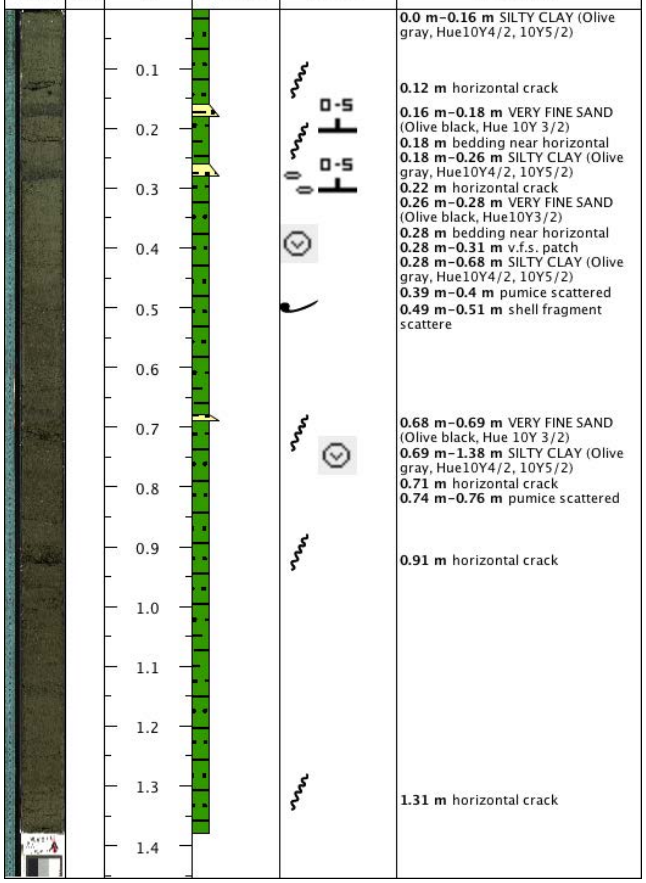

C9033C_8H_5

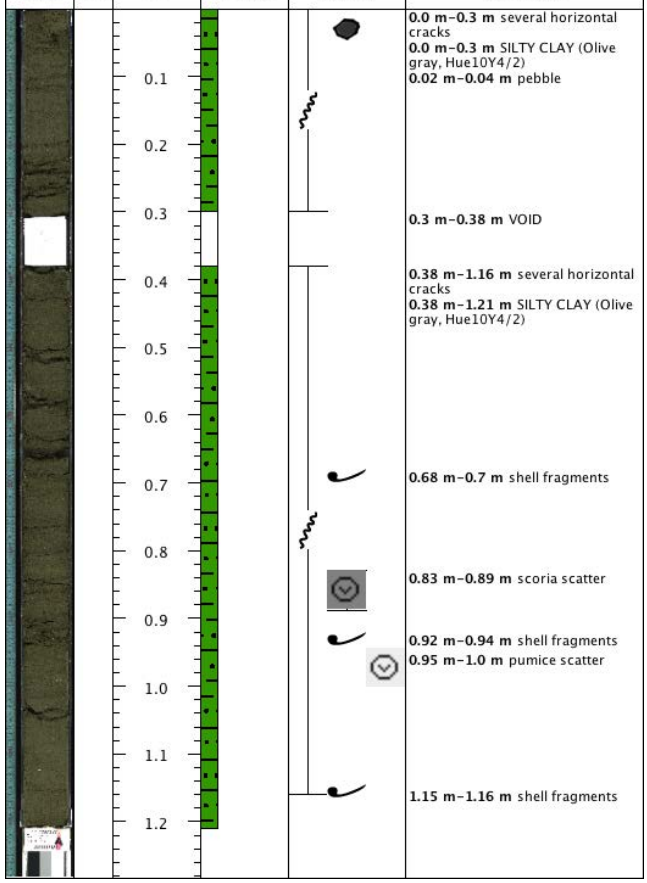

C9033C_8H_6

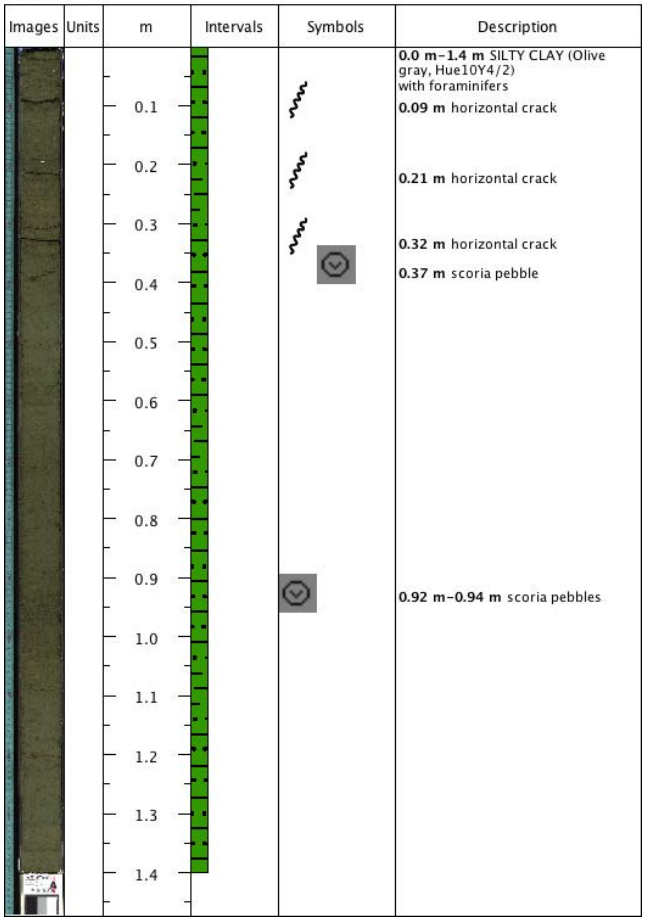

C9033C_8H_7

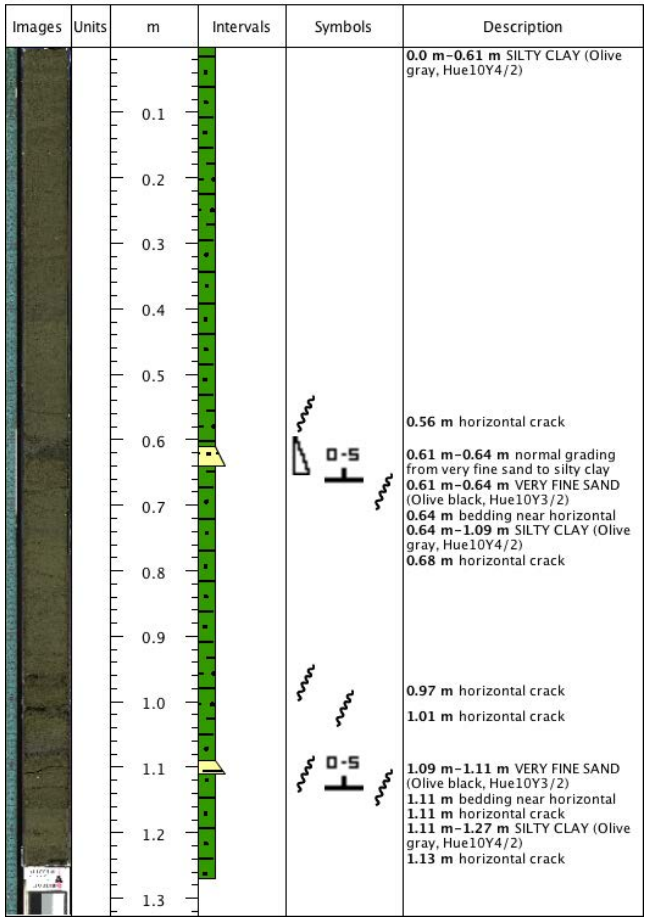

C9033C_8H_8

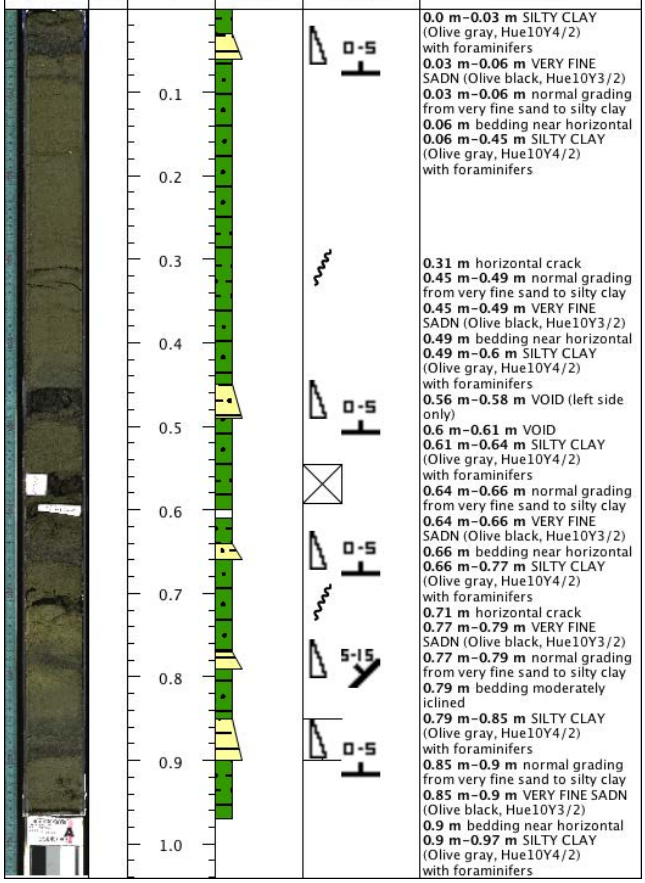

C9033C_8H_9

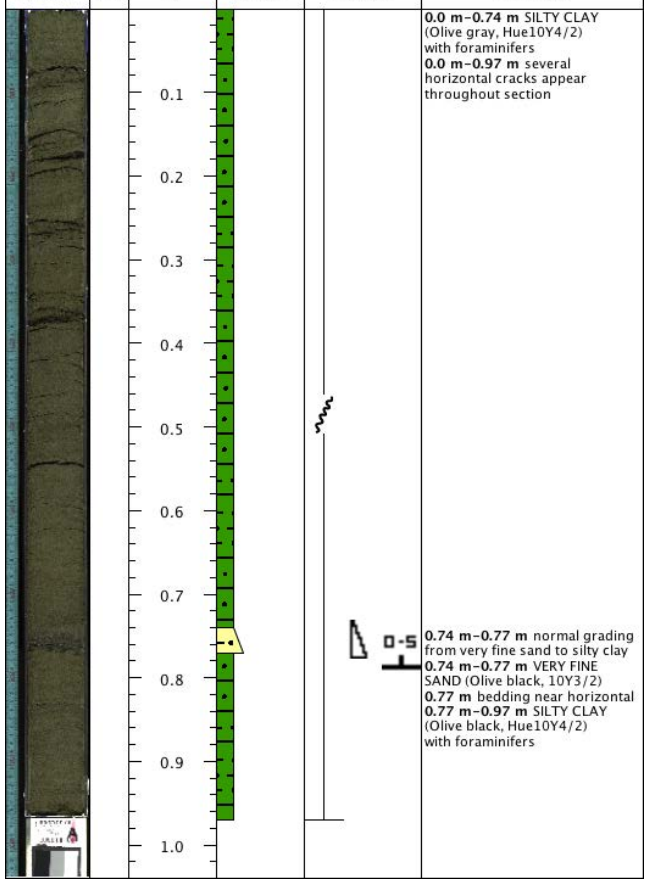

C9033C_8H_CC

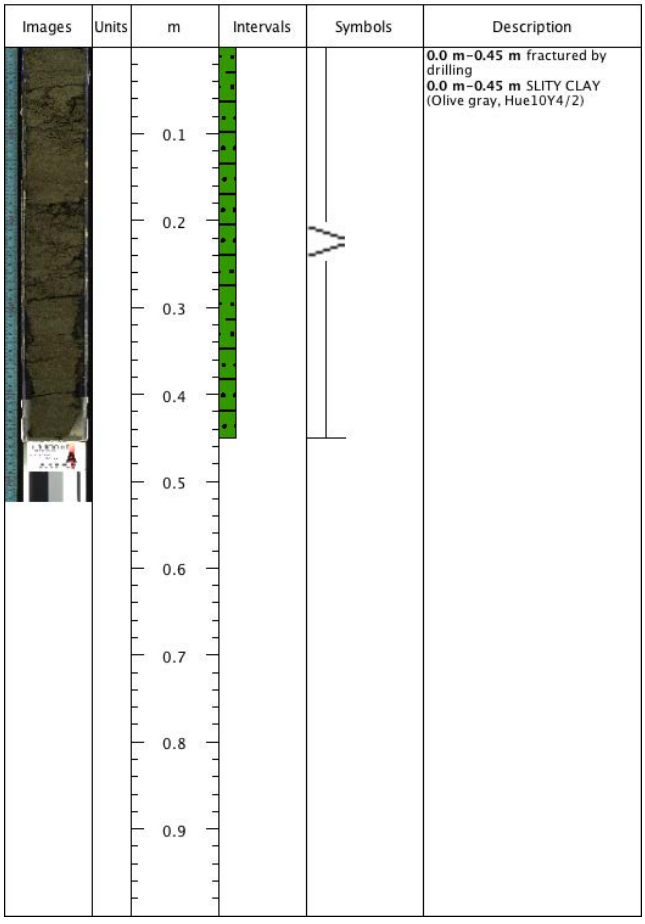

C9033C_9H_1

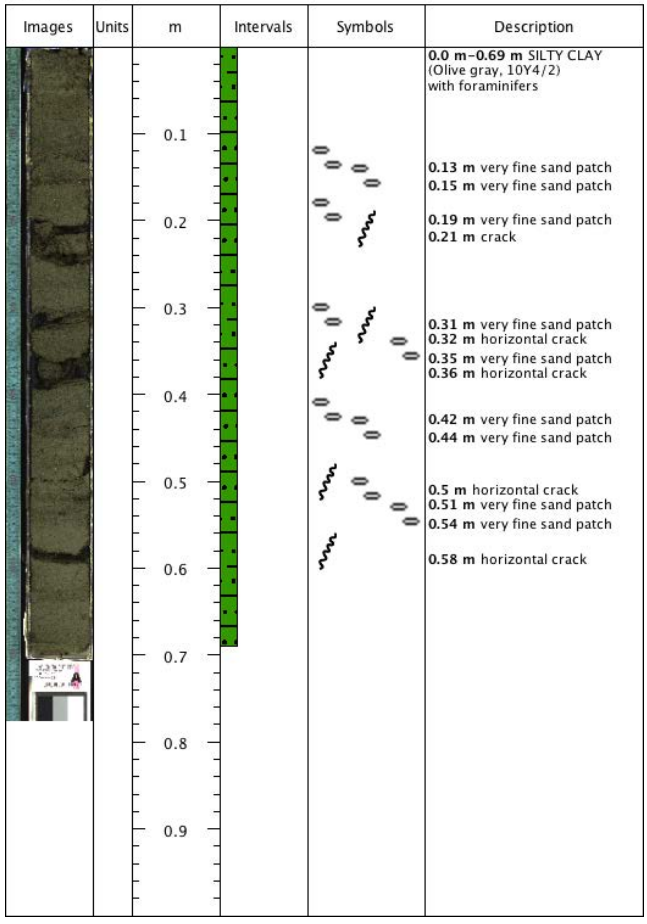

C9033C_9H_2

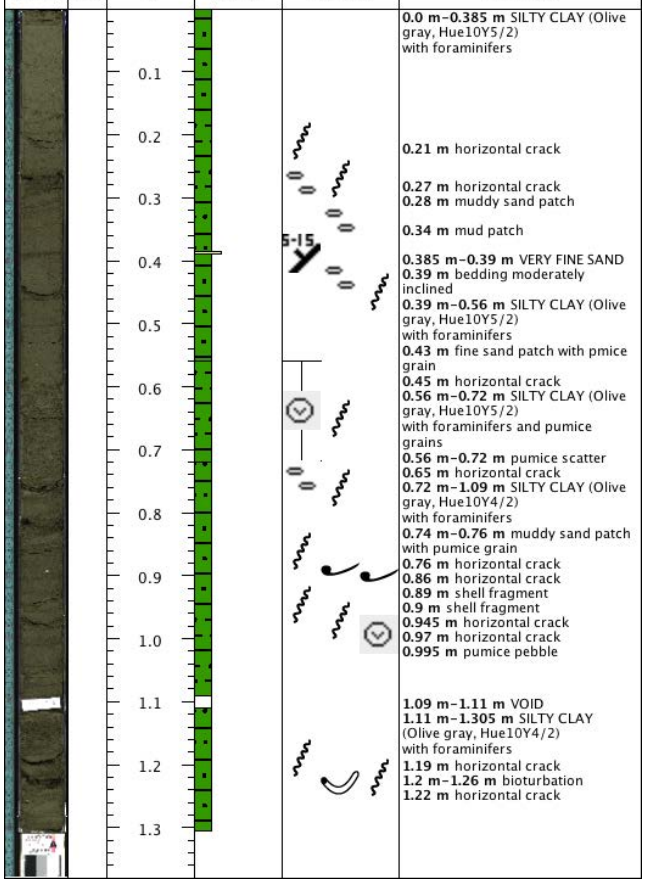

C9033C_9H_3

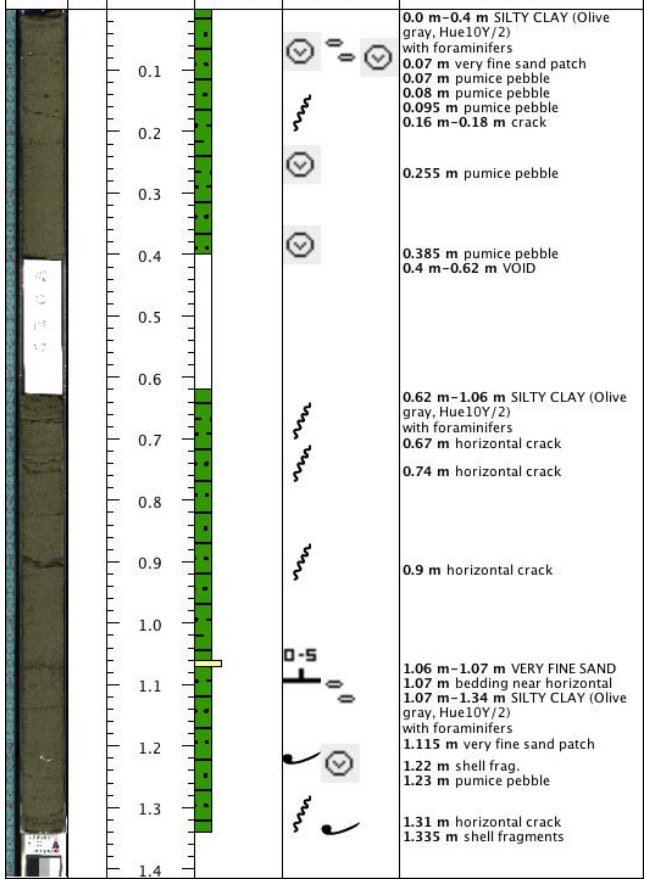

C9033C_9H_4

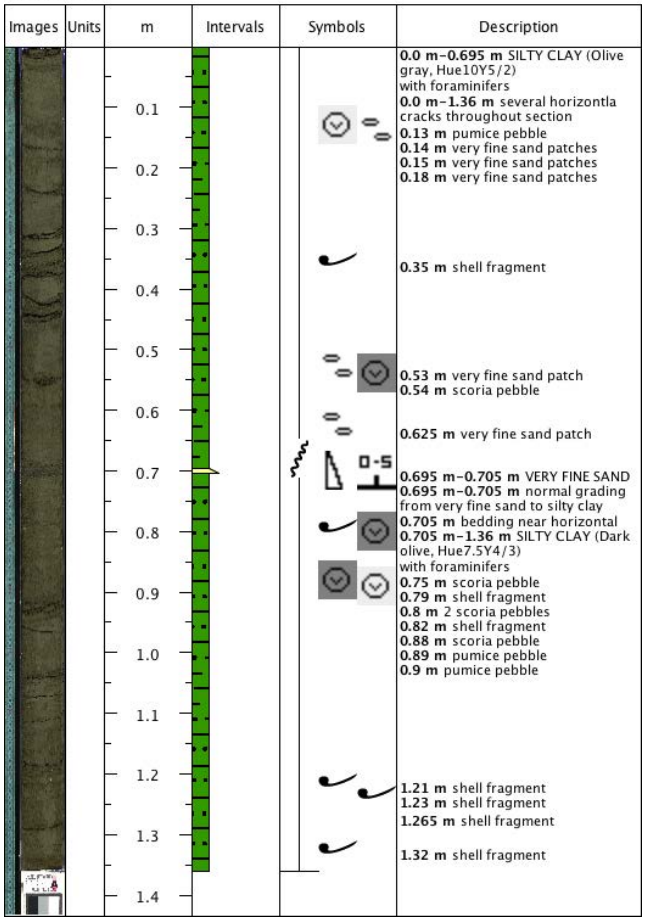

C9033C_9H_5

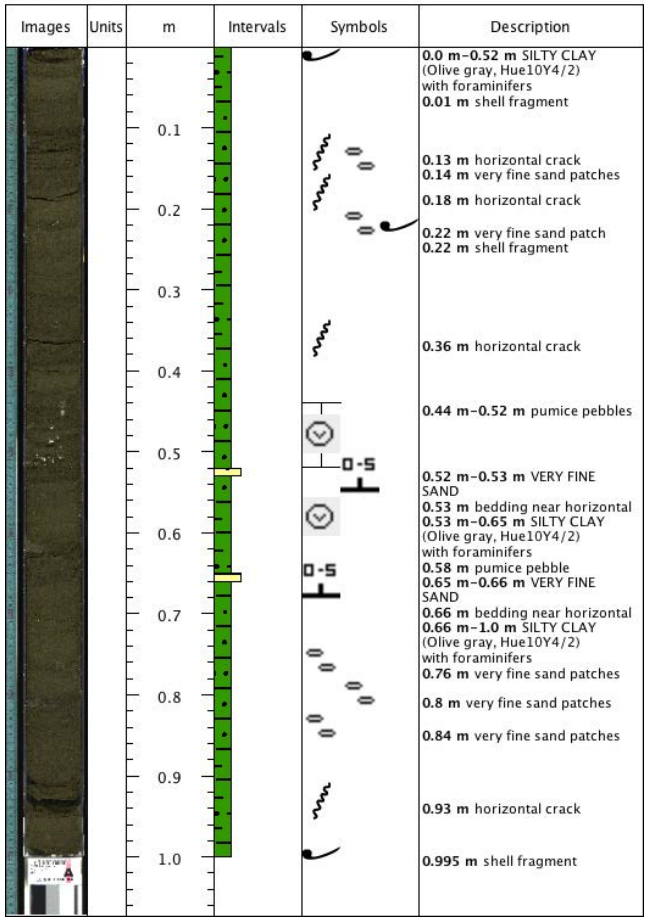

C9033C_9H_6

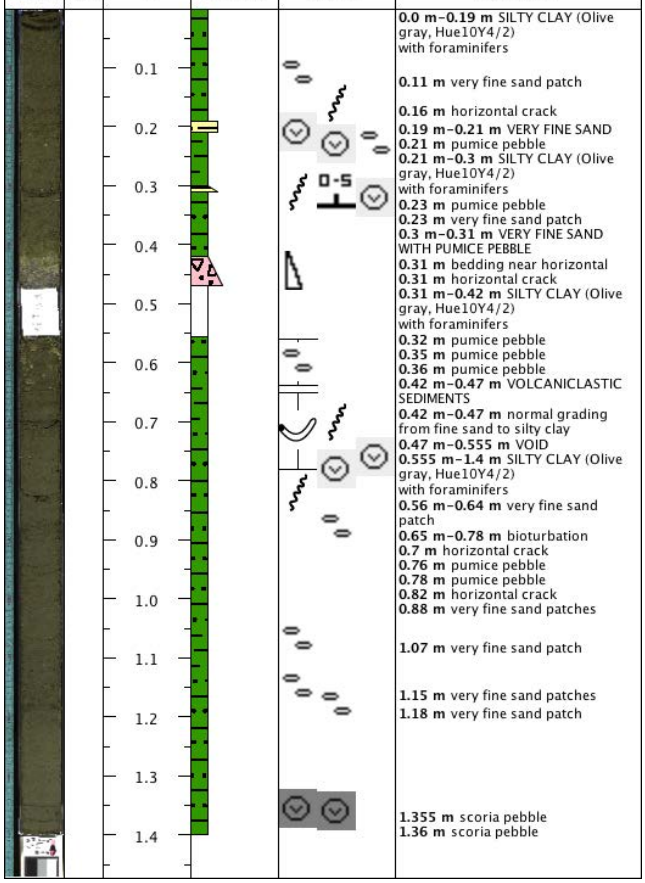

C9033C_9H_7

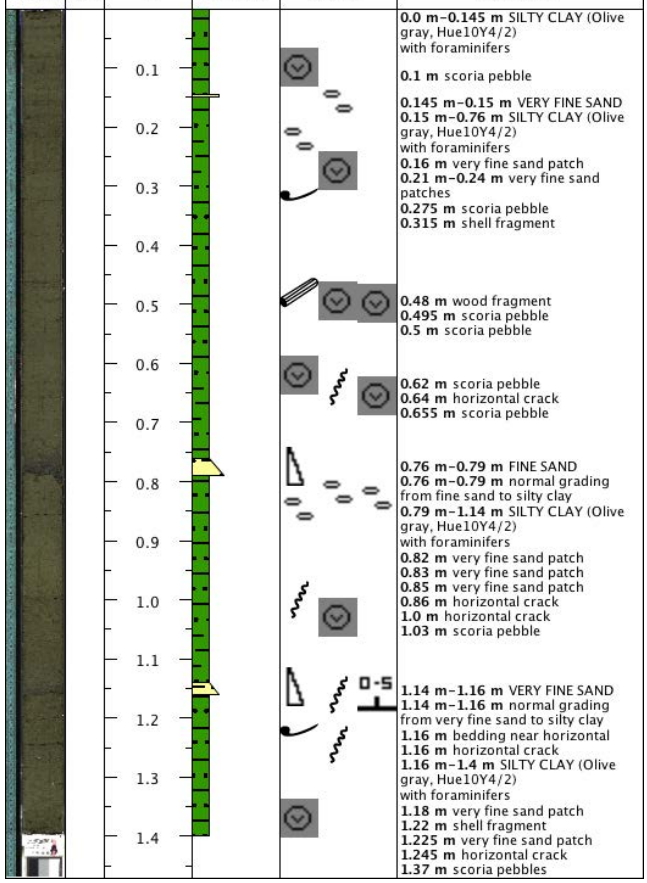

C9033C_9H_8

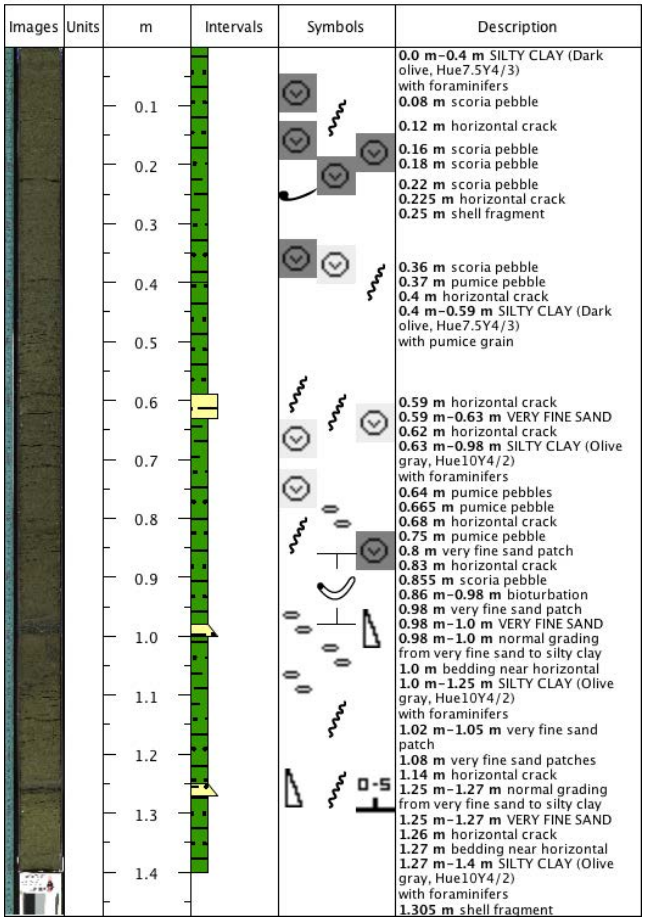

C9033C_9H_9

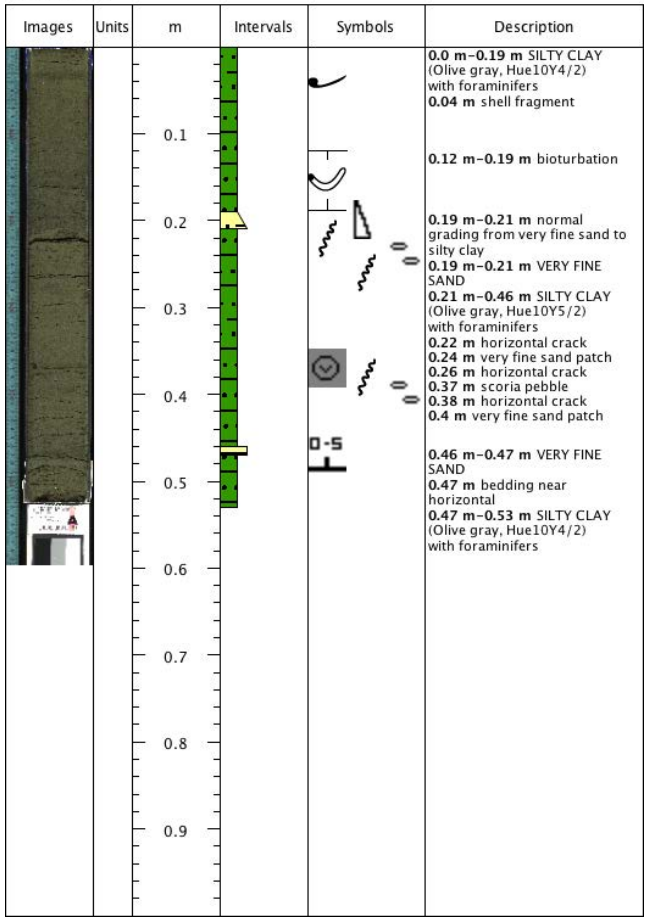

C9033C_9H_CC

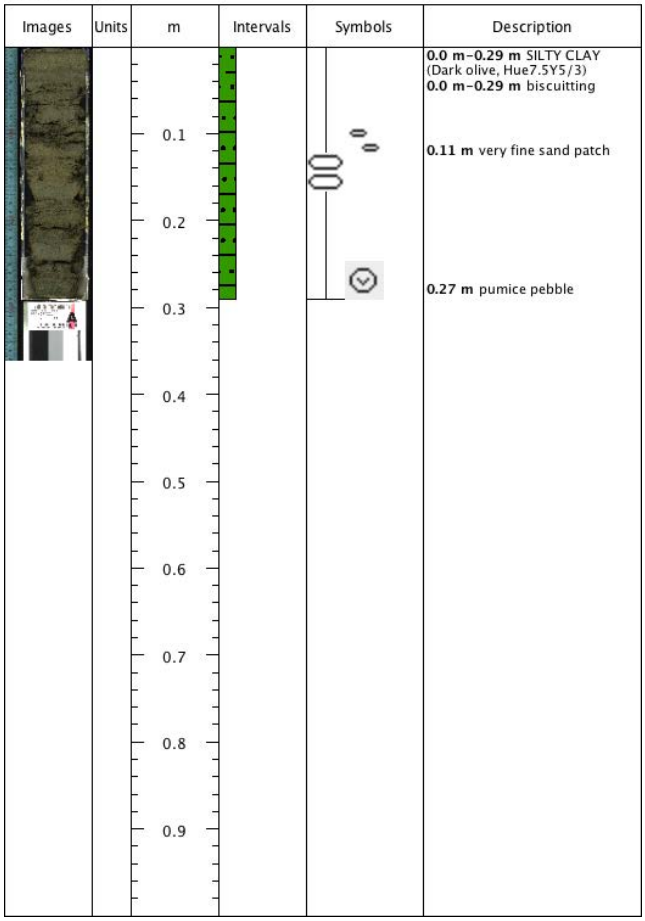

C9033C_10H_1

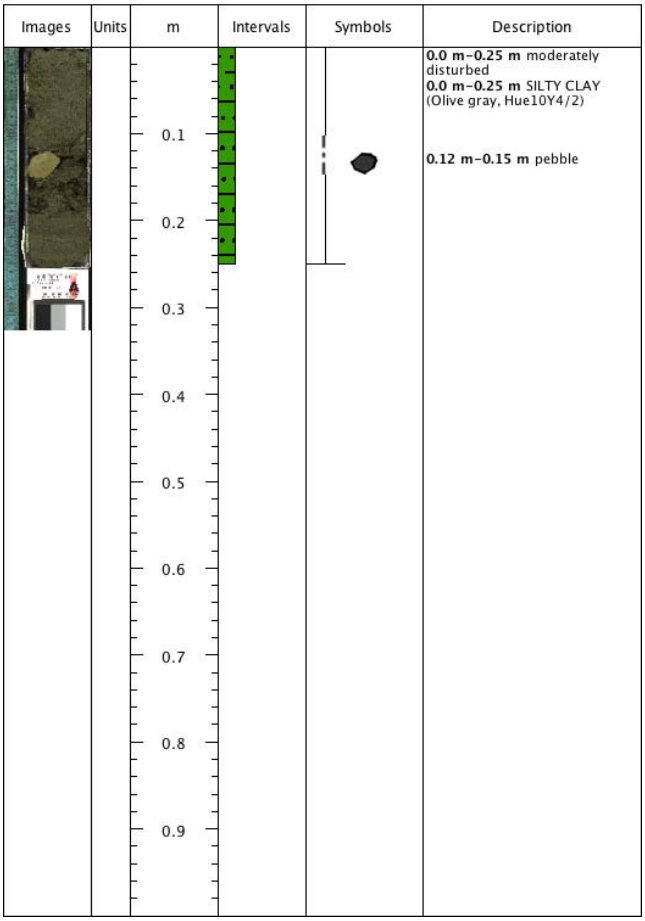

C9033C_10H_2

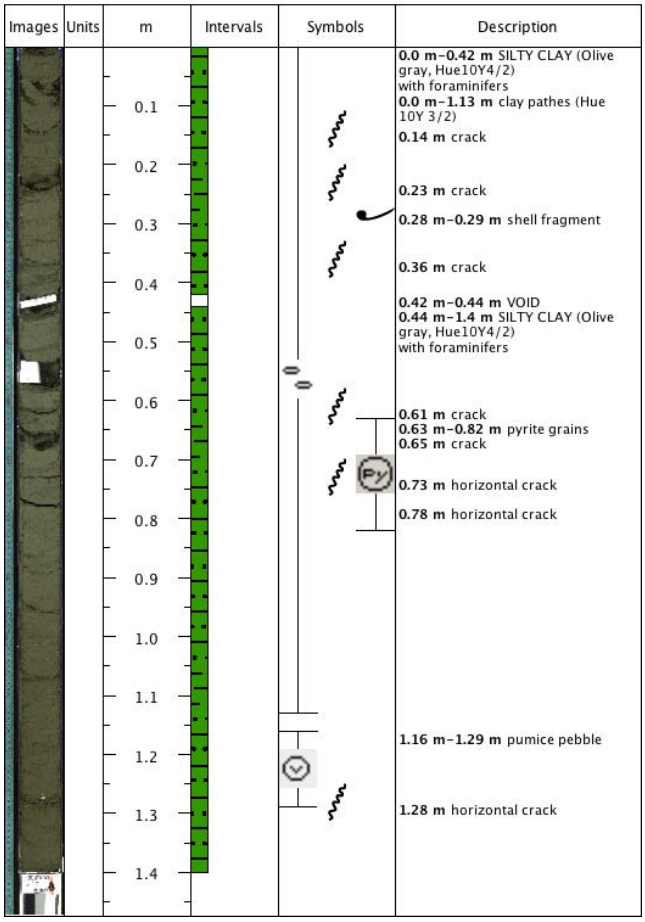

C9033C_10H_3

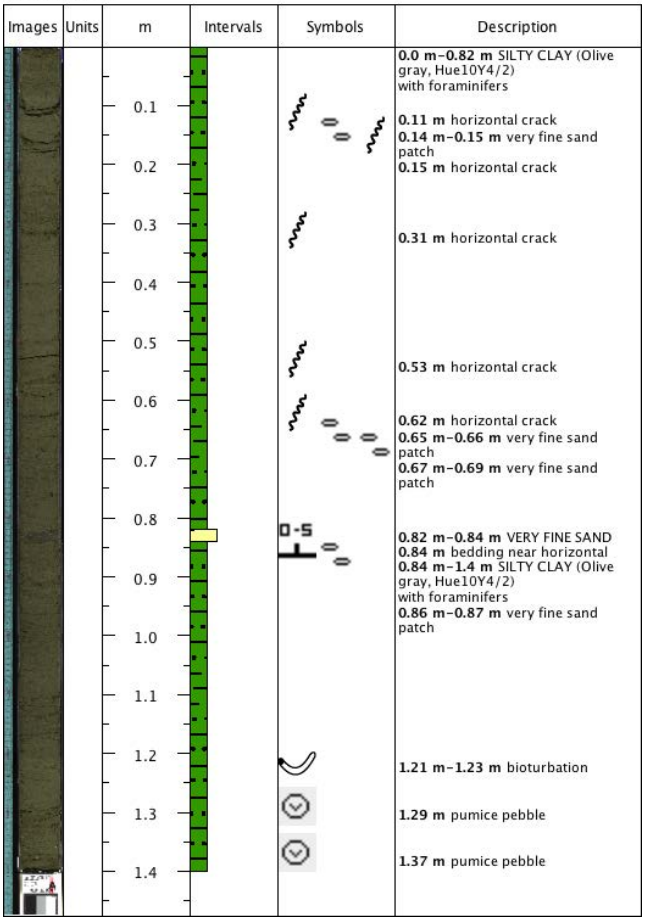

C9033C_10H_4

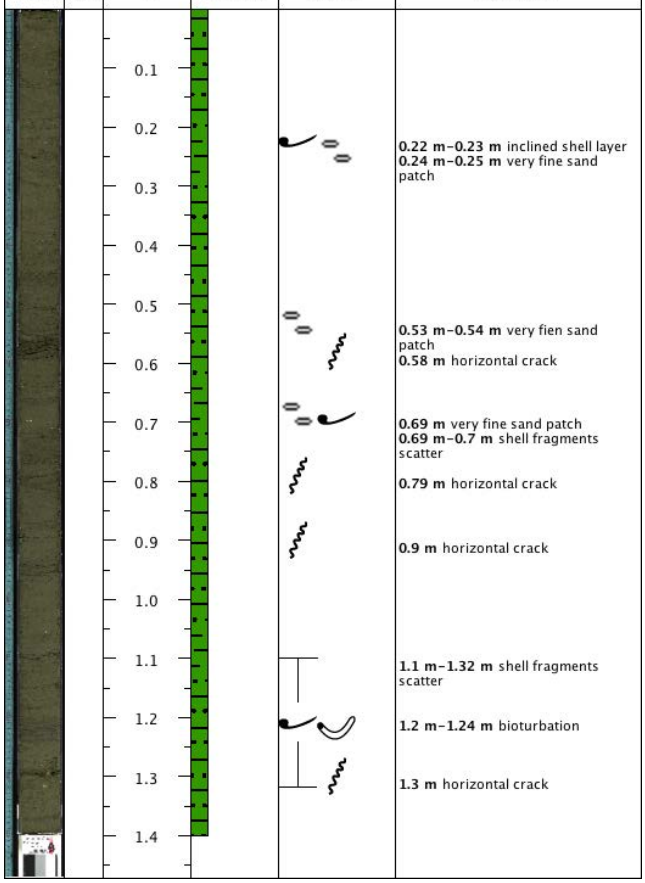

C9033C_10H_5

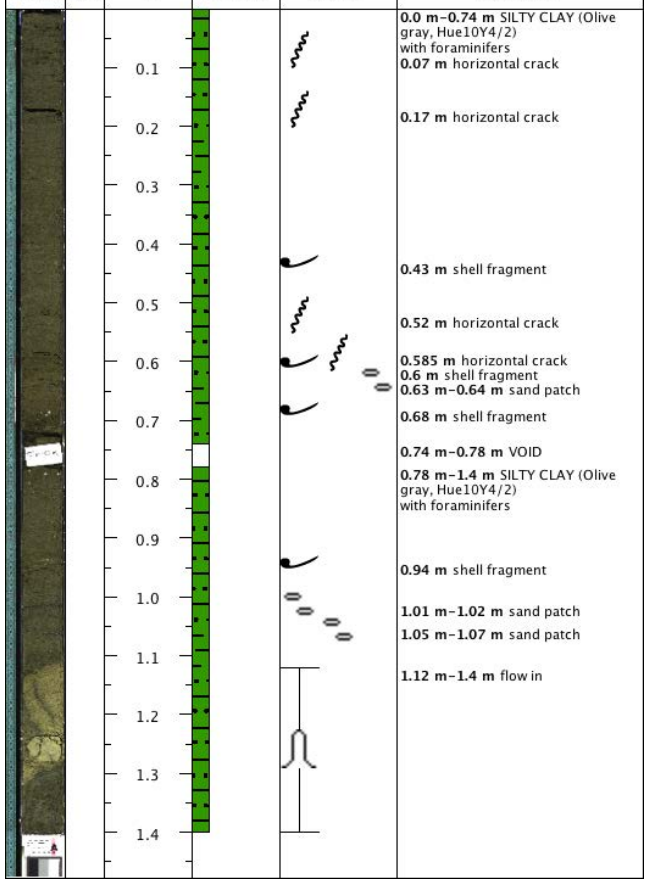

C9033C_10H_6

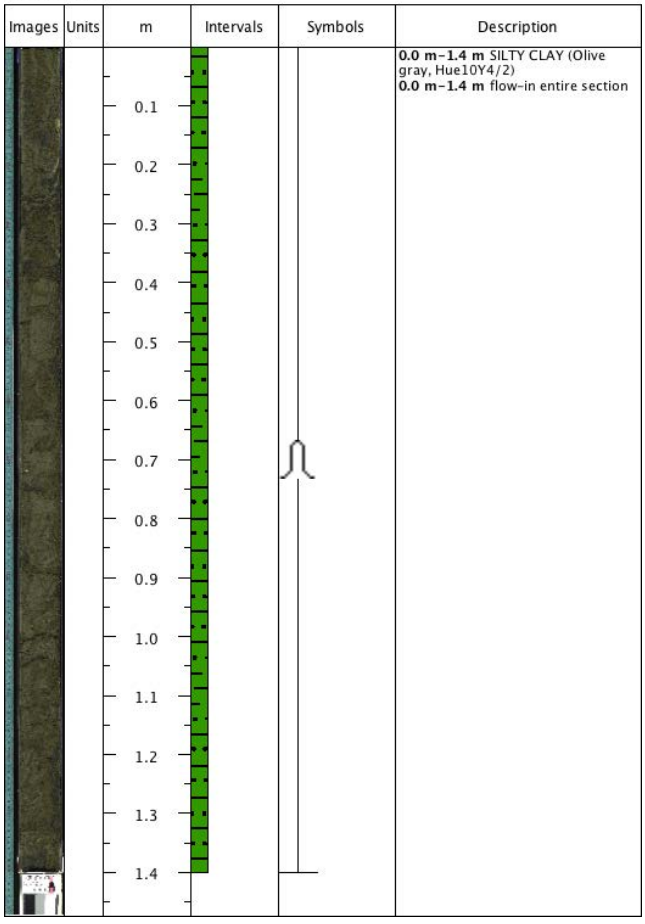

C9033C_10H_7

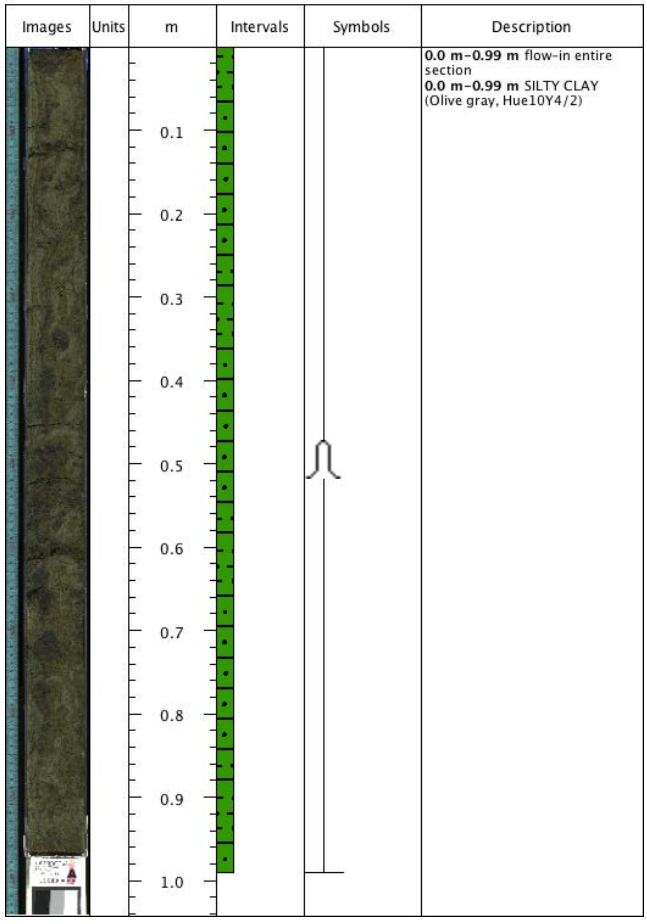

C9033C_10H_8

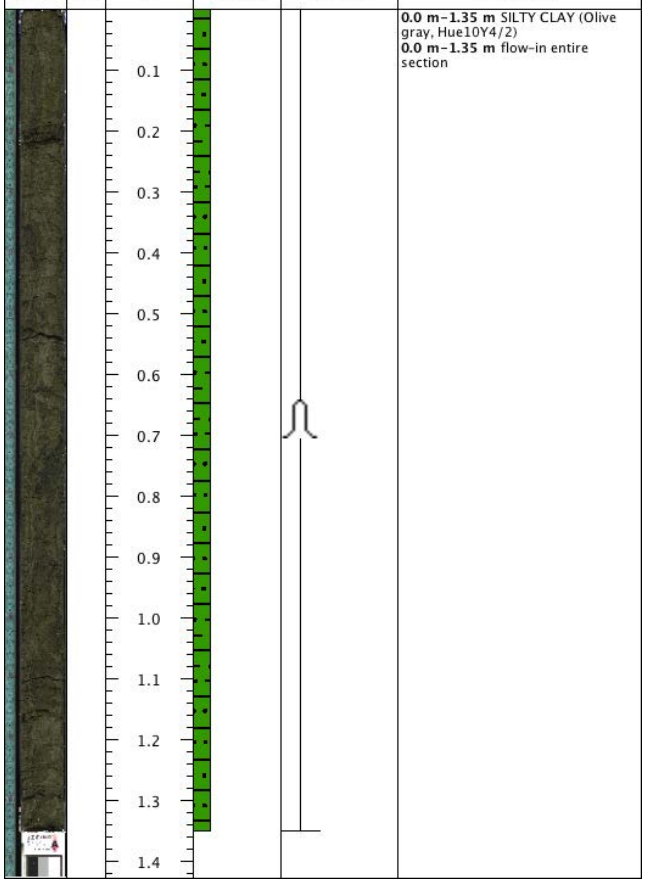

C9033C_10H_CC

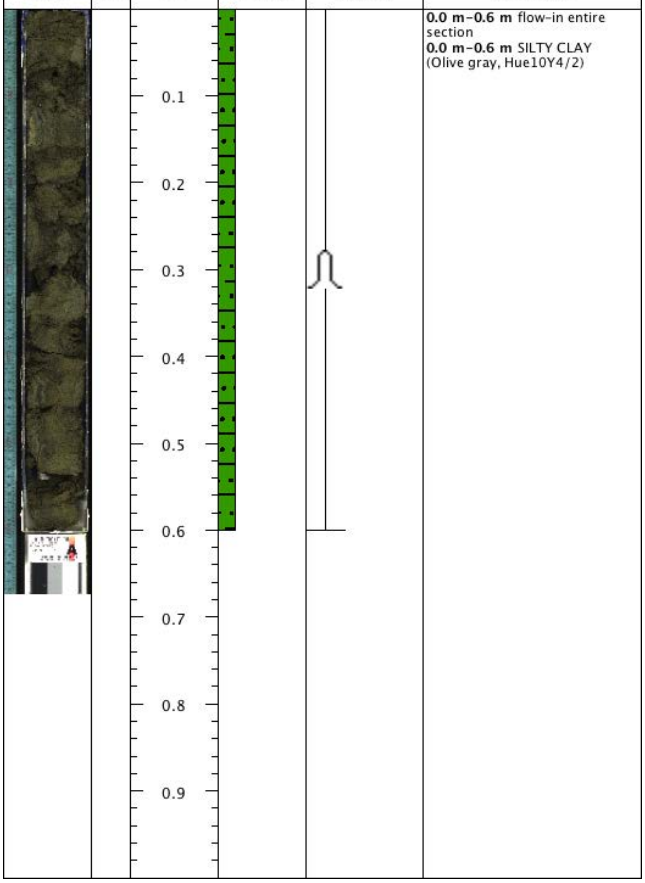

C9033C_11F_1

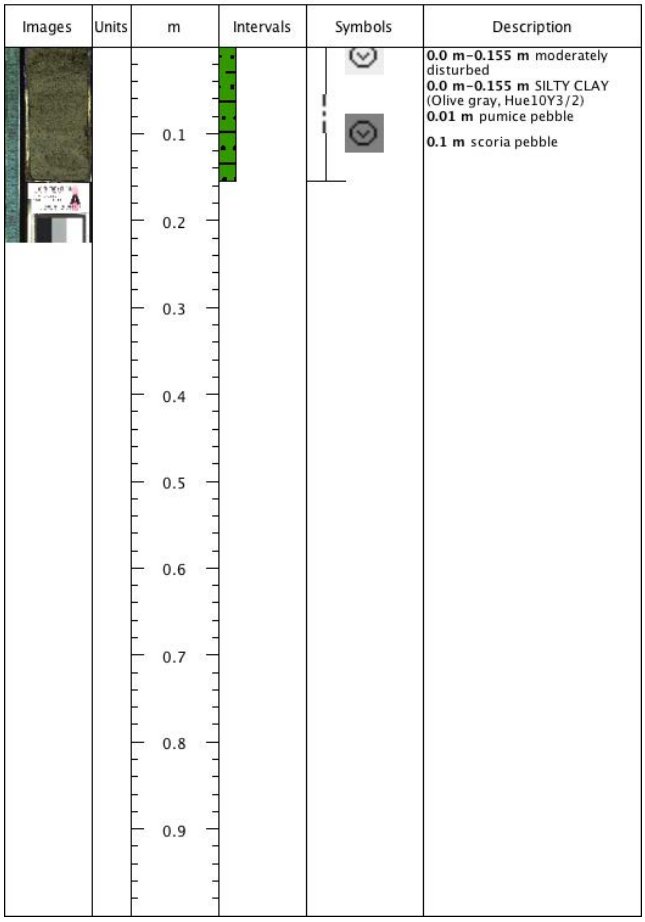

C9033C_11F_2

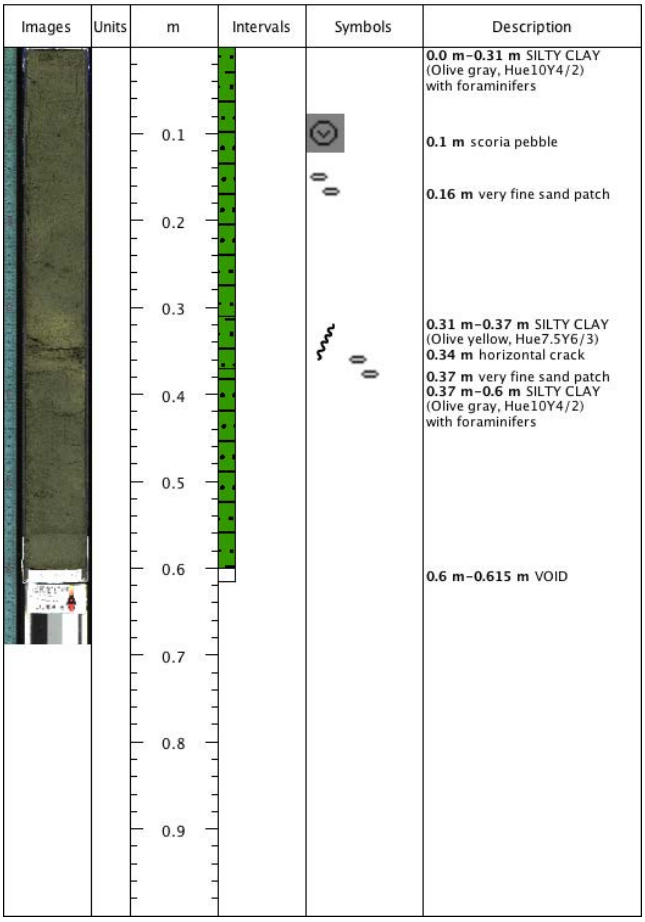

C9033C_11F_3

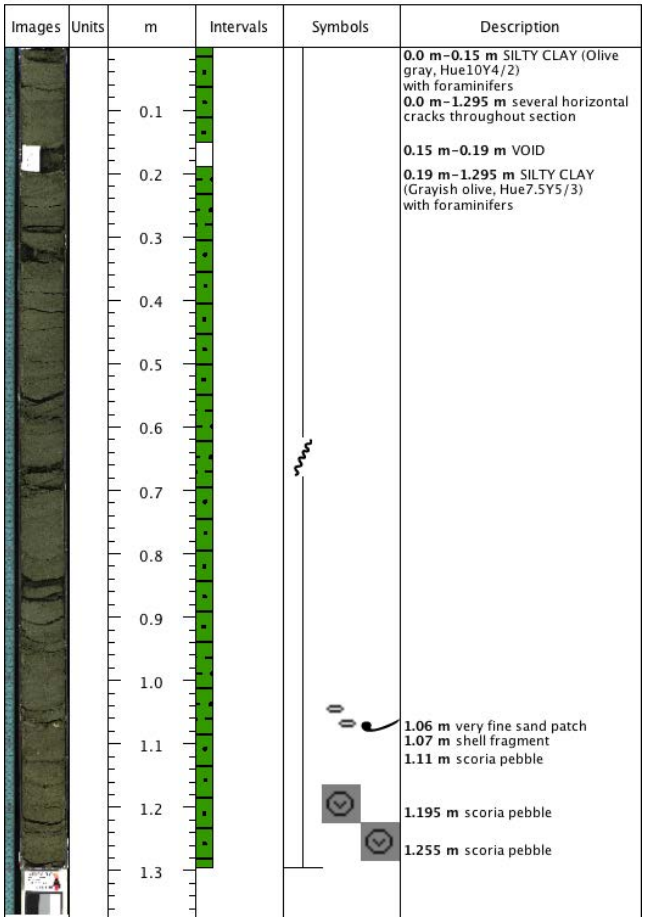

C9033C_11F_4

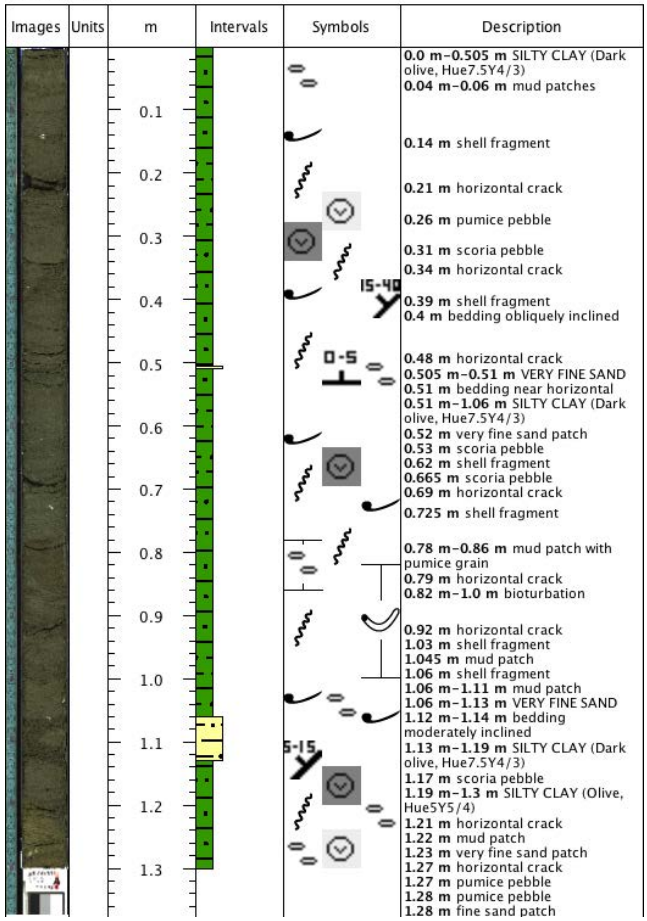

C9033C_11F_5

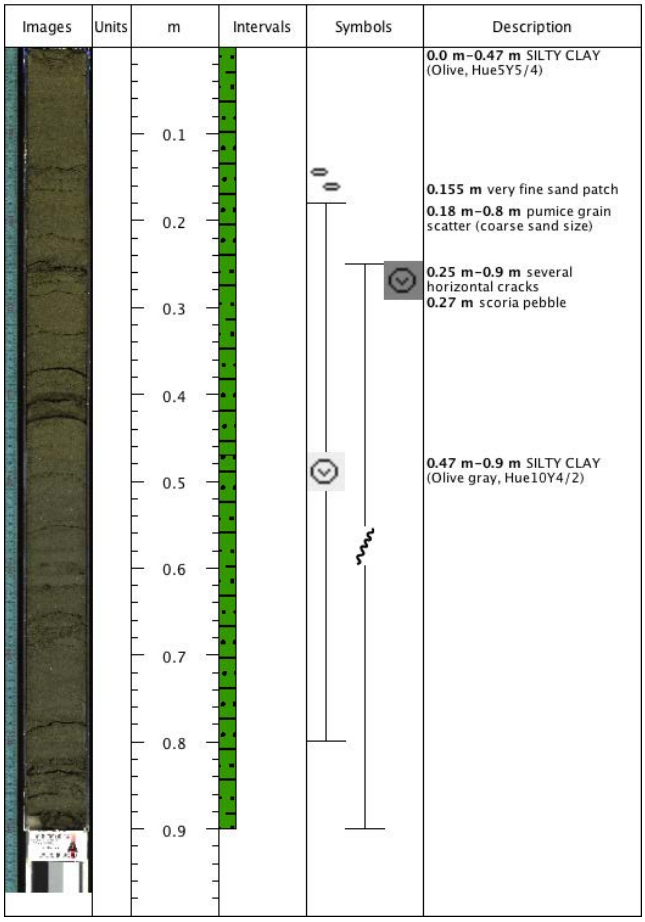

C9033C_11F_6

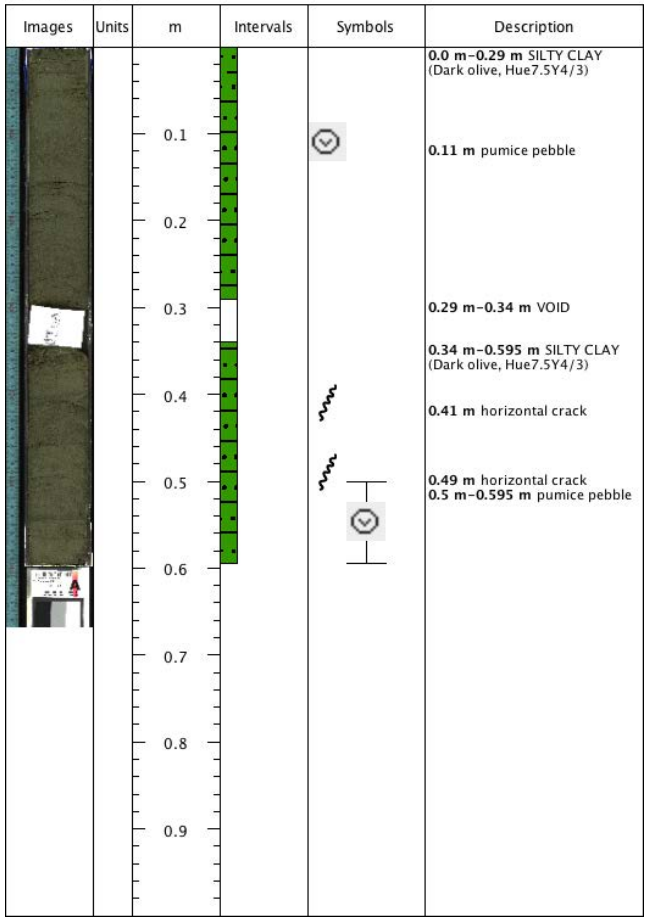

C9033C_11F_CC

Images	Units	m	Intervals	Symbols	Description
		0.1 0.2 0.3 0.4 0.5 0.6 0.7 0.8 0.9			**0.0 m–0.46 m** biscuitting **0.0 m–0.46 m** SILTY CLAY (Dark olive, Hue7.5Y4/3) **0.15 m** pumice pebble **0.31 m** shell fragment **0.32 m** shell fragment **0.4 m** shell fragment **0.41 m** very fine sand patch **0.43 m** shell fragment **0.44 m** very fine sand patch